NIRS—R—44

グループ研究「先端科学技術がもたらす環境負荷とその生物影響の認知基準化に関する研究」

（平成８～12年度）

最終報告書

平成13年11月

放射線医学総合研究所

Final Report on the Group Research :

Studies on the Comparative Evaluation on the Environmental Toxicants Released from Advanced Technology and Industry

(April 1996 - March 2001)

November 30 2001

National Institute of Radiological Sciences,

9-1, Anagawa 4-chome, Inage-ward, Chiba-shi 263-8555, Japan

目　次　Contents

1．概　況

近年の科学技術の発達に伴い、人類は遭遇したことのない種類や量の有害因子にさらされている。さらに、その曝露（被曝）様式は複雑化し、複合的な曝露の問題が顕在化してきている。本グループ研究は、平成８年に放医研の環境科学部門、安全解析部門、生物影響研究部門から、このような問題、特に、放射線と他の環境有害因子との関連や比較、複合影響に関心をもつ研究者により結成された。研究の焦点は放射線（放射性物質）を基準とした比較環境科学におかれ、原因物質の環境動態から、生態系への影響、生物学的影響をへて数学モデルに至る広範な研究を進め、すぐれた研究成果をあげた。本報告書は、その成果の概要を取りまとめたものである。

研究の主題を「環境負荷と生物影響の認知基準化」においた本研究では、当初２年間程度を放射線や有害物質の環境負荷や生物・生態系への影響を適切に比較し、その程度を基準化する（認知基準化）ための研究手法の開発に重点を置き、後半の３年間を放射線（放射性物質）と代表的な環境有害物質である重金属や先端科学技術産業で多用され始めている希土類元素の比較評価にあてた。研究の実施にあたっては、１）各々のサブグループで得られた成果をもとに環境動態や影響に関する数学的モデルを開発するサブグループ、２）環境中での有害物質の挙動・動態を中心とするサブグループ、３）生態系、特に、実験室内で制御できる実験生態系の開発とその利用に重点を置くサブグループ、４）生物学的影響を指標とし放射線と環境有害物質の影響の比較を行なうサブグループ、の４つのサブグループを編成した。各サブグループは適切に協力し、共同研究を実施することにより、当初の目標とした成果に加え、放射生態学や比較毒性学などの多方面で高く評価されている知見を得た。

第１サブグループでは、放射性物質等の有害物質の環境中における挙動や、その環境と人に及ぼす影響に関する理論・数学モデルの開発を目的とした。今般の研究期間においては、「健康リスク評価モデル」および「制御実験生態系もでる」の２つのモデルの開発を実際に行い、その開発過程からモデル化の利点や問題点を明らかにして行くこととした。健康リスクモデルとして、放射線への被曝により公衆にもたらされる健康影響を推定するモデルHESANSの開発を完了して。本モデルはすでにインターネット等を介して一般に公開され実用化されている。一方、SIM-COSMと名づけられた第２のモデルは、下記の第３サブグループとの協力のもとに、制御実験生態系（マイクロコスム）をコンピュータ上でシミュレートするものである。本モデルは、実験生態系の構成要素である微生物の増殖に非線型カイネティクスを導入したユニークなモデルであり、構成微生物相の増殖、生育、加齢などを模擬し、さらに、各種の有害物質（因子）への反応を的確に予測・模擬できるものである。本システムは、現在も実用化に向けて開発を続けており、実用化された折には、いわゆる「コンピュータ安全性試験」を可能にする画期的なものとなることが期待されている。

第２サブグループは、環境中の有害物質のレベルや挙動を評価するための基礎として、長半減期放射性核種や微量元素の分析法に関する研究を行なった。その結果、誘導電導プラズマ発光分析装置や、誘導電導プラズマ質量分析装置、イオンクロマトグラフィーなどの先端的分析装置を活用することにより、50 元素をこえる非常に多数の元素を高精度に安定して定量する手法の開発、改良に成功した。この方法を用いて、土壌や植物、菌類などの環境サンプル、ならびに実験動物の臓器などの元素分析を行い、本邦における環境中での長半減期放射性物質や微量元素の濃度を確定した。また、放射性ヨウ素や放射性セシウムの森林生態系における動態、環境中における $^{240}Pu/^{239}Pu$ 比の決定、放射性トレーサを用いた植物―土壌間の移行係数などについて研究を行なった。

第３サブグループは環境有害物質の影響やリスクを放射線との比較により評価できる制御実験生態系の確立とその利用に焦点をあてた研究を実施した。水生微生物生態系の一つであるマイコロコズムをこの目的のために導入し、種々の改良を行なった、その結果、生産者として藻類、消費者としてプロトゾア、分解者として大腸菌を使用したマイクロコズムの確立に成功し、これを用いてγ線や他の環境有害物質・因子（紫外線、酸性状態、Gd^{3+}, Cu^{2+}, Mn^{2+}, Ni^{2+} and Al^{3+}などの金属イオン）が生態系に及ぼす毒性の評価を行なった。その結果、本マイクロコズムは生態系に対する毒性を比較するための、これまでにない、すぐれた手法であることが判明した。

第４サブグループは比較毒性学の観点から放射線と環境有害物質の影響に関する研究を実施した。その結果、亜ヒ酸（砒素の酸化物）などの環境有害物質が放射線誘発DNA鎖切断の修復を阻害することを見出した。この知見は、放射線と環境有害物質の複合的な効果のメカニズムとして重要である。また、本サブグループでは、先端科学技術産業で広く使われ始めているガドリニウムの毒性について研究を行い、その細胞毒性には動物種差が認められること、Pu などの放射性物質に混合して吸入摂取されると、放射性物質の体内動態が大きく修飾されることを見出している。

このように、本研究グループは当研究所としては初めて生物・環境・安全解析関連研究者の統合により結成された研究グループであり、放射線（放射性物質）を環境有害物質の１つであるととらえ、他の環境有害物質も視野に入れて広く環境安全に関する研究を行なってきた。その結果、以下に示すように各サブグループにおいて当初の目標を達成する成果を得ただけでなく、相互の協力により環境科学、生態学において重要な知見を得、関連する分野の国際的な雑誌に発表することができた。

（グループリーダ、総合研究官、中村裕二）

1. Summary

We are now continuously exposed to a variety of environmental toxicants that are released from developing technology and industry. The style of exposures become complex and the combined effect of toxicants is concerned. This research group was established in 1996 by researchers gathering from environmental, risk analytical and biological fields, in order to investigate the comparative risk evaluation of radiation and other environmental toxicants.

The main subject of this group was, therefore, "Standardization of the perception of environmental and biological effects of radiation and other environmental toxicants". In the first two years, we concentrated our efforts to develop necessary methods, and then remaining 3 years were used for the comparative studies of radiation (radioactive nuclides) and environmental toxicants (especially heavy metals and rare earth elements). For efficient operation, the group was divided into 4 subgroups: 1) subgroup for mathematical model development, 2) subgroup studying the movement and kinetics of toxicants, 3) subgroup for developing a artificially controlled ecosystem, and 4) subgroup for comparative toxicology. These subgroups maintained tight cooperation, and obtained excellent research outcome described as followings.

The first sub-group, methodology development section, tried to develop the theoretical and mathematical models which could estimate the behavior of environmental toxicants and their biological and environmental impacts. Two kinds of models were developed; the first is a health risk estimation model, and another is computer simulation model of experimental exosystem. The first one, named HESANS (Health and Environment Safety Analysis Network System) is developed to estimate the health risk of radiation exposure to the population, and is now available through Internet as an interactive risk communication source. The second, named SIM-COSM, is also a computer model, and was developed to simulate the controlled microbial ecosystem (Microcosm), which was developed and used experimentally by the third sub-group. This model adopts the non-linear population dynamics of organisms in Microcosm, and well mimics the growth, foraging, maintenance, reproduction and death of microorganisms in the systems.

The second subgroup developed analytical methods for long-lived radionuclides and trace elements to obtain fundamental data on the levels and behavior of toxic substances in the environment, and established analytical methods using advanced instruments such as ICP-MS, ICP-AES, XRF and Ion-chromatography. This method allowed to analyze quantitatively more than 50 elements in variety of environmental samples (e.g. soil, plants, fungi, water) collected from different places in Japan. This subgroup also studied on the distribution and circulation of radiocesium and stable cesium in the forest ecosytem, the $^{240}Pu/^{239}Pu$ atom ratios in several soil samples collected in Japan and other countries, and soil-to-plants transfer factors of Cs, Sr, I, Co, Zn, Mn and Ce for several agricultural crops using radiotracer method.

The third sub-group concentrated their effort to construct controlled experimental ecosystems applicable for evaluating the effects and risks of environmental toxicants in comparison with radiation. One of aquatic microbial ecosystems, Microcosm, was introduced and improved for this purpose. The microcosm consisting of flagellate algae as a producer, ciliate protozoa as a consumer, and bacteria as a decomposer, was established and used for evaluating the ecotoxicity of radiation (γ -rays) and some other toxicants (ultraviolet radiation, acidification and metal ions such as Gd^{3+}, Cu^{2+}, Mn^{2+}, Ni^{2+} and Al^{3+}). The results indicate that Microcosm used here is a novel, unique and useful method for the comparison of toxicity to ecosystem.

The forth subgroup carried out the studies on the effects of radiation and environmental toxicants with respect to the comparative toxicology. They found that environmental toxicants such as arsenite (dioxide of arsenic) interfere with the repair of DNA double-strand breaks induced by gamma irradiation. The toxicity of gadolinium (Gd) was also investigated, since this elements began using widely in the advanced industry but its toxicity was not well known. It was demonstrated that cytotoxicity of Gd was remarkably high in mouse alveolar macrophages than in rat alveolar macrophages, and that this species differences may be attributable to the solubility of Gd hydoodxide in the phagolysosome. The administration of Gd also affects the metabolism of plutonium (Pu) in rat lung. Since the Gd is widely used as neutron absorber in the reprocessing of nuclear fuel, this finding is very important to estimate the combined effect of alpha radiation (Pu) and Gd.

As described above, this research group obtained a number of important findings with respect to the kinetics and effects of radioactive substances and environmental toxicant.

(Written by Group leader, Dr. Y. Nakamura)

第１サブグループ：

数学モデルによる環境動態・生物影響評価に関する研究

中村裕二、土居雅広、坂下哲哉

Model for Risk Estimation of Environmental and Biological Impacts of Radiation and Toxic Agents

Yuji Nakamura, Masahiro Doi and Tetsuya Sakashita (Methodology Development Section)

Abstract

The scope of this study is to develop the theoretical and mathematical models which could estimate the behavior of environmental toxicants and their biological and environmental impacts. To estimate the health risk of radiation exposure to the population, HESANS (Health and Environment Safety Analysis Network System) is developed by featuring updated risk projection models recommended by radiation protection authorities and national vital statistics. HESANS is open for the society through internet as an interactive risk communication source.

To know the mechanism of symbiotic ecology, controlled microbial ecosystem (Microcosm) is reproduced virtually in the computer as a Simulated Model Ecosystem (SIM-COSM). SIM-COSM is a kind of cell automata to regard each microbe as a "particle" wearing demographic parameters, and their living environment is divided by the lattice into the small square "patch". Particles show growth, foraging, maintenance, reproduction and death by changing their living environment and themselves interactively. The non-linear population dynamics of the particles cause the demographic and environmental stochasticities, which are studied theoretically to know the universal index of ecological hazard to compare the impacts of environmental toxicants mutually. Outcomes of these theoretical modeling and simulation are returned as a reference to the experimental Microcosm researches.

１．研究の目的

放射性物質（放射線）による生物・ヒトへの影響評価研究は、線量の概念、定義や線量　応答が比較的明瞭であり、低線量域から高線量域にわたって多くの知見が蓄積されてきた。これら放射性物質（放射線）の環境動態・生物影響評価を規準として、化学物質等の放射線以外の環境有害物質の環境負荷および生体影響を包括する影響及びリスクを評価する数学モデルを構築し、様々なエネルギー生産技術や科学技術のリスク（影響）の比較評価手法を開発することが本研究の目的である。

２．研究の方法

(b) 基礎情報データベースの整備と環境移行・発がんリスク推定システムの開発

放射性物質（放射線）の環境動態・生物影響評価の基礎となる情報収集・解析として、軽水炉の運用に伴う主要な放射性物質の動態パラメータ、人口動態統計データ、日本人の臓器重量に関する統計データ、等をデータベース化した。これら基礎情報データベースは、インターネットに接続したコンピュータにより操作できる計算機システム（環境・健康影響評価ネットワーク・システム、以下HESANS）に組み入れた。HESANSでは、わが国の軽水炉立地の安全評価指針に準拠した環境移行評価・住民等への外部放射線や食品摂取等の経路での内部放射線被ばくによる線量評価モジュール、国連科学委員会（UNSCEAR）、国際放射線防護委員会（ICRP）、米国原子力規制委員会（NUREG）、米国科学アカデミー・電離放射線の健康影響に関する検討委員会(BEIR)等が提案しているリスク推定モデルにより、様々な条件（被ばく線量・線量率、被ばく形態、被ばく時年齢、等）における健康影響リスク（発がん・遺伝的影響等の確率的影響の誘発リスク）を推定するモジュールを開発した。又、JAVA等のHTML技術によりインターネットに接続しているコンピュータから計算条件を入力し、web上で計算結果を得られるネットワーク・システムを開発した。

先端科学技術に伴う環境有害物質として、エネルギー、半導体関連の環境有害物質であるガドリニウム等の希土類元素と重金属元素について早期影響(半致死用量LD50)、晩発影響の発現に関するリスク情報をデータベース化した。

2-2　屋内ラドンによる肺がんリスク推定モデルの開発

公衆の放射線被ばく源として寄与の大きい家屋内ラドンの健康影響については、上述の主要なリスク推定モデルでは、米国等のウラン坑夫の疫学調査（コホート研究）に基づいて家屋内ラドン（Rn-222 ）の肺がん誘発リスクを推定している。しかし、坑道内作業環境と居住家屋内環境は大きく異なることから、スウェーデン国立放射線防護研究所とカロリンスカ医科大学環境医学研究所が共同で実施した「家屋内ラドンと肺がんに関する疫学調査（患者対照研究）」結果を基に、スウェーデンとの国際共同研究としてリスク推定モデルを開発した。1961年から1992年までのスウェーデン、日本の人口動態統計データを基礎データとしてデータベース化し、国別、時代別に実環境ラドンによる肺がん生涯リスクを比較解析した。

2-3　モデル実験生態系（マイクロコズム）の計算機シミュレーションコード（SIM-COSM）の開発

実環境生態系は、生物相、環境要因が複雑に入り組んでおり、環境負荷因子の影響は、実環境調査研究では、定性的に推定できるとしても、定量的に把握することは困難である。低線量放射線等の低用量の環境有害物質が環境生態系に与える負荷の機序を定量的に見いだすため、3種微生物で構成される水系制御実験生態系（マイクロコズム）を用いた環境負荷実験[1,2]が成果を挙げつつある。この実験モデル生態系（マイクロコズム）をひな形とし、個体ベースモデルを用いたオブジェクト指向型の並列計算シミュレーション・モデル（SIM-COSM）を開発し、生態系影響の数理解析を行った。プログラミング言語には、Uri Wilensky 教授（現在、米 North-eastern 大学）が、米マサチューセッツ工科大学メディア研究所において開発され、インターネットで無償公開されている StarlogoT を用いた（http://ccl.northwestern.edu/cm/）。

3．成果の概要

3-1　健康環境影響評価ネットワーク・システム

健康環境影響評価ネットワーク・システム（Health and Environmental Safety Analysis Network System: HESANS）は、インターネットの web サイトを構築する一連の HTML ページで構成されている。インターネットに接続した端末コンピュータから、ホームページのアドレスを閲覧すると、JAVA によって各種計算条件等の入力を求められ、インターフェースの指示に沿って、設定を進めていくと、web サイトのサーバー側で計算処理が行われ、結果が、端末コンピュータに引き渡され、図表として出力される。

HESANS の環境移行・線量評価モジュールは、緊急時被ばく評価、平常時被ばく評価、ライブラリ（核種、農作物、畜産物、家畜、臓器に関する各種パラメータ）のサブモジュールで構成されている。平常時被ばく評価・線量評価サブモジュールの初期入力画面を Fig. 1-(a)に示す。放射性物質放出位置の緯度経度、計算対象（大気中濃度、地表沈着濃度、内部被ばく線量（呼吸・食物）、外部被ばく線量（大気浮遊塵・地表沈着））から選択できる。

気象条件、放出源条件、放出核種等の設定画面を Fig. 1-(b)に示す。放出点の地上高、排気筒内径、排気速度、近隣の高層建築物の影響補正データ（建物高さ、床面積）、放出核種の設定、風向、卓越風向頻度、風速、大気安定度、降水量、降水割合、大気混合層高度等、気象データが設定される。

被ばく計算の条件設定画面を Fig. 1-(c) に示す。個人線量又は集団線量の選択、風による地表核種の再浮遊、飼料作物への土壌の付着、食品調理による核種の除去、土壌からの核種の洗出しによる除去、等、計算サブモジュールを含めるかどうかの選択、ライブラリ（核種、農作物、畜産物、家畜、臓器に関する各種パラメータ）のカスタマイズを行うことができる。

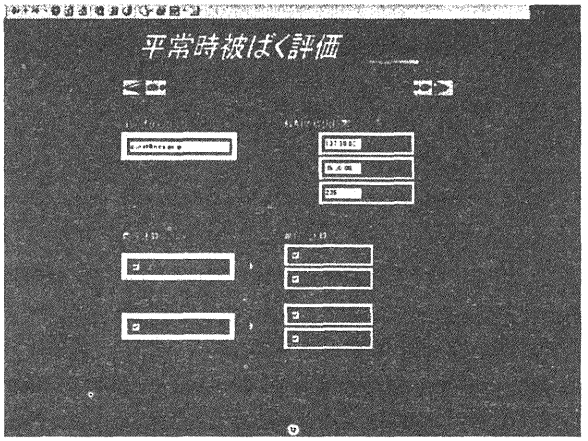

(a) home page : selection of exposure pathway

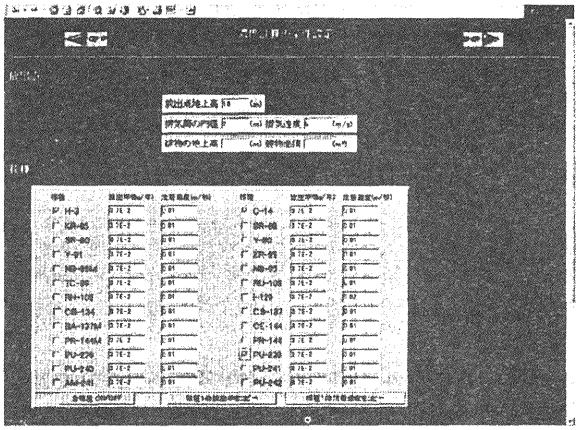

(b) setting of meteorological parameters and nuclides

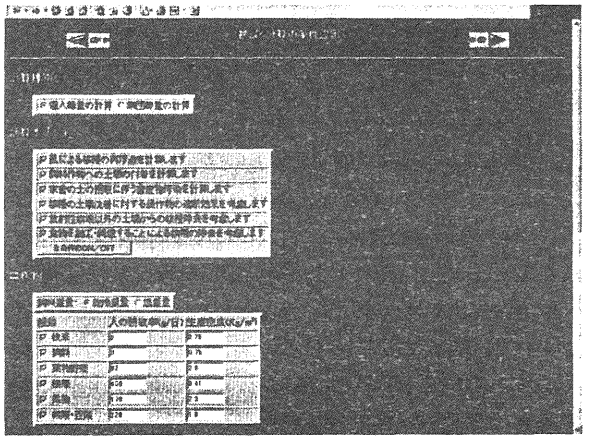

(c) setting of demographic parameters

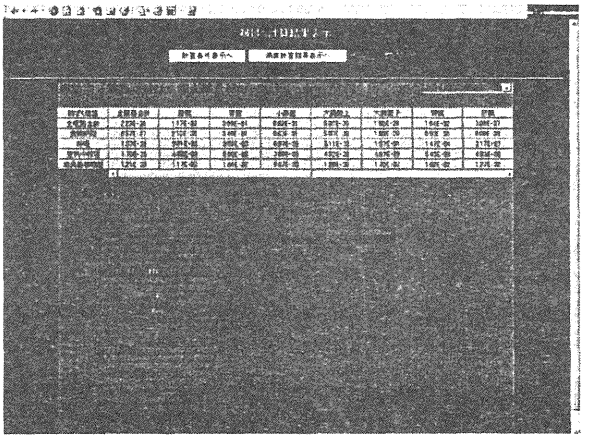

(d)　report of effective dose and organ dose

Fig.1　Environmental transfer and dose estimation modules of HESANS

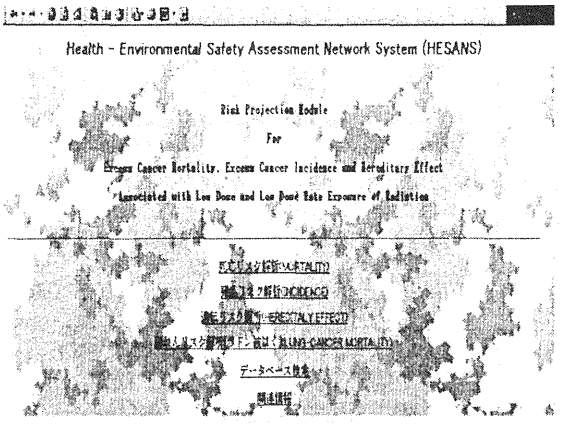

(a) home: selection of the health effect for projection

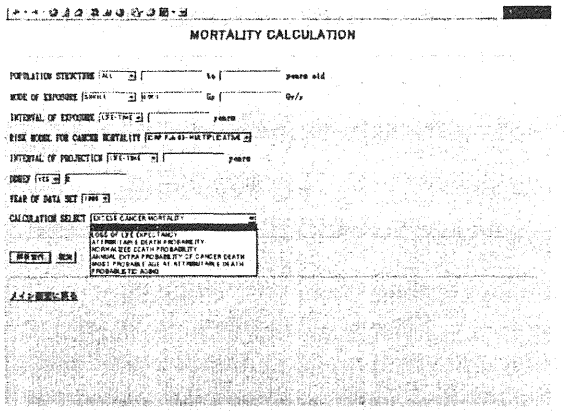

(b) selection of the risk model and parameter setting

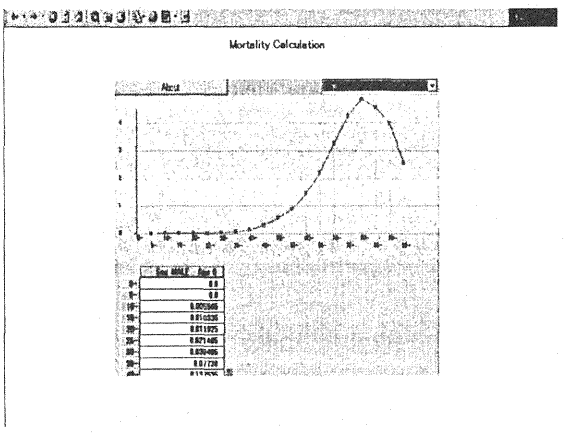

(c) Output :Excess lifetime risk of solid tumors by Age

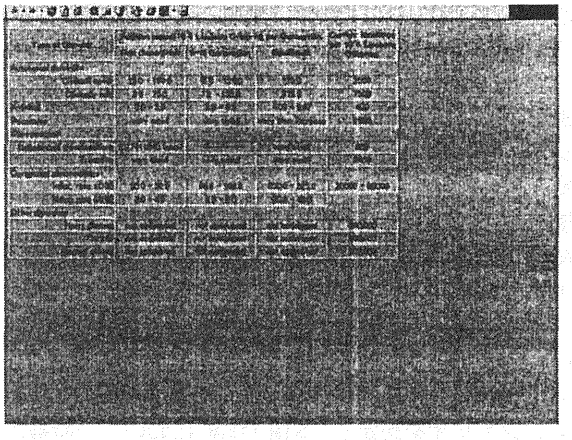

(d) Output :Excess risk of hereditary effects

Fig.2 Health risk projection module of HESANS

計算結果は、放射性物質の大気中濃度、地表沈着濃度については地図に重ね合わせた分布図として表示され、各被ばく経路（内部被ばく線量（呼吸・食物）、外部被ばく線量（大気浮遊塵・地表沈着））毎の臓器線量計算結果については、一覧表として表示される。臓器線量の出力例をFig. 1-(d)に示す。

HESANS の健康影響評価モジュールの初期設定画面をFig. 2-(a)に示す。解析するリスクは、死亡（致死がん）リスク、発がんリスク（非致死がんを含む）、遺伝リスク、家屋内ラドン肺がんリスクから選択する。モデル計算のデータベースもここから検索でき、年齢別死亡率、人口統計（年齢別、病症別）、臓器別がん死亡率（年齢別）、肺がん死亡率（年齢別、国別（日本、スウェーデン、米国））、平均寿命（国別（日本、スウェーデン、米国））について、1961 年から 1992 年について整備されている。

致死がんリスクを推定するサブモジュールの設定画面を Fig. 2-(b)に示す。リスク推定モデルは、(財) 放射線影響研究所（相加・相乗）モデル、国連科学委員会 1988 年報告書（相加・相乗）モデル、国際放射線防護委員会 1990 年勧告（相加・相乗）モデル、米国原子力規制委員会（NUREG）モデル、米国科学アカデミー・電離放射線の健康影響に関する検討委員会（BEIR-V）モデルのなかから選択できる。リスクを推定する対象集団の年齢構成(国別)、被ばく態様（一回・連続被ばくの別、被ばく期間）、リスク推定期間（生涯リスク、特定期間リスク）、の選択、および線量・線量率効果係数（DDREF）が設定できるようになっている。リスク推定結果は、年齢別過剰致死がん確率として、図と表で示されるようになっている(Fig. 2-(c))。

遺伝的リスクは、国連科学委員会 1988 年報告書において示された倍加線量法により推定・評価することができる。その結果は、遺伝疾患毎に一覧表で示されるようになっている（Fig. 2-(d)）。

3-2 屋内ラドンによる肺がんリスク推定モデル

スウェーデン家屋内ラドンと肺がんに関する疫学調査（患者対照研究）結果を基に、スウェーデンとの国際共同研究として肺がんリスク推定モデル(二種類)を開発した。1961 年から 1992 年までのスウェーデン、日本の人口動態統計データから対象とする国と年代を選択し、ラドン濃度、平衡定数（通常は 0.4）、居住係数（通常は 0.8）を設定して、実環境ラドンによる肺がん生涯リスクを推定できる。又このモデルから単位ラドン平衡等価濃度（WLM）あたりの実効線量換算係数は 2.05-13.5 mSv と推定され、従来の疫学的アプローチによる換算係数（3.88 mSv /WLM）と呼吸気道モデルによる換算係数（15 mSv/WLM）間との違いを範囲の中に含む結果となった。

HESANS は研究者仕様であり、正確な結果を得るには、放射性物質の環境動態及び放射線健康影響に関する知識が必要であり、今後、一般の利用者を想定したユーザーインターフェースの開発が望まれる。

3-3 SIM-COSMによる制御微生物生態系個体群に対する放射線の効果解析

3種微生物で構成される制御微生物生態系（マイクロコズム）を基に、個体ベースモデリング手法を用いて、計算機上に生態系をシミュレーションするコード（SIM-COSM）の概念をFig. 3に示す。各微生物個体毎の人口動態学的パラメータ、増殖-拡散モデル、探餌行動モデル、各個体毎のエネルギー収支動態モデルにより、SIM-COSMにおけるシミュレーション計算結果は、培養初期（50日以内）の各微生物種の個体群動態を追従し、生物群の種内・種間相互作用および生物群と環境との相互作用をおおむね説明するものとなった（Fig. 4）。長期培養における生物群の種内・種間相互作用および生物群と環境との相互作用については、参照とする実験データが乏しく、今後の検討課題である。

γ線照射による制御微生物生態系（マイクロコズム）負荷のシミュレーションでは、各生物種の半数致死線量（細胞増殖死をもって害の指標とする）から、各生物種個体への直接影響（放射線にヒットした場合の致死）を確率論的な負荷として計算機モデルに与え、個体数の一時的で急激な変化後の個体群動態を推定した。テトラヒメナの半致死線量 4000 Gy、ユーグレナ 330 - 170 Gy、大腸菌 50 Gy（37%生残時）であることから、大腸菌の生存曲線で校正した致死的負荷（100 Gy、500Gy相当）を培養30日後に付与するシナリオを想定し、SIM-COSMにおいて一時被ばくによる各生物種の個体群動態を観察した。100 Gyと500Gyのγ線照射マイクロコズム実験と、SIM-COSMによるγ線負荷シミュレーション実験の結果との比較をFig. 5-(a)及びFig. 5-(b)に示す。Fig. 5-(b)では、大腸菌を捕食する従属栄養原生動物であるはずのテトラヒメナが、γ線による大腸菌絶滅後にも200日以上生存する実験結果が示されており、SIM-COSMによる予測（被ばく後40日程度で絶滅）と大きく異なっている。テトラヒメナが環

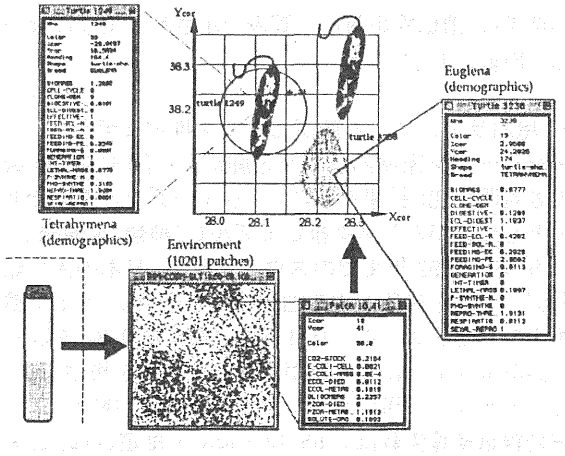

Fig.3 Schematic figure of the SIM-COSM concept as a object-oriented parallel base model, of which program code is developed with StarlogoT, an object-based parallel modeling languages (OBPML), developed and distributed by Professor Uri Wilensky, Center for Connected Learning and Computer-Based modeling, North-eastern University, of which web address is http://ccl.northwestern.edu/cm/.

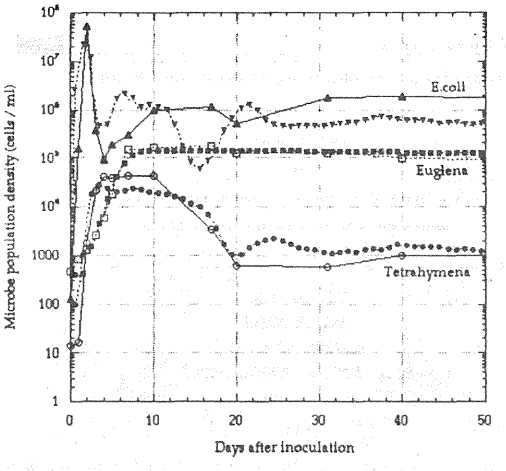

Fig.4 Population dynamics of Microcosm (Fuma et al.) and projection by SIM-COSM

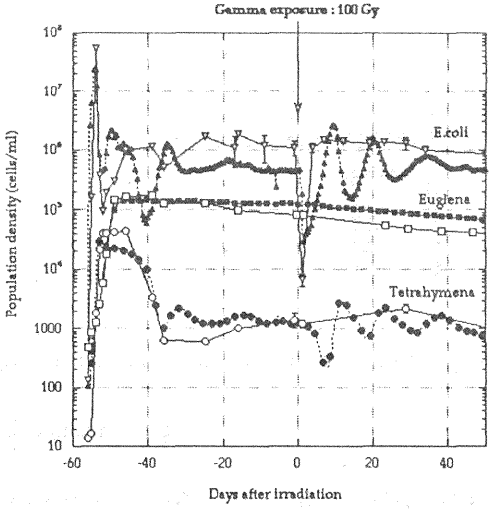

(a) γ-exposure : 100 Gy at 30 days after inoculation

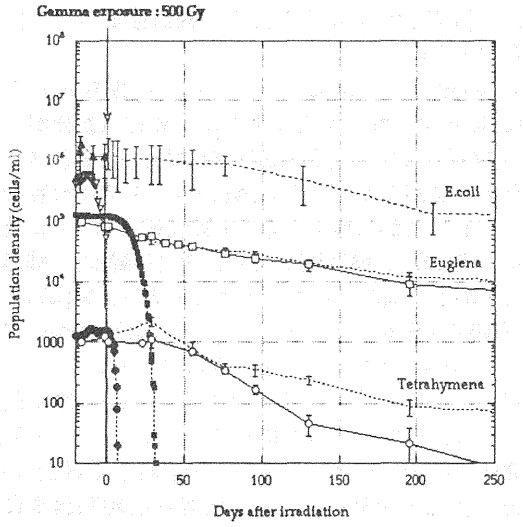

(b) γ-exposure : 500 Gy at 30 days after inoculation

Fig.5 Dose response of simulated microbes by SIM-COSM (●Tetrahymena、■Euglena、▲E.coli) and real microbes in Microcosm by Fuma et. al (○Tetrahymena、□Euglena、▽E.coli)

境の急激な変化、特に大腸菌個体数の一時的減少（Fig. 5-(a)）、又は絶滅（Fig. 5-(b)）に対応して、何らかの適応をしていることが示唆される。具体的には、従来は餌として利用しない死骸分解有機物や代謝産物等の捕食や、摂取エネルギー量との収支で代謝エネルギー量（maintenance cost）を生命維持に必要な最低限まで切り詰める、等の調整機構の存在が推測される。環境負荷因子に対する生態系システムとしての適応的なふるまいとその機序を明らかにするため、様々な計算条件においてシミュレーションを繰り返し、比較解析していくことが、今後の検討課題である。

放射線照射や他の環境有害物質の照射が、各生物種個体にとって致死的に作用しない低線量（用量）域の照射であっても、生理学的・人口動態学的な因子に影響を及ぼすことも考えられる。特に、この微生物生態系では、唯一の独立栄養原生動物であるユーグレナの光合成によって光エネルギーが利用されるため、この光合成の能率が放射線等の環境有害因子によって阻害（又は亢進）される場合には、生態系全体のエネルギーの流れ（フロー）に影響を与えることが予想される。

このような観点から、脂質分析・安定同位体比分析等を用いて、ユーグレナの光合成活性への放射線等環境有害物質の負荷に関する実験研究を実施し、線量（用量）効果関係を得た（流動促進研究、平成 10 年度　12 年度）。環境負荷因子が生態系のバランスを撹乱する因子の一つとして、今後、計算機モデルへの組み込みを検討している。

［参考文献］

1) Kawabata, Z. et al. : Synthesis of a Species-Defined Microcosm with Protozoa, J. Protozool. Research, 5, 23-26, 1985
2) Fuma et.al. : Effects of γ-rays on the populations of the steady-state ecological microcosm, Int.J.Radiat.Biology, 74 (1), 145-150, 1998.

［研究発表］

1) T. Sakashita,et al. ; Effects of atmospheric transport on temporal variations of 222Rn and its progeny concentration in the atmosphere, J. Nucl. Sci. and Technol., 34, 63-72 ,1998
2) M. Doi, F. Lagarde, R. Falk, G.A. Swedjemark.: Annual effective dose due to residential radon progeny in Sweden –evaluations based on current risk projection models and or risk estimates from a nationwide Swedish Epidemiological Study, 1-128, ISSN 0282-4434, Stockholm ,1996
3) M. Doi, S. Kobayashi : Surveys of concentration of radon isotopes in indoor and outdoor air in Japan, Environment International, 22, 649-655, 1996.
4) M. Doi, R. Falk, I. Ostergen: Intercomparison of passive radon dosimeters developed by NIRS (Japan) and SSI (Sweden), World Scientific, 39-44, ISBN-981-02-3443-0 Singapore, 1998.
5) M.Doi, Y. Nakamura, N.Ogiu, F.Lagarde, R.falk, G.A. Swedjemark: Effective dose doe to exposure to radon progeny for Swedish and Japanese Populations : An epidemiological approach, Radiation Research, 152, 166, 1999.
6) 土居雅広、中村裕二: BEIR VI にみるラドン影響の考え方、NIRS-M-140, 1343-0769, pp156-167, 2000
7) M. Doi, S. Fuma, T. Sakashita, H. Takeda, K. Miyamoto, Y. Nakamura, Z. Kawabata, Computer simulation of a Microorganic Ecology as a Self-sustaining System of Complexity, 4th International meeting on Theory and mathematics in Biology and Medicine, 152-153, Amsterdam, June, 1999.
8) 坂下、村上、飯田、池辺：クロスオーバー研究シンポジウム「放射性物質の環境移行研究の新たな展開」報告集、JAERI-conf 99-001, 119-134 , 1999.
9) M. Doi, S. Fuma, T. Sakashita, H. Takeda, K. Miyamoto, K. Yanagisawa, Y. Nakamura, Z. Kawabata, Ecological Impacts of Environmental Toxicants and radiation on the Microbial Ecosystem: A Model Simulation of Computational Microbiology, Proceedings of 10th International Congress of the International Radiation Protection,T-1-4,1-10, Hiroshima, 2000.
10) M.Doi, T. Sakashita, Y. Nakamura, N.Ogiu, F.Lagarde, R.falk, "Lifetime risk of Lung Cancer Due to Radon Exposure Projected to Japanese and Swedish populations, Health Physics , 80(6), 552-562, 2001.
11) 土居雅広、米原英典、甲斐倫明、緒方裕光：種々の分野のリスク概念に関する歴史的経緯と最近の動向，保健物理, 35(4), 421-433, 2000.

［口頭発表］

1) 坂下、藤高、井上、宮本、松本：第 26 回放医研環境セミナー、千葉、1998.
2) 土居、中村：閉鎖系マイクロコズムにおける環境と生物との相互作用に関するコンピュータシミュレーション、日本保健物理学会第 33 回研究発表会、浜松、1998
3) 土居、府馬、坂下、宮本、武田、中村、川端：確率的相互作用モデルによる制御実験生態系シミュレーション、日本生態学会第 46 回研究発表会、1999
4) M. Doi, S. Fuma, T. Sakashita, H. Takeda, K. Miyamoto, Y. Nakamura, Z. Kawabata, Computer simulation of a Microorganic Ecology as a Self-sustaining System of Complexity, 4th International meeting on Theory and mathematics in Biology and Medicine,Amsterdam, June, 1999.
5) 土居、府馬、坂下、宮本、武田、中村、川端：放射線の微生物生態系への影響に関するコンピュータ・シミュレーション、日本保健物理学会第 33 回研究発表会、大分、1999
6) 土居、府馬、坂下、宮本、武田、中村、川端:微生物制御実験生態系における個体群動態の環境負荷への応答特性モデル、第 9 回数理生物学シンポジウム、1999
7) 土居、府馬、坂下、宮本、武田、中村、川端：微生物生態系への放射線照射における環境負荷の計算機シミュレーション、日本生態学会第 47 回研究発表会、2000
8) 土居、府馬、坂下、宮本、武田、中村、川端：数理モデルによる放射線生態影響の計算機実験解析、日本放射線影響学会第 43 回研究発表会、2000
9) Sakashita, et al. :2nd International Conference on Applications of Stable IsotopeTechniques to Ecological Studies, Germany, Braunshcuweig, 2000.
10) 坂下、土居、中村、佐藤、山根、石井、府馬、武田、宮本、柳澤：ユーグレナ研究会第１６回研究発表会、岡山、2000. 11.

11) 坂下、土居、中村、石井、府馬、武田、宮本、柳沢：
日本微生物生態学会第１６回研究発表会、土浦、2000.

第２サブグループ：

微量成分の環境挙動解析に関する研究

村松康行、内田滋夫、吉田聡、坂内忠明、田上恵子

Analysis of the distribution and behavior of toxic and of tracer elements in the environment

Yasuyuki Muramatsu, Shigeo Uchida, Satoshi Yoshida, Tadaaki Ban-nai and Keiko Tagami

Abstract

In order to assess the levels and behavior of toxic substances in the environment, analytical methods for long-lived radionuclides and trace elements have been developed. Special attention is paid to the elements such as Pu, U, Th, Tc, Cs, Sr, I, Co, Cr, Cu, Mn, Zn and lanthanoid. Analytical methods mainly used were ICP-MS, ICP-AES, XRF and Ion-chromatography. Several data for these elements (nuclides) in variety of environmental samples (e.g. soil, plants, fungi, water) have been obtained. For soil, about 50 elements were determined in ca. 100 samples collected from different places in Japan and useful information on the distribution of many elements in Japanese soils were obtained. High iodine concentrations are found in upland soils, particularly in Andosol, while concentrations in lowland soils were considerably lower. Results on the distribution of radiocesium and stable cesium indicate that ^{137}Cs entered into the forest ecosystem is circulating. New data on the $^{240}Pu/^{239}Pu$ atom ratios in several soil samples collected in Japan and other countries have been obtained. It was found that the ratios could be used in identifying the source of contamination. Radiotracer techniques were also applied to study the transfer of radionuclides in the environment. Soil-to-plants transfer factors of Cs, Sr, I, Co, Zn, Mn and Ce were investigated for several agricultural crops usually consumed in Japan.

１．研究目的

第２サブグループにおいては、エネルギー産業等に由来する微量成分である放射性物質、重金属元素、レアーメタル等の環境中での分布と挙動並びに人への移行を予測するための生物地球化学的研究を実施した。特に、最新の高感度分析法を用い、環境構成物質（土壌、植物、水、菌類、動物等）中に含まれる種々の放射性及び安定元素の濃度と分布を調べることに重点を置いた。

初期に立てた目標は次の通りである。

(a)環境試料中に含まれる種々の放射性及び安定元素（微量元素）の高感度で精度が良い分析法を確立する。

(b)各種の生態系を構成する物質（様々な土壌、植物、水、菌類、動物等）について種々の放射性及び微量元素の分析を行い、各系及びそれを構成する物質がもつ元素組成の特徴を明らかにする。

(c)環境（主として農耕地並びに森林）における放射性及び安定元素について移行とそのメカニズムを明らかにする。

２．研究成果

本グループ研究が始まる以前、我々は環境放射生態学研究部において放射性核種を対象とした研究を行っていた。放射性核種の分析法については、従来の古典的な方法に頼っている面が多かった為、検出感度が悪く、測定時間もかかった。また、分析対象は農作物に中心を置き、主として放射性核種の移行を調べていた。しかし、本研究グループにおいては、単に放射性核種だけでなく、多くの安定元素（有害元素も含む）も分析し、総合的に研究を進めた。多元素を対象としたのは以下の理由からである。(1) 放射性核種も元素の一つであり、その環境移行はそれぞれの元素の物理・化学的特性に従っていることから、様々な元素と比較することで環境挙動をより正確に解明できる。(2) 放射性核種の環境移行は共存する安定元素（同位体）の量に左右される為、安定元素の濃度を把握しておく事は不可欠である。(3) 放射性核種の環境中での濃度は非常に低く直接分析は難しい為、安定元素を調べる事により、予想もしていなかった放射性核種が環境中へ放出された場合でもその挙動予測に役立つと考えられる。

本グループ研究を通し、今までは限られた種類の放射性核種だけしかデータが得られなかったが、多元素を対象にする事により、環境挙動を解明する上で科学的な裏付けもでき、研究の幅も広がった。また、ICP-MS（誘導結合プラズマ質量分析法）を積極的に用いる事により、今まで正確な分析が難しかった、Pu（$^{240}Pu/^{239}Pu$ 比）、^{99}Tc、U（$^{235}U/^{238}U$ 比）などの分析法（同位体分析も含める）を確立でき、環境中におけるデータを出す事が可能になった。さらに、対象を農耕地だけでなく、我が国の国土の７割近くを占める森林にも広げられた為、異なる生態系においてデータを比較し、解析する事ができた。特に、日本の各地から採取した代表的な土壌について、約 50 種類の元素（U, Th など天然放射性元素も含む）の分析を行い、今までに無かったデータをだすことができた。

このように、測定が難しかった核種の分析手法を確立し、

多くの元素も含めた研究を実施したことから、海外の研究者からも注目され、来訪者も多く研究協力も積極的に進めた。また、原子力基盤研究や放射能調査研究とも部分的に関連をもたせ研究を実施した。更に、1997 年に起きた動燃東海の事故時においては、タスクフォースのメンバーとして住民への相談や環境のモニタリングなどで協力した。そして、1999 年の JCO 事故時においては３人の被ばく患者の放射能測定・線量評価や周辺環境のモニタリング等で協力した。

本グループ研究や関連する研究テーマで、第２サブグループの関係した５年間の論文数は、原著論文だけでも 50 報近くあり（ほぼ全部が欧文）、その他（報文集、解説、著書、報告書など）も数多く出すことができた。

以下に、これらに関連して、本グループ研究を通じて得られた研究成果を述べる。

2.1 安定元素及び放射性物質の高感度分析法の確立

ICP-MS（高周波誘導結合プラズマ質量分析法）は、最近で最も進化した多元素同時分析法と言えるであろう。特に検出感度に優れ 1ppt (1pg/ml) 以下の測定も可能となった。我々はグループ研究に入る少し前からこの装置（四重極型）を環境試料の分析に本格的に応用しはじめた。グループ研究においては、ICP-MS の他にも、ICP-AES（高周波誘導結合プラズマ発光分析法）、イオンクロマトグラフ分析法、蛍光エックス線分析法、ガンマ線スペクトロメトリー等を用いた分析法を検討した。ここでは、主として ICP-MS に関する分析法に関する研究成果をまとめる。

2.1.1 多元素分析法

ICP-MS は元々半導体産業などで用いられたため、ここではまず環境分析への応用、つまり環境試料中の多元素の ICP-MS を用いた分析法を検討した。ICP-MS で測定するためには、水試料を除き、まず試料を溶液としなければならない。また、共存元素の影響や測定時の感度の変化（ドリフトなど）についても、試料の種類ごとに調べる必要がある。

水試料については、0.22μm のメンブラン濾紙で濾過した後、硝酸（高純度硝酸、多摩化学 AA-100）を加え、３％溶液とした。（長期間保存するときは５％程度の硝酸溶液にしたほうが目的元素の濃度変化は少ない。）固体試料については、粉末状態にした試料（約 100mg）をテフロン容器に入れ、硝酸、ふっ化水素酸、過塩素酸を加え、マイクロウェーブオーブンで加熱分解した。酸の量は試料の種類により異なり、例えば土壌試料では、硝酸（7ml）、ふっ化水素酸（3ml）、過塩素酸（0.5ml）である。また、植物試料では、まず硝酸（7ml）とふっ化水素酸（1ml）を加えマイクロウェーブオーブンで加熱分解した後に過塩素酸（0.5ml）を加えた。それをホットプレート（ホットブロック）上で蒸発乾固した。次に、硝酸に溶かし、さらに希釈した。硝酸の濃度は３％とし、定容した。測定時のドリフトなどを補正するための内部標準として Bi, In, Rh（20ppb）を添加した。

測定には四重極型 ICP-MS(Yokogawa PMS- 2000)を用いた。検出下限値は、多くの元素で溶液中の値として 1 ppt（1 pg/ml）以下であった。この値は土壌中のこれらの元素を分析するのに十分な感度である。地質調査所が作成した JB-1, JG-1, JR-2, JA-2 等の比較標準物質を使用し分析の質を確かめたところ、保証値と大変良い一致を示した。

2.1.2 U, Th の分析法

自然界に存在する U の同位体は ^{238}U（半減期：4.47x10^{9}年，存在比：99.2745％），^{235}U（半減期：7.04x10^{8}年，存在比：0.720％），^{234}U（半減期：2.45x10^{5}年，存在比：0.0055％）である。また、Th の自然界に存在する同位体は ^{232}Th（半減期：1.405x10^{10}年、存在比：100％）である。

U と Th の分析法には、アルファ線測定法、娘核種のガンマ線を測定する方法、放射化分析法、比色法などがある。しかし、前処理法が煩雑であったり、検出感度に問題があったりして、低濃度の分析は簡単ではない。我々は ICP-MS（誘導結合プラズマ質量分析装置）を用いる環境試料の分析方法について検討し、感度及び精度に優れた分析手法を確立できた。ここでは、分析操作の概要を述べる。

土壌や植物試料については、酸で分解して溶液にする必要がある。そこで、上で述べた安定元素（多元素）分析の方法と同様に、粉末試料をテフロン容器に入れ、硝酸、ふっ化水素酸、過塩素酸を加え、マイクロウェーブオーブンで加熱分解した。それを、蒸発乾固した後、硝酸に溶かし試料溶液とした（硝酸の濃度は通常 2-3％）。内部標準としては、U, Th と質量数が近い Bi を添加した。

測定には主として四重極型 ICP-MS(Yokogawa PMS-2000、Agilent 7500)を用いたが、二重収束型ICP-MS (Finnigan MAT ELEMENT)も使用した。検出下限値は、U, Th で溶液中の値として 1 ppt（1 pg/ml）以下であった。この値は土壌や植物中のこれらの元素を分析するのに十分な感度である。地質調査所が作成した JB-1, JG-1, JR-2, JA-2 等の比較標準物質を使用し分析の質を確かめたところ、保証値と大変良い一致を示した。

ウランの３つの同位体組成（^{238}U, ^{235}U, ^{234}U）をより正確に測定するためには、上記のように全分解した試料溶液をそのまま測定にかけるのではなく、化学操作を行い U を分離し測定することが不可欠である。通常、その化学分離操作は煩雑で時間がかかる。そこで、抽出クロマトグラフ樹脂である TEVA レジンを用いウラン分離・濃縮法を検討した。試料溶液を 6M 塩酸に調整した後、TEVA レジン（ミニカラム充填済）に通水し U を吸着させた。6M 塩酸溶液によりレジンを洗浄して共存多量元素を除去した後、U を 0.1M 硝酸により溶離した。溶離として用いた 0.1M 硝酸溶液 30mL 中にほぼ 100%のウランが回収できることがわかった。このとき、ほとんどの共存多量元素や Th 等は試料通水中及び洗液中に流出しており U のフラクションに混入しなかった。溶離液中のウラン同位体比は ICP-MS で求めた。本実験では、溶離液中のウラン濃度は 10-70ppb の範囲であったが、このとき ^{234}U についても十分カウントを得ることができた。また、本法よるウランの定量及び同位体比の測定結果は、アルファ線スペクトロメトリーの結果とよく一致していた。

2.1.3 Pu の分析法

プルトニウムの同位体は質量数 232～246 まで知られている。その中でも環境汚染を考える上で重要なものは、^{238}Pu（半減期：87.7 年）、^{239}Pu（24100 年）、^{240}Pu（6570 年）と ^{241}Pu（14.4 年）である。特に ^{239}Pu と ^{240}Pu は存在量が多いため注目されている。

環境中における Pu の濃度と動態を調べることは、原子燃料サイクルに係わる環境安全評価を行う上で大変重要と考えられる。Pu の分析は主として、アルファースペクトロメトリー法により行われているが、環境濃度は非常に低いため、分析操作に時間と手間がかかる。また、スペクトロメトリー法では、^{239}Pu と ^{240}Pu はエネルギーが近いため分離測定は難しい。ICP-MS は通常安定元素の分析に用いられているが、検出感度に富んでいることから、長半減期核種の分析にも適していると考えられている。しかし、プルトニウムの分析に ICP-MS を応用した例は少なく、化学分離法についてもあまり述べられていなかったので、分離濃縮法と測定法を検討した。また、環境関連の比較標準物質中のプルトニウム同位体に関するデータは殆ど出されていないので、IAEA の比較標準物質中の分析データの ^{240}Pu/^{239}Pu 比の分析も行った。

サンプル量は、プルトニウム濃度が比較的高い試料（$^{239+240}$Pu 濃度で 10Bq/kg 以上）では 1～10g とし、ビーカーに入れ８Ｎ硝酸（５倍量以上）を加え、スパイクとして既知量の ^{242}Pu を添加した。また、プルトニウム濃度が低い試料（一般の環境試料）は 10g～50g と多くのサンプルが必要であったため、予め 500℃で加熱し、有機物を分解した。硝酸による抽出はホットプレート上で４～６時間行った。それを温かいうちにガラス濾紙で濾過した。この抽出操作を２回ほど繰り返し、濾液を一つのビーカーにまとめた。それを飴状になるまでホットプレート上で加熱し、その後、硝酸に溶かし分離操作を行った。

プルトニウムの化学分離は、イオン交換樹脂（Dowex 1x8）を用いる方法と、抽出クロマトグラフ樹脂（TEVA）を用いる方法の２つを比較した。Dowex 1x8 による分離では飴状になった試料に８Ｎの硝酸を加えて溶かした。また、TEVA による分離では２Ｎの硝酸に溶かした。どちらの樹脂を用いる場合でも Pu の化学形を４価にそろえなければならない。そこで、$NaNO_2$, $HONH_3Cl$ 並びに H_2O_2 の３種の試薬を用いて化学収率等を比較検討した。

化学形を４価に調整した後、試料溶液を Dowex 1x8 または TEVA に通すことにより Pu は樹脂に保持される。同濃度の酸を流して洗浄の後、Dowex 1x8 の場合は５%NH_4I-10M塩酸溶液を、TEVA の場合は 0.1Mハイドロキノン溶液-９M塩酸溶液を用いて保持された Pu を溶離した。溶離液をホットプレート上で一旦蒸発乾固した後硝酸に溶かし、最終的には４％硝酸溶液として、測定に供した。ICP-MS によって測定したピークは ^{239}Pu, ^{240}Pu 及び ^{242}Pu である。また、必要に応じて、Fe などのマトリックス元素の濃度も測った。ICP-MS による ^{239}Pu の測定では、質量数 239 のところに $^{238}UH^+$が妨害を及ぼす可能性がある。このため ^{238}U を測定して除染係数を調べた。内部標準としては Bi を添加したが、最終的な濃度計算は既知量加えた ^{242}Pu に対する ^{239}Pu と ^{240}Pu の比を用いる同位体希釈法で行った。また、測定値の信頼性は Pu の同位体比のスタンダードである NBS-947 を測定し確認した。

なお、Pu は核燃料物質でありたとえ極少量を使用する場合でも規制を受ける。そのため、予め使用許可を取った。

何種類かの試薬（$NaNO_2$, $HONH_3Cl$ 並びに H_2O_2）を用い Pu の化学形を４価に調整する条件を検討したところ、$NaNO_2$ を用いた場合が Dowex 1x8 と TEVA ともに最も良い結果が得られた。H_2O_2 を用いた場合が収率が悪く化学形を４価にするのに十分でないと考えられる。

U の除染係数は Dowex 1x8 でも TEVA を用いた場合でもともに 10^4～10^5 程度であった。また、多くのマトリックス元素において除染係数は 10^4～10^5 程度であり、ICP-MS の測定に適する範囲まで下げることができた。今回分析に供した土壌では、U については Dowex 1x8 のほうが良く、また、希土類元素や鉄の分離には TEVA のほうが良い傾向にあった。

本分析法による ^{239}Pu の検出下限値は、試料溶液中の濃度として、0.05 mBq/ml（または 0.02 ppt 程度）であった。実際の土壌では、試料 20g を用いた場合、^{239}Pu では 0.1Bq/kg（乾燥）程度まで測定可能であった。^{240}Pu の検出下限値は、試料溶液中の濃度として 0.17 mBq/ml、20g の試料を用いた場合は 0.35Bq/kg（乾燥）であった。^{240}Pu と ^{239}Pu の検出下限値に差があるのは、^{240}Pu の方が半減期が短く放射能濃度が高くなるためである。UH^+が ^{239}Pu の測定に及ぼす影響は、溶液中の U 濃度が 1 ppb のとき ^{239}Pu のピークへの影響は約 0.03 ppt に相当する値であった。これは、検出下限値とほぼ同程度であり、測定には影響しない。化学分離操作により測定溶液中の U 濃度を 1 ppb 以下にするのは通常の試料ではそれほど難しくはない。

IAEA が作成した種々の比較標準試料を分析した結果、推奨値としてあげられている $^{239+240}$Pu の値と良い一致を示した。分析例をあげると（カッコ内は IAEA の推奨値）、IAEA-Soil-6: 1.0 Bq/kg (1.0 Bq/kg) ; IAEA-135: 211 Bq/kg (213 Bq/kg); IAEA-367: 39.5 Bq/kg (38 Bq/kg); IAEA-368: 29.8 Bq/kg (31 Bq/kg)であった。Pu の同位体比（^{240}Pu /^{239}Pu 原子比）について得られた値は、アイリッシュ海の堆積物（IAEA-135）: 0.21、アイリッシュ海の魚（IAEA-134）: 0.20、マーシャル諸島の堆積物（IAEA-367）: 0.31、ムルロワ環礁の堆積物（IAEA-368）: 0.04、オーストリーの土壌（IAEA-SOIL-6）: 0.19 であった。比較標準試料中の ^{240}Pu /^{239}Pu 比に関する IAEA の推奨値は示されていないことから、これらの値は今後分析を行う上での一つの参考値として役立つと思われる。

今回の研究結果から、環境中の Pu の分析に ICP-MS 法は大変有効と考えられ、今後、環境安全研究やモニタリングへの応用も期待できる。また、^{240}Pu /^{239}Pu 比も測定できることから、Pu の汚染源の同定などにも利用可能である。

2.1.4 Tc の分析法

^{99}Tc（物理学的半減期：21 万年）は核分裂生成物の一つであり、環境中には核実験のフォールアウトを通じ加わっている。また、原子燃料サイクルを考えた場合、重要な

核種の一つとみなされている。しかし、分析法が難しく、環境でのデータは極限られたものしか得られていなかった。そこで、最初に、ICP-MS 法による分析法の開発を行うとともに、^{99}Tc の標準物質についても検討した。すなわち、^{99}Tc の環境標準物質がないことから、^{99}Tc の濃度レベルが低い一般の環境試料を定量した場合、その値の妥当性を比較することができなかった。そこで、環境標準物質として利用可能な IAEA 比較標準物質をいくつか選択し、それらの ^{99}Tc の定量を行い、^{99}Tc の環境標準物質としての利用の可能性について検討した。

開発した分析法を **Fig.1** に示す。概要は以下の通りである。試料をビーカーに分取し、トレーサーとして ^{95m}Tc（半減期 61 日）を添加した。次に試料を灰化（450℃, 2h）した後、4M 硝酸により Tc を加熱抽出した（90℃, 3h)。濾過後、濾液は硝酸濃度で約 0.1M になるように希釈調整し、約 200mL の溶液とした。この溶液を TEVA・Spec レジンを充填したミニカラム（Eichrom 社製）に通水し、Tc の分離を行った。このとき、Ru を含むほとんどの共存元素はカラムを通過するが、Tc はレジンに強く収着する。カラムを 2M硝酸溶液で洗浄後、5mL の 8M硝酸溶液により Tc を溶離した。溶離液は 80℃以下）で一旦ドライアップした。2%硝酸溶液により乾固物を溶解し、回収率は ^{95m}Tc 濃度をγ線測定（アロカ、ARC-380）により求め、さらに ICP-MS（PMS-2000）により ^{99}Tc の定量を行った。

本分析法による平均回収率は 71±18%であり満足のいくものであった。標準試料の測定結果は(A) IAEA-373（チェルノブイリの牧草）: 0.86±0.07 Bq/kg, (B) IAEA-375（チェルノブイリの土壌）: 0.25±0.02 Bq/kg , (C) IAEA-135（アイリッシュ海堆積土）: 9.6±0.5 Bq/kg であった。以前我々が測定した日本の水田土壌中における ^{99}Tc 濃度は 0.02 - 0.11 Bq/kg であったことから、これらの環境標準物質中の ^{99}Tc 濃度は一般的な環境中の ^{99}Tc 濃度レベルよりも高く、チェルノブイリ事故やセラフィールド施設の影響を受けていることが示唆された。以上の結果から、これらの物質は ^{99}Tc の濃度も充分であり均一性も良いため、^{99}Tc の分析のための比較標準物質として使える可能性が示唆された。

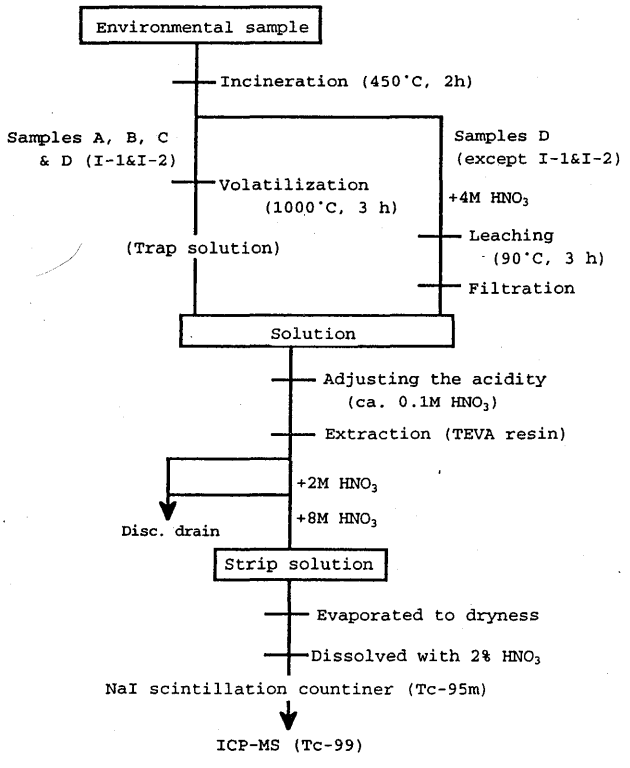

Fig. 1 Analytical method developed in the present study

また、本分析法を用いて、日本各地から 10 点の水田土壌を採取しそのフォールアウト ^{99}Tc 濃度を測定した。その結果、^{99}Tc 濃度は 6-110mBq/kg 乾土であった。この値を核分裂収率が同程度である ^{137}Cs の放射能濃度と比較すると、核分裂収率から得られる放射能濃度比、^{99}Tc/^{137}Cs は 2.16×10^{-4} であり、今回測定した土壌試料では 10^{-3} のオーダーであった。^{137}Cs が土壌に収着されやすい核種であることを考慮すると、得られた結果は、水田に降下・沈着したフォールアウト ^{99}Tc がほとんど表層土壌に蓄積されていることを示している。

2.2 生態系を構成する様々な物質における元素分布

2.2.1 土壌

土壌は環境の中で大変重要な働きを担っている。植物は土壌から養分を吸い、降水は土壌で浄化され地下へと流れていく。土壌中の元素の濃度に関しては、今まで主として土壌肥料学や植物栄養学の見地から研究されてきた。そのため、植物の生長に関係したような N, P, K, Fe, Ca, Mn, Zn などが中心で多くの微量元素に関するデータは限られている。そこで我々は ICP-MS 及び ICP-AES（発光分析法）を用い日本の代表的な土壌中の様々な元素を分析し、50 以上の元素についての分析値が得られた。

Fig.2 に本研究で得られた約 100 試料の土壌中の元素濃度の平均値を原子番号順にプロットした。（主要元素である Si や S はこの方法では測定されないので除いたが、C と N は他の方法で測定した。）この図より、土壌中に１％（10000ppm)程度またはそれ以上存在する元素は、Al, Fe, C, K, Ca, Mg, Na, (Si) であった。原子番号が隣り合う元素は、偶数番号の方が奇数番号よりも濃度が高い傾向が見られた。土壌の種類によっても濃度に差がある。例えば、U, Th, 軽希土類元素（La, Ce 等）などは西日本に特徴的な黄色土に高い。これは黄色土は花崗岩を母材としており、それの化学的特性を反映しているためである。黒ボク土では V, Co, Zn, Lu, Yb, Mo が高く、Rb, Cs, Ba, Tl, Th が低い傾向にあった。灰色低地土の元素濃度は多くの元素で全体の平均値とほぼ同じか少し高めであった。

土壌は地殻の岩石や堆積物が母材となり、それが風化作用を受け、さらに生物の作用により有機物が加わり生成したものである。そこで、我々が求めた土壌の化学組成を地殻の平均的な化学組成と比較してみると、土壌はNa, Mg, K, Ca, Rb, Sr 等の濃度が低い。これらの元素は風化作用により溶け出ていったものと考えられる。一方、Ti, Mn, Zn, Gd, Ta, Pb などは逆に土壌の方が少し高めであり、これらの元素は風化作用を受けてもそれほど減少しないと推定される。

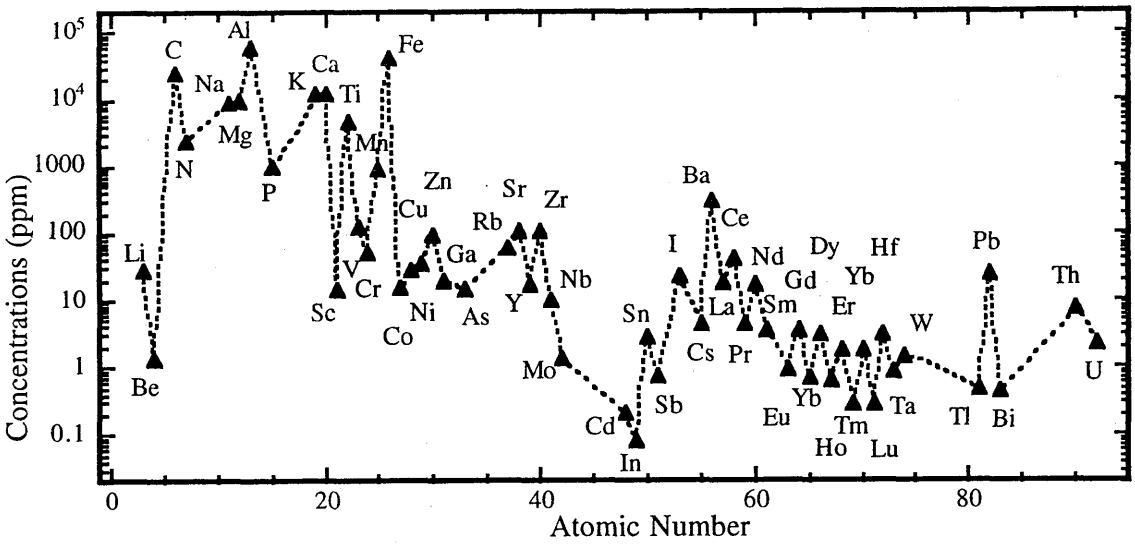

Fig.2. Elemental concentrations in Japanese soils (average of ca. 100 samples collected in Japan)

Table 1. Analytical results on the $^{240}Pu/^{239}Pu$ atom ratio and $^{239+240}Pu$ concentration in Japanese soils

Location	Soil type	$^{240}Pu/^{239}Pu$ (Atom ratio)		$^{239+240}Pu$ (Bq/kg)
Hitachinaka (Ibaraki)	Rice paddy	0.171	± 0.003	0.39
Ohmagari (Akita)	Forest	0.168	± 0.006	1.4
Rokkashomura (Aomori)	Forest	0.170	± 0.010	4.2
Rokkashomura (Aomori)	Field	0.168	± 0.008	0.43
Joetsu (Niigata)	Rice paddy	0.181	± 0.006	0.64
Ohtoyocho (Kochi)	Forest	0.179	± 0.005	1.8
Toyotomicho (Hokkaido)	Moor	0.176	± 0.005	1.5
Mean value (7)		0.173	± 0.01	1.5

地殻と比べ土壌に特異的に濃縮しているのは、C, N, Iの3元素でありそれらの濃縮率は 100 倍以上である。C と N については植物などの有機物が土壌に加わったためである。I は、もともと地殻を構成する岩石には極微量しか含まれておらず、海水から選択的に大気中に放出されたヨウ素が、乾性沈着あるいは雨に溶け湿性沈着した結果、土壌中の濃度が高くなったと考えられる。海水からの揮散は海洋微生物の作用により有機ヨウ素（ヨウ化メチル）が生成されることによりおこると考えられている。それが紫外線により分解されて無機ヨウ素となり、雨水に溶け土壌に入る。I^-（ヨウ化物イオン）と IO_3^-（ヨウ素酸イオン）は共に土壌に吸着しやすい。特に、黒ボク土への吸着は高く、I 濃度も高い。I 程ではないが As と Sb も土壌の方が数倍高い値であった、これも海からの影響があるのではないかと思われる。

次に元素間の相関を見る。U, Th, La, Ce, Yb, Lu についての関係を調べたところ、La と Ce 及び Yb と Lu の間、つまり隣り合った希土類元素の間には非常によい相関が見られた。しかし、離れた希土類元素間（例えば La と Lu）では相関はそれほど明らかではなかった。U と Th の相関はある程度みられた。Th と Ce (La) は比較的良い相関を示した。これは Th と軽希土元素はイオン半径が互いに似ていることに起因している。

Pu の分析データはある程度出されているものの、まだまだデータが不足している。特に、同位体組成（$^{240}Pu/^{239}Pu$ 比）に関しては極限られたものしかなかった。今回得られた土壌の Pu 濃度及び $^{240}Pu/^{239}Pu$ 原子比の分析例を **Table 1** に示す。濃度的には、農地に比べ森林土壌の方が高い傾向にあった。

我々が測定した日本の表層土壌中の $^{240}Pu/^{239}Pu$ 比は約 0.17 程度（長崎の試料を除く）であり、Krey が報告しているグローバルフォールアウトの平均値と良い一致を示している。但し、長崎の西山地区で採取した土壌の $^{240}Pu/^{239}Pu$ 原子比は約 0.04 と非常に低く、これは長崎に投下された Pu 爆弾の組成を反映していると考えられる。つまり、Pu 爆弾では ^{239}Pu が濃縮されているため $^{240}Pu/^{239}Pu$ 比が小さい。爆心地の近くでは飛び散った爆弾の材料の影響が大きく、そのため低い $^{240}Pu/^{239}Pu$ 比を示したと考えられる。

日本で採取した試料だけでなく、チェルノブイリやその他の地域の試料（IAEA の標準試料も含む）の分析も行っており、得られたデータを **Fig.3** にまとめた。

チェルノブイリの土壌試料では、約 0.4 程度という高い値が得られた。これは、燃焼度が高い燃料からの汚染を反映していると考えられる。（つまり、原子炉内で、^{238}U に中性子があたり ^{239}Pu が作られ、それに中性子が更に当たり ^{240}Pu が生成される。そのため、燃焼度が高い方が $^{240}Pu/^{239}Pu$ 比は高い傾向にある。）ムルロア環礁の堆積物（IAEA-368）から得られた $^{240}Pu/^{239}Pu$ 比は約 0.04 であり、これも長崎と同様 Pu 爆弾の材料を反映していると考えられる。マーシャル諸島の堆積物（IAEA-367)の値は約 0.3 であった。マーシャル諸島では水爆実験も含む種々な核実験を行っており、比較的高い $^{240}Pu/^{239}Pu$ 比が何に起因するのか現在のところ不明である。アイリッシュ海の堆積物（IAEA-135）においては、0.21 程度の値が得られた。この値はフォールアウトの値よりも少し大きい。セラフィールドの再処理施設で処理された使

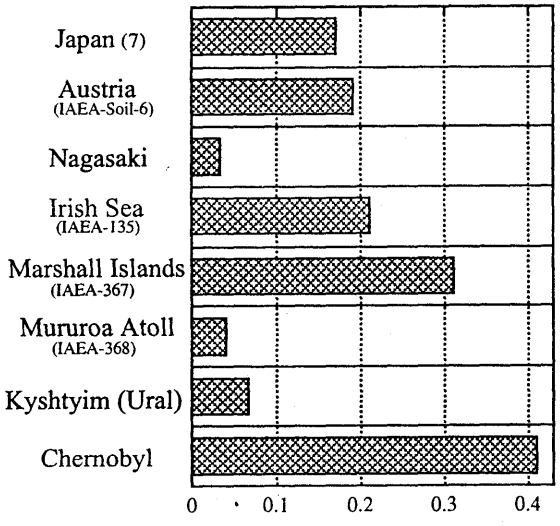

Fig. 3 The $^{240}Pu/^{239}Pu$ atom ratio in environmental samples (soil or sediment) from different origins

用済核燃料中の $^{240}Pu/^{239}Pu$ 比を反映していると考えられる。

原子炉や再処理施設の環境安全評価に関連して、環境中の濃度を測るだけでなく Pu の同位体比も調べることは重要と考えられる。同位体（特に $^{240}Pu/^{239}Pu$ 比）を測定することにより、プルトニウムの汚染源の同定も可能になる。また、汚染源周辺でのそれらの比を求めることは、プルトニウムの環境移行を解析する上でも役立つであろう。現在の科学技術庁の Pu 分析のマニュアルではアルファ線スペクトロメトリー法しか述べられていないが、さらに ICP-MS 法なども加え、また、分離法にも柔軟性を持たせる必要があろう。

2.2.2 植物・菌類

種々の農作物と森林生態系を形成する植物や菌類（キノコ）についても多元素分析を行っている。ここでは分析データの一例として、木の葉（広葉樹）、シダ、キノコの分析値を紹介する。植物は主として根から養分を吸収している。また、ここで用いたキノコも菌糸は土壌表層に存在している。そこで、植物（キノコ）と土壌との元素の濃度比を求めた。濃度比を調べることは、各元素の植物（キノコ）への移行や環境中での循環を評価する上で重要である。求めた濃度比を **Fig.4** に原子番号順に示した。移行比が１より大きい値を示したものは、P と K（木の葉、シダ、キノコ）、Rb と Cd（キノコ、シダ）であった。逆に、濃縮し難いものとしては、Ti, Ga, Zr, U, Th 等であった。その他興味深いものとしては、シダ類中の希土類元素があげられる。他の植物（木の葉以外も含む）やキノコに比べシダ類は希土類元素を格段に取り込みやすい。また、**Fig.4** からキノコは植物と比べ Cs と Rb を大変吸収しやすいことが分かる。しかし、おなじアルカリ元素でも K の値は３者でそれほど大きな差はない。チェルノブイリ事故の後各国でキノコ中に高い Cs-137 濃度が報告されたが、これは、キノコが安定セシウムを濃縮し易いことと関係している。しかし、キノコの種類によってセシウムの濃縮が大きく異なることも明らかになった。また、森林生態系におけるセシウムの分布に関する研究を行ったが、フォールアウトで加わった Cs-137 は系内では既に安定セシウムと混ざり、

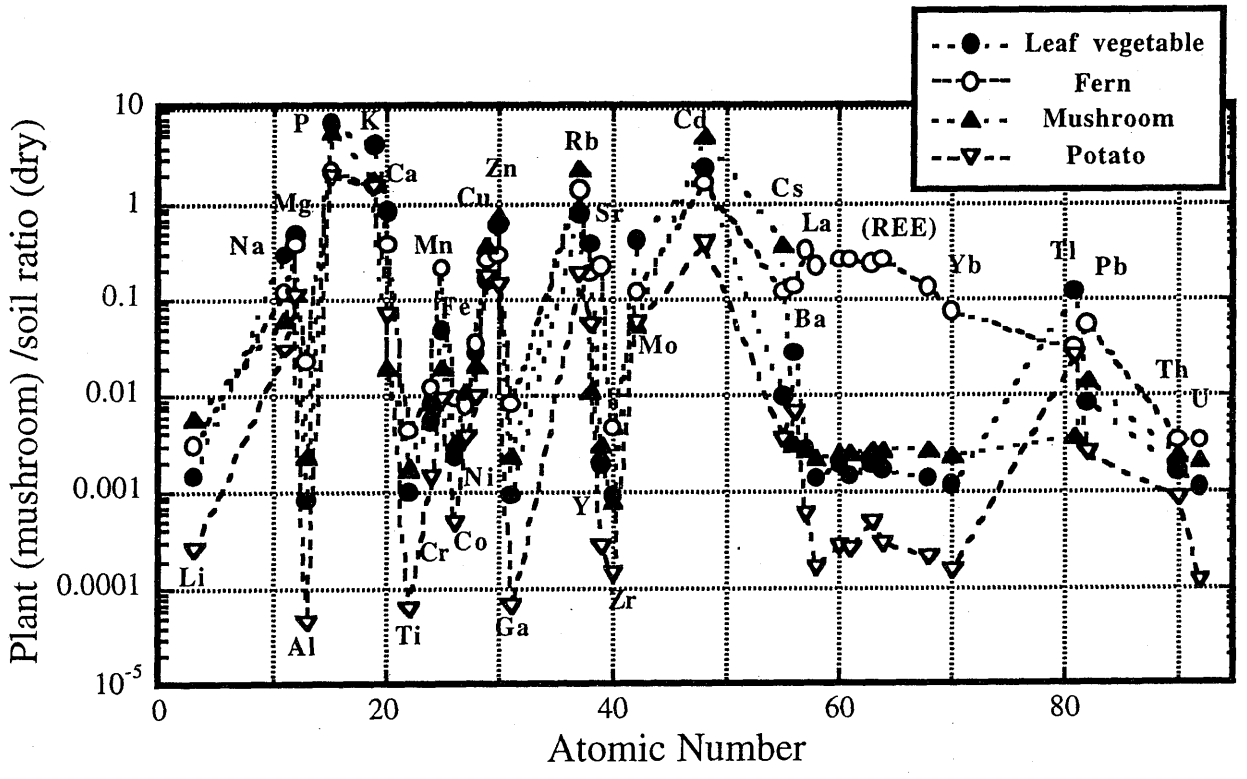

Fig. 4 Plant (mushroom) / soil concentration ratios for leaf vegetables, ferns, potatos and mushrooms (dry weight basis)

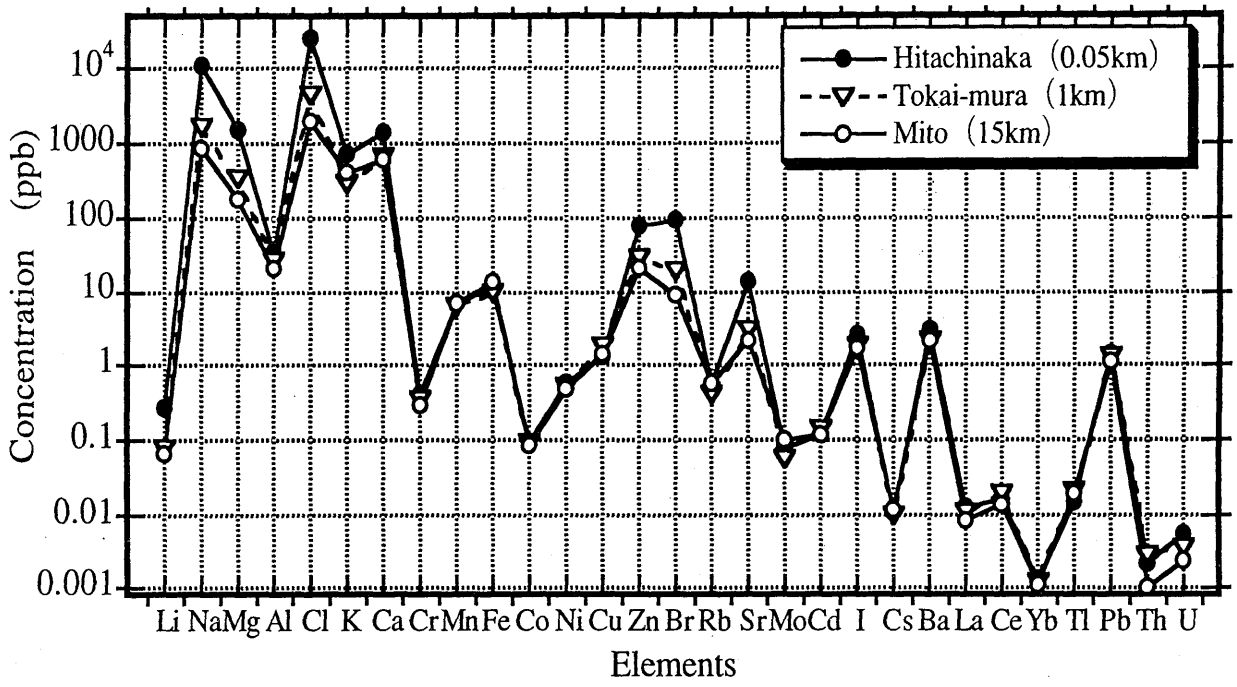

Fig. 5 Elemental concentrations in rain water samples collected from Hitachinaka, Tokai-mura and Tokyo with different distance from the coast.

Cs-137/Cs 比はほぼ一定で同様な挙動を取っていることが分かった。

2.2.3 天然水

酸性雨や温暖化の問題に関連して天然水の化学組成とその変化に関する研究が重要となっている。森林に酸性雨が降り注ぐと樹冠や土壌から特定の元素が溶出し地下水や河川に入る。また、温暖化によって生態系や土壌のバランスが変化し新たに溶出する元素も出てくる可能性がある。さらに、今後先端技術産業の発展とともに今まで用いられなかった元素（レアーメタルなど）が環境に加わることも予想される。しかし、天然水中の微量元素に関する信頼できるデータは海水を除いては少ないのが現状である。そのため、雨水、河川水、湖沼水、地下水などについてバックグラウンドデータを取った。　水試料の ICP-MS による分析は上で述べた固体試料とは異なり前処理操作が楽であり、主に濾過と酸等による調整だけで済む。しかし、天然水中の多くの元素は濃度が低いため検出限界が問題になる。また、低濃度の元素を測定する場合は他の元素の分子イオン等の妨害を受けやすいので注意が必要である。

Fig.5 に雨水の分析結果を示す。試料の採取場所はひたちなか市の海岸（放医研那珂湊放射生態学センターの裏：海岸より 50m），東海村（海岸より 1 km）及び水戸（海岸より 2 km）の 3 地点である。それらを ICP-MS 及び ICP- 発光法で分析し約 30 元素についてのデータが得られた。海からの距離が近い程明らかに多い元素は Li，Cl，Na、Mg、Zn、Br，Sr ，U であった。また、Rb、I 、Ba、La も海岸で採取した降雨中に高い傾向があった。Mn、Fe、Co、Ni、Cu、Mo、Cd、Cs、Tl、Pb などは 3 地点ともほぼ同じ値を示した。

ヨウ素は、放射生態学的にもまた、栄養学的にも重要な元素であるが、今まで分析が難しかったのでデータが不足している。ICP-MS を用いることにより濃縮操作なしにヨウ素を分析でき、今まであまり知られていなかった雨水や陸水中のヨウ素濃度に関するデータが得られた。雨水中のヨウ素濃度は 1 ～ 3 ppb 程度であり、春先に高く、夏場に低い傾向にあった。雨水中の濃度は、降水量とも関係していると考えられる。つまり、雨の降る量や期間が少ないと、大気中のヨウ素濃度は高くなり雨水に溶ける（又はウォッシュアウトされる）量も多くなると推定される。事実降り始めの雨の濃度は高い傾向にあった。また、化学形態についても ICP-MS にイオンクロマトを接続し形態別分離測定を行い、I^- と IO_3^- の 2 つが確認できた。

ヨウ素以外の元素の季節変化は La、Ce、Yb、Th についても春先に高く夏場に低い傾向が見られた。一方、Ni、Cu、Cr、Cd、Mo、Zn などは春先に顕著なピークはなく、上述の元素とは異なった挙動をとると思われる。K、Rb は 11 月に高い値が観測され、大気中に舞い上がった枯れ葉など植物起源の成分からの影響の可能性もあろう。天然水中の元素の存在量と水を通じた環境中での元素の循環に関しては、河川水や地下水などについて得られたデータと合わせて解析中である。

2.3 農耕地並びに森林移行とそのメカニズム

2.3.1 農耕地

農耕地における放射性核種の農作物への移行を、RI トレーサ実験により調べた。用いたトレーサは、Cs-137、Sr-85、Mn-54、Zn-65、Co-60、I-125 である。我が国の土壌として最も一般的な黒ボク土をポットに入れ、上記の核種を添加し、それに作物を植え、バイオトロン中で栽培した。収穫後、可食部をサンプリングし、Ge 半導体検出器又は

NaI シンチレーションカウンターを用いて測定した。

得られた値をもとに、土壌－植物移行係数（Transfer Factor）を求めた。尚、移行係数は作物中の放射性核種の濃度を土壌中の濃度で割った値として定義される。

今まで我が国の農作物への移行係数値についてのデータは極限られていたが、本研究を通してデータをとることができた。これまでの実験で得られたデータを **Table 2** にまとめる。今まで殆どデータがなかった米についての移行係数値が得られたのは意味深い。

全般的に見ると、葉菜類は根菜や穀類に比べて移行係数値（湿重量）は低い傾向にあった。但し亜鉛については穀類で高い値が見られ、これは植物の生長に関連した元素であるためと考えられる。（以前の我々の研究でも若い葉の方が古い葉に比べて Zn の値が明らかに大きかった。）

移行係数（湿重量で表した場合）が最も低い値を示したものは、Sr と I ではサツマイモ、Cs と Co ではタマネギ、Mn と Zn ではトマトであった。これらの値は重さをもとにしているため、水分や貯蔵デンプンの含量が多くなると相対的に濃度が低くなったものと考えられる。Cs、Mn、Zn、Co については、ホウレンソウで高い移行係数値が見られた。これは、植物の種類に関係していると思われるが、葉面積が広く蒸散量も多いことにも影響されている可能性もある。また、I の場合は、セリの移行係数値が高かった。これは、湛水状態で栽培したため、土壌からヨウ素が溶けだし、植物に移行したためと考えられる。Ce の移行係数は他の核種に比べて著しく低かった。この元素は半導体に用いられる希土類の廃棄物の中に大量に含まれており、環境安全の面からも注目されている。また、Pu と化学的挙動が似ていると考えられ、Pu のアナログとして使われることがある。Ce の低い移行係数値から考え、もしもこの元素による土壌汚染が生じた場合でも、農作物へ取り込まれる量は少ないと推定される。

Table 2 には比較として IAEA がまとめた代表的な移行係数値（IAEA 1982）も示してある。葉菜のセシウムの値は、IAEA の値より数倍高い傾向にあった。これは、黒ボク土が放射性セシウムを可給態の状態で吸着するため、農作物がこの核種を取り込み易かったと考えられる。一方、ヨウ素の場合、ほとんどの移行係数の値は、IAEA の値より 1 桁低かった。これは、畑状態の黒ボク土へのヨウ素の吸着力が強く、植物に吸収され難かったためと考えられる。その他の元素については、元素分析の結果から推定して、例えば、U、Th、希土類元素では通常 0.001 以下と非常に小さな値であった。

2.3.2 森林

チェルノブイリ事故の後、放射性 Cs が森林に長期間残留することが明らかになってきた。事故から 10 年以上たっても森林の動植物中の濃度はほとんど低下していない。なかでも特にキノコは放射性 Cs を蓄積しやすく、被ばく線量評価の面で注目されている。森林内での放射性 Cs の長期的な挙動を解明するためには、森林内にもともと存在する安定 Cs や関連するアルカリ及びアルカリ土類元素を含めた総合的な研究が有効と考えられる。そこで、放射性 Cs による汚染の程度が異なる国内外数カ所の森林で土壌、植物、キノコを採取し、放射性 Cs と関連安定元素を ICP-MS や ICP-AES で定量した。

植物と比較するとキノコは、明らかに Rb と Cs 濃度が高く、Ca と Sr 濃度が低かった。キノコ中の ^{137}Cs, Cs, Rb の濃度は、同じ森林で採取した植物に比べて 1 桁高い。これは、キノコが本質的に Cs を吸収しやすいことを示している。

1 つの森林で採取したキノコ中の ^{137}Cs と安定 Cs との間

Table 2　Transfer factors of edible parts of agricultural products by radiotracer experiments

	agricultural products*	Cs	Sr	Mn	Zn	Co	I	Ce
cereals	brown rice (dried)	0.017	0.06	0.21	3.0	0.006	0.006	≦0.0002⁺
	wheet (dried)	0.10	0.24	2.4	2.9	0.019		≦0.01⁺
leaf vegetables	cabbage	0.13	0.13	0.23	0.11	0.013	0.0016	0.00009
	Chinese cabbage	0.15	0.15	0.27	0.34	0.018	0.0013	
	spinach	0.17	0.30	1.51	1.74	0.18	0.0031	0.0015
	komatsuna	0.057	0.44	0.30	0.17	0.016	0.016	0.0027⁺
	Japanese parsley	0.079					0.24	0.00079⁺
	lettuce	0.055	0.18	0.72	0.24	0.0048	0.00076**	0.00087
	onion	0.002	0.13	0.038	0.12	0.0009		≦0.09⁺
fruit vegetables	tomato	0.061		0.014	0.021	0.0018	0.0003	0.00087
	sweet peper	0.080		0.029	0.052	0.016		
root vegetables	carrot	0.014	0.12	0.23	0.21	0.005	0.0009	0.0002
	radish	0.02	0.05	0.02	0.04	0.004	0.0015	≦0.0001⁺
	turnip	0.026	0.25	0.030	0.14	0.0021	0.0013**	
potatos	sweet potato	0.050	0.040	0.095	0.12	0.0043	0.0002	0.00011
bean	soy bean (dried)	0.13					0.0029	0.0004
IAEA		0.03	0.3	0.5	0.4	0.03	0.02	0.002

*TFs were calculated with wet weight of agricultural products expect for "dried".

** means the experiment was carriedout with other Andosols.

⁺ the data from reference

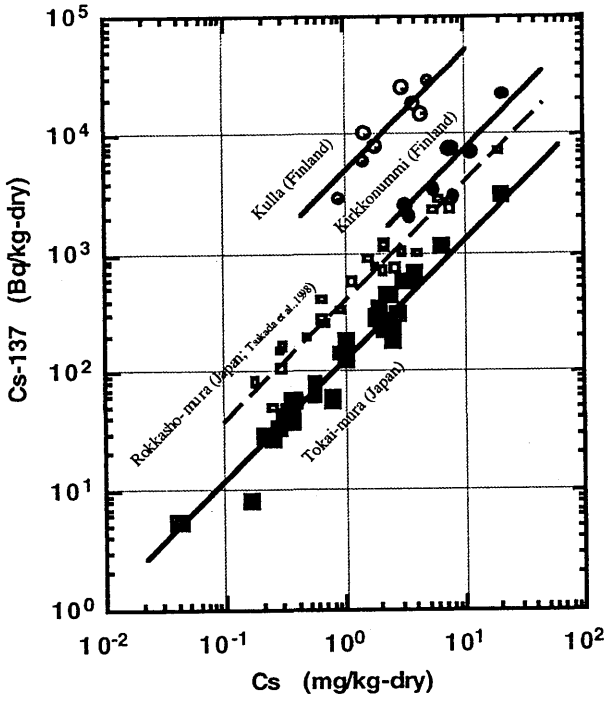

Fig. 6 Relationships between Cs-137 and stable Cs in mushrooms collected from different forests. (Data for Rokkasho-mura are from Tsukada et al. (1998).)

には、キノコの種類に関わらず正の相関が見られた(**Fig.6**)。すなわち、放射性 Cs は安定 Cs と共にキノコに取り込まれていることが明らかとなった。両者の比は森林ごとにほぼ一定であった。このことから、核実験のフォールアウトやチェルノブイリ事故によって森林に沈着した ^{137}Cs は生物的物質循環の中で安定 Cs とほぼ平衡状態になっていることが示唆された。森林ごとの比の違いは、各森林への放射性セシウムの沈着量の違い、土壌中の安定セシウム濃度の違い、森林の植生や土壌の違い等に起因すると考えられる。今後、森林の元素循環モデルを用いてこれらの比を再現できれば、安定 Cs 濃度を用いてキノコ中の放射性 Cs 濃度を予測することが可能と考えられる。

日本の森林土壌中の ^{137}Cs と Pu 濃度の深度分布を調べたところ、両核種ともほとんどが表層（10cm 以内）に存在し、深さとともに減少した。これらのデータから考え、フォールアウトで加わったこれらの核種は、40 年前後経った今も、地表の極表面に留まっていることが分かった。

[研究発表]

原著論文（peer-review された論文）のみのリストである。但し、他の研究課題（原子力基盤、放調など）と関係するものも含む。

（研究論文）

1) Muramatsu, Y., Yoshida, S., Uchida, S. and Hasebe, A.: Iodine desorption from rice paddy soil. Water, Air and Soil Pollution, 86, 359-371 (1996).
2) Yoshida, S., Muramatsu, Y., Tagami, K. and Uchida, S.: Determination of major and trace elements in Japanese rock reference samples by ICP-MS. Int. J. Environmental Analytical Chemistry, 63, 195-206 (1996).
3) Muramatsu, Y., Uchida, S., Sumiya, M. and Ohmomo, Y.: Deposition velocity of gaseous organic iodine from the atmosphere to rice plants. Health Phys., 71, 757-762 (1996).
4) Muramatsu, Y. and Yoshida, S.: Behaviour of iodine-129 in the soil-plant system. Österreichishe Bodenkundlichen Gesellschaft Heft 53, 207-214 (1996).
5) Schnetger, B. and Muramatsu, Y.: Determination of halogens, with a special reference to I, in geological and biological samples using pyrohydrolis for preparation and ICP-MS and IC for measurement. Analyst, 121, 1627-1631 (1996).
6) Yoshida, S., Muramatsu, Y. and Ban-nai, T.: Accumulation of radiocesium and trace elements in mushrooms collected from Japanese forests. Österreichishe Bodenkundlichen Gesellschaft Heft, 53, 251-258 (1996).
7) Tagami, K. and Uchida, S.: Microbial role in immobilization of technetium in soil under waterlogged conditions. Chemosphere, 33, 217-225 (1996).
8) Tagami, K. and Uchida, S.: Aging effect on technetium in soil under aerobic and anaerobic conditions. Toxicol. Environ. Chem., 56, 235-247 (1996).
9) Tagami, K. and Uchida, S.: Analysis of technetium-99 in soil and deposition samples by inductively coupled plasma mass spectrometry. Appl. Radiat. Isot., 47, 1057-1060 (1996).
10) Yasuda, H., Ambe, S. and Uchida, S.: Distribution coefficients of platinum group metals between soil solid and liquid phase. Environ. Technol., 17, 1151-1154 (1996).
11) Uchida, S. and Tagami, K.: Separation and concentration of technetium using a Tc-selective extraction chromatographic resin. J. Radioanal. Nucl. Chem., 221, 35-39 (1997).
12) Uchida, S. and Tagami, K.: Improvement of Tc separation procedure using a chromatographic resin for direct measurement by ICP-MS. Anal. Chim. Acta, 357, 1-3 (1997).
13) Ban-nai, T., Muramatsu, Y. and Yoshida, S.: Concentrations of ^{137}Cs and ^{40}K in edible mushrooms collected in Japan and radiation dose due to their consumption. Health Physics, 72, 384-389 (1997).
14) Yoshida, S. and Muramatsu, Y.: Determination of major and trace elements in mushroom, plant and soil samples collected from Japanese forests. Intern. J. Environ. Anal. Chem., 67, 49-58 (1997).
15) Ban-nai, T., Muramatsu, Y., Yoshida, S., Uchida, Y., Shibata, S., Ambe, S., Ambe, F. and Suzuki, A.: Multitracer Studies on the Accumulation of Radionuclides in Mushrooms. J. Radiat. Res., 38, 213-218 (1997).
16) Tagami, K. and Uchida, S.: Concentration of global

fallout ^{99}Tc in rice paddy soils collected in Japan. Environ. Pollut., 95, 151-154 (1997).

17) Yoshida, S., Muramatsu, Y., Tagami, K. and Uchida, Y.: Concentrations of lanthanide elements, Th, and U in 77 Japanese surface soils. Environment International, 24, 275-286 (1998).

18) Muramatsu, Y. and Wedepohl, K. H.: The distribution of iodine in the earth's crust. Chemical Geology, 147, 201-216 (1998).

19) Yoshida, S. and Muramatsu, Y.: Concentration of alkaline earth elements in mushrooms and plants collected in a Japanese pine forest, and their relationship with ^{137}Cs. J. Environ. Radioact, 41, 183-205 (1998).

20) Schnetger, B., Muramatsu, Y. and Yoshida, S.: Iodine (and other Halogens) in twenty six geological reference materials by ICP-MS and ion chromatography. Geostandards Newsletter, 22, 181-186 (1998).

21) Yoshida, S., Muramatsu, Y. and Uchida, S.: Soil-solution distribution coefficients, Kds, of I^- and IO_3^- for 68 Japanese Soils. Radiochimica Acta, 82, 293-297 (1998).

22) Tagami, K. and Uchida, S.: Aging effect on bioavailability of Mn, Co, Zn and Tc in Japanese agricultural soils under waterlogged condition. Geoderma., 84, 3-13 (1998).

23) Tagami, K., Uchida, S. and Garcia-Leon, M.: Comparison of a radiation counting method and ICP-MS for the determination of Tc-99 in environmental samples. J. Radioanal. Nucl. Chem., 234, 147-151 (1998)

24) Muramatsu, Y. and Yoshida, S.: Effects of microorganisms on the fate of iodine in the soil environment. Geomicrobiology J., 16, 85-93 (1999).

25) Rühm, W., Yoshida, S., Muramatsu, Y., Steiner, M. and Wirth, E.: Distribution patterns for stable ^{133}Cs and their implications with respect to the long-term fate of radioactive ^{134}Cs and ^{137}Cs in a semi-natural ecosystem. J. Environ. Radioactivity, 45, 253-270 (1999).

26) Muramatsu, Y., Uchida, S., Tagami, K., Yoshida, S. and Fujikawa, T.: Determination of plutonium concentration and its isotopic ratio in environmental materials by ICP-MS after separation using ion-exchange and extraction chromatography. J. Anal. At. Spectrom., 14, 859-865 (1999).

27) Sekine, T., Konishi, M., Kudo, H., Tagami, K. and Uchida, S.: Separation of carrier free ^{95m}Tc from niobium targets irradiated with alpha-particles. J. Radioanal. Nucl. Chem., 239 (3), 483-487 (1999).

28) Uchida, S. and Tagami, K.: Use of IAEA Reference Materials (IAEA-373 and 375) as Low-level ^{99}Tc References. J. Radioanal. Nucl. Chem., 240, 357-359 (1999).

29) Uchida, S., Tagami, K., Wirth, E. and Rühm, W.: Concentration level of ^{99}Tc in forest soils collected within the 30-km zone around the Chelnobyl reactor. Environ. Pollut., 105, 75-77 (1999).

30) Uchida, S. and Tagami, K.: A rapid separation method for determination of Tc-99 in environmental waters by ICP-MS. Radioactivity and Radiochemistry, 10, 23-29 (1999).

31) Ambe, S., Shinonaga, T. Ozaki, T., Enomoto, S., Yasuda, H. and Uchida, S.: Ion competition effects on the selective absorption of radionuclides by Komatsuna (Brassica rapa var. perviridis), Environ. Exp. Bot., 41, 185-194 (1999).

32) Uchida, S., Tagami, K., Rühm, W. and Wirth, E.: Determination of ^{99}Tc deposited on the ground within the 30-km zone around the Chernobyl reactor and estimation of ^{99}Tc released into atmosphere by the accident. Chemospere, 39, 2757-2766 (1999).

33) Yoshida, S. and Muramatsu, Y.: Use of stable elements for predicting radionuclide transport, I. linkov and W. R. Schell (eds.) Contaminated Forests. 41-49 (1999).

34) Tagami, K. and Uchida, S.: Chemical transformation of techneitum in soil during the change of soil water conditions. Chemosphere, 38, 963-971 (1999)

35) Tagami, K. and Uchida, S.: Comparison of the TEVA Spec resin and liquid-liquid extraction methods for the separation of technetium in soil samples. J. Radioanal. Nucl. Chem., 239, 643-648 (1999)

36) Tagami, K. and Uchida, S.: Use of a Combustion Apparatus for Low-level ^{99}Tc separation from soil samples. Radioact. Radiochem., 10, 30-34 (1999)

37) Gerzabek, M. H., Muramatsu, Y., Strebl, F. and Yoshida, S.: Iodine and bromine contents of some Austrian soils and relations to soil characteristics. J. Plant Nutr. Soil Sci., 162, 415-419 (1999).

38) Ban-nai, T., Muramatsu, Y. and Yanagisawa, K.: Transfer of selected radionuclides (Cs, Sr, Mn, Co, Zn and Ce) from soil to root vegetables. J. Radioanal. Nucl. Chem., 241, 529-531 (1999).

39) Shiraishi, K., Muramatsu, Y., Los, I. P., Korzun, V. N., Tsigankov, N. Y. and Zamostyan, P. V.: Estimation of dietary iodine and bromine intakes of Ukrainians. J. Radioanal. Nucl. Chem., 242, 199-202 (1999).

40) Shiraishi, K., Ban-nai, T., Muramatsu, Y. and Yamamoto, M.: Comparison of stable cesium and radiocesium on dietary intakes by Japanese subjects using 18 food categories. J. Radioanal. Nuclear Chemistry, 242, 687-692 (1999).

41) Muramatsu, Y., Ishikawa, Y., Yoshida, S. and Mori, T.: Determination of thorium organs from Throtrast patients by inductively coupled plasma mass spectroscopy and x-ray fluorescence. Radiation Research, 152, 97-101 (1999).

42) Shiraishi, K., Tagami, K., Muramatsu, Y. and Yamamoto, M.: Contributions of 18 food categories to intakes of ^{232}Th and ^{238}U in Japan. Health Physics, 78, 28-36 (2000).

43) Ban-nai, T., Muramatsu, Y., Tagami, T., Uchida, S., Yoshida, S., Kimura, S. and Watanabe, Y.: Levels of

radionuclides in plant samples collected around the uranium conversion facility following the criticality accident in Tokai-mura. J. Environ. Radioactivity, 50, 131-143 (2000).

44) Yoshida, S., Muramatsu, Y., Tagami, K., Uchida, S., Ban-nai, T., Yonehara, H. and Sahoo, S.: Concentrations of uranium and $^{235}U/^{238}U$ ratios in soil and plant samples collected around the uranium conversion building in the JCO campus. J. Environ. Radioactivity, 50, 161-172 (2000).

44) Komura, K., Yamamoto, M., Muroyama, T., Murata, Y., Nakanishi, T., Hoshi, M., Takada, J., Ishikawa, M., Takeoka, S., Kitagawa, K., Suga, S., Endo, S., Tosaki, N., Mitugashira, T., Hara, M., Hashimoto, T., Takano, M., Yanagawa, Y., Tsuboi, T., Ichimasa, M., Ichimasa, Y., Imura, H., Sasajima, E., Seki, R., Saito, Y., Kondo, M., Kojima, S., Muramatsu, Y., Yoshida, S., Shibata, S., Yonehara, H., Watanabe, Y., Kimura, S., Shiraishi, K., Ban-nai, T., Sahoo, S. K., Igarashi, Y., Aoyama, M., Hirose, K., Uehiro, T., Doi, T., Tanaka, A. and Matsuzawa, T.: The JCO criticality accident at Tokai-mura, Japan: an overview of the sampling campaign and preliminary results. J. Environ. Radioactivity, 50, 3-14 (2000).

45) Muramatsu, Y., Rühm, W., Yoshida, S., Tagami, K., Uchida, S. and Wirth, E.: Concentrations of ^{239}Pu and ^{240}Pu and their isotopic ratios determined by ICP-MS in soils collected from the Chernobyl 30-km zone. Environ. Sci. & Technol, 34, 2913-2917 (2000).

46) Tagami, K. and Uchida, S.: Separation of rhenium by an extraction chromatographic resin for determination by ICP-MS. Anal. Chim. Acta, 405, 227-229 (2000)

47) Amachi, S., Muramatsu, Y. and Kamagata, T.: Radioanalytical determination of biogenic volatile iodine emitted from aqueous environmental samples. J. Radioanal. Nucl. Chem., 246, 337-342, (2000).

48) Müller, J., Ruppert, H., Muramatsu, Y. and Schneider, J.: Reservoir sediments – a memory of mining and industrial development (Talsperre Malter, Eastern Erzgebirge, Germany). Environmental Geology, 39, 1341-1351 (2000).

49) Nakanishi, T., Hosotani, R., Komura, K., Muroyama, T., Kofuji, H., Murata, Y., Kimura, S., Sahoo, S. K., Yonehara, H., Watanabe Y. and Ban-nai T.: Residual neutron-induced radionuclides in a soil sample collected in the vicinity of the criticality accident site in Tokai-mura, Japan: A Progress Report. J. Environ. Radioactivity, 50, 61-68 (2000)

50) Shinonaga, T., Gerzabek, M. H., Strebl, F. and Muramatsu, Y.: Transfer of iodine from soil to cereal grains in agricultural areas of Austria. Sci. Total Environ., 267, 33-40 (2001).

51) Muramatsu, Y., Yoshida, S., Tagami, K., Uchida, S. and Rühm, W.: ICP-MS analysis of environmental plutonium. Plutonium in the Enviroment, Kudo, A., (Editor), Elsevier Science Ltd. Amsterdam, 63-77 (2001).

52) Amachi, S., Kamagata, Y., Kanagawa, T. and Muramatsu, Y.: Bacteria mediate methylation of iodine in marine and terrestrial environments. Applied and Environmental microbiology, 67, 2718-2722 (2001).

(その他の論文 - 総説、Proceedings、著書など)

1) S. Yoshida, Y. Muramatsu and T. Ban-nai: Accumulation of radiocesium and trace elements in mushrooms collected from Japanese forests. Proceedings of International Symposium on Radioecology 1996, Ten Years Terrestrial Radioecological Research Followimg the Chernobyl Accident, Vienna, 251-258 (1996).

2) 村松康行: 環境における 129I の挙動 放医研環境セミナー報文集、No.23、NIRS-M-113, 57-68 (1996)

3) 吉田 聡、村松康行：地球規模の放射能汚染と菌類、日本菌学会会報、37, 25-30 (1996).

4) 吉田 聡：日本の土壌に対するヨウ素の吸着について、環境中微量物質の挙動パラメータ検討専門研究会報告書、京都大学原子炉実験所、KURRI-KR-1, 65-66 (1996).

5) 吉田 聡：「チェルノブイリ後 10 年間の陸上放射生態学研究会議」に参加して、保健物理、31, 386-388 (1996).

6) S. Yoshida, Y. Muramatsu, K. Tagami and S. Uchida: Multi-element analysis using ICP-MS to determine soil-to-plant and soil-to-mushroom transfer factors. Proceedings of International Workshop on Improvement of Environmental Transfer Models and Parameters, Tokyo, 174-180 (1996).

7) Ban-nai, T., Muramatsu, Y., Yoshida, S. and Yanagisawa, K.: Studies on the transfer of Cs, Sr, Co, Mn and Zn from soil to plants and from medium to mushrooms by using radiotracer. Proceedings of International Workshop on Improvement of Environmental Transfer Models and Parameters, Nuclear Cross-Over Research, Tokyo, 181-190 (1996).

8) Ban-nai, T., Muramatsu, Y., Yoshida,S. and Yanagisawa, K.: Radiotracer experiments on the uptake of radionuclides by mushrooms and vegetables. Proceedings of International Symposium on Ionizing Radiation - Protection of the Natural Environment, The Swedish Radiation Protection Institute, 628-633, (1996).

9) 内田滋夫：農耕土壌中における微量元素の挙動、「地域環境と潅漑排水（丸山利輔編著）」, 180-183、（社）畑地農業振興会、東京、(1997).

10) 村松康行、吉田聡: ICP-MS による環境試料の多元素分析 放射線科学、40、164-170 (1997)

11) 村松康行、吉田聡: キノコと放射性セシウム RADIOISOTOPES, 46, 450-463 (1997)

12) Uchida, S. and Tagami, K.: Concentrations of Global Fallout ^{99}Tc and ^{137}Cs and Their Behaviour in Rice Paddy Fields., *in the Proceedings of the International Conference on Radiation Dosimetry and Safety*, pp174-178, (1997).

13) Tagami, K. and Uchida, S.: Aging Effect on the Bioavailability of Tc, Cs and Co in Agricultural Soils under Aerobic and Anaerobic Conditions., *in Proceedings of the International Conference on Radiation Dosimetry and Safety*, pp179-183, (1997).
14) Uchida, S. and Tagami, K.: A rapid separation method for determination of Tc-99 in environmental waters by ICP-MS., *in Proceedings of Rapid radioactivity Measurements in Emergency and Routine Situations*, pp. 181-186, (1997).
15) Tagami, K. and Uchida, S.: Use of a Combustion Apparatus for Low-level ^{99}Tc separation from soil samples., *in Proceedings of Rapid radioactivity Measurements in Emergency and Routine Situations*, pp. 187-191, (1997).
16) 吉田 聡： 森林中の植物・きのこへの Cs-137 及び微量安定元素の移行、 「環境中微量物質動態」専門研究会報告書、 京都大学原子炉実験所 、 KURRI-KR-18, 23-26 (1997).
17) 内田滋夫：表層土壌中における Tc-99 の挙動 ーバッチ法による Tc の分配係数ー、 「環境中微量物質動態」専門研究会報告書（京都大学原子炉実験所：KURRI-KR-18）, pp. 73-78, (1998).
18) 田上恵子、内田滋夫：土壌中におけるフォールアウト Tc-99 の挙動、「環境中微量物質動態」専門研究会報告書（京都大学原子炉実験所：KURRI-KR-18）, pp. 79-86, (1998).
19) S. Yoshida, Y. Muramatsu, W. Ruhm and A. Rantavaara: Behavior of radiocesium and related stable elements in forest ecosystems. Proceedings of International Meeting on Influence of Climatic Characteristics upon Behavior of Radioactive Elements, Rokkasho-mura, Aomori (1997. 10) 213-220 (1998).
20) S. Yoshida, Y. Muramatsu, W. Ruhm and A. Rantavaara: Behavior of trace elements and radionuclides in soil-plant systems. In: Comparative Evaluation of Environmental Toxicants (Proceedings of International Workshop on Comparative Evaluation of Health Effects of Environmental Toxicants Derived from Advanced Technologies, Chiba,1998. 1), eds. J. Inaba and Y. Nakamura. Kodansha Scientific Itd., pp. 47-55 (1998).
21) W. R. Schell and S. Yoshida: Behavior and modelling of radionuclide and non-radionuclide toxicants in the environment. In: Comparative Evaluation of Environmental Toxicants (Proceedings of International Workshop on Comparative Evaluation of Health Effects of Environmental Toxicants Derived from Advanced Technologies, Chiba,1998. 1), eds. J. Inaba and Y. Nakamura. Kodansha Scientific Itd., pp. 57-74 (1998).
22) Ban-nai, T., Muramatsu, Y., Yanagisawa, K. and Uchida, S: Studies on Transfer of Radionuclides from Soil to Vegetables. Proceedings of International Workshop on Comparative Evalution of Health Effects of Environmental Toxicants Derived from Advanced Technologies (Tokyo, Kodansha Scientific Ltd.), 279-280, (1998).
23) Ban-nai, T., Muramatsu, Y., Yanagisawa, K. and Uchida, S: Studies on Transfer of Radionuclides from Soil to Vegetables. Proceedings of International Workshop on Comparative Evalution of Health Effects of Environmental Toxicants Derived from Advanced Technologies (Supplement. NIRS-M-130), 95-105, (1998).
24) Muramatsu, Y., Ban-nai, T., Yoshida, S. and Uchida, S.: Transfer of some selected radionuclides and trace elements from soil to plant. Proceedings of International Meeting on Influence of Climatic Characteristics upon Behavior of Radioactive Elements, Rokkasho-mura, Aomori, 189-196 (1998).
25) Muramatsu, Y., Yoshida, S.: On the environmental behavior of radioactive and stable iodine. Proceedings of the International Workshop on Comparative Evaluation of Health Effects of Environmental Toxicants Derived from Advanced Technologies, edited by J. Inaba & Y. Nakamura, Supplement, NIRS-M-130, ISBN-4-938987-05-8, 45-58, (1998).
26) Muramatsu, Y. and Yoshida, S.: On the environmental behavior of radioactive and stable iodine. Proceedings of the International Workshop on Comparative Evaluation of Health Effects of Environmental Toxicants Derived from Advanced Technologies, edited by J. Inaba & Y. Nakamura, (Tokyo, Kodansha Scientific Ltd.), 267-269, (1998)
27) 村松康行: 地球規模の放射性物質の分布と移動、月刊地球, vol.22, 69-79 (1998)
28) 田上恵子、内田滋夫：水中のウラン濃度の ICP-MS 法のよる直接測定、「保健物理と放射能動態」専門研究会報告書（京都大学原子炉実験所：KURRI-KR-30）, pp. 110-115, (1999).
29) 内田滋夫、田上恵子：水試料中の Tc-99 の迅速・勘弁な分析法の検討、「保健物理と放射能動態」専門研究会報告書（京都大学原子炉実験所：KURRI-KR-30）, pp. 116-123, (1999).
30) 村松康行, 吉田 聡: ICP-MS を用いた環境試料中の Pu, U, Th の分析 RADIOISOTOPES, VOL.48, 472-487, (1999)
31) 渡利和男、稲葉次郎、今井靖子、村松康行、西村義一、明石真言：「放射線と人体・暮らしの中の放射線」研成社（1999）
32) 村松康行: 陸上環境における Pu, U, Th の分布と挙動 放医研環境セミナー報文集 No.26、128-137、（1999）
33) S. Yoshida and Y. Muramatsu: Use of stable elements for predicting radionuclide transport. In: Contaminated Forests (Proceedings of NATO Advanced Research Workshop, Contaminated Forests: Recent Developments in Risk Identification and Future Perspective, Kiev, Ukraine, 1998. 6), eds. I.Linkov and W.R.Schell. Kluwer Academic Publishers, Netherland, pp. 41-49 (1999).
34) Tagami, K. and Uchida, S.: Some considerations on the fate of ^{99}Tc in Paddy Fields, *in "Workshop Proceedings on Comparative Evaluation of Environmental Toxicants, Supplement (Eds.: Inaba, J. and Nakamura, Y.)"*, NIRS-M-130, pp. 113-119, 1999.
35) 田上恵子、内田滋夫：ICP-MS 法を用いた土壌-土壌溶液間のウラン、トリウム等の分配係数の測定について、京都大学原子炉実験所「天然バリア Kd」専門研究会報告書、pp. 115-158, KURRI-KR-44、1999.

36) 内田滋夫:分配係数におよぼす土壌乾燥処理の影響、京都大学原子炉実験所「天然バリア Kd」専門研究会報告書、pp. 163-168, KURRI-KR-44、1999.
37) 村松康行: 原子放射線の影響に関する国連科学委員会(UNSCEAR)第 49 回会議に出席して、放影協ニュース, VOL 7, No. 24, 11-12 (2000)
38) 村松康行: UNSCEAR 会議に出席して 放射線科学, Vol. 43, No. 8, (2000)
39) 村松康行, 矢後長純: 第 37 回理工学における同位元素研究発表会から Isotope News, No.556, 33-34 (2000)
40) 天知誠吾、村松康行: 土壌から大気へのヨウ素の揮発—バクテリアによるヨウ素のメチル化—放射線科学、43, 317-322、(2000)
41) 天知誠吾、鎌形洋、村松康行: 地球規模でのヨウ素サイクルに貢献するバクテリア 化学と生物、印刷中、(2001)
42) Muramatsu, Y., Ishigure, N., Noda, Y., Yonehara, H., Yoshida, S., Yukawa, M., Tagami, K., Ban-nai, T., Uchida, S., Akashi, M., T. Hirama, T. and Nakamura,Y.: Estimation of radiation doses based on ^{24}Na produced in biological materials from three exposed patients in the Tokai-mura criticality accident. Proceedings, International Symposium on the Criticality Accident in Tokai-mura, December 2000, Chiba.
43) 吉田 聡: 日本の土壌に対するヨウ素の分配係数、「天然バリア Kd」専門研究会報告書、京都大学原子炉実験所、KURRI-KR-44, 183-186 (2000).
44) S. Yoshida, T. Ban-nai, Y. Muramatsu, K. Tagami and S. Uchida: Determination of fission products and uranium isotopes in soil and plant samples collected in JCO campus. Proceedings of the First Workshop on Environmental Radioactivity, KEK, Tsukuba, Ibaraki (2000. 3) 179-182 (2000).
45) S. Yoshida, Y. Muramatsu, M. Steiner, M. Belli, A. Pasquale, B. Rafferty, W. Ruhm, A. Rantavaara, I. Linkov, A. Dvornik and T. Zhuchenko: Relationship between radiocesium and stable cesium in plants and mushrooms collected from forest ecosystems with different contamination levels. Proceedings of 10th Internatiomnal Congress of the International Radiation Protection Association (IRPA-10), Hiroshima, Japan (2000. May) P-11-244 (2000).
46) I. Linkov, S. Yoshida and M. Steiner: Fungi contaminated by radionuclides: critical review of approaches to modeling. Proceedings of 10th Internatiomnal Congress of the International Radiation Protection Association (IRPA-10), Hiroshima, Japan (2000. May) P-4b-255 (2000).
47) Tagami, K. and Uchida, S.: Global fallout Technetium-99 Levels in Japanese Paddy Soils., The 10th International Congress of The International Radiation Protection Association (IRPA-10), P-4a-231(5p), (2000).
48) Uchida, S., Tagami, K. and García-León, M.a: Redetermination of Low-level ^{99}Tc in Planchet Samples by ICP-MS. The 10th International Congress of The International Radiation Protection Association (IRPA-10), P-4a-243(6p), (2000).
49) 田上恵子、内田滋夫:環境標準物質中 Tc-99 の ICP-MS による定量, in Proceedings of the First Workshop on Environmental Radioactivity (Ed. T. Miura), pp. 97-104, KEK Proceedings 2000-13, (2000).
50) 田上恵子、内田滋夫:マーシャル諸島で採取した土壌中の Tc-99 の分析, in Proceedings of the First Workshop on Environmental Radioactivity (Ed. T. Miura), pp. 105-112, KEK Proceedings 2000-13, (2000).
51) Muramatsu, Y., Yoshida, S. and Amachi S Roles of Microbial activities on the distribution and speciation of iodine in the soil environment. *in Proceedings of the International Workshop on Distribution and Speciation of Radionuclides in the Environment (Eds.: Inaba, J., Hisamatsu, S. and Ohtsuka, Y.)"*, ISBN 4-9980604-3-0 C3040,. 58-65, (2001).
52) Yoshida, S. Muramatsu, Y., Tagami, K. and Uchida, S.: Determination of uranium isotopes in soil and plant samples collected on the JCO grounds, *in Proceedings of the International Workshop on Distribution and Speciation of Radionuclides in the Environment (Eds.: Inaba, J., Hisamatsu, S. and Ohtsuka, Y.)"*, ISBN 4-9980604-3-0 C3040, pp. 38-44, (2001).
53) Ban-nai, T., Hisamatsu, S., Yanai-Kudo, M., Hasegawa, H., Torikai, Y.: The concentration of Cs, Sr and other elements in the water samples collected n the paddy field. In: Distribution andspeciation of radionuclides in the environment - Proceedings of the International Workshop on Distribution and Speciation of Radionuclides in the Environment- . 227-232, (2001).
54) Tagami, K. and Uchida, S.: Distribution of Technetium-99 in Surface Soils, *in Proceedings of the International Workshop on Distribution and Speciation of Radionuclides in the Environment (Eds.: Inaba, J., Hisamatsu, S. and Ohtsuka, Y.)"*, ISBN 4-9980604-3-0 C3040, pp. 38-44, (2001).
55) Uchida, S and Tagami, K.: Time Dependence on Plant Availability of Radionuclides in Two Japanese Soils under Upland and Paddy Field Conditions, *in Proceedings of the International Workshop on Distribution and Speciation of Radionuclides in the Environment (Eds.: Inaba, J., Hisamatsu, S. and Ohtsuka, Y.)"*, ISBN 4-9980604-3-0 C3040, pp. 239-245 (2001).
56) 坂内忠明:霧箱の歴史. 放射線教育、4:4-17 (2001)

(口頭発表)

1) Muramatsu, Y., Yoshida, S. and Tagami, K.: Determination of trace elements in precipitation collected in Japan by ICP-MS. 26th International Symposium on Environmental Analytical Chemistry, Vienna, April 1996..
2) Muramatsu, Y. and Yoshida, S.: Behaviour of iodine-129 in the soil-plant system. International Symposium of the Austrian Soil Science Society "ten Years Terrestrial Radioecological Research Following the Chernobyl Accident", Vienna, April 1996.
3) Uchida, S. and Tagami, K.: Eco-Informa'96 (4th International Conference on Global Networks for Environmental Information), Lake Buena Vista, Florida, USA, 4-7 November, 1996.
4) Tagami, K. and Uchida, S.: Eco-Informa'96 (4th

International Conference on Global Networks for Environmental Information), Lake Buena Vista, Florida, USA, 4-7 November, 1996.

5) S. Yoshida and Y. Muramatsu: Determination of trace elements in mushroom, pant and soil samples collected from Japanese forests, 26th International Symposium on Environmental Analytical Chemistry, Vienna, 1996.4.

6) S. Yoshida, Y. Muramatsu and T. Ban-nai : Accumulation of radiocesium and trace elements in mushrooms collected from Japanese forests, International Symposium on Radioecology 1996, Ten Years Terrestrial Radioecological Research Followimg the Chernobyl Accident, Vienna, 1996.4.

7) J. Zhang, C.-Q. Liu, T. Ishii, S. Yoshida and K. Nakamura: The rare earth elements of the rain water over Japan, International Marine Symposium, Mutsu, 1996.11.

8) Ban-nai, T., Muramatsu, Y., Yoshida, S. and Yanagisawa, K: Radiotracer experiments on the uptake of radionuclides by mushrooms and vegetables. International Symposium on Ionsizing Radiation : Protection of the Natural Environment, Stokholm, Sweden, 1996. 5.

9) 田上恵子、内田滋夫、M. Garcia-Leon：第 39 回日本放射線影響学会、豊中、1996.11.

10) 坂内忠明、吉田　聡、村松康行：放射性核種のキノコへの移行に関する RI トレーサー実験. 日本農芸化学会 1996 年度大会、京都、1996. 4.

11) 坂内忠明、村松康行、吉田　聡、内田滋夫、柴田貞夫、安部静子、安部文敏: マルチトレーサー法を用いたきのこへの無機元素の移行に関する研究. 第 33 回理工学における同位元素研究発表会 東京, 1996. 7.

12) 村松康行、 坂内忠明、柳沢啓、吉田聡、内田滋夫：土壌から植物への放射性 I, Cs, Sr, Tc, Mn, Co, Zn の移行に関する研究、日本放射線影響学会第 39 回大会、大阪（千里）、1996. 11.

13) 村松康行、 坂内忠明、柳沢啓、吉田聡：原子力施設周辺住民の放射性及び安定元素摂取量に関する調査研究、放射能調査研究発表会、千葉、1996.12

14) 吉田聡、村松康行：森林内の植物・きのこにおける放射性セシウムと微量元素、1996 年度日本地球化学会年会、札幌、1996.8.

15) Uchida, S. and Tagami, K.: Concentrations of global fallout ^{99}Tc and ^{137}Cs and their behaviour in rice paddy fields., International Conference on Radiation Dosimetry and Safety, Taipei, Taiwan, R.O.C., 31 March – 2 April, 1997.

16) Tagami, K. and Uchida, S.: Aging effect on the bioavailability of Tc, Cs and Co in agricultural Soils under aerobic and anaerobic conditions., International Conference on Radiation Dosimetry and Safety, Taipei, Taiwan, R.O.C., 31 March – 2 April, 1997.

17) Muramatsu, Y. and Yoshida, S.: Effects of microorganisms on the fate of iodine in the environment. XII International Symposium on Environmental Biogeochemistry, Monopoli /Bari (Italy) 1997.

18) Muramatsu, Y., Ban-nai, T., Yoshida, S. and Uchida, S.: Transfer of some radionuclides and trace elements from soil to plant. International Meeting on Influence of Climatic Characteristics upon Behavior of Radioactiove Elements. Rokkasho Village, Japan, 1997. 10.

19) Tagami, K., Uchida, S. and Garcia-Leon, M.: Comparison of a radiation counting method and ICP-MS for the determination of Tc-99 in environmental samples., International Conference on Methods and Applications of Radioanalytical Chemistry, Kona, Hawaii, USA, 6-11 April, 1997.

20) Tagami, K. and Uchida, S.: Plant availability of Mn, Zn, Co, Sr, Cs and Tc in Japanese agricultural soils under upland and paddy field conditions, International Symposium Bio-trace Elements'97 (BITREL'97), Hachioji, Tokyo, 2-4 August, 1997.

21) Tagami, K. and Uchida, S.: Comparison of the TEVA spec resin and liquid-liquid extraction methods for the separation of Tc in soil samples., Asia-Pacific Symposium on Radiochemistry, Kumamoto, 6-9 October, 1997.

22) Uchida, S. and Tagami, K.: A rapid separation method for determination of Tc-99 in environmental waters by ICP-MS. Rapid radioactivity Measurements in Emergency and Routine Situations. Teddington, U. K., 15-17 October, 1997.

23) Tagami, K. and Uchida, S.: Use of a combustion apparatus for low-level ^{99}Tc separation from soil samples., Rapid radioactivity Measurements in Emergency and Routine Situations. Teddington, U. K., 15-17 October, 1997.

24) Tagami, K. and Uchida, S.: Chemical transformation of technetium in soil during the change of soil water conditions., Sixth International Conference on the Chemistry and Migration Behaviour of Actinides and Fission Products in the Geosphere, Sendai, 26-31 October, 1997.

25) Uchida, S. and Tagami, K.: Sorption of technetium onto 129 surface soils collected in Japan., Sixth International Conference on the Chemistry and Migration Behaviour of Actinides and Fission Products in the Geosphere, Sendai, 26-31 October, 1997.

26) S. Yoshida and Y. Muramatsu : Concentration of trace elements and radiocesium in mushrooms, plants and soils collected in forest ecosystems, RIKEN International Symposium, Bio-Trace Elements '97, Hachioji, Tokyo, 1997.8.

27) S. Yoshida and Y. Muramatsu: Transfer of trace elements and radionuclides in Japanese forests, XIII International Symposium on Environmental Biogeochemistry, Monopoli (Bari), Italy, 1997.9.

28) S. Yoshida, Y. Muramatsu, W. Ruhm and A. Rantavaara: Behavior of radiocesium and related stable elements in forest ecosystems, International Meeting on Influence of Climatic Characteristics upon Behavior of Radioactive Elements, Rokkasho-mura, Aomori, 1997.10.
29) S. Yoshida, Y. Muramatsu and S. Uchida: Soil-solution distribution coefficients, Kds, of I^- and IO_3^- for 51 Japanese Soils, Sixth International Conference on the Chemistry and Migration Behavior of Actinides and Fission Products in the Geosphere, Sendai, 1997.10.
30) 吉田聡, 村松康行：森林内の植物・きのこにおける微量元素、理研シンポジウム、生体微量元素 '97、和光市、1997.3.
31) 田上恵子、内田滋夫、Garcia-Leon：第 34 回理工学における同位元素研究発表会, 東京, 1997. 7.
32) 藤川　敬, 田上恵子, 内田滋夫：第 34 回理工学における同位元素研究発表会, 東京, 1997. 7.
33) 吉田 聡： 森林中の植物・きのこへの Cs-137 及び微量安定元素の移行、平成９年度 京都大学原子炉実験所 専門研究会「環境中微量物質動態」、熊取、1997.12.
34) 村松康行、 内田滋夫、吉田聡、田上恵子：ICP-MS を用いた土壌中の U, Th, Pu の分析、第 34 回理工学における同位元素研究発表会 東京, 1997. 6-7.
35) 村松康行：地殻におけるヨウ素の分布と挙動、1997 年度日本地球化学会年会, 八王子, 1997.9.
36) 村松康行：地球規模の放射性物質の分布と挙動、放医研環境セミナー、千葉、1997. 12.
37) 村松康行：放射性ヨウ素（I-129）及び安定ヨウ素の環境中での分布と挙動、平成９年度京都大学原子炉実験所専門研究会「環境中微量物質動態」、熊取（大阪）、1997.12.
38) 坂内忠明：科学館における放射線関連の展示. 第 34 回理工学における同位元素研究発表会 東京、1997. 7.
39) S. Yoshida and Y. Muramatsu: Behavior of trace elements and radionuclides in soil-plant systems, International Workshop on Comparative Evaluation of Health Effects of Environmental Toxicants Derived from Advanced Technologies, Chiba, 1998.1.
40) W. R. Schell and S. Yoshida: Behavior and modelling of radionuclide and non-radionuclide toxicants in the environment, International Workshop on Comparative Evaluation of Health Effects of Environmental Toxicants Derived from Advanced Technologies, Chiba, 1998.1.
41) Tagami, K. and Uchida, S.: Some considerations on the fate of ^{99}Tc in Paddy Fields, Workshop on Comparative Evaluation of Environmental Toxicants, Chiba, Japan, 28-30 January, 1998.
42) Ban-nai, T., Muramatsu, Y., Yanagisawa, K. and Uchida, S: Studies on transfer of radionuclides from soil to vegetables. International Workshop on Comparative Evalution of Health Effects of Environmental Toxicants Derived from Advanced Technologies , Chiba, 1998. 2.
43) S. Yoshida and Y. Muramatsu: Recent developments of forest radioecology in Japan - Possible use of stable elements for predicting the behavior of long-lived radionuclides -, NATO Advanced Research Workshop, Contaminated Forests: Recent Developments in Risk Identification and Future Perspective, Kiev, Ukraine, 1998.6.
44) Muramatsu, Y.: Possibility to use I-129 in the thyroid dose reconstraction and its problems,Seventh Symposium on Chernobyl-related Health Effects, organized by Radiation Effects Association, Tokyo, 1998.11.
45) Tagami, K. and Uchida, S.: Separation of ^{99}Tc in soil samples using a combination of a combustion apparatus and a chromatographic resin and the determination by ICP-MS, Workshop in "Technetium-1998", UK, 8-9 April 1998.
46) Tagami, K. and Uchida, S.: Time Dependence on Plant Availability of Mn, Zn, Co, Sr, Cs and Tc in Japanese Agricultural Soils., First International Conference on Applied Sciences and the Environment (ASE 98), Cadis, Spain, 5-7 October, 1998.
47) Uchida, S. and Tagami, K.: Some Considerations on the Accumulation of Global Fallout ^{99}Tc in Rice Paddy Fields, First International Conference on Applied Sciences and the Environment (ASE 98), Cadis, Spain, 5-7 October, 1998.
48) 村松康行, 吉田聡, 田上恵子, 内田滋夫, 藤川敬：ICP-MS による環境試料中の Pu の分析と同位体比の測定第３６回理工学における同位元素研究発表会 東京, 1998. 6-7.
49) 田上恵子、内田滋夫、Rühm, W., Steiner, M. and Wirth, E.：日本影響学会第 41 回大会、長崎、1998.12.
50) 田上恵子、内田滋夫：環境試料中の ^{99}Tc 定量分析のための標準物質について、第 42 回放射化学討論会、仙台、1998.9.
51) 田上恵子、内田滋夫：日本の水田土壌中の 99Tc 濃度レベル、第 42 回放射化学討論会、仙台、1998.9.
52) 吉田　聡、村松康行：森林生態系における放射性セシウムの挙動とキノコへの蓄積、日本地球化学会 1998 年度年会、福岡、1998.10.
53) 吉田　聡：陸圏と放射能：森林における放射性核種の挙動-キノコを中心にして-、日本放射線影響学会第 41 回大会、長崎、1998.12.
54) 村松康行, 吉田聡： 地殻におけるヨウ素の分布と挙動＜その 2＞海底に沈んだヨウ素は何処にいくか, 日本地球化学会 1998 年度年会, 福岡、1998. 10.
55) 天知誠吾、鎌形洋一、村松康行、金川貴博：ヨウ素循環に関与する環境微生物の生態の解明、第 14 回日本微生物生態学会、京都、1998.11.
56) 村松康行, 吉田聡, 田上恵子, 内田滋夫, 藤川陽子, Rühm, Wirth： ICP-MS を用いた環境試料中の $^{240}Pu/^{239}Pu$ 比に関する研究, 日本放射線影響学会第 41 回大会, 長崎、1998. 12.
57) 塚田祥文、坂内忠明、長谷川英尚：農作物における

部位別元素濃度について、日本保健物理学会第 33 回研究発表会、静岡、1998.5
58) 坂内忠明：科学館における放射線関連の展示．放射線教育に関する国際シンポジウム、神奈川、1998. 12.
59) 内田滋夫、田上恵子、Rühm, W., Steiner, M. and Wirth, E.：チェルノブイル周辺の森林における土壌から植物への Tc-99 の移行、日本原子力学会 1999 年春の年会、東広島市、1999. 3.
60) Muramatsu, Y. , Ishikawa, Y. , Yoshida, S. and Mori, T.: Determination of Th in organs from Thorotrast patients by ICP-MS and XRF, International workshop on health effects of thorotrast, radium, radon and other alpha-emitters 1999, Tokyo, 1999. 1.
61) Muramatsu, Y. : Determination of Th, U and Pu in biological and environmental materials by ICP-MS. Bundesamt fuer Strahlenschutz (BfS) Berlin, invited lecture, 1999.10.
62) Tagami, K. and Uchida, S., Hamilton, T. and Robison, W.: Measurement of technetium-99 in Marshall Islands soils by ICP-MS, Conference on Low Level Radioactivity Measurement Techniques, Mol, Belgium, 18-22 October, 1999.
63) Uchida, S., Tagami, K., Rühm, W., Steiner, M. and Wirth, E.: Separation of Tc-99 in soil and plant samples collected around the Chernobyl reactor using a Tc-selective chromatographic resin and determination of the nuclide by ICP-MS., Conference on Low Level Radioactivity Measurement Techniques, Mol, Belgium, 18-22 October, 1999.
64) Tagami, K. and Uchida, S.: The Use of ICP-MS for the measurement of low-level technetium-99 in environmental samples, CITAC'99 Japan Symposium on Practical Realization of Metrology in Chemistry for the 21st Century, Tsukuba, Japan, 9-11 November, 1999.
65) Tagami, K. and Uchida, S.: Determination of technetium-99 in environmental standard reference materials by ICP-MS, CITAC'99 Japan Symposium on Practical Realization of Metrology in Chemistry for the 21st Century, Tsukuba, Japan, 9-11 November, 1999.
67) Tagami, K. and Uchida, S.: Development of a separation method for ^{99}Tc in environmental samples using a TEVA resin and its concentration levels in Japan, The Second Japanese-Russian Seminar on Technetium, Shizuoka, Japan, 29 November – 2 December, 1999.
68) S. Yoshida, Y. Muramatsu, M. Steiner, M. Belli and B. Rafferty: Concentrations of radiocesium and related stable elements in different comppartments of forest ecosystems, XIVth International Symposium on Environmental Biogeochemistry, Huntsville, Canada, 1999.9.
69) 村松康行、田上恵子、吉田聡、内田滋夫、田中睦、藤川敬：環境試料中の Pu の濃度及び同位対比の ICP-MS による測定，第 36 回理工学における同位体元素研究発表会，東京,1999, 7.
70) 村松康行、吉田聡、U. Fehn：ヨウ素の地殻における分布と挙動〈その 3〉海底堆積物の沈み込みに伴うヨウ素の挙動，日本地球化学会年会，つくば，1999.9-10
71) 村松康行、吉田聡、天知誠吾：ヨウ素の生物地球化学的サイクルについて—^{129}I の長期的挙動との関連で—，放射線影響学会第 42 回大会，広島，1999. 9
72) 吉田 聡、村松康行、M. Steiner、M. Belli、B. Rafferty：森林生態系内の植物における放射性 Cs と関連安定元素の関係、日本放射線影響学会第 42 回大会、広島、1999.9.
73) 吉田 聡：日本の土壌に対するヨウ素の分配係数、平成１１年度 京都大学原子炉実験所 専門研究会「天然バリア Kd」、熊取、1999.11.
74) 天知誠吾、鎌形洋一、村松康行、金川貴博 :ヨウ素循環に関与する環境微生物の貢献度,、第 15 回日本微生物生態学会、高知、1999.11.
75) 田上恵子、内田滋夫、García-Tenorio, R. : ICP-MS による環境試料中のウラン同位体測定、第 43 回放射化学討論会、つくば、1999.10.
76) 吉田 聡、坂内忠明、村松康行、田上恵子、内田滋夫：JCO 敷地内で採取した土壌と植物中の放射性核種の分析、「環境放射能」研究会、つくば、2000.3.
77) Muramatsu, Y., Noda, Y., Yonehara, H., Yoshida, S., Yokawa, M., Tagami, K., Nakamura, Y. and Akashi, M.: Estimation of neuttron fluences for three heavily exposed patients based on activation of biological materials from the Tokai-mura criticality accident. Workshop on the Criticality Accident at Tokai-mura, IRPA Satellite Meeting, 2000.5.
78) Muramatsu, Y., Ishigure, N., Noda, Y., Yonehara, H., Yoshida, S., Yukawa, M., Tagami, K., Bannai, T., Uchida, S., Akashi, M., Hirama T. and Nakamura Y.: Estimation of radiation doses based on ^{24}Na produced in biological materials from three exposed patients in the Tokai-mura criticality accident, International Symposium on the Criticality Accident in Tokai-mura, 2000.12, Chiba.
79) Tagami, K. and Uchida, S.: Global fallout Technetium-99 Levels in Japanese Paddy Soils., The 10th International Congress of The International Radiation Protection Association, Hiroshima, Japan, May, 14-19, 2000.
80) Uchida, S., Tagami, K. and García-León, M.: Redetermination of Low-level ^{99}Tc in Planchet Samples by ICP-MS. The 10th International Congress of The International Radiation Protection Association, Hiroshima, Japan, May, 14-19, 2000.
81) Tagami, K. and Uchida, S.: Distribution of Technetium-99 in surface soils, *The International Workshop on Distribution and Speciation of Radionuclides in the Environment*, Rokkasyo, Aomori, Japan, October 11-13, 2000.
82) Uchida, S and Tagami, K.: Time dependence on plant availability of radionuclides in two Japanese soils under

upland and paddy field conditions, *The International Workshop on Distribution and Speciation of Radionuclides in the Environment,* Rokkasyo, Aomori, Japan, October 11-13, 2000.

83) Ban-nai, T., Hisamatsu, S., Yanai-Kudo, M., Hasegawa, H. and Torikai, Y.: The concentration of Cs, Sr and other elements in the water samples collected n the paddy field. *The International Workshop on Distribution and Speciation of Radionuclides in the Environment,* Rokkasyo, Aomori, Japan, October 11-13, 2000.

84) Muramatsu, Y., Yoshida, S. and Amachi, S.: Roles of Microbial activities on the distribution and speciation of iodine in the soil environment. *The International Workshop on Distribution and Speciation of Radionuclides in the Environment,* Rokkasyo, Aomori, Japan, October 11-13, 2000.

85) Yoshida, S. Muramatsu, Y., Tagami, K. and Uchida, S.: Determination of uranium isotopes in soil and plant samples collected on the JCO grounds, *The International Workshop on Distribution and Speciation of Radionuclides in the Environment,* Rokkasyo, Aomori, Japan, October 11-13, 2000.

86) S. Yoshida, Y. Muramatsu, M. Steiner, M. Belli, A. Pasquale, B. Rafferty, W. Ruhm, A. Rantavaara, I. Linkov, A. Dvornik and T. Zhuchenko: Relationship between radiocesium and stable cesium in plants and mushrooms collected from forest ecosystems with different contamination levels, 10th Internatiomnal Congress of the International Radiation Protection Association (IRPA-10), Hiroshima, Japan, 2000.5.

87) I. Linkov, S. Yoshida and M. Steiner: Fungi contaminated by radionuclides: critical review of approaches to modeling, 10th Internatiomnal Congress of the International Radiation Protection Association (IRPA-10), Hiroshima, Japan, 2000.5.

88) S. Yoshida, T. Ban-nai, Y. Muramatsu, K. Tagami and S. Uchida: Determination of fission products and uranium isotopes in soil and plant samples collected around the uranium conversion building in JCO campus, Workshop on The Criticality Accident at Tokai-mura, Hiroshima, Japan, 2000.5.

89) 村松康行、吉田聡、坂内忠明、田上惠子、内田滋夫：JCO 転換試験棟周辺で採取した環境試料中の放射性核種の濃度と同位体比, 第 37 回理工学における同位体元素研究発表会、東京、2000. 7.

90) 田上恵子、内田滋夫：ICP-MS による岩石・土壌試料中のレニウム分析法の検討、第 37 回理工学における同位元素研究発表会、東京、2000.7.

91) 田上恵子、内田滋夫：ＩＣＰ-ＭＳによる環境試料中Ｕ同位体比測定のための分離濃縮法、第４回分析化学東京シンポジウム、幕張、2000.9.

92) 田上恵子、内田滋夫：ICP-MS 法による環境水中のレニウム分析法の検討、第 44 回放射化学討論会、神戸、2000.9.

93) 天知誠吾、 鎌形洋一、金川貴博、 村松康行：ヨウ素の揮発に与える環境微生物の影響, 第 37 回理工学における同位体元素研究発表会、東京、2000. 7.

94) 吉田 聡、村松康行、田上恵子、内田滋夫、坂内忠明、米原英典、SAHOO Sarata Kumar： JCO 敷地内で採取した土壌・植物中の 235U と 238U、 日本放射線影響学会第 43 回大会、東京、2000.8-9.

95) 高橋千太郎、孫学智、N. V. Chandrasekharane、久保田善久、佐藤宏、田場裕一、吉田聡： 重粒子線照射によるラット脳組織の損傷：組織学的変化、元素組成の変動、および遺伝子の発現、 日本放射線影響学会第 43 回大会、東京、2000.8-9.

96) 吉田 聡、村松康行： 二重収束型 ICP-MS を用いた土壌・植物中の U・Pu の濃度と同位体比の測定、2000 年度日本地球化学会第 47 回年会、山形、2000.9.

97) 坂内忠明, 村松康行, 田上惠子, 内田滋夫, 吉田聡, 木村真三, 渡辺嘉人： JCO 敷地内で採取した植物中の人工放射性核種, 日本放射線影響学会第 43 回大会, 東京, 2000.8-9.

98) 村松康行, 野田豊, 米原英典, 石榑信人, 湯川雅恵, 田上恵子, 中村裕二, 明石真言：東海村の臨界事故で被曝した 3 人の作業員の血液、尿、嘔吐物等の放射能測定と中性子フルエンスの推定, 日本放射線影響学会第 43 回大会, 東京, 2000.8-9.

99) 村松康行：上総層群中のヨウ素はどこから来たか？-地殻におけるヨウ素の分布との関係から考える -、第３回ヨウ素利用研究シンポジューム、千葉、2000. 11.

100) 天知誠吾、鎌形洋、金川貴博、 村松康行：ヨウ素の揮発に関与する環境微生物、第３回ヨウ素利用研究シンポジューム、千葉、2000. 11.

101) 村松康行：臨界事故で被ばくした作業員の血液、尿、嘔吐物等のガンマー線測定と中性子フルエンスの推定、放医研環境セミナー、千葉、2000. 12.

102) 吉田 聡、坂内忠明、村松康行、田上恵子、内田滋夫：JCO ウラン転換棟周辺で採取した土壌・植物中の核分裂生成物とウラン同位体、第 28 回放医研環境セミナー、千葉、2000.12.

103) 渡辺嘉人、木村真三、坂内忠明、サフーサラタクマール、小藤久毅、米原英典：臨海事故後のウラン加工工場敷地内で採取した植物試料中のβ線放出核種の濃度測定、日本放射線影響学会第 43 回大会、東京、2000. 8-9.

104) 吉田 聡、村松康行：ICP-MS を用いた長半減期核種および安定元素の分析と環境挙動解析への応用、第２回「環境放射能」研究会、つくば、2001.3.

105) 内田滋夫：移行パラメータについて、第９回原子力研究総合センターシンポジウム、東京、2001.1.

106) 高橋知之、駒村美佐子、内田滋夫：水田土壌中 ^{90}Sr 移行評価モデルの不確実性に関する検討、日本原子力学会「2001 年春の年会」、東京、2001.3.

第３サブグループ：
制御実験生態系の構築に関する研究

武田 洋、宮本霧子、柳澤　啓、府馬正一、井上義和、
渡辺嘉人（人間環境研究部）、石井伸昌（科学技術特別研究員）

Studies on Construction of Controlled Experimental Ecosystems for ecotoxicity evaluation.

Hiroshi Takeda, Kiriko Miyamoto, Kei Yanagisawa, Shoichi Fuma, Yoshikazu Inoue ,
Yoshito Watanabe (Division of Human Radiation Environment), Nobuyoshi Ishii (JSTC, Research Fellow)

The aim of the third sub-group was to construct controlled experimental ecosystems applicable for an ecotoxicity evaluation at the community level and to evaluate the relative ecotoxicity for various toxic agents in comparison with radiation. As a model of aquatic microbial ecosystem, a microcosm was constructed and the stability and reproducibility as an experimental tool were investigated. This microcosm consists of flagellate algae *Euglena gracilis Z* as a producer, ciliate protozoa *Tetrahymena thermophila B* as a consumer, and bacteria *Escherichia coli DH5 α* as a decomposer. Three species in the microcosm interact with each other and their populations can be maintained for more than one year. The microcosm was used for evaluating the ecotoxicity of radiation (γ- rays) and some other toxicants (ultraviolet radiation ; UV-C, acidification and metals such as Gd^{3+}, Cu^{2+}, Mn^{2+}, Ni^{2+} and Al^{3+}). This microcosm test could evaluate not only direct effects but also secondary effects, which should be taken into account for ecological risk assessment. The results indicate that the toxicity of 500 or 1,000 Gy γ- rays is equivalent to 50 kerg/mm^2 UVC, pH4 acidification, 300 μM Gd^{3+}, 100 μM Cu^{2+}, 10,000 μM Mn^{2+} and 100 μM Ni^{2+} , respectively. This suggests that microcosm tests are useful for comparative evaluation of ecotoxicity. By using this experimental model ecosystem, the combined effects from radiation and some other toxicants are now being investigated.

１．緒言

本グループ研究では、人だけでなく生態系を対象として各種有害因子による影響を評価する手法の開発が課題であった。生態系は無機的環境要素と様々な生物種で構成され、その機能は生物種間の相互作用による物質やエネルギーの流れによって支えられている。このような生態系の構造や機能への影響を評価する目的では、自然の生態系はあまりに複雑で解析が困難である。そこで我々は、自然生態系の基本的要素を包含しながらも、室内実験が可能な制御実験生態系を利用することとした。制御実験生態系とは、自然生態系の空間的スケールや構成要素をある程度制御した条件下で操作実験が可能なモデル生態系である。本研究では水圏生態系のモデルであり、フラスコや試験管サイズでの実験が可能なマイクロコズムを用いて、様々な有害因子による負荷実験を行なった。主に用いたマイクロコズムは、水圏微生物生態学の基礎的研究のために最近開発されたもので、ユーグレナ、テトラヒメナ、大腸菌の３者微生物で構成されたものである。この３者マイクロコズムの生物間相互作用や実験系としての再現性や安定性についての検討は、開発者らによっても短期的には行なわれていたが、我々の研究目的に必要な長期間実験にも使用可能であるかを検討することから本研究を開始した。なお、この３者微生物で構成されるマイクロコズム以外に、藻類とミジンコで構成されるマイクロコズムも一部本研究に使用した。一方、有害因子としては、放射線（^{60}Co-γ線）を始めとし、紫外線（UV-C）、電磁場、酸性化および金属類（銅；Cu^{2+}、ニッケル；Ni^{2+}、ガドリニウム；Gd^{3+}、アルミニウム；Al^{3+}、マンガン；Mn^{2+}）を負荷実験に使用した。本研究では、これらの有害因子の相対的な危険度を評価することを一義的な目標としたが、生態系における影響の発現と防御のメカニズムを解析するための基礎的情報の取得にも努めた。このため、マイクロコズムを構成する微生物単独培養系でも同様な負荷実験を行った。

２．実験および結果

2-1. ３者マイクロコズムの実験系としての有効性の検討

本研究に用いた３者マイクロコズムは愛媛大学の川端らによって開発されたもので、生産者として鞭毛虫ユーグレナ (*Euglena gracilis Z*)、消費者として繊毛虫テトラヒメナ（*Tetrahymena thermophila B*）、分解者として大腸菌（*Echerichia coli DH5 α*）から構成されたものである。これら３者の微生物はいずれも無菌株として分譲されたものを使用している。マイクロコズムを培養するための基本培地は、無機栄養塩および金属塩を含んだ Taub 培地を用い、これに有機物としてプロテオースポリペプトンを0.5mg/mlとなるように添加したものをマイクロコズム培地として使用した。このマイクロコズム培地を、フラスコやネジ口試験管に一定量を入れ、オートクレーブ滅菌後、テトラヒメナ、ユーグレナ、大腸菌を接種し、マイクロコズムを培養した。なお、培養条件は、温度 25 度℃、照度 2,500lux（明暗周期 12 時間）で静置培養とし、培養開始後様々な時点で、マイクロコズム構成微生物の個体数密度（Population density）を計測した。ユーグレナとテトラヒメナは顕微鏡

観察により個体数を計測し、また大腸菌は PB 培地により混釈平板法で生菌数（コロニー形成能力を持つ菌）を測定した。まずは、この３者マイクロコズムの基礎データを得るため、また安定性や再現性を確認するために、以下のようにマイクロコズム構成生物種の単独、２者及び３者の長期間培養実験を行った。

単独培養実験

マイクロコズムを構成する３種微生物をそれぞれ単独に培養した場合、テトラヒメナは培養開始２０日目には死滅した。一方、大腸菌は培養開始直後に急速に増殖したが、その後は次第に減少し２５０日目以降はその減少速度が早くなる傾向を示した。ユーグレナは他の生物種に比べ安定した個体数密度を維持したが、200 日目以降は減少する傾向を示した。この結果、マイクロコズムを構成する個々の生物種の単独培養では、長期間安定した個体数密度を維持することは出来ないことが判明した。

２者培養実験

２種の微生物を組み合わせて培養した場合、比較的安定な個体数密度を維持したのはユーグレナのみで、大腸菌とテトラヒメナはその共存者によって異なる個体数密度とその経時的変化を示した。大腸菌は共存者がユーグレナの場合よりテトラヒメナの場合にその個体数密度は低く押さえられた。また、テトラヒメナはユーグレナとの共存では培養開始後 30 日目に死滅し、テトラヒメナの被捕食者（餌）である大腸菌との共存でも培養開始後 30 日目以降次第にその個体数は減少し、300 日目には死滅した。このように、マイクロコズム構成生物種の中で外部からの光エネルギーを利用して生存できるユーグレナ以外の生物種は、２者培養においても安定した個体数密度を維持することは出来なかった。なお、ユーグレナもテトラヒメナとの組み合わせでは、培養開始後 200 日以降にはその個体数は減少し、一年間近くその個体数密度が安定していたのは、大腸菌との組み合わせの場合のみであった。

３者マイクロコズム培養実験

３者の微生物（ユーグレナ、テトラヒメナ、大腸菌）を組み合わせて培養した場合には、各生物種の個体数密度が培養開始 40 日目以降ほぼ一定となり、３者の生物種が相互作用し共存関係が成立したものと推定された。このような結果は、以前川端研究室で行われた結果と一致することから、この３者マイクロコズムが再現性のある実験系であることが確認された。また今回の実験で、生物種間の共存関係は一年以上維持されることが判明し、長期間の影響評価実験にも利用できる可能性を示した。Fig.1 に示したように、各生物の個体数は次第に減少する傾向はあるが、３者系としてはほぼ 1000 日間維持することが出来た。

３者マイクロコズムの共存系が成立するメカニズムについては、以下のようなことがこれまでの実験から明らかになっている。マイクロコズム培地中にはプロテオースペプトンが存在し、これを栄養素として、まず大腸菌とユーグレナが増殖し、テトラヒメナは餌である大腸菌がある程度増殖した時点でその個体数を増加させる。プロテオースペプトンは大腸菌やユーグレナの増殖に伴い比較的短期間で枯渇するが、葉緑体を持つユーグレナが系外から唯一供給される光エネルギーを物質エネルギー（有機物）に変換し、これを系内の栄養源として供給する。ユーグレナによるこの光合成過程では、分解者である大腸菌によって供給される無機物が利用される。また、各微生物の代謝産物や死骸が互いに他の微生物の生存と増殖に促進的に働くことを明らかにしている。Fig.2 には、このような３者マイクロコズムの生物種間相互作用を示している。

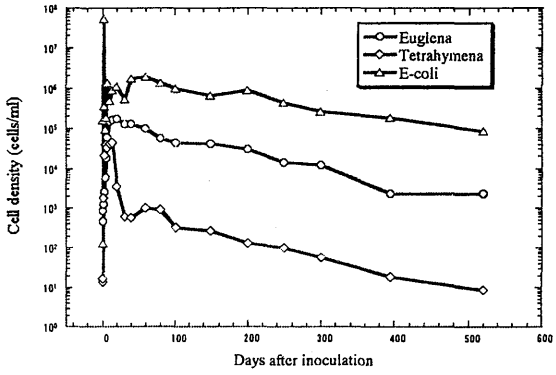

Fig. 1. Variations in the population density of three microbes in the microcosm after inoculation.

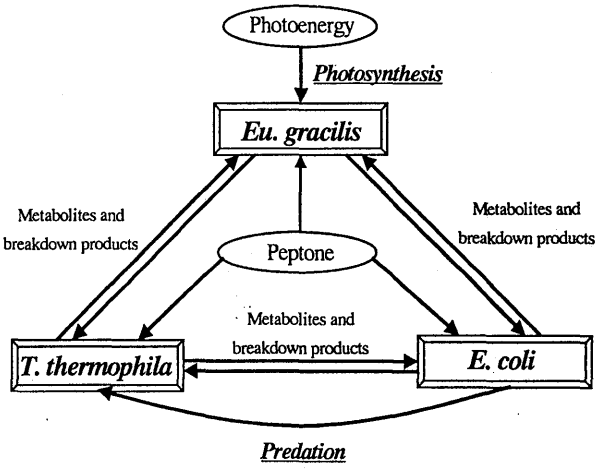

Fig. 2. Interactions among three microbes in the microcosm.

2-2.各種有害因子の負荷による安定期３者マイクロコズム構成生物種の個体数変化

培養開始後各構成生物の個体数密度がほぼ一定となる安定期の３者マイクロコズムに、放射線（γ線）、紫外線(UV-C)、酸性化および重金属類を負荷し、マイクロコズム構成生物の個体数変化を調べた。その結果から各有害因子の比較影響評価を試みた。

放射線

培養開始後 56 日目の安定期にある３者マイクロコズムへの放射線（^{60}Co-γ線）の負荷実験を行った。負荷したγ線の線量は 0、50、100、500、1000、5000 Gy とし、負荷前後のマイクロコズム構成生物種の個体数変化を調べた。50 と 100 Gy の照射で、大腸菌の個体数が照射直後一時的

な減少を示し、500 Gy の線量で大腸菌は死滅した。他の生物種は、500 Gy 以上の線量で経時的な個体数変化が見られ、5000 Gy の線量ですべての生物種が照射直後に死滅した。このように、マイクロコズムへの放射線影響はその線量に依存した応答を示した。Fig.3 には 500 Gy 照射の結果を示している。

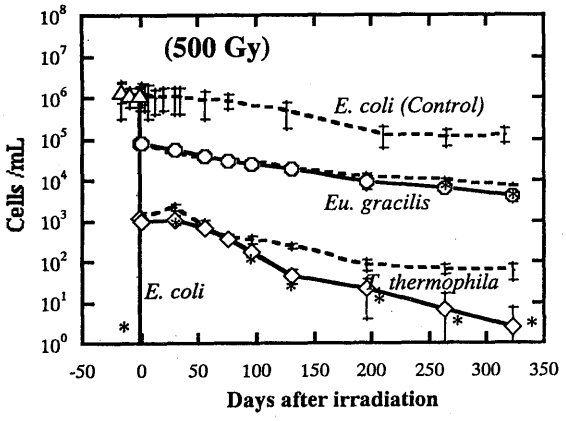

Fig. 3. Effects of γ-rays on the populations in the microcosm.

なお、テトラヒメナの放射線に対する半致死線量（LD50）は約 4000Gy であることが明らかにされており、500Gy や 1000Gy の照射でテトラヒメナの個体数に減少が見られたのは放射線による直接的な影響ではなく、被捕食者である大腸菌が死滅したことによる間接的影響のためと考えられた。また、1000Gy の照射でテトラヒメナの個体数が一時的にコントロールより増加したり、またその後の個体数減少の程度が 500Gy 照射の場合より少ないのは、大腸菌の死骸を利用することで競争関係にあるユウグレナが 1000Gy の照射で個体数が減少したことに関連しており、これも間接的な影響と推定された。このように、放射線によるマイクロコズム系への影響には直接的な影響だけでなく系内の生物種間相互作用に基づく間接的な影響も観察された。

紫外線

培養開始後 70 日目の安定期にある 3 者マイクロコズムへの紫外線（UV-C）負荷実験を行った。負荷した紫外線の線量は、0、1、10、50、100 kerg/mm2 であった。1kerg/mm2 の線量からすべての生物種が照射直後一時的に個体数の減少を示し、50 kerg/mm2 の線量ではユーグレナとテトラヒメナが死滅し、100 kerg/mm2 の線量では 3 生物種すべてが死滅した。なお、50 kerg/mm2 の線量を負荷した場合、大腸菌は一時的にその個体数を減少させるが、その後は増殖ししばらくの期間はコントロールよりむしろ高い個体数を維持した。これは、大腸菌の捕食者であるテトラヒメナが紫外線の直接影響によって死滅し、紫外線による致死効果を免れた大腸菌がテトラヒメナに補食されることなく、また培地中のプロテオースペプトンを他生物種と争うことなく利用し増殖したためと推定された。大腸菌で見られたこのような個体数の経時的な変化も、マイクロコズム系内の生物種間相互作用に基づく間接的影響と見なすことができる。

酸性化

酸性化は 1 Nの硫酸と硝酸の等量混合液を用い、マイクロコズム培養開始後 67 日目および 128 日目の培地を pH4 に調製した。培養開始 67 日目に酸性化したマイクロコズムでは、大腸菌の個体数が一時的に減少するが、酸性負荷後 10 日目前後に対照と同じ個体数に回復した。この回復は共存者であるユーグレナによる培地の中性化によりもたらされるものと考えられた。一方、128 日目に酸性化したマイクロコズムでは、まず大腸菌が死滅し、それに引き続きテトラヒメナも死滅した。このテトラヒメナの死滅は被捕食者である大腸菌の死滅による間接影響であると推測された。このように、マイクロコズムの酸性化に対する緩衝能力は培養期間によって異なることが判明した。

金属類

銅（Cu^{2+}）：安定期のマイクロコズムに $CuSO_4$ 溶液を加え、その構成生物種の個体数に与える影響を調べた。1μM 及び 10μM Cu^{2+}ではどの生物種にも影響が見られなかった。100μM では、まず大腸菌がすみやかに死滅し、次いでテトラヒメナも死滅したがユーグレナには影響が見られなかった。ニッケル（Ni^{2+}）：安定期のマイクロコズムに $NiSO_4$ 溶液を加え、その構成生物種の個体数に与える影響を調べた。1μM 及び 10μM Ni^{2+}では、どの生物種にも影響が見られなかった。100μM では、まずテトラヒメナがすみやかに死滅し、次いで大腸菌も死滅したがユーグレナには影響が見られなかった。他の金属では、まず大腸菌が死滅し、次いでテトラヒメナが死滅するという順序であったが、Ni^{2+}ではこれが逆であった。1000μM では、テトラヒメナと大腸菌がすみやかに死滅し、次いでユーグレナも死滅した。

マンガン（Mn^{2+}）：安定期のマイクロコズムに MnCl2 溶液を加え、その構成生物種の個体数に与える影響を調べた。100μM Mn^{2+}では、大腸菌が一時的に減少したが、ユーグレナとテトラヒメナには影響が見られなかった。500μM では、大腸菌とテトラヒメナが一時的に減少したが、ユーグレナには影響が見られなかった。1000μM では、大腸菌とテトラヒメナが一時的に減少したが、ユーグレナは対照よりも個体数が若干増加した。10000μM では、大腸菌がすみやかに死滅し、次いでテトラヒメナも死滅したが、ユーグレナは対照よりも個体数が若干増加した。

ガドリニウム（Gd^{3+}）：安定期のマイクロコズムに GdCl3 溶液を加え、その構成生物種の個体数に与える影響を調べた。50μM Gd^{3+}では、どの生物種にも影響が見られなかった。100μM では、大腸菌が一時的に減少したが、その後すみやかに回復し、個体数は対照よりも増加した状態で維持された。ユーグレナとテトラヒメナには影響が見られなかった。300μM では大腸菌は、ほぼ死滅し、テトラヒメナは一時的に減少したが、ユーグレナには影響が見られなかった。1000μM では、全生物種がすみやかに死滅した。

アルミニウム（Al^{3+}）：酸性雨により土壌から溶出したアルミニウムが、湖沼などの水圏生態系に影響を及ぼす可能性が指摘されている。そこで、マイクロコズムを使って、アルミニウムが水圏微生物生態系に及ぼす影響を評価した。生産者であるユーグレナ、消費者であるテトラヒメナ、分解者である大腸菌から構成されるマイクロコズムの定常期

Table 1. Effect levels of ionizing radiation and other toxic agents on the microcosm.

Effects	γ-ray (Gy)	UV (kerg/mm²)	Electric field	Magnetic field	Acidification	Metals (μM)				
						Cu	Mn	Gd	Ni	Al
No damge	—	1	1000 V ×3h25min	0.1 T ×3h34min	pH4.5	10	—	50	10	10
Population decrease	50-100	10	—	—	pH 4	—	100-1000	100	—	100-500
Extinction of one or two species	500-1000	50	—	—	pH 3.5	100	10000	300	100	—
Extinction of all species	5000	100	—	—	—	—	—	1000	1000	1000

*: − denotes "not examined".

に$AlCl_3$を加え、各生物種の個体数に与える影響を調べた。10μMのアルミニウム負荷では影響が見られなかった。100μM では、ユーグレナが負荷51日目以降でコントロールよりも減少したが、大腸菌には影響が見られず、テトラヒメナでは負荷直後に一時的な増加が認められた。500μMでは、アルミニウム負荷直後に大腸菌は大きく減少したが、速やかに回復し個体数は一旦コントロールより多くなった後コントロールと同程度になった。ユーグレナとテトラヒメナは、負荷直後にそれぞれのコントロールよりも一時的に増加した。1000μM では、まず大腸菌が、次いでテトラヒメナが速やかに死滅し、その後ユーグレナも死滅した。このように、基本的にはマイクロコズムに対するアルミニウムの影響は濃度依存的であったが、一部の構成生物（ユーグレナ）に着目するとその影響には必ずしも濃度依存性が見られなかった。

2-3. 3者マイクロコズム構成生物の個体数変化を指標にした比較影響評価

安定期にある3者マイクロコズムへの様々な有害因子（γ線、紫外線、電磁場、酸性化および金属類）負荷実験によって見られた直接的および間接的影響を、その程度によって、1：影響が見られないレベル、2：構成微生物のいずれかに個体数の一時的減少が見られるレベル、3：構成微生物の1種または2種が死滅するレベル、4：構成微生物のすべてが死滅するレベルの4段階に分けて比較した。例えば、1種または2種が死滅する第3のレベルは放射線では500Gyから1000Gyに相当し、このレベルの影響は50 kerg/mm2の紫外線（UV-C）、pH4.0への酸性化、100μMの銅（Cu^{2+}）あるいはニッケル（Ni^{2+}、300μMのガドリニウム（Gd^{3+}）、1,000μM のアルミニウム（Al^{3+}）、10,000μMのマンガン（Mn^{2+}）にMのマンガン（Mn^{2+}）に相当することが判明した（Table1）。

このように放射線と他の有害因子による影響の程度が数値化され、さらに明解な比較指標として有害物質の濃度1μM/Lによる影響の程度を放射線の吸収線量であるグレイ（Gy）に換算して表すと、重金属Mn^{2+}、Al^{3+}、Gd^{3+}、はそれぞれ0.05Gy、0.5Gy、1.7Gy、そしてNi^{2+}とCu^{2+}は5Gyになると試算された。

2-4. 物質動態の解析法およびその変化を指標にした影響評価法の検討

生態系が有する機能への影響を評価するためには、構成生物種への直接的な影響だけでなく、生物種間の物質循環やエネルギー流を解析する必要がある。この物質動態解析のためのモデル実験系として、藻類－ミジンコ－グッピィーで構成したボトルおよび水槽サイズのマイクロコズムを構築した。この実験系を用いて、炭素の安定同位体^{13}Cを利用したトレーサー実験を行なった。

<u>$^{13}CO_2$アナライザによる淡水プランクトン中の^{13}C濃度分析</u>

^{13}Cの分析には$^{13}CO_2$アナライザ（日本分光 EX-130）を用いた。この装置は試料を酸素気流中で燃焼し生成した炭酸ガスを装置の吸収セルに導入して$^{12}CO_2$,$^{13}CO_2$の赤外線吸光度を測定し^{13}C濃度を計算する。通常検量線はnaturalのグリシンおよび^{13}C濃度が99atom%のグリシンを使用して作成する。その方法はnatural試料として炭素量100μgから1000μgまで100μg毎に対応する量のグリシンを用いて調製し、^{13}Cの試料は^{13}C濃度99atom%のグリシンを炭素量として1.1μgから11μgまで1.1μg毎にとり両者を燃焼分析した際の$^{12}CO_2$,$^{13}CO_2$による赤外線吸収信号から作成する。この$^{13}CO_2$アナライザを使用して淡水中に生育する動物性プランクトン(ミジンコ)への食物連鎖を介した炭素の移行を調べた。

実験に用いたアクリル樹脂製の容器に、貯水池から採取し実験室内で繁殖させた藻類の培養液3リットルを入れ、$^{13}CO_2$ (99 atom%) 350ppmを添加した混合ガスを通気した。これを天然光の条件下に置きオオミジンコ（Daphnia magna）を入れて培養し、適時（4-8時間後）採取した。採取したミジンコは1個体ずつ石英製の燃焼容器に入れて凍結乾燥しミジンコ有機成分中^{13}C濃度を求めた。この結果、天然光の条件下で$^{13}CO_2$通気開始後数時間で藻類に^{13}Cは取り込まれ、さらに^{13}Cはミジンコに移行していることが確認された。今後この^{13}Cトレーサー法を用いて、様々な有害因子を負荷した場合にモデル生態系内の物質循環がどのような影響を受けるかについて調べることとした。

<u>紫外線負荷によるミジンコへの^{13}C取り込みへの影響</u>

^{13}Cトレーサー法によるモデル生態系への影響研究として、紫外線負荷の場合の実験を行なった。すなわち、藻類およびミジンコで構成されるモデル生態系に紫外線（UV-B）を照射し、その照射直後に$NaH^{13}CO3$を添加し24時間培養後にミジンコに取り込まれた^{13}C濃度を測定した。なお、藻類の培養は水田土壌1kgに乾燥鶏糞5gを添加して水10リットルを加えて攪拌し温室内に放置した。約10日で藻類が増殖し緑色に変化した。溶液中のプランクトンを顕微鏡で観察したところ増殖した藻類はイカダモ、

クロレラおよびムレミカズキモであった。また紫外線照射はUV-Bランプを使用して95μw/cm2で15分、30分、60分間行った。本実験の結果、ミジンコへの^{13}Cの取り込みが30分間以上の紫外線照射によって低下することが判明した。これは紫外線の照射によりミジンコの藻類摂食量が低下したためと考えられる。以前より、ミジンコを使用した有害物質の毒性試験法は行なわれてきたが、そのエンドポイントとして実質的には致死率を指標にしている。^{13}Cをトレーサーとした物質移行を影響指標として場合、ミジンコが死亡しない線量における照射の影響を検出することが可能であり、より感度の高い生態系影響指標として利用できる可能性が示唆された。

2-5. 3者マイクロコズムによる放射線と酸性化の複合影響評価

生態系は様々な有害因子に曝露される可能性がある。したがって,放射線の生態系影響を評価するためには、放射線とそれ以外の有害因子の複合影響を考慮する必要がある。そこで、放射線と酸性化が水圏微生物生態系（マイクロコズム）に与える複合影響について検討した。放射線負荷は^{60}Coをソースとし、線量率72Gy/minのγ線を100Gy照射した。また、酸性化負荷は酸性雨を模擬した0.1N硝酸+0.1N硫酸等量混合液をマイクロコズム培地に加えｐＨ４とした。実験は、56日間培養した安定期のマイクロコズムに放射線および酸性化をそれぞれ単独に負荷した場合と放射線負荷直後にｐＨ４酸性化負荷した場合、そしていずれの負荷も与えない場合の４つのシリーズで行った。負荷を与えた後、各シリーズのマイクロコズム構成生物の個体数、クロロフィルα量、ATP量、培地のｐＨとイオン濃度（NO_3^-、SO_4^{2-}、NH_4^+など）が120日間にわたって測定した。

その結果,放射線単独負荷では、負荷直後に大腸菌の個体数がコントロールよりも有意に減少したが、その後はコントロールレベルまで回復した。その他の生物種には影響が見られなかった。酸性化単独負荷では、大腸菌がコントロールよりも減少する傾向が見られ、テトラヒメナは有意に減少し、ユーグレナはわずかに増加した。これに対し、放射線と酸性化の複合負荷では、負荷直後に大腸菌がコントロールよりも有意に減少した。その後個体数は回復したが、コントロールよりも少ない傾向を示した.テトラヒメナは有意に減少し、ユーグレナはわずかに増加した.以上の結果より、放射線と酸性化による複合負荷はマイクロコズム構成生物の個体数変化に対し相加的な影響を与えることが判明した。

3.考察

放射線とその他様々な有害因子による生態系への影響を比較評価する目的で我々が用いたモデル生態系（３者マイクロコズム）は、非常にシンプルではあるが、生産者、消費者、分解者という生態系の基本的な構造と機能の一部を含んだ実験系である。この実験系は、期間に制限はあるが構成している生物種を単独培養あるいは２者培養することが可能である。本研究では、３者マイクロコズムで見られた影響が発現するメカニズムを解析するため、必要に応じて単独培養への負荷実験を行った。その結果、３者マイクロコズムへの負荷実験では、生物間あるいは生物と有害因子間での相互作用による間接影響や二次的影響の評価も可能であることを明らかにした。

現在、生態系への影響評価については、放射線影響研究の分野でも重要な課題であり、IAEAやICRPも取り上げている。マイクロコズムは生物間相互作用による放射性物質の動態や放射線による生態系影響発現機構の解析ツールとして放射線環境安全研究に有効に利用できると期待される。

本研究での成果

① 生態系影響研究のモデル実験系として３者マイクロコズムを構築
② 物質動態解析研究のモデル実験系として藻類－ミジンコ－グッピィーで構成したボトルおよび水槽サイズのマイクロコズムを構築
③ 炭素動態解析のための^{13}Cトレーサー法を確立
④ ３者マイクロコズムでの放射線（γ線）、紫外線（UV-C）、電磁場、酸性化、金属類の影響解析
⑤ ３者マイクロコズムでの各種有害因子の比較影響評価

研究発表

（研究論文）

1) Fuma,S., Miyamoto,K., Takeda,H., Yanagisawa.K., Inoue,Y., Sato,N., Hirano,M. and Kawabata,Z.: Ecological effects of radiation and other environmental stress on aquatic microcosm. Proceedings of the international Workshop on Comparative Evaluation of Health Effects of Environmental Toxicants Derived from Advanced Technologies, 131-144. (1998)
2) 武田　洋：制御実験生態系の構築に向けて、月刊地球 No.22、p.158-167. (1998)
3) Fuma,S., Takeda,H., Miyamoto,K., Yanagisawa,Y., Inoue,Y., Sato,N., Hirano,M. and Kawabata,Z.*, : Effects of γ-rays on the populations of the steady-state ecological microcosm. Int.J.Radiat.Biol., 74, 145-150. (1998)
4) Takeda,H., Fuma,S., Miyamoto,K., Nishimura,N and Inaba,J.: Biokinetics and dose estimation of radiocarbon in rata. Radiation Protection Dosimetry, 79, 169-174. (1998)
5) Nishimura,Y., Takeda,H., Watanabe,Y., Yukawa,M., Inaba,J. Sato,I.and Matsusaka,N.: Placental transfer of radiosilver in rats. Radiation Protection Dosimetry,79, 323-326, 1998.
6) Wang B., Takeda H., Dao W., Zhou X., Odaka T., Ohyama H., Yamada T. and Hayata I.: Induction of apoptosis by beta radiation from tritium compounds in mouse embryonic brain cells. : Health Physics, 77, 16-23. (1999)
7) Fuma,S., Takeda,H., Miyamoto,K., Yanagisawa,K., Inoue,Y., Ishii,K., Sugai,C, Ishii,C. and Kawabata,Z. : Simple aquatic microcosm for ecotoxicity screening at the community level., Bull.Environ.Cont.Toxicol.65, 699-706. (2000)
8)Yanagisawa,K., Takeda,H., Miyamoto,K. and S.Fuma : Transfer technetium from paddy soil to rice seeding. Journal of Radioanalytical & Nuclear Chemistry, 243, 403-408. (2000)
9) 武田 洋：モデル生態系を用いた放射線の生態系影響研究、Radioisotopes, 49, 319-322. (2000)

10) Fuma,S., Takeda,H., Miyamoto,K., Yanagisawa,K., Inoue,Y., Ishii,K., Sugai,C, Ishii,C. and Kawabata,Z. : Ecological evaluation of gadolinium toxicity compared with other heavy metals using an aquatic microcosm. Bull.Environ.Cont.Toxicol., 66, 231-238. (2001)

11) Takeda,H., Lu,H.M., Miyamoto,K., Fuma,S., Yanagisawa,K., Ishii,N. and Kuroda,N. : Comparative biokinetics of tritium in rats during continuous ingestion of tritiated water and tritium-labeled food. Int.J.Radiat.Biol., 77, 375-381. (2001)

（口頭発表）

1) 府馬正一、武田洋、宮本霧子、柳澤啓、井上義和 、佐藤尚衛、川端善一郎：マイクロコズムを用いた放射線の生態系影響評価の試み、日本放射線影響学会第39回大会、1996.11月、大阪.

2) 武田洋、宮本霧子、府馬正一、柳澤啓、井上義和 、佐藤尚衛、平野眞由美、川端善一郎：マイクロコズムに対する放射線と紫外線の比較影響評価、第44回日本生態学会大会、1997.3月、札幌.

3) 宮本霧子、武田洋、府馬正一、柳澤啓、井上義和 、佐藤尚衛、平野眞由美、川端善一郎：マイクロコズムを用いた生態系に対する酸性化影響研究の試み、第44回日本生態学会大会、1997.3月、札幌.

4) Takeda,H., Fuma,S., Miyamoto,K., Nishimura,Y. and Inaba,J.: Biokinetics and dose estimationof radiocarbon in rata. Workshop on Intakes of Radionuclides. 1997. 9.15-18, Avignon,France

5) 府馬正一、武田洋、宮本霧子、柳澤啓、井上義和、佐藤尚衛、平野眞由美、川端善一郎：マイクロコズムを用いたγ線と酸性化の生態系影響の比較、日本放射線影響学会第４０回大会、京都、1997.11.

6) Takeda,H., Fuma,S., Miyamoto,K., Yanagisawa,K., Inoue,Y., Sato,N., Hirano,M. and Kawabata,Z.: Comparative evaluation of ecological effects of γ-radiation and UVC-radiation using an aquatic microcosm. International Workshop on Comparative Evaluation of Health Effects of Environmental Toxicants Derived from Advanced Technologies, 1998.1. 28-30. Chiba

7) Miyamoto,K.,Fuma,S., Takeda,H., Yanagisawa,K., Inoue,Y., Sato,N., Hirano,M. and Kawabata,Z.: Effects of acidification on the population of growth stage aquatic microcosm. International Workshop on Comparative Evaluation of Health Effects of Environmental Toxicants Derived from Advanced Technologies, 1998.1. 28-30. Chiba

8)Yanagisawa,K., Takeda,H., Miyamoto,K., Fuma,S.; Transfer of technetium from paddy soil to rice seedling. International Workshop on Comparative Evaluation of Health Effects of Environmental Toxicants derived from Advanced Technologies.1998.1.28-30, Chiba.

9) 府馬正一、武田洋、宮本霧子、柳澤啓、井上義和 、佐藤尚衛、平野眞由美、川端善一郎：Ｃｕ、Ｎｉ、Ｍｎが安定期のマイクロコズムに与える影響の比較評価、第４５回日本生態学会、京都、1998.3

10) 宮本霧子、武田洋、府馬正一、柳澤啓、井上義和 、佐藤尚衛、平野眞由美、川端善一郎：増殖期の三者マイクロコズムにおける培地の酸性緩和過程について、第４５回日本生態学会、京都、1998.3

11) 佐藤尚衛、平野眞由美、宮本霧子、武田洋、府馬正一、柳澤啓、井上義和 、川端善一郎：安定期マイクロコズムにおける酸性化影響の解析、第４５回日本生態学会、京都、1998.3

12) 武田 洋：マイクロコズム実験系を利用した３H 動態解析研究、科研費基盤研究（A）「トリチウム放出事故時の農・畜産・水産物及び環境中のトリチウム残留に関する研究」班成果報告会、平成１０年１月２１日、東京

13) Fuma,S., Takeda,H., Miyamoto,K., Yanagisawa,Y., Inoue,Y., Sato,N., Hirano,M. and Kawabata,Z.*, : Evaluation of gadolinium ecotoxicity as compared with other heavy metals by using aquatic microcosm. 8th Annual Meeting of SETAC-Europe April 14-18. 1998. Bordeaux, France.

14) Takeda,H., Miyamoto,K., Fuma,S., Yanagisawa,Y., Inoue,Y., Sato,N., Hirano,M. and Kawabata,Z.*, : An aquatic microcosm for assessing the ecological toxicity of various toxicants. 8th Annual Meeting of SETAC-Europe April 14-18. 1998. Bordeaux, France.

15) Miyamoto,K., Takeda,H., Fuma,S., Yanagisawa,Y., Inoue,Y., Sato,N., Hirano,M. and Kawabata,Z.*, : Effects of acidification on aquatic microcosm. 8th Annual Meeting of SETAC-Europe April 14-18. 1998. Bordeaux, France.

16) 柳澤 啓、武田 洋、宮本霧子、府馬正一：テクネチウムの化学形と土壌からイネ幼植物への移行、第３６回理工学における同位元素研究発表会、東京、1999.7

17) 武田 洋、宮本霧子、府馬正一、柳澤 啓、黒田典子：提案したトリチウム体内動態モデルによる公衆への線量係数の算定、第３６回理工学における同位元素研究発表会、東京、1999.7

18) 武田 洋、府馬正一、宮本霧子、柳澤 啓、岩倉哲男：食物として投与した放射性炭素の動物体内動態、日本放射線影響学会第４２回大会、広島、1999.9

19) 府馬正一、武田 洋、宮本霧子、柳澤 啓、川端善一郎：マイクロコズムを用いた環境負荷因子の比較影響研究、日本放射線影響学会第４２回大会、広島、1999.9

20) 府馬正一、武田 洋、宮本霧子、柳澤 啓、井上義和 、石井伸昌、菅井一憲、川端善一郎：マイクロコズムを用いたガドリニウムの生態系影響評価、第５回日本環境毒性学会・バイオアッセイ研究会合同研究発表会、東京、1999.9

21) 石井伸昌、府馬正一、宮本霧子、武田 洋、柳沢 啓、川端善一郎：印旛沼周辺水域におけるウイルス様粒子の分布、日本陸水学会第６４回大会、滋賀、1999.10

22) 石井伸昌、川端善一郎、那須正夫：微生物相互作用による Escherichia coli 自然形質転換の抑制、日本微生物生態学会第１５回大会、高知、1999.11

23) Fuma, S., Takeda, H., Miyamoto, K., Yanagisawa, K., Inoue, Y., Ishii, N., Sugai, K. and Kawabata, Z.[*1]: Factors to be considered for ecotoxicity assessment: suggestion from microcosm study, SETAC 20th Annual Meeting, Philadelphia USA, 1999.11.

24) 府馬正一、武田 洋、宮本霧子、柳澤 啓、井上義和、石井伸昌、菅井一憲、石井千歳、川端善一郎：マイクロコズムを用いたニッケルの生態系影響評価 —単一生物種試験との比較— 第４７回日本生態学会、広島、2000.3

25) 武田 洋、宮本霧子、府馬正一、柳澤 啓、井上義和 、

石井伸昌、川端善一郎：生態毒性研究に用いる３種マイクロコズムの構造的特性の検討、第４７回日本生態学会、広島、2000.3
26) 府馬正一、武田 洋、宮本霧子、川端善一郎、柳澤 啓、井上義和 、石井伸昌、菅井一憲、石井千歳：マイクロコズムを用いたマンガンの生態系影響評価 —単一生物種試験との比較— 第３４回日本水環境学会、京都、2000.3
27) 柳澤啓、武田洋、宮本霧子、府馬正一、石井伸昌：$^{13}CO_2$アナライザーによる淡水プランクトンを用いたトレーサー実験，第37回理工学における同位元素研究発表会，東京，2000.7.
28) 府馬正一，石井伸昌、武田 洋，宮本霧子，柳澤 啓，井上義和、川端善一郎：モデル実験生態系に対するγ線と酸性化の複合影響，日本放射線影響学会第 43 回大会，東京、2000.8.
29) 石井伸昌，松井一彰，武田 洋，府馬正一，宮本霧子，柳澤 啓，川端善一郎. 原生生物による Escherichia coli の細胞外遺伝子受容能力の抑制. 日本微生物生態学会第 16 回大会. 茨城. 2000.11
30) 宮本霧子、武田 洋、府馬正一、石井伸昌、柳澤 啓、石井千歳、畠山 崇、菅井一憲、川端善一郎：安定期三者マイクロコズムの各構成生物種細胞数に対する UVC の影響. 日本生態学会第 48 回大会. 熊本. 2001.3
31) 石井伸昌，武田 洋，土居雅広，府馬正一，宮本霧子，柳澤 啓，川端善一郎. 原生生物による生細菌摂食速度の測定方法. 日本生態学会第 48 回大会. 熊本. 2001.3
32) K.Yanagisawa,H.Takeda, K.Miyamoto, S.Fuma and N.Ishii : Determination of ^{13}C concentration in biological materials using infrared absorption method. Eight International Conference on Low-level Measurements of Actinides and Long-lived Radionuclides in Biological and Environmental Samples. 16-20 Oct. 2000. Oarai,Ibaraki,Japan

第４サブグループ：

生体内挙動・影響の解析および新しい毒性評価法に関する研究

高橋千太郎、久保田善久、佐藤宏、孫学智（科学技術特別研究員）

Metabolism and Effect of Environmental Toxicants and New Risk Assessment

Sentaro Takahashi, Yoshihisa Kubota, Hiroshi Sato (Environmental and Toxicological Sciences Research Group), and Xue-Zhi Sun (JSTC, Research Fellow)

The effect of arsenite(As) or nickel(Ni) on the repair of DNA double-strand breaks (dsbs) was studied in γ-irradiated Chinese hamster ovary cells using pulse-field gel electrophoresis. Both As and Nil inhibited repair of DNA dsbs in a concentration- dependent manner; 0.08 mM As significantly inhibited the rejoining of dsbs, while 76 mM Ni was necessary to observe a clear inhibition. The mean lethal concentrations for the As and Ni treatments were approximately 0.12 and 13 mM, respectively. This indicates that the inhibition of repair by As occurred at a concentration at which appreciable cell survival occurred, but that Ni inhibited repair only at cytotoxic concentrations at which the cells lost their proliferative ability.

The cytotoxicity of gadolinium (Gd) was investigated in alveolar macrophages (AM) cultured in vitro. The viability of rat AM was decreased by exposure to gadolinium at doses more 3 μM, while mouse AM appeared to be resistant even up to 1000 μM Gd exposure. The phagocytic activity of mouse AM was higher than that of AM and mouse AM took up a larger amount of Gd than rat AM. Therefore, the marked difference in the cytotoxic response to gadolinium between mouse and rat alveolar macrophages could not be attributed to the phagocytic activities for the colloidal form of Gd. The cytotoxic sensitivity of AM to Gd present in non-colloidal form was almost the same between mouse and rat AM. Therefore, it is suggested that the extent to which Gd-colloid phagocytosed. is dissolved in the phagolysosome or the subsequent process to exhibit the cytotoxicity may be different between mouse and rat AM

The effect of Gd on the lung retention, excretion, and translocation of plutonium (Pu) was also studied in rats instilled intratracheally with Pu-hydroxide with and without Gd. The lung retention of Pu was higher and the fecal excretion was lower in the rats administered Pu-hydroxide containing a high concentration of Gd (Pu-GdH) than those administered pure Pu-hydroxide colloid. The administration of Pu-GdH induced the inflammatory reactions in the lung. The delayed alveolar clearance of Pu in the rats administered Pu-GdH may be attributable to the change in physicochemical characteristics of colloid and the inflammation induced in the lung by Gd.

科学技術の発展に伴って種々の化学物質が環境中に放出されるようになり、その人体への影響が懸念されている。本研究の目的は、重金属や希土類元素などの有害元素の毒性を放射線の生体影響を基準として明らかにするとともに、放射線との複合影響についても検討し、これら環境中有害物質と放射線の人体への影響を相互に比較できる形で提示することを目的としている。新しい毒性評価手法に関する研究として、一般毒性を評価するためにチャイニーズハムスターの卵巣由来の細胞（CHO, Chinese hamster ovary）を、吸入毒性（呼吸器毒性）を評価するために培養肺マクロファージ（AM, Alveolar Macrophage）を使用した細胞毒性試験法を開発してきた。これらの細胞毒性試験法を使用し、環境毒性物質として重金属や希土類元素の毒性を評価した。幾つかの重金属は環境毒性物質として歴史的に有名で、人に及ぼす影響は今日まで種々の毒性評価試験法でかなり詳細に解明されてきている。近年、重金属のいくつかについてはX線に誘発されたDNA損傷の修復過程に及ぼす影響を指標とした毒性評価が報告されるようになってきた。ニッケル、カドミウム、水銀、コバルト、鉛、銅などである。ヒ素についても同様の報告がある。しかしその影響は一様ではない。例えば、ニッケルはX線や紫外線で起こるDNA損傷の修復は抑制するが、水銀は紫外線誘発のDNA損傷の修復は抑制しない。DNA損傷の修復が不完全な場合、細胞は細胞死、突然変異などを引き起こすと考えられる。DNA損傷にはいくつかのタイプがあるが、特にDNA二重鎖切断（double strand break, dsb）が重要と考えられるが、DNA-dsbの修復に対する金属の効果についてはほとんど知られていない。そこで本研究ではγ線で誘発されたDNA-dsbの修復に対するヒ素(As)とニッケル(Ni)の効果について検討した。一方、先端科学技術の急速な発展に伴い希土類元素の中には新たな利用目的が見出され産業界で大量に使用されているにも関わらず人に及ぼす影響が十分に検討されていない元素が幾つかある。ランタノイドの１元素であるガドリニウム（Gd）は磁性体として近年多種の工業製品に使用されており、また原子力の分野では中性子吸収体として、医学分野ではMRIの強力な造影剤として利用されるなど広範で多量の利用にも関わらず、体内に摂取した場合の毒性としては粒子状物質を取り込む能力（貪食能）を持っている細胞、特にマクロファージに特異的に取り込まれ、その細胞機能を阻害することが分かっている程度であった。そこで環境毒性の観点からこのGdに着目し、その毒性をAMを使用した細胞毒性試験法で解明した。また、Gdは使用済み核燃料の再処理工程で使用されているため、この工程での事故発生時にはプルトニウム(Pu)とGdを同時に体内へ摂取する可能性が高い。Gdが生体に種々の影響を与えることはすでに報告されており、

Gdの共存によりPuの体内挙動が影響を受けることは十分に考えられる。そこで、ラットにPuとGdの共沈水酸化コロイドを気管内挿管法により投与し、その後のPuの動きをみた。

実験方法

DNA-dsbの修復阻害

CHO-K1細胞$1.5x10^6$を35mmの培養用ディッシュに蒔き、[^{14}C]チミジンを添加して24時間培養し、DNAを標識した。種々の濃度のヒ素(As)、ニッケル(Ni)を負荷して2時間培養後、^{137}Cs-γ線40Gyを照射してDNA-dsbを誘発させた。更に培養を続けてDNA-dsbを修復させた後、トリプシン処理により細胞を回収して0.5%アガロースゲルに懸濁し、氷冷下モールドに注入してゲルを固めplugとした。Plugはプロテナーゼ Kで氷冷下、1時間、更に50℃で一晩処理して蛋白を分解し、洗浄操作を行った後リボヌクレアーゼで処理した。plugはTBEバッファー中でパルスフィールド電気泳動を24時間行った。ゲルを切り出し、plugとlaneそれぞれに含まれる^{14}Cの放射活性を液体シンチレーションカウンターで測定し、次式によりDNA-dsbの割合をFARとして算出した。

FAR (fraction of activity released) ＝

lane中の放射活性/(plug中の放射活性+lane中の放射活性)

カドミウムを種々の濃度で添加した。48時間後、トリパンブルー色素排除試験法により肺マクロファージの生存率を調べた。肺マクロファージの形態学的変化、DNAの断片化等は常法により検討した。貪食能は細胞にラテックス粒子を添加して一定時間培養し、固定染色後に顕微鏡下で細胞あたりの粒子数を計測することにより判定した。また、細胞内に取り込まれたガドリニウムの量はICP-MSで測定した。

プルトニウムの体内挙動に対するガドリニウムの影響

2種類の濃度 (Low(L)、High(H)) のGdを含む共沈コロイド (Pu-Gd-L群、Pu-Gd-H群) およびGdを含まないコロイド (Pu群) をそれぞれSD系ラットに投与した。4週間後に肺、肝、腎、脾、大腿骨を摘出し、糞尿は経時的に採取した。各臓器 および糞尿中に含まれるPuの放射活性を計測し、初期排泄終了後の肺に存在するPu量に対する臓器、糞尿中のPu量の割合を算出した。一方、Gdの肺への影響は、重量の変化、肺洗浄 細胞のタイプと数の変化を指標にして検討した。

結　果

DNA-dsbの修復阻害

Asは8－800μMでいずれも生存率が90%以上で毒性は見られな

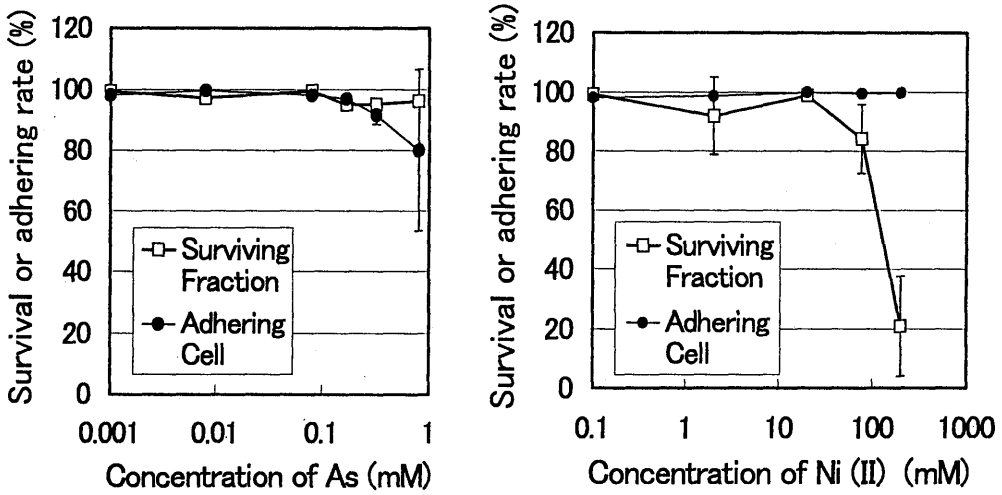

Fig. 1. Cell viability determined by the trypan blue dye exclusion test and the percentage of adherent cells after 2.5 h exposure to As. or Ni. Vertical bars indicate the SD for 6 to 12 cultures obtained from at least three independent experiments.

DNA-dsbの修復率は以下の式より算出した。

修復率 ＝

[(FAR(0)-FAR(BL))-(FAR(30)-FAR(BL))]/(FAR(0)-(FAR(BL))

ただし、FAR(0)は照射直後のFAR値、FAR(30)は照射後30分(37℃)のFAR値、FAR(BL)は非照射で未負荷の場合のFAR値。一方、細胞毒性はトリパンブルー色素排除試験とコロニー形成試験を常法により実施することにより判定した。

ガドリニウムの細胞毒性

肺洗浄によって採取したマウス及びラットの肺マクロファージを常法に従って培養し、ガドリニウムと、対照として重金属の

かった。Niは20mM以下では毒性はなかったが、200mMでは生存率が20%まで低下した(Fig.1)。コロニー形成試験で見た細胞の増殖能はAs、Niともに濃度増加に伴って低下し、平均致死濃度はAsが0.121mM、Niが13.3mMであった(Fig.2)。Asを負荷した場合、0.12mMまでは照射直後のFAR値(修復なし)は対照群と同レベルであったが、それ以上では濃度増加に伴ってFAR値は高くなった(Fig.3)。30分間の修復後はAs0.08mM以上で有意に高いFAR値を示し、DNA-dsbの修復が抑制された。

ガドリニウムの細胞毒性

Gd添加後48時間の生存率を見ると非常に興味ある結果が得ら

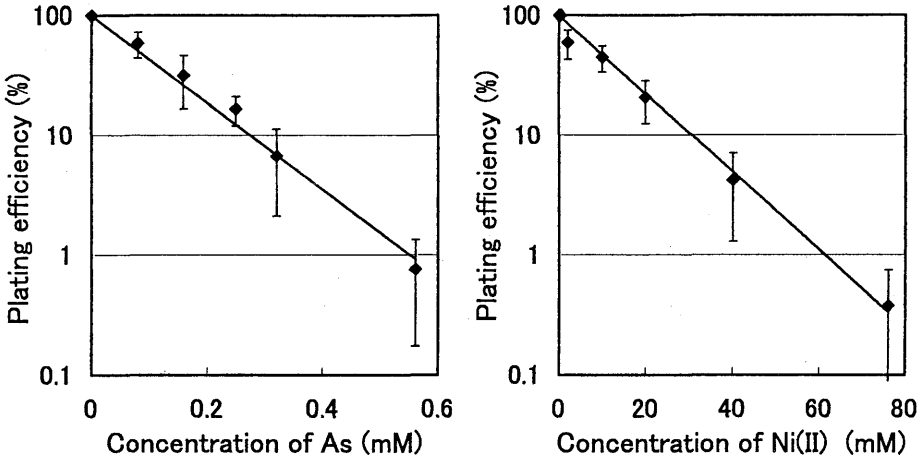

Fig. 2. Cell survival as determined by the colony-forming assay after 2.5 h exposure to As or Ni. Vertical bars indicate the SD for 6 to 9 cultures obtained from at least three independent experiments.

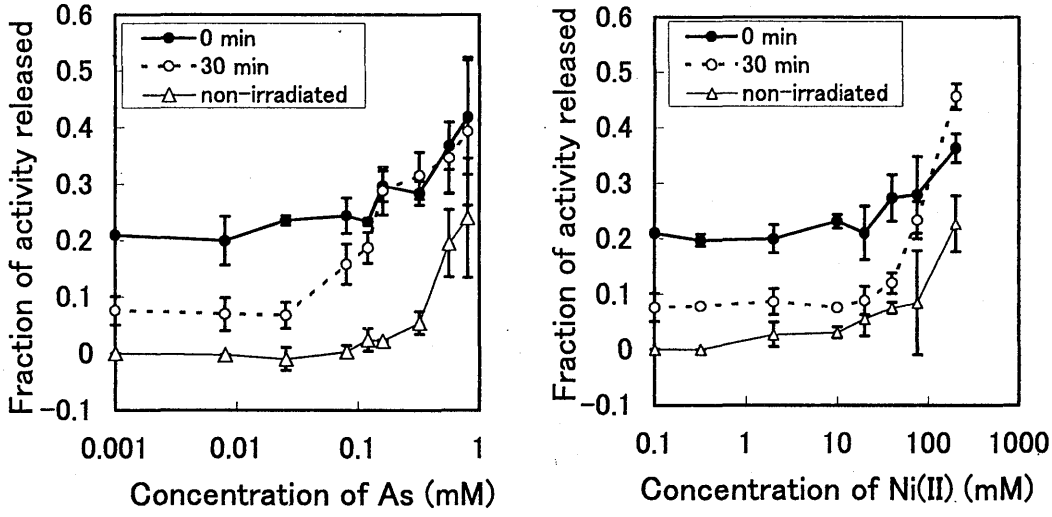

Fig. 3. FAR values assayed immediately after irradiation (●) or 30 min after the repair incubation with As or Ni(II) (○). FAR values for the nonirradiated cells are also shown (△). Vertical bars indicate the SD the 6 to 12 cultures from at least three independent experiments.

れた（Fig. 4）。カドミウムでは2系統のマウスと2系統のラットの肺マクロファージ何れも、類似した用量-生存率曲線を描き、カドミウム濃度の増加に伴って生存率が低下した。一方、ガドリニウムではラットの肺マクロファージの生存率はガドリニウムの濃度と共にほぼ直線的に低下するのに対し、マウスの肺マクロファージは1mMのガドリニウムでほとんど死なず、3mMで急激な生存率の低下を示した。すなわちマウスとラットの肺マクロファージでガドリニウムの細胞毒性に対して顕著な感受性の相違が認められた。この相違が何に起因するのかを明らかにするために2-3の実験を行った。高濃度のガドリニウムを細胞培養液に溶解すると肉眼でも明らかな沈殿物の形成が観察される。また幾つかの希土類元素は細胞培養液のような中性pHではコロイドと呼ばれる粒子状の物質を作ることが報告されている。マクロファージは粒子状物質を異物として認識し、細胞内に取り込み、細胞内で溶解、分解する能力を特化させた細胞であるため、細胞培養液中で形成されたガドリニウムのコロイドを細胞内に取り込み、それがガドリニウムのマクロファージに対する細胞毒性に関与しているのではないかと推察された。そこで細胞培養液中で形成されるコロイドをフィルタで除去した場合ガドリニウムの細胞毒性が軽減されるか検討した（Fig. 5）。カドミウムの肺マクロファージに対する細胞毒性はカドミウムを含む細胞培養液のフィルタ処理で全く変化しなかった。一方ガドリニウムの場合、ラット肺マクロファージに対する細胞毒性はフィルタ処理によって顕著に軽減されるのに対し、マウス肺マクロファージに対する細胞毒性はフィルタ処理に全く影響されなかった。そしてフィルタ処理したガドリニウムによるラット肺マクロファージの細胞生存率曲線はマウス肺マクロファージの生存率曲線とほぼ一致し、1mMでほとんど影響されず、3mMで生存率の急激な低下を示した。ガドリニウムのコロイドを細胞内に取り込む能力がマウスとラットの肺マクロファージで異なるのか検討するために、ガドリニウムを添加して一定時間培養後細胞内に取り込まれたガドリニウムの量をICP-MSで測定した（Table 1）。ガドリニウムに対して高感受性であるラット肺マクロファージがより高いガドリニウム取り込み量を示すという予想に反し、一貫してマウス肺マクロファージの方がより多く

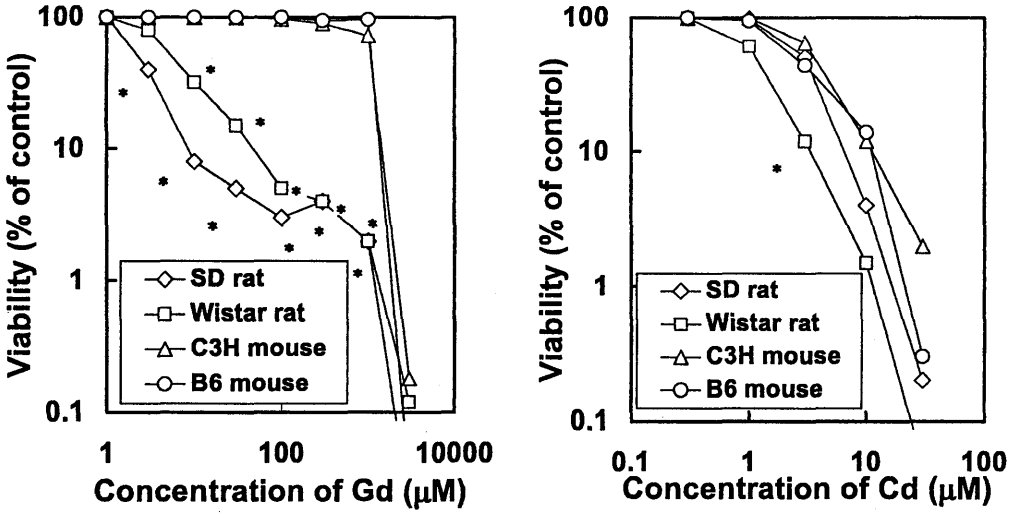

Fig. 4. The viability of mouse and rat alveolar macrophages after 48hr of exposure to Gd and Cd. The viability was expressed as the percentage of the viable cell number to that in control culture. Each data point is a mean of three separate experiments. Asterisks indicate the statistically significant difference from C3H and B6 mice at the corresponding concentration of Gd or Cd.

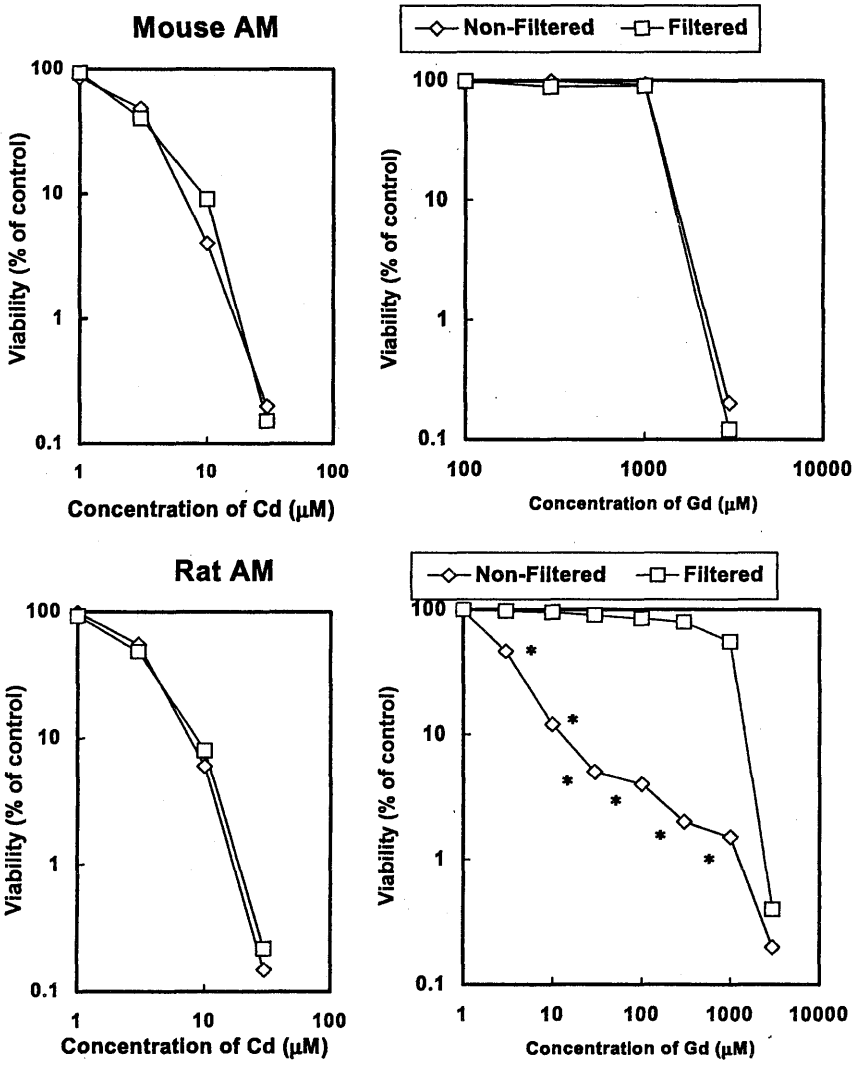

Fig, 5. Effects of filtration of Gd and Cd preparations on cell viability determined at 48 hr of culture in B6 mouse (upper) and SD rat (lower). Each data point is a mean of 3 separate experiments. Asterisks indicate the statistically significant difference from those exposed to filtered Gd.

Table 1. The uptake of Gd by B6 mouse and SD rat AM after 0, 4 and 10 hrs.

Incubatioin Time (hr)	Incubation Temperature (℃)	AM	% Gd[a] ExpI	% Gd[a] ExpII
0	-	B6 mouse	0.06	n.d.
0	-	SD rat	n.d.	0.10
4	4	B6 mouse	0.28	0.36
4	4	SD rat	0.22	0.27
4	37	B6 mouse	1.12	0.96
4	37	SD rat	0.58	0.60
10	4	B6 mouse	0.27	0.40
10	4	SD rat	0.31	0.26
10	37	B6 mouse	1.40	2.00
10	37	SD rat	0.78	0.86

[a] The amount of Gd per 10^6 AM, expressed as a percentage of total amount of Gd added, i.e. 2ml of 300μM Gd

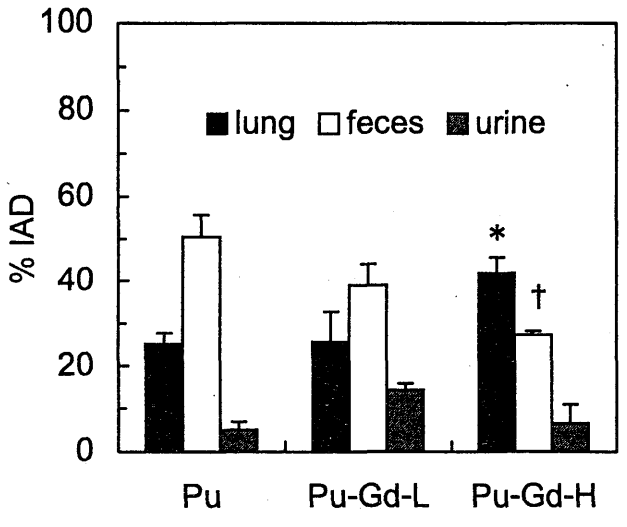

Fig. 6. Lung retention and cumulative excretion of ^{239}Pu in feces and urine 4 weeks after intratracheal instillation of ^{239}Pu-hydroxide, Pu-Gd-L, and Pu-Gd-H. Vertical bar shows SD of three rats.
*p<0.05. †;p<0.01, ‡;p<0.005.

のガドリニウムを取り込んでいた。

プルトニウムの体内挙動に対するガドリニウムの影響

コロイド投与4週間後の肺への残留率は、Pu-Gd-H群が対照群(Pu群)に対して有意に高く(Fig. 6)、糞への排泄率が低い結果が得られた(Fig. 7A)。尿中排泄は Pu-Gd-L 群で有意に高い値を示した(Fig. 7B)。肺から肝、骨へ移行して残留しているPu量は3群ともほぼ同レベルで違いがみられなかった。体重に対する肺の重量の割合はPu-Gd-H群で有意な増加がみられた。Gd単独投与群では肺洗浄細胞の数が4日まで経時的に増加し、その後減少したが、洗浄細胞中への好中球の混在がみられた。

考 察

As、Niともに DNA-dsb 修復を阻害する結果が得られたが、阻害濃度がNiは40mM以上に対しAsは0.08mM(生存率50%以上)の低濃度で DNA-dsb の修復を阻害した。As と Ni が X 線あるいは紫外線により誘発される DNA 損傷の修復を毒性のない濃度で阻害するとの報告は多い。しかし、本研究では DNA-dsb の修復を低濃度で阻害したのは As のみであり、Ni では低濃度での修復阻害は見られなかった。As が修復阻害を示した濃度は、井戸水中の As 濃度が 0.014mM という報告があり、環境レベルと比較して高い濃度ではない。As に汚染された環境中では人で 0.14mM 以上にもなった例もある。As や Ni による DNA-dsb の修復阻害のメカニズムは明らかでないが、As は特異的に突然変異を誘発することが報告されており、本研究でγ線に誘発された DNA-dsb の修復を阻害することを初めて見いだしたことにより、As による突然変異のメカニズムを解明できるかもしれない。

細胞培養液中で形成されたガドリニウムのコロイドはラット肺マクロファージの細胞毒性に密接に関与するが、マウス肺マクロファージには毒性を示さない、3mM 以上のガドリニウムではコロイド形成以外の原因、おそらくイオン状のガドリニウムが細胞毒性に関与し、その毒性はマウスとラットの肺マクロファージで差が認められないことを示した。このことから、ガドリニウムコロイドによる細胞毒性のマウスとラット肺マクロファージ間の顕著な相違はガドリニウムコロイドの取り込み量によるのではなく、それ以降の機序、コロイドの細胞内での溶解、イオン化

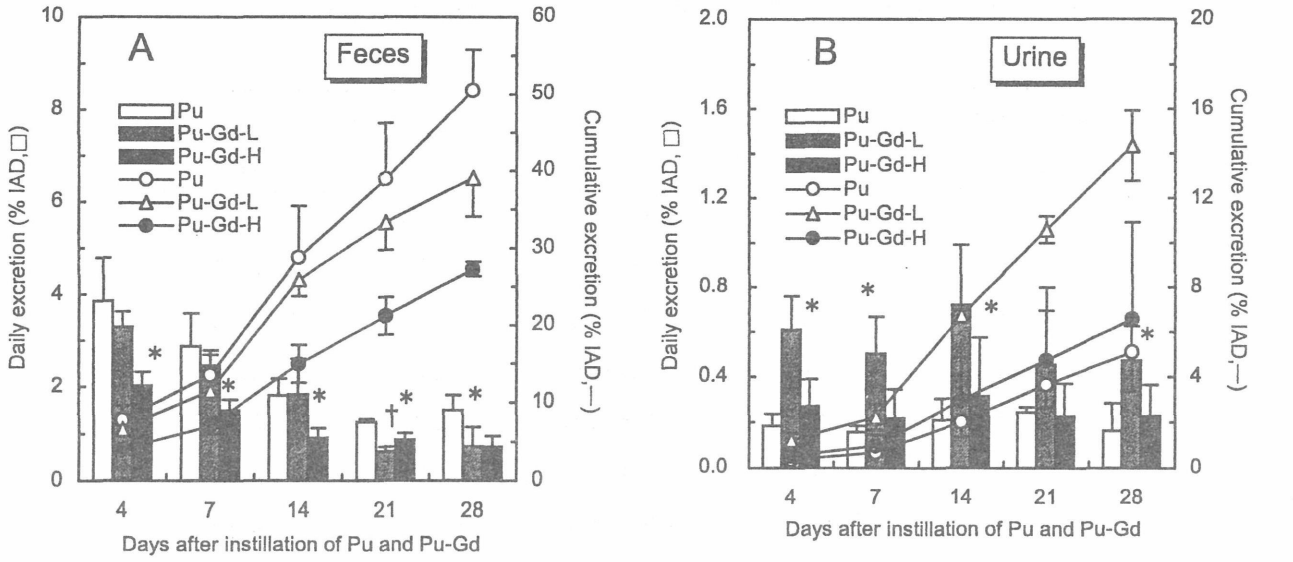

Fig. 7. Daily and cumulative excretion of ^{239}Pu in feces (A) and urine (B) following intratracheal instillation of ^{239}Pu-hydroxide (Pu), Pu-Gd-L and Pu-Gd-H. Vertical bar shows SD of 3 rats. *p<0.05, †p<0.02

或いはイオン化ガドリニウムの細胞内構成成分との反応における相違によると推察された。本研究では先端科学技術の急速な発展に伴い多量に且つ広範な用途に使用されるようになった物質の一例としてガドリニウムを取り上げ、人に及ぼす影響を細胞毒性を指標として検討したのであるが、その細胞毒性に実験動物間の顕著な種差を見出すという予想外の成果を得た。このことから環境汚染物質の影響を総合的且つ精緻に評価するためには、多くの毒性試験それぞれの長短を正しく認識して可能な限り多くの毒性評価を行いその情報を得ること、毒性発現機序の解明までを行うことが重要であると認識された。

Gd を肺に単独投与したラットの肺洗浄細胞中に炎症性細胞である好中球の存在が確認されたことから、Pu と Gd の共沈水酸化コロイドを投与したラットでも炎症が引き起こされていることが推察された。一般に、炎症が起きている肺では沈着粒子の肺からのクリアランスが遅くなることが知られており、共沈水酸化コロイドを投与して4週間後の Pu の肺残留率が高いのは、Gd により肺に炎症が起こったためと考えられる。Pu の水酸化物は lysosome での可溶化を経て細胞外へ放出されることや lysosome が炎症に重要な役割を果たしていることを考慮すると、Gd が lysosome での Pu の可溶化に抑制的に作用している可能性があるが、現時点ではその機序は明らかではない。

結　論

γ 線により誘発されたDNA-dsbの修復がAsで阻害されたことは、Asと放射線の複合影響が環境中で起こりうることを考慮すると非常に重要である。また、Niは本研究での実験条件では毒性を示す高い濃度でのみDNA-dsbの修復を阻害したが、他のタイプのDNA損傷の修復は低濃度で阻害されることからDNA-dsbの修復に対する影響をより明らかにするためにさらに検討が必要である。 GdのAMに対する毒性はGdの細胞内への取り込み量と取り込まれたGdの細胞内での溶解性に依存したが、マウスとラットのAMに対するGdの毒性の大きな違いはGdコロイドに対する貪食能とは関係がなく、取り込まれたGdコロイドの細胞内での溶解過程の違いに依存することが示唆された。すなわち、ラットのAMは細胞内でより活発にGdコロイドを溶解、あるいは溶解されたGdに対してより感受性が高いために毒性が強く現れたと考えられる。Gdとの共存により水酸化コロイドとして摂取されたPuははいからのクリアランスが影響を受けることがわかった。詳細なメカニズムは不明であるが、事故によりPuとGdが同時に体内に取り込まれ、Gdの量が肺に炎症を誘発し、Puの水酸化物の物理化学的性質を変化させるような高いレベルの場合は通常よりPuの肺への滞留時間が長くなり被爆線量が高くなることが予想された。

研究発表

（研究論文）

1) Sato, H., Takahashi, S., Suzuki, K., Esaka, F. and Furuya, K.: Changes in the concentrations of metal elements in various organs of the mouse following multiple intraperitoneal administration of Ca-DTPA, *J. Health Phys.*, **31**, 41-48, 1996.

2) Kubota, Y., Takahashi, S. and Sato, H.: Effect of a maternall injection of ^{239}Pu on the number of CFU-S in the foetal liver of the C3H and BDF1 mouse, *Int. J. Radiat. Biol.*, **72**, 71-78, 1997.

3) Takahashi, S., Kubota, Y. and Sato, H.: Mutant frequencyes in *lacZ* transgenic mice following the internal irradiation from ^{89}Sr or the external γ-ray irradiation, *J. Radiat. Res.*, **39**, 53-60, 1998.

4) 高橋千太郎、久保田善久、孫学智、佐藤宏：ラジオルミノグラフィー用の市販イメージングプレートのα線放出核種およびポジトロン核種に対する感度とダイナミックレンジ, *RADIOISOTOPES*, **47**, 32-38, 1988

5) Takahashi, S., Oishi, M., Takeda, E., Kubota., Y., Kikuchi, T. and Furuya, K.: Physicochemical characteristics and toxicity of nickel oxide particles calcined at different temperatures, *Biol. Trace Element Res.*, **69**, 161-174, 1999.

6) Okayasu, R., Takahashi, S., Yamada, S., Hei, T. K. and Ullrich, R. L.: Asbestos and DNA double strand breaks, *Cancer Res.*, **59**, 298-300, 1999.

7) Sato, H., Yamada, Y., Ishigure, N., Nakano, T., Enomoto, H.,

Takahashi, S., Kubota, Y. and Inaba, J.: Retention, excretion and translocation of 239Pu in rats following inhalation of $^{239}PuO_2$ calcined at 1150 and 400℃, *J. Radiat. Res.*, **40**, 197-204, 1999.

8) Okinaga, K., Takahashi, S., Tsugoshi, T., Kudo, Y., Furuya, K. and Araki, Y.: Characterization of suspended particulate matter in the air in subways and corresponding above-ground areas, *J. Jpn. Soc. Atmos. Environ.*, **35**, 12-20, 2000.

9) Takahashi, S., Takahashi, I., Sato, H., Kubota, Y., Yoshida, S. and Wistar rats by inductively coupled plasma-atomic emission spectrometry and mass spectrometry, *Laboratory Animals*, **34**, 97-105, 2000.

10) Kubota, Y., Takahashi, S., Takahashi, I. and Patrick, G.: Different cytotoxic response to gadolinium between mouse and rat alveolar macrophages, *Toxicol. in Vitro*, **14**, 309-319, 2000.

11) Takahashi, S., Takeda, E., Kubota, Y. and Okayasu, R.: Inhibition of repair of radiation-induced DNA double-strand breaks by nickel and arsenite, *Radiat. Res.*, **154**, 686-691, 2000.

12) Kubota, Y., Takahashi, S., Sun, X.-Z., Sato, H., Aizawa, S. and Yoshida, S.: Radiation-induced tissue abnormalities in fetal brain are related to apoptosiss immediately after irradiation, *Int. J. Radiat. Biol.*, **76**, 649-659, 2000.

13) Sato, H., Takahashi, S. and Kubota, Y.: Effects of gadolinium on the retention and translocation of ^{239}Pu-hydroxide, *Health Phys.*, **80**, 164-169, 2001.

（口頭発表）

1) 久保田善久、高橋千太郎、佐藤宏：肺マクロファージの増殖能を指標とした大気中粒子状物質の毒性試験法環境科学会 1996 年会、東京、1996. 9.

2) 沖永希世、高橋千太郎、津越敬寿、工藤善之、古谷圭一：地下街および地下鉄液構内における浮遊粒子状物質の粒子径分布と元素組成、環境科学会 1996 年会、東京、1996. 9.

3) 佐藤宏、久保田善久、高橋千太郎：ガドリニウム、イットリウム、カドミウムの培養ラット肺胞マクロファージに対する細胞毒性、環境科学会 1996 年会、東京、1996. 9.

4) 沖永希世、古谷圭一、高橋千太郎、久保田善久、竹内亮、森本兼尋：MSTO-211H 細胞を用いた大気中浮遊微粒子の細胞毒性試験法の開発、環境科学会 1997 年会、福岡、1997. 10.

5) 久保田善久、高橋千太郎、沖永希世、佐藤宏：カドミウム、ガドリニウムの培養細胞に及ぼす細胞毒性、環境科学会 1997 年会、福岡、1997. 10.

6) 沖永希世、高橋千太郎、津越敬寿、古谷圭一、荒木庸一：都市地下空間における大気中粒子状物質の挙動とその特性化、第 58 回分析化学討論会、福岡、1997. 5.

7) 沖永希世、高橋千太郎、古谷圭一、荒木庸一：地下鉄駅構内とその近傍の地上部分における化学特性とその細胞毒性について、日本分析化学討論会第 46 年回、東京、1997. 10.

8) Okayasu, R., Takahashi, S. , Ullich R.: Induction of DNA double strand breaks in CHO-K1 and xrs-5 cell with asbestos, American Association for Cancer Research, 89th Annual

9) 高橋千太郎、竹田絵里子、岡安隆一、久保田善久、古谷圭一：環境中有害粒子状物質による DNA 二重鎖切断: アスベストと酸化ニッケル、環境科学会 1998 年会、筑波、1998. 9.

10) 沖永希代、八向真帆、高橋千太郎、久保田善久、古谷圭一：地下鉄駅構内における浮遊粒子状物質の季節変動: 細胞毒性試験と多環芳香族炭化水素類の分析、環境科学会 1998 年会、筑波、 1998.9.

11) 八向真帆[1]、工藤善之[1]、沖永希世[1]、古谷圭一[1]、久松由東[2]、高橋千太郎[3]（[1]東京理科大学理学部、[2]国立公衆衛生院、[3]放射線医学総合研究所）：地下鉄構内と地上大気中の多環式芳香族炭化水素量の比較、大気環境学会、札幌、1998. 9.

12) 山下美穂[1]、工藤善之[1]、古谷圭一[1]、高橋千太郎[2]（[1]東京理科大学理学部、[2]放射線医学総合研究所）：地下鉄構内における粗粒子粉塵の特性化、大気環境学会、札幌、1998. 9.

13) 高橋千太郎、竹田絵里子、久保田善久、古谷圭一：環境中有害金属および放射線による CHO 細胞の DNA 損傷と修復阻害、第 41 回日本放射線影響学会、長崎、1998. 12.

14) 久保田善久、高橋千太郎、山田裕、竹田絵里子：マウス肺マクロファージの放射線による活性酸素産生とアポトーシス誘発の関係、第 41 回日本放射線影響学会、長崎、1998. 12.

15) 高橋千太郎、久保田善久、佐藤宏、孫学智：α核種及びポジトロン核種に対する IP の感度：^{239}Pu の組織局所線量推定への利用、第 16 回ラジオルミノグラフィー研究会、東京、1999. 4.

16) 佐藤宏、久保田善久、孫学智、高橋千太郎：気管内投与された水酸化 Pu の動態に対する Gd の影響、日本保健物理学会第 34 回研究発表会、大分、1999. 5.

17) 高橋功、高橋千太郎、佐藤宏、吉田聡、村松康行：ラット臓器中の安定元素の ICP-AES および ICP-MS による定量、日本保健物理学会第 34 回研究発表会、大分、1999. 5.

18) 古谷圭一、工藤善之、佐藤英晃, 中条健一、荒木庸一、高橋千太郎：地下鉄構内における浮遊粒子状物質の挙動と細胞毒性、第 40 回大気環境学会年会、三重、1999. 9.

19) Okayasu, R., Takahashi, S., Koshi, Y., Kubota, Y. and. Bedford, S.: Inhibition of radiation induced DNA double strand break repair by metal elements, 91st Annual Meeting of the American Association for Cancer Research., San Francisco, 2000. 3. .

6. 主要論文一覧 List of Major Publications

ページ (pages)	Authors and Titles
41	Bannai, T. et al. Multitracer studies on the accumulation of raionuclides in mushrooms
47	Doi, M. et al. Life time risk of lung cancer due to radon exposure projected to Japanese and Swedish populations
58	Fuma, S. et al. Effects of γ-rays on the population of the steady-state ecological microcosm
64	Kubota, Y. et al. Different cytotoxic response to gadolinium between mouse and rat alveolar macrophages
75	Matsui, K., Ishii, N. et al. Survical of genetically modified Escherichia coli carrying extraneous antibiotics resistance gene through microbial interactions
82	Miyamato, K. et al. Effect of acidification of the population of growth stage aquatic microcosm
86	Muramatsu, Y. et al. Determination of plutonium concentration and its isotopic ratio in environmental materials by ICP-MS after separation using ion-exchange and extration chromatography
93	中村裕二；人間活動と地球放射線環境
98	Nakamura, Y. Report on International Workshop on Comparative Evaluation of Health Effects of Environmental Toxicants Derived from Advanced Technologies (in Japanese)
102	Sakashita, T., et al. Effect of atmospheric transport on temporal variations of ^{222}Rn and its progeny concentration in the atmosphere
112	Sato, H. et al. Effect of gadlinium on the retention and translocation of ^{239}Pu-hydroxide
118	Sun, X-Z., et al. Different patterns of abnormal neuronal migration in the cerebral cortex of mice prenatally exposed to irradiation
128	Tagami, K., et al Concentration of global fallout ^{99}Tc in raice paddy soils collected in Japan
132	Takahashi, S. et al. Inhibition of repair of radiation-induced DNA double strand breaks by nickel and arsenite
138	Takeda, H. et al. Comparative biokintics of tritium in rats during continuous ingestion of tritiated water and tritium-labeled food
145	Uchida, S. et al. Determination of 99Tc dposited on the ground within the 30-km zone around the Chernobyl reactor and estimation of ^{99}Tc released into atmosphere by the accident
155	Yanagisawa, K. et al. Transfer of technetium from paddy soil to rice seedling.
151	Yoshida, S. et al. Concentration of alkali and alkaline earth elements in mushrooms and plants collected in a Japanese pine forest, and their relationship with ^{137}Cs

J. RADIAT. RES., 38, 213–218 (1997)

Multitracer Studies on the Accumulation of Radionuclides in Mushrooms

TADAAKI BAN-NAI[1]*, YASUYUKI MURAMATSU[1], SATOSHI YOSHIDA[1], SHIGEO UCHIDA[1], SADAO SHIBATA[2], SHIZUKO AMBE[3], FUMITOSHI AMBE[3] and AKIRA SUZUKI[4]

[1]Environmental & Toxicological Sciences Research Group, National Institute of Radiological Sciences, Isozaki 3609, Hitachinaka-shi, Ibaraki 311–12,
[2]Division of Radiation Research, National Institute of Radiological Sciences, 4–9–1 Anagawa, Inage-ku, Chiba-shi, Chiba 263,
[3]The Institute of Physical and Chemical Research (RIKEN), 2–1 Hirosawa, Wako-shi, Saitama 351–01,
[4]Faculty of Education, Chiba University, 1–33 Yayoi-cho, Inage-ku, Chiba-shi, Chiba 263, Japan

(Received, May 27, 1997)
(Revision received, August 22, 1997)
(Accepted, September 8, 1997)

Mushroom/Multitracer/Accumulation/Cultivation experiment/Radionuclide

We used the multitracer technique to study the transfer of several radionuclides to two mushroom species. Radionuclides accumulated in the fruiting bodies of the mushrooms in the order of ^{83}Rb > ^{65}Zn > ^{54}Mn > ^{22}Na > ^{75}Se and ^{85}Sr > ^{60}Co > ^{88}Y, ^{102}Rh, ^{139}Ce, ^{143,144}Pm, ^{146,153}Gd and ^{173}Lu > ^{175}Hf. The concentration ratio values for ^{83}Rb, ^{65}Zn and ^{54}Mn in the fruiting bodies were more than 10, whereas those for ^{60}Co, ^{88}Y, ^{102}Rh, ^{121m}Te, ^{175}Hf and the rare earth elements were less than 1. There were major differences in the accumulations of the alkali elements.

INTRODUCTION

Mushrooms accumulate Cs, including radiocesium[1,2]. After the Chernobyl reactor accident, high concentrations of radiocesium were found in European mushrooms[3–6]. Cesium-137 concentrations in mushrooms are markedly higher than those in autotrophic plants[7–9]. In a previous study[10], we calculated the contribution of mushrooms collected in Japan to the total Japanese intake of ^{137}Cs (on average) as 32%, whereas the intake for ^{40}K was only 1.7%. Mushrooms therefore are considered important in estimating the internal radiation dose of ^{137}Cs obtained from foods.

In terms of the forest ecosystem, mushroom species have important functions in the decomposition of plant materials and the absorption of elements, such as K and P, from soil[11]. In a previous study[12], we reported results of laboratory experiments on the accumulation of the radiotracers ^{137}Cs, ^{85}Sr, ^{60}Co, ^{54}Mn and ^{65}Zn in three mushroom species and one higher plant (*Medicago sativa*). Mushrooms tended to accumulate

*Corresponding author

large amounts of Cs, but there were marked differences among the mushroom species. Accumulations were low for Sr and Co. There still is little data available on the transfer of various nuclides to mushrooms, in comparison to the known data on the transfer of other biological materials[13–15]. Reliable data on the accumulation of other nuclides in mushrooms are needed for doing radioecological and environmental studies.

A multitracer, produced by irradiating targets with high-energy heavy-ions[16], can be used to study the behaviors of various elements in the environment. Ambe *et al.*[13] made a multitracer study of the absorption of radionuclides through the roots of rice and soybean plants cultivated in nutrient solutions or soil and obtained the distributions of the radionuclides of 24 elements (Be, Na, Sc, Mn, Co, Zn, Se, Rb, Sr, Y, Zr, Nb, Ru, Rh, Ag, Te, Ce, Pm, Eu, Gd, Yb, Lu, Hf and Ir) in the grain, leaves, stems and roots.

We used the multitracer technique to study the transfer of several radionuclides (elements) from a medium (mixture of yeast extract and malt extract) to two mushroom species. The multitracers contained 17 nuclides, including ones related to fission products (Sr, Ce, Te), activation products (Mn, Co, Zn) and natural radionuclides (Rb).

MATERIALS AND METHOD

Multitracer

The radioactive tracers were produced by irradiating thin gold foil with a ^{14}N beam accelerated to 135 MeV/nucleon in the RIKEN Ring Cyclotron[16]. The irradiated foil was dissolved in *aqua regia*, and the solution obtained evaporated to dryness. The residue was dissolved in 3 M HCl. Gold was extracted from the solution with ethyl acetate. The aqueous solution with the multitracer was adjusted to 0.05 M HCl. Details of the separation procedure are described in Ambe *et al.*[16]. In our study, the irradiated gold foil was cooled for more than 4 months before the separation. The radionuclides used were ^{22}Na, ^{54}Mn, ^{60}Co, ^{65}Zn, ^{75}Se, ^{83}Rb, ^{85}Sr, ^{88}Y, ^{102}Rh, ^{121m}Te, ^{139}Ce, ^{143}Pm, ^{144}Pm, ^{146}Gd, ^{153}Gd, ^{173}Lu and ^{175}Hf. Chloride was the chemical form of these nuclides in the multitracer.

Mushrooms Cultivation

Two mushroom species, *Hebeloma vinosophyllum* and *Coprinus phlyctidosporus*, were used in the culture experiment. The medium solution was comprised of yeast extract (2 g), malt extract (10 g) and agar (15 g) dissolved in distilled water (1000 ml), then 25 ml portions were poured into flasks (200 ml), and the multitracer was added. The pH of the solution was adjusted to 6.0 with 0.1N–NaOH, and the mixture autoclaved. Three flasks per mushroom species containing the medium solution and multitracer were prepared and incubated at 25°C. After about one month, the mushrooms produced fruiting bodies. The concentrations of radionuclides in the mushroom samples (whole fruiting bodies) were measured with a Ge-detector. Details of the counting procedures are described elsewhere[17]. The mean values of the three flasks were calculated for each species. The concentration ratio, defined as the radionuclide activity in the fruiting bodies of the mushroom (Bq/g, wet wt.) divided by the radionuclide activity in the medium at the beginning of the experiment (Bq/g, wet wt.), was calculated.

RESULTS AND DISCUSSION

The accumulations of the multitracer in the fruiting bodies of the two mushroom species are shown as concentration ratios in Table 1.

Figure 1 shows radionuclides that had mean concentration ratio values (with standard deviation) higher than 1. The ratios were in the order of Rb > Zn > Mn > Na > Se and Sr. Markedly high values of more than 10 were found for Rb (27), Zn (21) and Mn (11). The elements Co, Ce, Y, Rh, Te, Pm, Gd, Lu and Hf had concentration ratios lower than 1 (Fig. 2). The concentration ratios of Mn, Zn and Sr found for the mushrooms in this study were almost the same as the values reported previously[12]. Because the concentration ratios of radioactive Rb, Zn and Mn are markedly high, in order to protect against radiation attention must be paid to the levels of these nuclides in contaminated forest ecosystems.

In a previous study[12], we found that radionuclide accumulation for mushrooms was in the order of Zn > Mn > Sr > Co, whereas for the higher plant (*Medicago sativa*) the order was Sr > Zn and Mn > Co. Mascanzoni[18] also reported a tendency for the low accumulation of Sr in mushrooms collected from Swedish forests. Ambe *et al.*[13] found a decreasing tendency in the transfer factor for soybean stem of the order Sr > Rb > Zn > Mn > Se > Na. Yoshida and Muramatsu[2] analyzed many major and trace elements in mushrooms, higher plants (tree leaf) and soil samples collected from a pine forest and found a high accumulation of Rb and Cs and a low accumulation of Mg, Ca, Sr and Ba in mushrooms as compared with the higher plants. There is a characteristic difference in the accumulation of Sr between mushrooms and higher plants.

Interestingly, there are specific differences in the accumulation of alkali elements. We found that Rb is highly accumulated in mushrooms, whereas the concentration ratio of Na is significantly lower than that of

Table 1. Concentration ratios of radionuclides in the fruiting bodies of two mushroom species

	H. vinosophyllum	*C. phlyctidosporus*	average
^{22}Na	2.3 ± 0.3[a]	1.8 ± 0.5[a]	2.1
^{54}Mn	12 ± 2	11 ± 2	11
^{65}Zn	24 ± 4	18 ± 2	21
^{75}Se	2.7 ± 0.1	0.7 ± 0.1	1.7
^{83}Rb	32 ± 5	22 ± 3	27
^{85}Sr	2.0 ± 1.1	0.7 ± 0.2	1.4
^{60}Co	0.67 ± 0.48	0.64 ± 0.13	0.66
^{88}Y	0.52 ± 0.46	0.26 ± 0.08	0.39
^{102}Rh	0.47 ± 0.19	0.20 ± 0.05	0.34
^{121m}Te	0.63 ± 0.19	—	—
^{139}Ce	0.47 ± 0.40	0.43 ± 0.09	0.45
^{143,144}Pm	0.48 ± 0.37	0.32 ± 0.07	0.40
^{146,153}Gd	0.45 ± 0.37	0.21 ± 0.01	0.33
^{173}Lu	0.47 ± 0.39	0.16 ± 0.03	0.32
^{175}Hf	0.27 ± 0.15	0.07 ± 0.03	0.17

[a]The mean values with standard deviation for three flasks

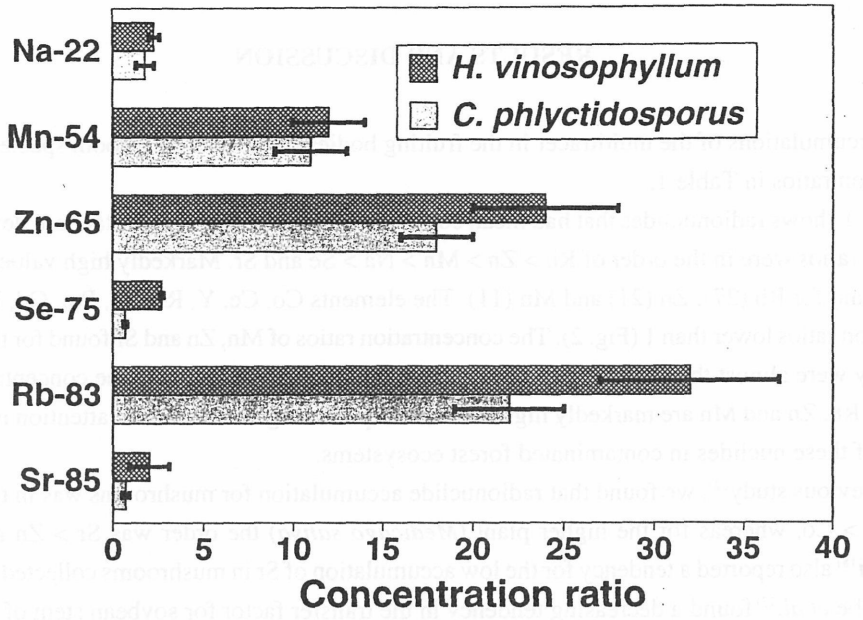

Fig. 1. Concentration ratios of the multitracer in fruiting bodies of mushrooms (I)
Note: The mean values are for three flasks. Solid lines show the range of standard deviation.

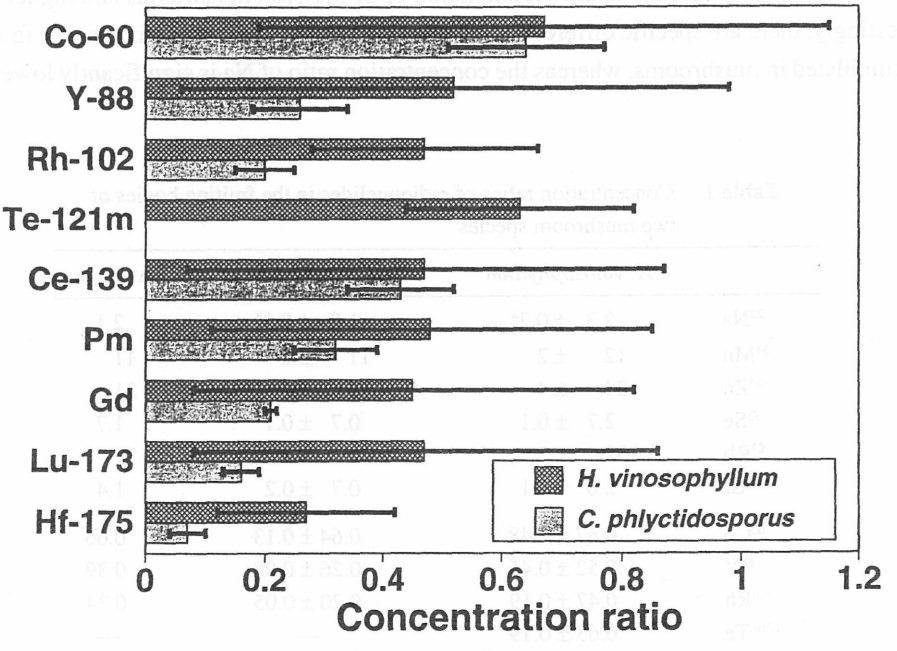

Fig. 2. Concentration ratios of the multitracer in fruiting bodies of mushrooms(II)
Note: The mean values are for three flasks. Solid lines show the range of standard deviation.

Rb. There were no Cs isotopes in the multitracer used in this study. In a previous study using ^{137}Cs, however, we found that it tended to be accumulated in mushrooms, the concentration ratios being 21 ± 1, 14 ± 3 and

2.6 ± 0.3, respectively for *H. vinosophyllum, F. velutipes*, and *C. phlyctidosporus*. The concentration ratio of Rb for *H. vinosophyllum* (32) was somewhat larger than that of Cs. Differences in the concentration ratios among the species for Rb seemed to be smaller than for Cs. The concentration ratio of Cs for *H. vinosophyllum* was about 8 times that for *C. phlyctidosporus*[12], whereas the ratio of Rb in *H. vinosophyllum* in the experiment reported here was only about 1.5 times that for *C. phlyctidosporus*. Ingrao *et al.*[19] found no marked correlation between the concentrations of Cs and Rb in mushrooms collected in the field (R = 0.5).

In the present experiment, a small amount of Se was detected in the Silicon plug used to cover the flasks and in the activated charcoal supplemented with tetramethylendiamine in a dish placed in the incubator. We assumed that Se, added as an inorganic form, was converted to a gaseous organic species by the biological activity of the fungi. Chau *et al.*[20] reported that inorganic and organic selenium compounds are converted to volatile selenium compounds by microorganisms in lake sediments. The volatile selenium compound produced would be dimethyl selenide.

The chemical composition of the medium was determined by inductively coupled plasma mass spectrometry (Yokogawa, PMS-2000). The element concentrations (on a wet weight basis) obtained (data for Na, K, Ca, Mn, Zn and Sr were published in our previous study[12]) are 2400 ppm for Na; 1000 ppm for K; 77 ppm for Ca; 2.6 ppm for Zn; 1.9 ppm for Sr; 0.5 ppm for Rb; 0.3 ppm for Mn; 0.03 ppm for Co; < 0.01 ppm for Se, Ce and Hf; and < 0.003 ppm for Y, Te, Gd and Lu. Elsewhere[12] we found that the concentration ratios of mushroom to medium for Cs, Sr and Co were not markedly affected by coexisting stable elements (up to 10 ppm in the medium), whereas the ratio of Mn decreased as the amount of stable Mn in the medium increased. Because the concentrations of most elements (except Na, Sr and Zn) found in this study are very low, the concentration ratio of the relevant nuclide may not be much affected by coexisting stable elements. Sodium is known to function in the control of osmotic pressure and ionic strength in the cell. A high Na concentration could be the cause of the low Na concentration ratio.

The concentration ratios of Co, Y, Rh, Te, Ce, Pm, Gd, Lu and Hf are very low (Fig. 2). This suggests that there would be no particular accumulation of these elements in mushrooms in the case of contamination. The concentration ratios of the rare earth elements in *C. phlyctidosporus* tended to decrease with increasing atomic number, but the data are limited.

Uptake experiments using a multitracer provided information about the concentration ratios of several nuclides (elements) in mushrooms. Because there is little available information on the accumulation of elements in mushrooms, our findings can be used to understand the behavior of radionuclides in the environment and to estimate possible radiation doses due to the consumption of mushrooms.

REFERENCES

1. Haselwandter, K. (1978) Accumulation of the radioactive nuclide ^{137}Cs in fruitbodies of basidiomycetes. Health Phys. **34**: 713–715.
2. Yoshida, S. and Muramatsu, Y. (1998) Determination of major and trace elements in mushroom, plant and soil samples collected from Japanese forests. Intern. J. Environ. Anal. Chem. in press.
3. Haselwandter, K., Berreck, M. and Brunner, P. (1988) Fungi as bioindicators of radiocaesium contamination: pre- and post-Chernobyl activities. Trans. Br. mycol. Soc. **90**: 171–174.
4. Teherani, D. K. (1988) Determination of ^{137}Cs and ^{134}Cs radioisotopes in various mushrooms from Austria one year

after the Chernobyl incident. J. Radioanal. Nucl. Chem., Lett. **126**: 401–406.
5. Baldini, E., Bettoli, M. G. and Tubertini, O. (1989) Further investigation on the Chernobyl pollution in forest biogeocenoses. Radiochimica Acta **46**: 143–144.
6. Battiston, G. A., Degetto, S., Gerbasi, R. and Sbrignadello, G. (1989) Radioactivity in mushrooms in northeast Italy following the Chernobyl accident. J. Environ. Radioactivity **9**: 53–60.
7. Muramatsu, Y., Yoshida, S. and Sumiya, M. (1991) Concentration of radiocesium and potassium in basidiomycetes collected in Japan. Sci. Total Environ. **105**: 29–39.
8. Yoshida, S., Muramatsu, Y. and Ogawa, M. (1994) Radiocesium concentrations in mushrooms collected in Japan. J. Environ. Radioactivity **22**: 141–154.
9. Yoshida, S. and Muramatsu, Y. (1994) Concentrations of radiocesium and potassium in Japanese mushrooms. Environ. Sci. **7**: 63–70.
10. Ban-nai, T., Yoshida, S. and Muramatsu, Y. (1997) Concentrations of ^{137}Cs and ^{40}K in edible mushrooms collected in Japan and radiation dose due to their consumption. Health Phys. **72**(3): 384–389.
11. Ogawa, M. (1981) The mycorrhiza. In: Microorganisms in Soil, Ed. Soil Microbiological Society of Japan, pp. 279–297, Hakuyusha, Tokyo. (In Japanese)
12. Ban-nai, T., Yoshida, S. and Muramatsu, Y. (1994) Cultivation experiments on uptake of radionuclides by mushrooms. Radioisotopes **43**: 77–82 (in Japanese).
13. Ambe, S., Ohkubo, Y., Kobayashi, Y., Iwamoto, M., Maeda, H. and Yanokura, M. (1995) Multitracer study of transport and distribution of metal ions in plants. J. Radioanal. Nucl. Chem. **195**: 305–313.
14. IAEA (1982) Generic Models and Parameters for Assessing the Environmental Transfer of Radionuclides from Routine Releases, IAEA Safety Series No. 57, IAEA, Vienna.
15. Tateda, Y. and Koyanagi, T. (1996) Concentration factors for ^{137}Cs in Japanese coastal fishes (1984–1990). J. Radiat. Res. **37**, 71–79.
16. Ambe, S., Chen, S. Y., Ohkubo, Y., Kobayashi, Y., Iwamoto, M., Maeda, H., Yanokura, M., Takematsu, N. and Ambe F. (1995) "Multitracer" a new tracer technique — its principle, features and application. J. Radioanal. Nucl. Chem. **195**: 297–303.
17. Ban-nai, T., Muramatsu, Y. and Yanagisawa, K. (1995) Transfer factor of some radionuclides (radioactive Cs, Sr, Mn, Co and Zn) from soil to leaf vegetables. J. Radiat. Res. **36**: 143–154.
18. Mascanzoni, D. (1992) Determination of ^{90}Sr and ^{137}Cs in mushrooms following the Chernobyl fallout. J. Radioanal. Nucl. Chem., Articles **161**: 486–488.
19. Ingrao, G., Belloni, P. and Santaroni, G. P. (1992) Mushrooms as biological monitors of trace elements in the environment. J. Radioanal. Nucl. Chem., Articles **161**: 113–120.
20. Chau, Y. K., Wong, P. T. S., Silverberg, B. A., Luxon, P. L. and Bengert, G. A. (1976) Methylation of selenium in the aquatic environment. Science **192**: 1130–1131.

Paper

LIFETIME RISK OF LUNG CANCER DUE TO RADON EXPOSURE PROJECTED TO JAPANESE AND SWEDISH POPULATIONS

Masahiro Doi,* Yuji Nakamura,* Tetsuya Sakashita,* Nobuko Ogiu,* Frédéric Lagarde,† and Rolf Falk‡

Abstract—**Lifetime risk projections depend greatly on both background lung cancer rates and the selection of the risk model. Since background lung cancer rates differ from subject populations and the time, etiological risk of lifetime lung cancer mortality per unit radon exposure in WLM should be estimated for each subject population and the time of interest. To answer quantitatively how much are the differences among the projected risks for different populations, the Swedish case-control-study-based risk projection model was applied to the Japanese and Swedish populations from 1962 to 1997 as subject populations because of their distinct trends of lung cancer rates. To compare the results with the reference population and authorized risk projection models, U.S. population 1997 and the two risk projection models in BEIR VI report were applied, respectively. Lifetime risk of lung cancer mortality projected for Japanese, Swedish, and U.S. populations in 1997 per radon progeny exposure were estimated to range from 1.50 (0.40–3.19) × 10^{-4} WLM^{-1} to 9.86 (2.62–20.9) × 10^{-4} WLM^{-1}, which could be compared to the detriment associated with a unit effective dose. Conclusive dose conversion coefficients in this study ranged from 2.05 (0.55–4.37) to 13.5 (3.59–28.6) mSv WLM^{-1}, and within this range the discrepancy between dosimetric and epidemiological approaches was included.**

Health Phys. 80(6):552–562; 2001

Key words: radon; risk analysis; epidemiology; alpha particles

INTRODUCTION

The Committee on the Biological Effects of Ionizing Radiations (U.S) reviewed the four epidemiological studies (Lundin et al. 1971; Muller et al. 1983; Radford and Renard 1984; Howe et al. 1986; Hornung and Meinhardt 1987) in the BEIR IV report (NRC 1988). As the substantial revision of BEIR IV report, the recent BEIR VI report (NRC 1999) reviewed 11 miner studies and reexamined all approaches to assess the lung cancer risk posed by residential radon exposure. The BEIR VI report discussed uncertainties related to the induction of lung cancer at low level radon exposure and the combined impact of tobacco smoking, exposure to the mine dust, arsenic, diesel exhaust, Silica and Mycotoxins, and concluded that uncertainties posed by these known risk factors were not significant. And two risk projection models based on the pooled analysis of epidemiological studies of miners (Lubin et al. 1995) were authorized to extrapolate to estimate the potentially important public lung cancer risk posed by indoor radon exposure. It also emphasized that miner-based risk projection is an indirect evidence of lung cancer risk of residential radon exposure and must be validated by direct evidence of lung cancer risk of residential radon proved in the reliable epidemiological study.

BEIR committee reviewed some case-control studies on residential radon and lung cancer and their meta-analysis (Lubin and Boice 1997) and regarded them as inconclusive because of some potential limiting factors and errors in estimation of cumulative radon progeny exposure (NRC 1999). BEIR committee listed several formidable limitations of these case-control studies on residential radon and lung cancer studies and expressed a rather negative view of whether these limitations could be addressed to achieve more definitive results. But if they were not definitive, they showed direct evidence of indoor radon risk.

It is trivial that risk projections with an excess relative model depend greatly on background lung cancer rate of the subject population and also the selection of the risk model. But it is not answered quantitatively how much are the differences in the projected risks for different subject populations.

Lung cancer is one of the leading causes of cancer death in most of the developed countries, and several environmental toxins have been suspected to raise the background lung cancer risk. Particularly, daily cigarette smoking showed up as the most common cause of lung

* Environmental and Toxicological Sciences, Research Group, National Institute of Radiological Sciences, 4-9-1, Anagawa, Inage, Chiba, Japan; † Division of Epidemiology, Institute of Environmental Medicine, Karolinska Institute, Box 210, S171 77, Stockholm, Sweden; ‡ Division of Environmental Monitoring and Dosimetry, Swedish Radiation Protection Institute, S17116, Stockholm, Sweden.

For correspondence or reprints contact: M. Doi, Environmental and Toxicological Sciences, Research Group, National Institute of Radiological Sciences, 4-9-1, Anagawa, Inage, Chiba, Japan, or email at masa_doi@nirs.go.jp

(*Manuscript received* 11 *November* 1999; *revised manuscript received* 6 *October* 2000, *accepted* 6 *February* 2001)

0017-9078/01/0

cancer, and year trends of cigarette consumption, sales, and smoking prevalence are different by the population and the times.

ICRP proposed the reference population, for which survival probability and the age-specific lung cancer mortality rate were derived by Land and Sinclair (1991) from the average values of the five countries (i.e., Japan, the United States, Puerto Rico, the United Kingdom and China).

A conclusive lifetime lung cancer mortality coefficient was projected for the reference population with miner-based relative risk projection model and was estimated to be 2.83×10^{-4} WLM^{-1} (Working Level Month)[§][‖] (ICRP 1994a). This value was compared to the estimate of BEIR IV, 3.5×10^{-4} WLM^{-1} projected for U.S. population 1980–1984 with time since exposure model (NRC 1988).

ICRP (1994a) divided this etiological lifetime lung cancer mortality coefficient by the detriment coefficient for effective dose of 5.6×10^{-5} mSv^{-1} for adult workers and 7.3×10^{-5} mSv^{-1} for members of the public (ICRP 1991) and recommended effective dose conversion factors of 5.06 mSv WLM^{-1} (or 1.43 mSv per mJ h m^{-3}) for workers and 3.88 mSv WLM^{-1} (or 1.10 mSv per mJ h m^{-3}) for members of the public. These reference dose conversion factors are general estimates, but it must be emphasized that the confidence intervals are included in these estimates substantially.

The ICRP has endorsed a dosimetric human respiratory tract model in Publication 66 (ICRP 1994b), and the modal value of 15 mSv WLM^{-1} was evaluated by the model (Birchall and James 1994), which is 3 to 4 times larger than the above conversion conventions. Sensitivity analysis of each parameter in the respiratory tract model, including quality factor of 20 for alpha-particle exposure, was performed substantially by Birchall and James (1994) but could not explain such a discrepancy consistently. The BEIR VI report also reviewed the discrepancy between epidemiological and dosimetric approaches and discussed the uncertainty in the quality factor of alpha-particle in the dosimetric model (NRC 1999).

It must be reconfirmed before discussing about the discrepancy that the projected lung cancer risk of radon exposure is proportional to the survival probability and the age-specific lung cancer mortality rate of the subject population.

The first objective of this study is to estimate the etiological risk of lifetime lung cancer mortality for applying the Japanese and Swedish populations to a Swedish case-control study-based relative risk projection model in contrast to the miner-based risk projection models in BEIR VI report (NRC 1999). The second objective is to apply these models to the Japanese, Swedish, and U.S. populations in 1997, and to compare the dose conversion factors with their confidence intervals.

MATERIAL AND METHODS

Japanese and Swedish populations from 1962 to 1997 were selected as subject populations because Japanese population is just the opposite of Swedish population in the indoor radon exposure as well as the smoking rate. U.S. population was selected as a reference population because it was thoroughly examined in BEIR IV and VI reports (NRC 1988, 1999).

JAPANESE POPULATION

Residential radon concentrations in Japan were relatively low in comparison with those in other countries (UNSCEAR 1993). A recent nationwide indoor radon survey was commenced for 940 houses (Sanada et al. 1999). Radon concentration in the Japanese houses showed approximately a log-normal distribution of which arithmetic and geometric means were 15.5 and 12.7 Bq m^{-3}, respectively. Only one house exceeded the action level of 150 Bq m^{-3} settled by the U.S. EPA (1986).

Smoking rate of Japanese male has been high in comparison with other countries. In 1965, 82.3% of Japanese males were smoking, and although it has tended to go downward, still 55.2% of Japanese males were smoking in 1997.

Smoking rate of total female had been very low, and it tended to be reduced gradually; it reached down to 15% in 1997. But the smoking rate of Japanese women in the 20–29 y age group has been constantly increasing since 1965, as illustrated in Appendix A.

By the census population study (Hirayama 1979), daily cigarette smoking is showed as the largest cause of lung cancer, of which excess relative risk and attributable risk in males were 3.76 and 67.2%, respectively. As the reflection of these conditions, malignant neoplasm by site is changing its pattern drastically in these 40 y in the Japanese population. In 1960, stomach cancer for males and females was the most common, accounting for 52.3% of all deaths from cancer for males and 39.2% for females, while lung cancer for males and females was 7.2% and 3.6%, respectively (Ministry of Health and Welfare 1962). Death rates by stomach cancer for both sexes are decreasing, and, instead, lung cancer has been increasing consistently for both males and females. According to the statistics in 1997, lung cancer was the most common type of cancer for males, accounting for 21.4% of all cancer deaths (for females lung cancer accounted for 11.7% of all cancer deaths). Fig. 1 shows the age-specific lung cancer mortality rates by sex, $r_o(a)$, for the Japanese population from 1962–1997, which were calculated by the age-specific lung cancer cases in *Vital Statistics of Japan* (Ministry of Health and Welfare

[§] 1 WL (working level) is equivalent to the equilibrium equivalent radon concentration of 100 pCi L^{-1} or 3,700 Bq m^{-3} (EEC). Assuming an equilibrium factor of 0.4, 1 WL is approximately equal to a radon gas concentration of 9,250 Bq m^{-3}.

[‖] 1 WLM (working level month) is an exposure to 1 WL for 170 h and is equal to 3.54 mJ h m^{-3} (ICRP 1994a).

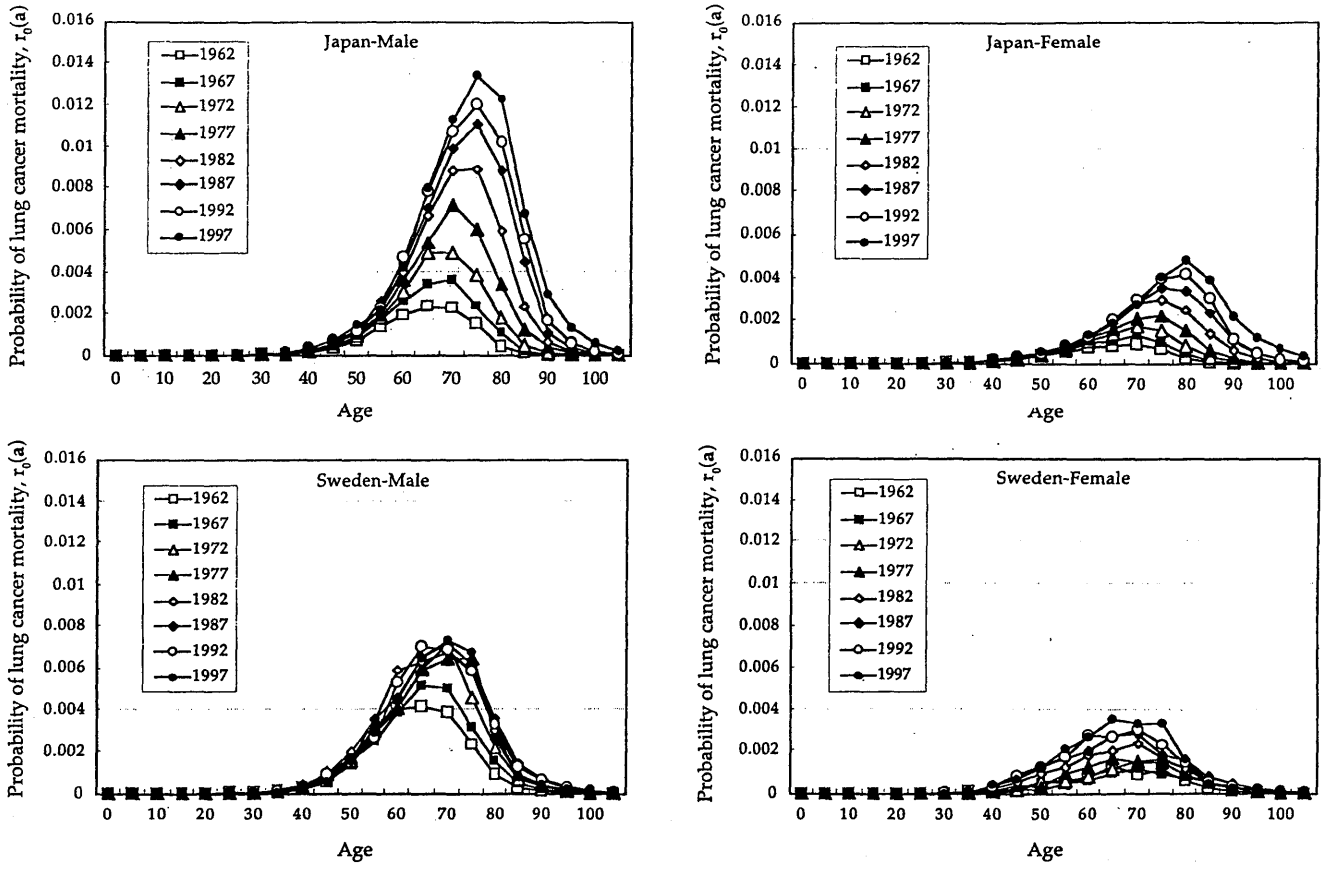

Fig. 1. Probability of lung cancer mortality by age in the presence of other causes of death for the Swedish and Japanese populations from 1962 to 1997 (calculated after Swedish Cancer Registry, Statistisk Årsbok, and Japan vital statistics).

1962–1997). A constant increase of background lung cancer mortality for Japanese males and females, which might reflect the year trend of smoking rates, is illustrated in Appendix A. Fig. 2 shows life expectancy of Japanese males and females shown in *Vital Statistics of Japan* (Ministry of Health and Welfare 1962–1997).

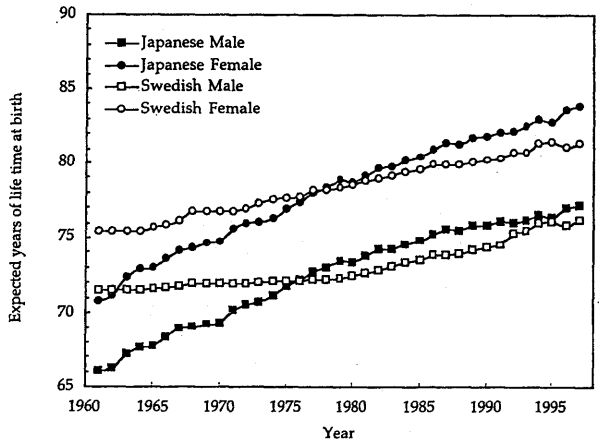

Fig. 2. Trends of life expectancy at birth of the Swedish and Japanese populations in 1961–1997 (reproduced after Swedish Statistisk Årsbok 1964–1999, and Japan vital statistics 1962–1997).

SWEDISH POPULATION

Residential radon concentrations in Sweden were regarded as some of the highest in the world (UNSCEAR 1993). As a rough guide to represent nationwide indoor radon concentration, 506 houses including 191 apartments in multi-family houses were measured in 1982, and the radon concentration showed approximately a log-normal distribution, of which arithmetic and geometric means of detached houses were 122 and 69 Bq m^{-3}, respectively (Swedjemark and Mjönes 1984). Average radon concentration in the houses built since 1981 was surveyed to be 50 Bq m^{-3}, which might be caused by some social countermeasures to indoor radon, i.e., alm-shale concrete was not used in any houses built after 1975, and the building construction to decrease the inflow of soil gas has been improved by the Swedish 1980 building code (Swedjemark and Åkerblom 1994).

The proportion of smokers is steadily decreasing in Sweden. The proportion of daily smokers for men 16–84 y has decreased from 36% in 1980 to 22% in 1995, while

the proportion of daily smokers among women decreased during the corresponding period from 29% to 23% (Swedish National Board of Health and Welfare 1998). The proportion of smokers among men has decreased significantly since the 1960's, but among women has changed its trend to decline since the latter 1970's.

The Swedish Cancer Registry was established in 1958, and has collected statistics of cancer incidence in Sweden. Regulations of the National Board of Health and Welfare require that physicians send clinical reports of all cancer cases and pathologists send reports for every cancer diagnosis. This means that most of the cancer cases are noted twice in separate reports by the Registry. The background lung cancer mortality by age, $r_o(a)$ for Swedish males and females are evaluated from Swedish Cancer Registry data from 1962–1997 (Swedish National Board of Health and Welfare 1964–1999, Statistiska Centralbyrån 1964–1999), of which results are shown in Fig. 1. Recent vital statistics of Sweden are distributed by the Swedish National Board of Health and Welfare (http://www.sos.se/sos/publ/skrift/skrifte.htm). Fig. 1 shows background lung cancer mortality of Swedish males had almost been saturated during the 1990's, while that of females still increased gradually. These figures might reflect partly the trends of age-specific smoking rates in the 1960's and 1970's for Swedish males and females. As illustrated in Appendix A, smoking rates of Swedish males began to decrease in 1970, while those of Swedish females increased constantly. Fig. 2 shows the life expectancy of Swedish males and females from 1961 to 1997 (Statistiska Centralbyrån 1964–1999).

U.S. POPULATION

As the reference of the above subject populations, recent U.S. population figures were selected. The lung cancer mortality rates of the U.S. population for 5-y age groups and sex in 1997 were derived from the number of lung cancer deaths reported by the U.S. Department of Health & Human Services (http://www.cdc.gov/nchs/data/gmwki_97.pdf) and populations by U.S. Census Bureau (http://www.census.gov/population/www/estimates/uspop.html). Life expectancy for females was 79.4 y and for males 73.6 y in 1997 (National Center for Health Statistics 1999).

RISK PROJECTION MODEL

Etiological risk of lifetime lung cancer mortality due to radon progeny exposure is evaluated at a radon progeny exposure rate of 0.1 WLM y^{-1} by adopting the relative risk projection model to the background lung cancer mortality of the subject population. Assuming 0.8 as an occupation factor and 0.4 as an equilibrium factor, 0.1 WLM y^{-1} is given by the indoor radon gas concentration of 22.4 Bq m^{-3}.

According to the definition of relative risk, expected risk is expressed in proportion to the control (or background) lung cancer mortality of the subject population. This is a first simple approximation, and some modifying factors must be taken into consideration for more precise projection as the risk models in BEIR VI report (NRC 1999).

Excess relative risk and covered exposure period could be derived from each case-control study on residential radon and lung cancer or their meta-analysis (Lubin and Boice 1997; NRC 1999). For this study, a Swedish nationwide case-control study (Pershagen et al. 1994) was selected because it was based on the well-authorized cancer registry and radon monitoring, and the result showed the clear pattern of increasing relative risk with time-weighted mean radon exposure (Pershagen et al. 1993, 1994).

Because a subsequent study accounting for random error in the exposure assessment confirmed that measurements of radon concentration are more valid when study subjects who slept near open windows were excluded (Lagarde et al. 1997), a relative risk coefficient obtained by conditional logistic regression of all study subjects except those who slept near an open window was adopted in this study. Confounding by known risk factors, i.e., smoking, occupation, and urban living, was adjusted in the multivariate analysis. The resulting excess relative risk of lung cancer (thereafter abbreviated as ERR) was 0.020 (95% CI 0.0055–0.0433) WLM^{-1}.

Since the Swedish epidemiological study (Pershagen et al. 1993, 1994) covered an average exposure period of 32.5 y for each case and control subject, estimated excess relative risk corresponds only to 32.5 y of cumulative radon exposure and does not reflect the lifetime risk of lung cancer mortality. Hence, radon exposure incurred 32.5 y or more before age at risk may be weighted more or less in the risk projection analysis, depending on hypotheses about the etiological relevance of such exposure.

Taking this into account, the risk projection model based on the Swedish case-control study is mathematically expressed as follows:

$$r(a) = r_o(a)[1 + \beta \times (W_1 + RF \times W_2)],$$

where

$r(a)$ = lung-cancer mortality rate for given age and calendar period by age a;
$r_o(a)$ = background of lung cancer mortality rate in the population by age a;
β = excess relative risk per unit radon progeny exposure per WLM, = 0.020 (95% CI: 0.0055–0.0433) WLM^{-1} (Pershagen et al. 1993, 1994);
W_1 = cumulative exposure in WLM incurred between 3 y and 32.5 y before age a;
W_2 = cumulative exposure in WLM incurred 32.5 y or more before age a; and
RF = reduction factor for cumulative exposure, W_2.

The 3-y lag period in the model is based on the assumption that radon progeny exposures have no substantial effect on the lung cancer mortality for at least 3 y (Pershagen et al. 1994). The reduction factor, *RF* is introduced in this model to account for modification of the risk coefficient related to exposure outside the 32.5-y period. This ad-hoc procedure allows conjectural extensions of the model to a wider time-frame in conjunction with values for *RF* varying from unity to zero. The lifetime risk of lung cancer mortality per unit WLM is the integration of $[r(a)-r_0(a)]$ over the expected years of life divided by the lifetime exposure.

As the reference of the above model, two miner-based risk projection models authorized in BEIR VI report (NRC 1999) were also adopted to the subject populations. The Exposure-Age-Duration (EAD) model and the Exposure-Age-Concentration (EAC) model are the extrapolations from miner studies to the residential radon exposure and its lung cancer risk. Mathematical notations of EAD and EAC models are summarized in Appendix B.

RESULTS AND DISCUSSION

Fig. 3 shows the trend of etiological risk of lung cancer mortality per lifetime radon progeny exposure, projected to Japanese and Swedish populations by sex since 1962–1997, by applying the Swedish case-control-study-based risk projection model in the case of $RF = 0$. Error bars reflected the 95% confidence intervals of excess relative risk of the Swedish case-control-study (Pershagen et al. 1994).

Lifetime lung cancer risk for Japanese males increased constantly, from 0.99 (0.26–2.11)–4.87 (1.69–10.3) $\times$ 10^{-4} WLM^{-1} from 1962–1997. For Swedish males, the lifetime lung cancer risk was estimated to be 1.77 (0.47–3.77) $\times$ 10^{-4} WLM^{-1} in 1962, which was larger than that for Japanese male. It increased to reach the maximum of 2.93 (0.78–6.23) $\times$ 10^{-4} WLM^{-1} in 1982, and then gradually decreased to 2.70 (0.72–5.75) $\times$ 10^{-4} WLM^{-1} in 1997. This estimate was around half of that for Japanese males.

Lifetime lung cancer risk for Japanese and Swedish females was similar to increase constantly. From 1962–1997, it increased from 0.41 (0.11–0.87)–1.79 (0.47–

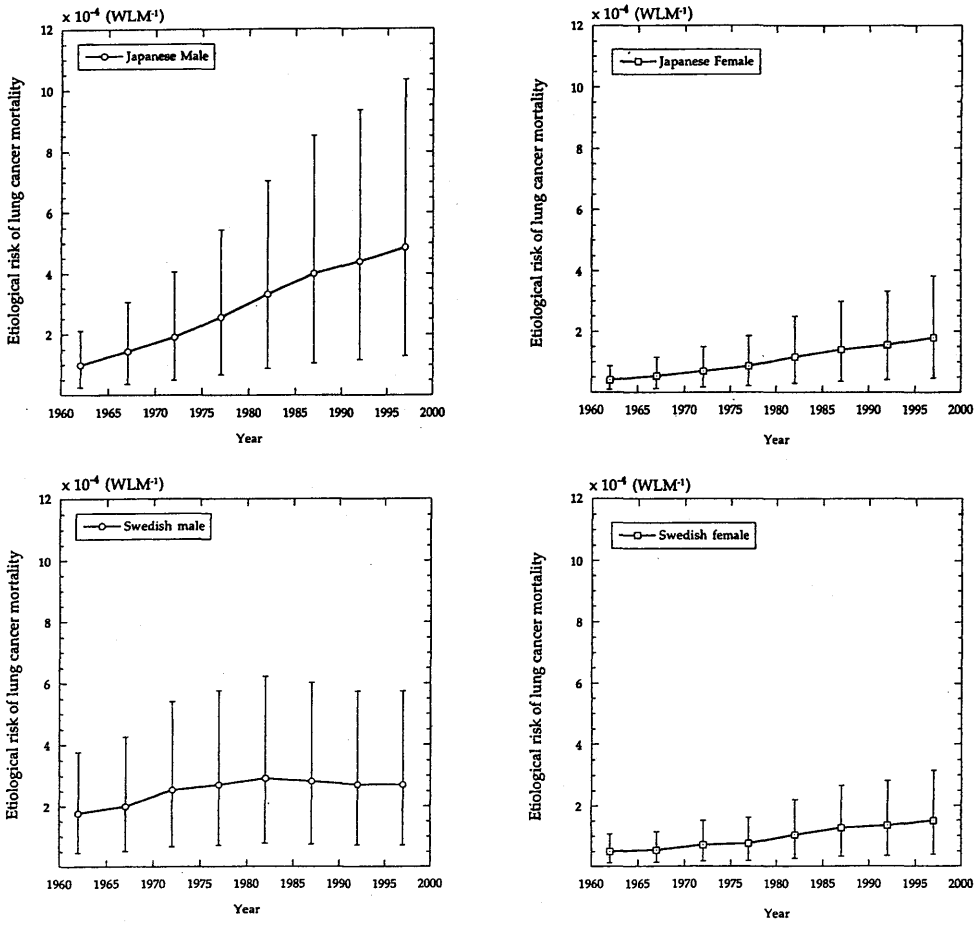

Fig. 3. Etiological risk of lung cancer mortality projected to the Japanese and Swedish populations from 1962–1997 by the Swedish case-control-study-based risk projection model in the case of $RF = 0$ at an exposure rate of 0.1 WLM y^{-1}.

3.82) $\times$ 10^{-4} WLM^{-1} for Japanese females, and from 0.51 (0.13–1.08)–1.50 (0.40–3.19) $\times$ 10^{-4} WLM^{-1} for Swedish females.

The lung cancer mortality for Japanese males might be on the rise, while the total smoking rate decreased constantly. It may partly be explained that smoking rates in young age groups of Japanese males were more than 80%, and they did not decrease significantly before 1980 as shown in Fig. A2. In addition, per capita cigarette consumption of Japanese population increased constantly until 1980 as shown in Fig. A3. These may suggest that total exposure to tobacco of Japanese male was not necessarily decreased. Fig. A2 also shows the constant increase of smoking rates in the 20–29 y age groups of Japanese females since 1962, which may cause the increase of lung cancer risk for Japanese females as suggested in Fig. 3.

Swedish lung cancer mortality and smoking habits are discussed in the Swedish public health report (Swedish National Board of Health and Welfare 1998). Indeed, there are several complex reasons that influence the lung cancer mortality of each subject population, and careful epidemiological and biological analyses are required to understand the true situation. In the Swedish case-control study, a weak interaction was found between tobacco smoking and radon exposure, which was more than additive and less than multiplicative (Pershagen et al. 1994). Detailed discussions on tobacco smoking and radon exposure are shown in Appendix C, BEIR VI report (NRC 1999).

When the relative risk projection model was applied, etiological lung cancer risk due to lifetime radon exposure reflected the trend of background lung cancer mortality of each subject population by sex and age. Fig. 4 shows the age-specific etiological risk of lung cancer mortality for Japanese, Swedish, and U.S. populations by sex in 1997 at an exposure rate of 0.1 WLM y^{-1} by applying the three risk projection models. Swedish-case-control-study-based model with $RF = 0$ was applied, and the results were plotted with those of the two risk projection models in BEIR VI report (NRC 1999). Fig. 5 shows total etiological risk of lung cancer mortality per lifetime radon progeny exposure at an exposure rate of 0.1 WLM y^{-1} for Japanese, Swedish, and U.S. populations in 1997 projected by applying the above three risk projection models. Error bars in Fig. 5 reflect the 95% confidence intervals of excess relative risk for each risk projection model.

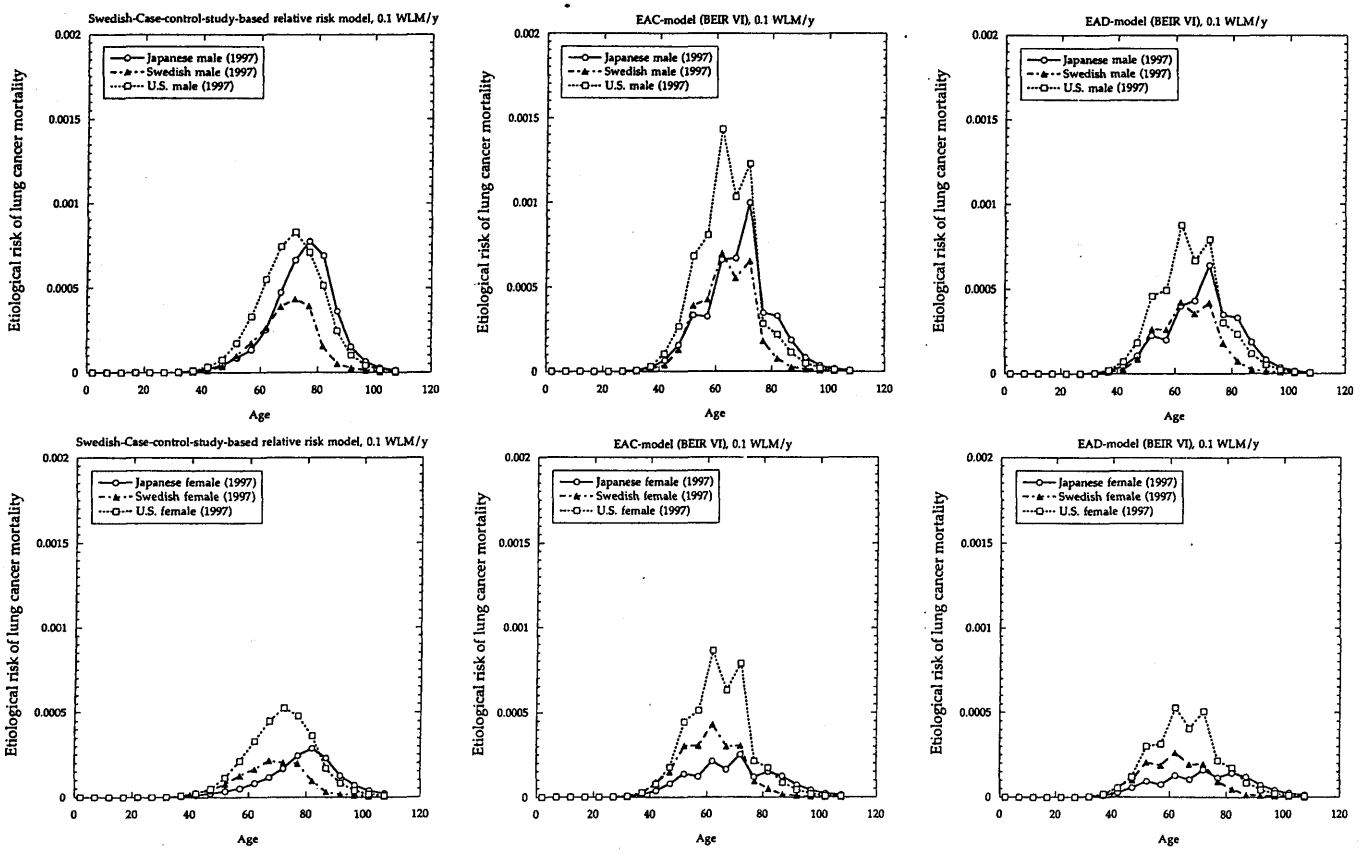

Fig. 4. Etiological risk of lung cancer mortality by age projected to the Japanese, Swedish, and U.S. populations in 1997 by the Exposure-Age-Duration (EAD) model, Exposure-Age-Concentration (EAC) model (BEIR VI, National Research Council 1999), and the Swedish case-control-study-based risk projection model in the case of $RF = 0$ at an exposure rate of 0.1 WLM y^{-1}.

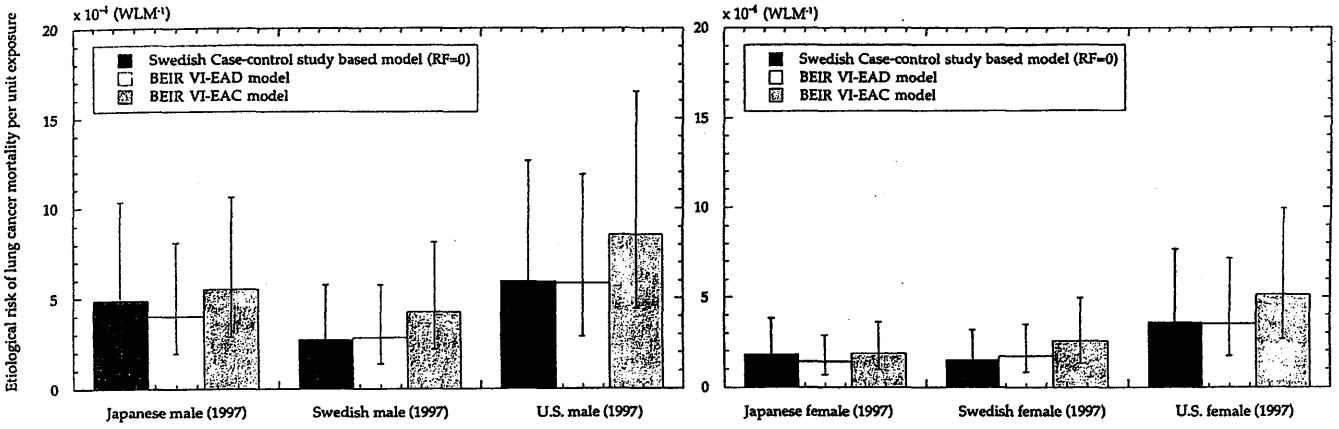

Fig. 5. Etiological risk of lung cancer mortality projected to the Japanese, Swedish, and U.S. populations in 1997 by the Exposure-Age-Duration (EAD) model, Exposure-Age-Concentration (EAC) model (NRC 1999), and the Swedish case-control-study-based risk projection model in the case of $RF = 0$ at an exposure rate of 0.1 WLM y^{-1}. Error bars reflect the 95% confidence interval of excess relative risk coefficient of each model.

As shown in Figs. 4 and 5, the largest risk projections were given by the Exposure-Age-Concentration model (NRC 1999) for all subject populations. For Japanese and U.S. populations, the minimum radon risk estimates were given by the Exposure-Age-Duration model (NRC 1999), while for Swedish populations they were given by the Swedish case-control-study-based model.

Since the Swedish case-control study corresponded to 32.5 y of exposure at a constant radon concentration of each case-control study subject (Pershagen et al. 1994), the risk related to exposure outside the 32.5-y period must be included in the lifetime lung cancer risk estimate by weighting the reduction factor, *RF*, from unity to zero. Table 1 shows the etiological lifetime lung cancer mortality per lifetime radon progeny exposure projected to Japanese, Swedish, and U.S. populations (1997) by applying the risk projection model in the case of $RF = 0$, 0.5, and 1.0, respectively. In comparison with miner-based EAD and EAC models in Fig. 5, *RF* might be fixed to zero for Japanese and Swedish populations and 0.5 for the U.S. population at most. Consequently, lifetime lung cancer risk coefficients projected for Japanese, Swedish, and U.S. populations (1997) were included in the range from 1.50 (0.40–3.19) $\times 10^{-4}$ WLM^{-1} (Swedish female, $RF = 0$) to 9.86 (2.62–20.9) $\times 10^{-4}$ WLM^{-1} (U.S. male, $RF = 0.5$) as listed in Table 1.

The ICRP has recommended the conversion from radon progeny exposure to effective dose by a direct comparison of the detriment associated with a unit effective dose and a unit radon progeny exposure (ICRP 1994a). According to this method, the lifetime risk of lung cancer mortality per lifetime radon progeny exposure was compared with nominal risk coefficients for stochastic effects on atomic bomb survivors per unit effective dose, namely 7.3×10^{-5} mSv^{-1} for the whole population (ICRP 1991). By a comparison of the above range of lung cancer mortality coefficients and the above nominal detriment coefficients, the possible range of conversion factors was estimated from 2.05 (0.55–4.37) to 13.5 (3.59–28.6) mSv WLM^{-1}. ICRP proposed the nominal dose conversion factor of 3.88 mSv WLM^{-1} for the general public by an epidemiological approach (ICRP 1991), which was based on the lifetime lung cancer risk coefficient of 2.83×10^{-4} WLM^{-1} for the reference

Table 1. Etiological lifetime lung cancer mortality per lifetime radon progeny exposure projected to Japanese, Swedish, and U.S. populations in 1997 by applying the risk projection model in the case of $RF = 0$, 0.5, and 1.0, respectively. *RF* is a risk weighting factor of the cumulative exposure incurred more than 32.5 y before the age at risk comparing to the exposure incurred between 3 and 32.5 y before the age.

		Excess life-time lung cancer mortality per 10,000 person WLM (95% CI)		
		Swedish-Epi-study-based risk projection model		
Population	Sex	$RF = 0$	$RF = 0.5$	$RF = 1.0$
Japan 1997	Male	4.87 (1.69–10.3)	8.40 (2.23–17.8)	11.9 (3.17–25.2)
	Female	1.79 (0.47–3.82)	3.19 (0.85–6.79)	4.59 (1.22–9.76)
Sweden 1997	Male	2.70 (0.72–5.75)	4.40 (1.17–9.36)	6.09 (1.62–13.0)
	Female	1.50 (0.40–3.19)	2.40 (0.64–5.11)	3.30 (0.88–7.03)
U.S. 1997	Male	5.94 (1.58–12.6)	9.86 (2.62–20.9)	13.8 (3.67–29.0)
	Female	3.61 (0.96–7.69)	6.02 (1.60–12.8)	8.42 (2.24–17.9)

population (Land and Sinclair 1991) with the miner-based risk projection model.

On the other hand, the dosimetric approach by the computer-aided human respiratory tract model implies the arithmetic mean of effective dose per potential alpha energy exposure to be 17.2 mSv WLM^{-1}, with a modal value of approximately 15 mSv WLM^{-1} (ICRP 1994b; Birchall and James 1994, 1999). The respiratory tract *in vivo/in vitro* biodosimetry approach using rats by Brooks et al. (1999) found the absorbed dose per exposure for nasal epithelial cell and for deep lung epithelial cells to be 0.22–0.47 mGy WLM^{-1} and 1.13–1.34 mGy WLM^{-1}, respectively. Taking a radiation-weighting factor for alpha particles of 10 to 20, these dosimetric approaches showed good agreement.

The estimated dose conversion coefficient in this study ranged from 2.05 (0.55–4.37) to 13.5 (3.59–28.6) mSv WLM^{-1}, and within this range the discrepancy between dosimetric and epidemiological approaches was included. It is important to assess the uncertainties within these alternative approaches and the selection of the models, and it is also important to account for a possible dependence on the background lung cancer mortality of subject populations and their time trends.

CONCLUSION

To answer quantitatively how much are the differences among the projected risks for specific populations with different risk projection models, the Swedish case-control study-based risk projection model was applied to the Japanese and Swedish populations 1962–1997 and U.S. population 1997.

When the relative risk projection model was applied, etiological lung cancer risk due to lifetime radon exposure reflected the trend of background lung cancer mortality of each subject population by sex and calendar year. For Japanese males, estimated lifetime lung cancer risk of radon exposure showed a significant increase from 0.99 (0.26–2.11) in 1962 to 4.87 (1.69–10.3) $\times$ 10^{-4} WLM^{-1} in 1997.

For Swedish males it increased from 1.77 (0.47–3.77) $\times$ 10^{-4} WLM^{-1} in 1962 to the maximum of 2.93 (0.78–6.23) $\times$ 10^{-4} WLM^{-1} in 1982. For Japanese and Swedish females, it increased constantly from 0.41 (0.11–0.87)–1.79 (0.47–3.82) $\times$ 10^{-4} WLM^{-1} for Japanese females, and from 0.51 (0.13–1.08)–1.50 (0.40–3.19) $\times$ 10^{-4} WLM^{-1} for Swedish females. Significant increase of lifetime lung cancer risk for Japanese males during 1962–1997 reflected the increase of background lung cancer mortality rates, which may partly be caused by their trends of smoking habit from the 1930's to the 1970's.

Lifetime risk of radon exposure and lung cancer mortality projected for Japanese, Swedish, and U.S. populations in 1997 ranged from 1.50 (0.40–3.19) $\times$ 10^{-4} WLM^{-1} to 9.86 (2.62–20.9) $\times$ 10^{-4} WLM^{-1}, which could be compared to the detriment associated with a unit effective dose, namely 7.3 $\times$ 10^{-5} mSv^{-1} for the general population. Conclusive dose conversion coefficients in this study ranged from 2.05 (0.55–4.37) to 13.5 (3.59–28.6) mSv WLM^{-1}, which included the estimates of dosimetric and epidemiological approaches.

Acknowledgments—Much appreciation should be expressed to Gun Astri Swedjemark, the former Director of the Division of Environmental Radiology, Swedish Radiation Protection Institute, and her staff for their kind coordination throughout this cooperative study and their invaluable support.

The authors wish to express their deepest gratitude to Göran Pershagen, Institute of Environmental Medicine, Karolinska Institute, for his kind encouragement and invaluable academic direction throughout this work. The authors would also like to express their hearty appreciation to Anita Enflo, Swedish Radiation Protection Institute, for her invaluable support to realize this collaborative work.

REFERENCES

Birchall, A.; James, A. C. Uncertainty analysis of the effective dose per unit exposure from radon progeny and implications for ICRP risk-weighting factors. Radiat. Protect. Dosim. 53:133–140; 1994.

Birchall, A.; James, A. C. The new ICRP respiratory tract model and radon dosimetry, indoor radon. Exposure and its health consequences—Quest for the true story of environmental radon and lung cancer. Inaba, J.; Yonehara, H.; Doi, M., eds. Tokyo: Kodansha Scientific Ltd.; 1999: 49–65.

Brooks, A. L.; Khan, M. A.; Bao, S.; Braby, L. A.; Johnson, N. F.; Cross, F. T. Radon induced micronuclei in respiratory tract biodosimetry, indoor radon. Exposure and its health consequences—Quest for the true story of environmental radon and lung cancer. Inaba, J.; Yonehara, H.; Doi, M., eds. Tokyo: Kodansha Scientific Ltd.; 1999: 67–82.

Hirayama, T. Cancer epidemiology in Japan. Environmental Health Perspectives 32:11–15; 1979.

Hornung, R. W.; Meinhardt, T. J. Quantitative risk assessment of lung cancer in U.S. Uranium miners. Health Phys. 52:417–430; 1987.

Howe, G. R.; Nair, R. C.; Hewcombe, H. G.; Miller, A. B.; Abbatt, J. D. Lung cancer mortality (1950–1980) in relation to radon daughter exposure in a cohort of workers at the Eldorado Beaverlodge uranium mine. J. Natl. Cancer Inst. 77:357–362; 1986.

ICRP. Recommendations of the International Commission on Radiological Protection. Oxford: Pergamon Press; Publication 60; 1991, 1990.

ICRP. Protection against radon-222 at home and at work. Oxford: Pergamon Press; Publication 65; 1994a.

ICRP. Human respiratory tract model for radiological protection. Oxford: Pergamon Press; Publication 66; 1994b.

Japan Tobacco, Inc. History book of Japan Tobacco, Inc. Vol. 4. Tokyo: Japan Tobacco, Inc.; Private Publication; 1963: 698–701 (in Japanese).

Japan Tobacco, Inc. History book of Japan Tobacco, Inc. Vol. 5. Tokyo: Japan Tobacco, Inc.; Private Publication; 1978: 194–197 (in Japanese).

Japan Tobacco, Inc. History book of Japan Tobacco, Inc. Vol. 6. Tokyo: Japan Tobacco, Inc.; Private Publication; 1990: 2083 (in Japanese).

Lagarde, F.; Pershagen, G.; Åkerblom, G.; Axelson, O.; Bäverstam, U.; Damber, L.; Enflo, A.; Svartengren, M.; Swedjemark, G. A. Residential radon and lung cancer in Sweden:

Risk analysis accounting for random error in the exposure assessment. Health Phys. 72:269–276; 1997.

Land, C. E.; Sinclair, W. K. The relative contributions of different organ sites to the total cancer mortality associated with low-dose radiation exposure. In: Risks associated with ionizing radiations. Oxford: Pergamon Press; Annals of the ICRP 22(1):31–57; 1991.

Lubin, J. H.; Boice, J. D., Jr. Lung cancer risk from residential radon: meta-analysis of eight epidemiological studies. J. Natl. Cancer Inst. 89:49–57; 1997.

Lubin, J. H.; Boice, J. D., Jr.; Edling, C.; Hornung, R. W.; Howe, G. R.; Kunz, E.; Kusiak, R. A.; Morrison, H. I.; Radford, E. P.; Samet, J. M.; Tirmarche, M.; Woodward, A.; Yao, S. X.; Pierce, D. A. Lung cancer in radon exposed miners and estimation of risk from indoor exposure. J. Natl. Cancer Inst. 87:817–827; 1995.

Lundin, F. E.; Wagoner, J. K.; Archer, V. E. Radon daughter exposure and respiratory cancer: quantitative and temporal aspects. Joint Monograph No. 1: NIOSH and NIEHS. Washington, DC: U.S. Dept. of Health, Education and Welfare, Public Health Service; 1971.

Ministry of Health and Welfare. Vital statistics of Japan. Tokyo: Ministry of Health and Welfare, Statistics and Information Department; 1962–1997 (in Japanese).

Muller, J.; Wheeler, W. C.; Gentleman, J. F.; Suranyi, G.; Kusiak, R. Study of mortality of Ontario miners 1955–1977. Part I. Toronto: Ontario Ministry of Labour, Ontario Workers Compensation Board; 1983.

National Center for Health Statistics. National Vital Statistics Report 47:8–11; 1999.

National Research Council. Committee on the biological effects of ionizing radiation. Health risks of radon and other internally deposited alpha-emitters. BEIR IV. Washington, DC: National Academy Press; 1988.

National Research Council. Committee on the biological effects of ionizing radiation. Health effects of exposure to radon. BEIR VI. Washington, DC: National Academy Press; 1999.

Pershagen, G.; Axelson, O.; Clavensjö, B.; Damber, L.; Desai, G.; Enflo, A.; Lagarde, F.; Mellander, H.; Svartengren, M.; Swedjemark, G. A.; Åkerblom, G. Radon i bostäder och lung cancer. En landsomfattande epidemiologisk undersökning, IMM-rapport 2/93. Stockholm: Karolinska Institute; 1993 (in Swedish).

Pershagen, G.; Axelson, O.; Clavensjö, B.; Damber, L.; Desai, G.; Enflo, A.; Lagarde, F.; Mellander, H.; Svartengren, M.; Swedjemark, G. A.; Äkerblom, G. Residential radon exposure and lung cancer in Sweden. New England J. Med. 330:159–164; 1994.

Radford, E. P.; Clair Renard, K. G. St. Lung cancer in Swedish iron miners exposed to low doses of radon daughters. New England J. Med. 310:1485–1494; 1984.

Sanada, T.; Fujimoto, K.; Miyano, K.; Doi, M.; Tokonami, S.; Uesugi, M.; Takata, Y. Measurement. of nationwide indoor Rn concentration in Japan. J. Environmental Radioact. 45:129–137; 1999.

Statistiska Centralbyrån, Statistisk Årsbok '64-'99. Sveriges officiella statistisk. Stockholm: Statistica Centralbyrån; 1964–1999 (in Swedish).

Swedish National Board of Health and Welfare. Cancer incidence in Sweden 1962–1997. Stockholm: Swedish National Board of Health and Welfare; Centre for Epidemiology; 1964–1999.

Swedish National Board of Health and Welfare. Sweden's public health report. Stockholm: Swedish National Board of Health and Welfare; 1998.

Swedjemark, G. A.; Mjönes, L. Radon and radon daughter concentrations in Swedish homes. Radiat. Protect. Dosim. 7:341–345; 1984.

Swedjemark, G. A.; Åkerblom, G. The Swedish radon program: thirteen years of experience and suggestions for future strategy. Radiat. Protect. Dosim. 56:201–205; 1994.

United Nations Scientific Committee on the Effects of Atomic Radiation. Sources and effects of ionizing radiation. New York: United Nations; 1993.

U.S. Environmental Protection Agency. A citizen's guide to radon. Washington, DC: Environmental Protection Agency; EPA Report 86-0004; 1986.

APPENDIX A

Trends of smoking rate as a significant contributor to background lung cancer mortality of Japanese and Swedish populations from 1962 to 1998

As the health habit of the subject populations that may be tied-in with the background lung cancer mortality, the smoking rate of Japanese and Swedish populations by sex from 1962–1998 are illustrated in Fig. A1 (Japan Tobacco Inc. 1963, 1978, 1990; Swedish National Board of Health and Welfare 1998).

Trends of smoking rate of Japanese populations by 10-y age group from 1962 to 1998 was shown in Fig. A2 (Japan Tobacco Inc. 1963, 1978, 1990). Per capita cigarette consumption rate of Japanese population more

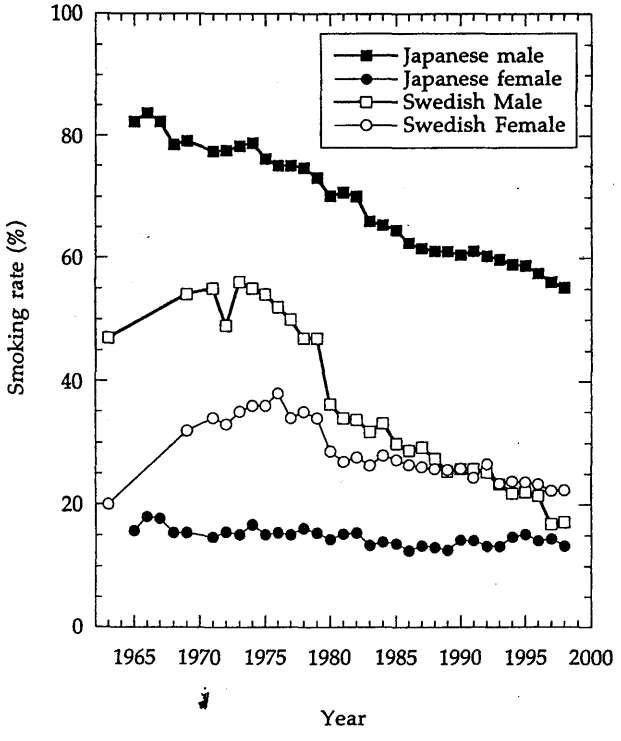

Fig. A1. Smoking rate of Japanese and Swedish males and females from 1962–1998.

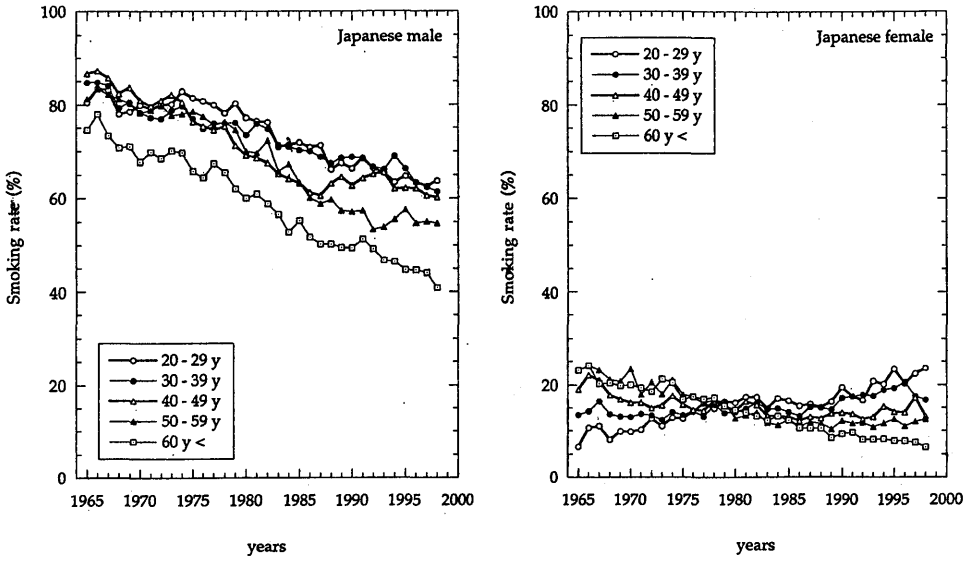

Fig. A2. Smoking rate of Japanese populations by 10-y age group from 1962–1998.

than 15 y old from 1920 to 1998 was shown in Fig. A3 (Japan Tobacco Inc. 1963, 1978, 1990). Detailed information on Japanese smoking rate and cigarette consumption rate are distributed by the Japanese Ministry of Health and Welfare (http://www.health-net.or.jp/kenkonet/tobacco/front.html).

APPENDIX B

The miner-study based models in BEIR VI report, 1999

The BEIR committee developed the revised risk model of lung cancer risk associated with radon exposure, incorporating an updated assessment of dose-effect relationship from the latest review of historical miner cohort studies, and an associated extrapolations from miners to the general population.

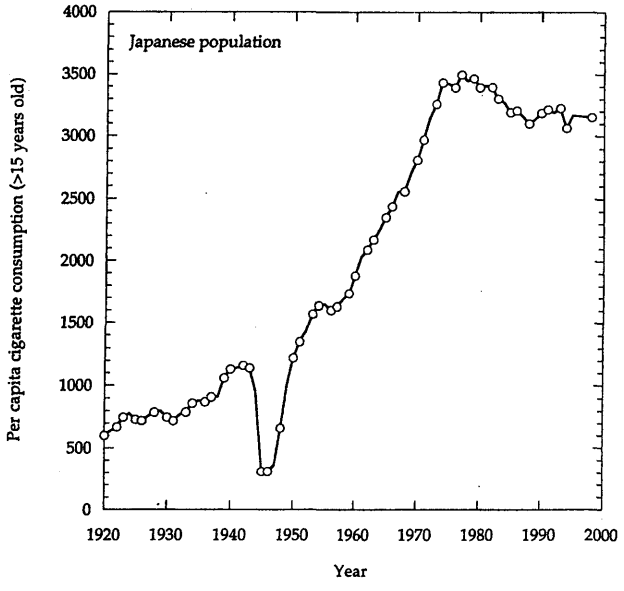

Fig. A3. Per capita cigarette consumption rate of Japanese population more than 15 y old during 1920–1998.

The Exposure-Age-Duration (EAD) model is described as:

$$r(a) = r_o(a) \times [1 + \beta \times \phi(a) \times \gamma \times (W_1 + 0.72 \times W_2 + 0.44 \times W_3)],$$

where

β = excess relative risk, 0.553 (95%CI 0.271–1.125) $\times 10^{-2}$ per WLM;
$r(a)$ = lung-cancer mortality rate for given age and calendar period; and
$r_o(a)$ = background or baseline of lung cancer mortality rate in the population.

Time-since-exposure Windows:

- W_1: cumulative exposure in WLM incurred between 5 y and 14 y before age a;
- W_2: cumulative exposure in WLM incurred between 15 y and 24 y before age a; and
- W_3: cumulative exposure in WLM incurred 25 y or more before age a.

Attained age: $\phi(a)$: 1.0 when age a is less than 55 y, 0.52 when a is 55–64 y, 0.28 when a is 65–74 y, and 0.13 when a is 75 years or more.

Duration of exposure: $\gamma = 1.0$ when duration is less than 5 y, 2.78 when duration is 5–14 y, 4.42 when duration is 15–24 y, 6.62 when duration is 25–34 y, and 10.20 when duration is 35 y or more.

The Exposure-Age-Concentration (EAC) model is described as

$$r(a) = r_o(a)[1 + \beta \times \phi(a) \times \gamma \times (W_1 + 0.78 \times W_2 + 0.51 \times W_3)],$$

where

β = Excess relative risk, 7.681 (95%CI 3.969–14.864) $\times 10^{-2}$ per WLM;
$r(a)$ = lung-cancer mortality rate for given age and calendar period; and
$r_o(a)$ = background or baseline of lung cancer mortality rate in the population.

Time-since-exposure windows:

- W_1 = cumulative exposure in WLM incurred between 5 y and 14 y before age a;
- W_2 = cumulative exposure in WLM incurred between 15 y and 24 y before age a; and
- W_3 = cumulative exposure in WLM incurred 25 y or more before age a.

Attained age: $\phi(a)$ = 1.0 when age a is less than 55 y; 0.57 when a is 55–64 y; 0.29 when a is 65–74 y; and 0.09 when a is 75 y or more.

Exposure rate (1 WL = 3,700 Bq m^{-3} EEC): γ = 1.0 when exposure rate is less than 0.5 WL; 0.49 when exposure rate is 0.5–1.0 WL; 0.37 when exposure rate is 1.0–3.0 WL; 0.32 when exposure rate is 3.0–5.0 WL; 0.17 when exposure rate is 5.0–15.0 WL; and 0.11 when exposure rate is 15 WL or more.

■ ■

INT. J. RADIAT. BIOL 1998, VOL. 74, NO. 1, 145–150

Effects of γ-rays on the populations of the steady-state ecological microcosm

S. FUMA†*, H. TAKEDA†, K. MIYAMOTO†, K. YANAGISAWA†, Y. INOUE†, N. SATO†, M. HIRANO† and Z. KAWABATA‡

(Received 3 October 1997; accepted 25 February 1998)

Abstract. *Purpose*: To investigate the dose–response of an aquatic microcosm exposed to γ-rays and to test the suitability of micro-cosms for elucidation of the mechanisms that account for such ecological effects.
Materials and methods: The microcosm used in this study consisted of algae *Euglena gracilis* Z as a producer, protozoa *Tetrahymena thermophila* B as a consumer and bacteria *Escherichia coli* DH5α as a decomposer. After the steady-state microcosm was irradiated with ^{60}Co γ-rays at various dose levels, the population densities of each species were measured.
Results: Irradiation at up to 100 Gy did not affect the population of the microcosm except for a temporary decrease of *E. coli* just after irradiation. At 500 or 1000 Gy, *E. coli* died out just after irradiation. Only *Eu. gracilis* and *T. thermophila* could survive. Their populations, however, decreased compared with that of each control, except for a temporary increase of *T. thermophila* after 1000 Gy irradiation. These population changes were attributable to the extinction of *E. coli* in addition to the direct effects of radiation. Irradiation at 5000 Gy extinguished all species in the microcosm.
Conclusions: The response of the microcosm to radiation was dose-dependent over a range of high doses. The microcosm was also shown to be suitable for examining not only direct effects but also secondary effects.

1. Introduction

Ecosystems are exposed to various kinds of toxic agents derived from human activities. For conservation of ecosystems, the activities which are more harmful to ecosystems should be replaced with less harmful ones if possible. Therefore, the ecological effects of a toxic agent should be evaluated, as compared with other agents, in a proper way. For instance, the evaluation of the ecological effects of radiation compared with acidification will be a help to the decision-making of energy choice between nuclear power generation and thermal power generation.

The authors have started comparative studies with various toxic agents, in comparison with ionizing radiation. The reasons why radiation was chosen as a standard are: (1) radiation is one of the agents which potentially affects ecosystems, especially in the case of severe nuclear accidents such as Chernobyl and nuclear waste disposal to the deep sea or underground; and (2) dose estimation and the biological effects of radiation are investigated better than other toxic agents.

Radiation effects on wild organisms have been well investigated (IAEA 1976, 1988, 1992, NCRP 1991). However, the ecological effects of radiation have scarcely been investigated at the community level and there are few mechanistic studies of the ecological effects of radiation. Radiation may affect ecosystems, not only directly, but also secondarily because ecosystems consist of many species that have a wide range of radiosensitivities (Sparrow *et al.* 1967) and have complex interactions, for example predator–prey interactions. After one species has been damaged directly by radiation, another species which is more resistant to radiation may also be affected by the disappearance of interaction with that damaged species. Radiation effects on ecosystems cannot therefore be deduced from the effects on each organism isolated from the ecosystem, as shown in the case of ultraviolet radiation (Bothwell *et al.* 1994) or some chemicals (Mosser *et al.* 1972, Hutchinson and Czyrska 1975, Taub 1976, Wilkes 1978, Crow and Taub 1979).

Radiation effects on ecosystems have been observed in high-background radiation areas (Léonard *et al.* 1981), nuclear test sites (Templeton *et al.* 1971) and natural fields irradiated experimentally (Woodwell 1967, Hinckley 1971) or contaminated by the accidents of nuclear facilities (Kozubov and Taskaev 1990, Krivolutsky and Pokarzhevsky 1990). These approaches, however, have not always led to correct evaluation of radiation effects and could not always contribute to the elucidation of the mechanisms which account for the ecological effects of radiation, because natural ecosystems are extremely complex and are affected by many variable factors

*Author for correspondence.
†Environmental and Toxicological Sciences Research Group, National Institute of Radiological Sciences, 9–1 Anagawa-4-chome, Inage-ku, Chiba-shi 263–8555, Japan. email fuma@nirs.go.jp
‡Department of Environmental Conservation, Ehime University, Tarumi 3–5-7, Matsuyama 790–8566, Japan.

0955–3002/98 $12.00

apart from radiation. An attempt has therefore been made to evaluate the radiation effects on ecosystems by using a microcosm.

Microcosms are experimental ecosystems constructed in the laboratory to have some of the physical, chemical and biological elements of natural ecosystems. Microcosms contain interactions among those elements as do natural ecosystems. Microcosms provide biotic or abiotic simplicity, controllability and replicability (Beyers and Odum 1993). It has been demonstrated that microcosms can act as fairly realistic models of natural ecosystems (Beyers 1963, Cooke 1967, Gorden *et al.* 1969). Microcosms have therefore been used for studies of basic ecology or the evaluation of ecological effects of toxic agents at the community level (Beyers and Odum 1993).

This paper investigated the effects of γ-rays on populations of a steady-state aquatic microcosm. The aim was: (1) to investigate the dose–response in an aquatic microcosm exposed to γ-rays; and (2) to test the suitability of microcosms for the elucidation of mechanisms that account for ecological effects.

2. Materials and methods

2.1. *Microcosm*

The microcosm used in this study was synthesized by Kawabata *et al.* (1995). It consisted of flagellate algae *Euglena gracilis* Z as a producer, ciliate protozoa *Tetrahymena thermophila* B as a consumer and bacteria *Escherichia coli* DH5α as a decomposer. The culture medium was a half-strength modified #36 Taub and Dollar's salt solution (Taub and Dollar 1968) containing proteose peptone (Difco Laboratory, Detroit, MI, USA) of 500 mg/l. The microcosm was cultured in an incubator with fluorescent lamps under a 2500 lx and a 12 h light–dark cycle at 25°C.

In the microcosm the population change of each organism reached a steady state 50 days after inoculation as a result of interactions among the species. All species can co-exist in the microcosm for as long as 1 year. When *T. thermophila* was cultured alone in the microcosm medium it died out without reaching a steady state and *Eu. gracilis* and *E. coli* when cultured alone in the microcosm medium could not exist so stably as they do in the microcosm.

In the microcosm, proteose peptone mainly contributes to the growth of *Eu. gracilis* and *E. coli* in the early stage of culture. After exhaustion of proteose peptone, the microcosm is maintained with energy which *Eu. gracilis* fixes by photosynthesis. Each species is supported with metabolites or the breakdown products of the other two species. *T. thermophila* cannot exist without *E. coli* because *T. thermophila* grazes *E. coli* as its staple food (Nakajima and Kawabata 1996).

2.2. *Procedures*

The microcosms were synthesized in 250 ml polypropylene bottles with screw caps (Nalgene, Rochester, NY, USA) containing 150 ml culture medium. They were irradiated with ^{60}Co γ-rays (0, 50, 100, 500, 1000, 5000 Gy) at a dose rate of 50 Gy/min on the 56th day after the beginning of the culture. Four bottles of microcosm were irradiated with γ-rays at each dose and five bottles of microcosm were kept as unirradiated controls.

The population density of each organism was measured before irradiation and over 320 days after irradiation. The population of *Eu. gracilis* and *T. thermophila* was counted microscopically in a 1 mm deep chamber of 50 × 20 mm^2, having a 1 mm^2 grid. The number of viable *E. coli* was measured by counting colonies formed in a broth–agar medium (extract bonito: 3·0 g; polypeptone: 3·0 g; NaCl: 5·0 g; agar powder: 15·0 g; distilled water: 1 l; pH adjusted to 7·0) after incubation at 25°C for 5 days.

3. Results and discussion

3.1. *Radiation effects on the cell populations of the microcosm*

Figure 1 shows the changes in the population densities of the three species in the irradiated microcosm compared with non-irradiated controls. The patterns of changes observed can be separated into three groups as follows.

3.1.1. *50 or 100 Gy irradiation.* At 50 or 100 Gy, the population of *E. coli* in the microcosm decreased just after irradiation compared with controls. Irradiation at 100 Gy decreased *E. coli* more significantly than at 50 Gy. However, in both cases *E. coli* soon recovered to control levels, and then its population density was maintained at control level. Irradiation at 50 or 100 Gy did not affect the populations of *Eu. gracilis* and *T. thermophila*. It is therefore concluded that the microcosm used in this study is resistant to up to 100 Gy γ-irradiation.

3.1.2. *500 or 1000 Gy irradiation.* At 500 Gy, *E. coli* died out shortly after irradiation. After 500 Gy, the population density of *Eu. gracilis* in the microcosm was unchanged for a long time, and then became lower than that of the controls. This decrease was first observed on the 264th day after irradiation. This decrease is, therefore, thought to be a secondary effect rather than a direct effect of radiation. That is, it is

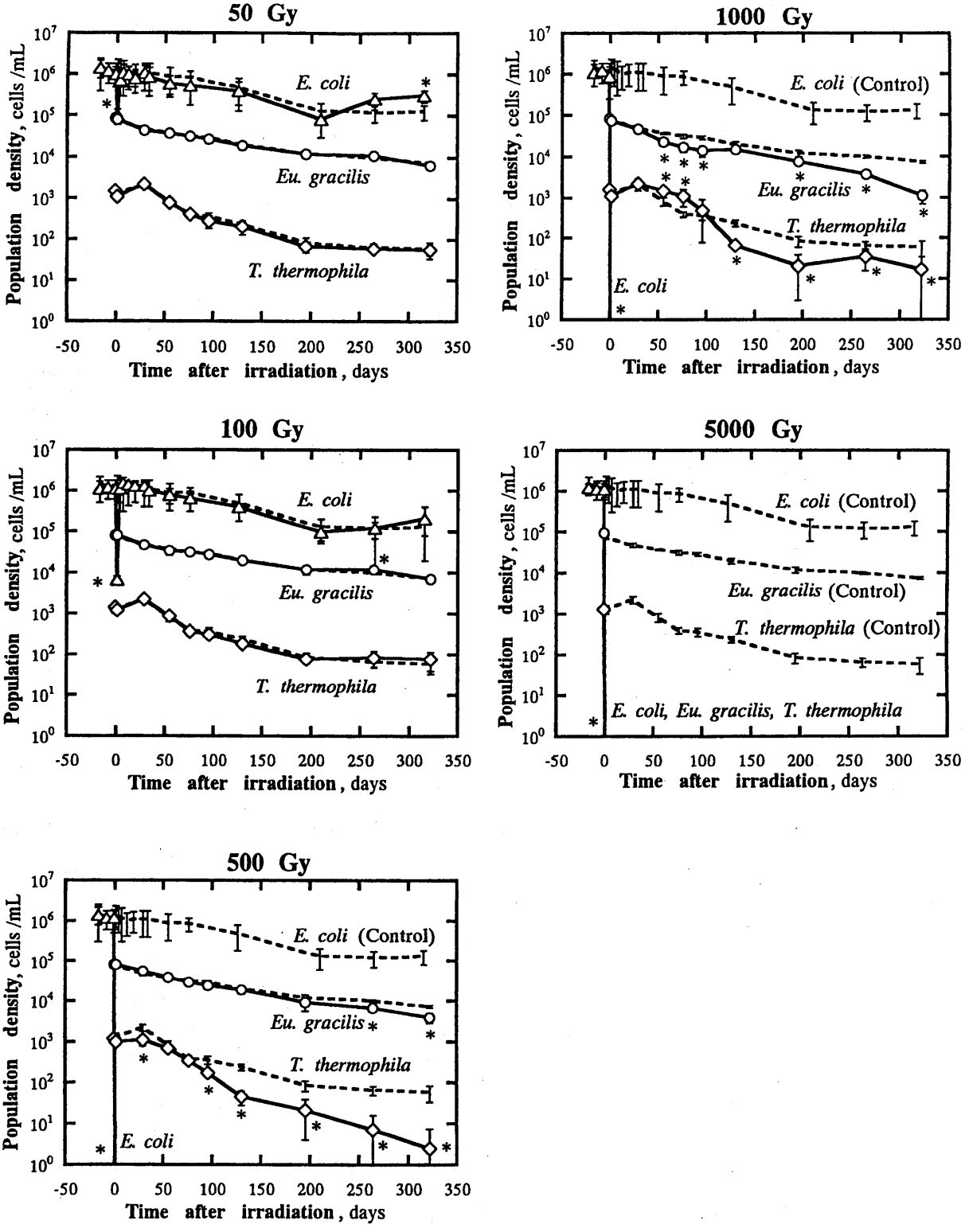

Figure 1. Population changes in the microcosm after irradiation with γ-rays. Solid lines represent results of irradiated microcosms. Broken lines represent results of controls. Error bars are standard deviations. Asterisks indicate statistically significant differences ($p<0{\cdot}05$, Student's *t*-test).

thought that the extinction of *E. coli* in the irradiated microcosm decreased *Eu. gracilis* because metabolites of *E. coli* contribute the growth of *Eu. gracilis* in the microcosm (Nakajima and Kawabata 1996).

After 500 Gy irradiation, the population of *T. thermophila* in the microcosm decreased compared with that of controls. This decrease is not thought to be direct damage of radiation because lethal dose (LD_{50}) for pure-cultured *Tetrahymena priformis* is elucidated to be approximately 4000 Gy (Elliott 1959). It is thought that 500 Gy irradiation decreased *T. thermophila* by extinguishing *E. coli* in the microcosm; *T. thermophila* cannot exist without *E. coli*, which *T. thermophila* grazes as a staple food (Nakajima and Kawabata 1996).

At 1000 Gy, *E. coli* in the microcosm died out just after irradiation. After 1000 Gy irradiation, the population of *Eu. gracilis* in the microcosm decreased compared with controls. This decrease was more significant than the decrease after 500 Gy irradiation. Irradiation at 1000 Gy also began to decrease *Eu. gracilis* earlier than that after 500 Gy. These results suggest that the decrease of *Eu. gracilis* in the microcosm irradiated with 1000 Gy γ-rays was caused by direct radiation damage in addition to the secondary effects.

After 1000 Gy irradiation, the population of *T. thermophila* in the microcosm increased temporarily, and then decreased compared with controls. However, irradiation at 1000 Gy did not decrease *T. thermophila* as much as 500 Gy. This population change is thought to be a result of secondary effects rather than direct effects of radiation because *Tetrahymena* is radioresistant. The mechanism is thought to be that as a result of the direct effect of 1000 Gy irradiation, breakdown products of *E. coli* were left in the microcosm. These contributed to the growth of *T. thermophila*. Since dead *E. coli* also contribute to the growth of *Eu. gracilis*, the latter competes with *T. thermophila* (Nakajima and Kawabata 1996). The decrease of *Eu. gracilis* after 1000 Gy irradiation also provided *T. thermophila* with an advantage in the competition for breakdown products of *E. coli*. Therefore, *T. thermophila* temporarily increased in the microcosm after irradiation. When the consumption of breakdown products was largely complete, *T. thermophila* decreased. However, 1000 Gy irradiation did not decrease *T. thermophila* as much as 500 Gy irradiation because 1000 Gy irradiation decreased *Eu. gracilis*, whose breakdown products contribute to the growth of *T. thermophila* (Nakajima and Kawabata 1996).

Gamma irradiation at 500 or 1000 Gy extinguished *E. coli* in the microcosm. This resulted in the disappearance of interactions between *E. coli* and the other two species that are necessary to their survival. As a result of the disappearance of these interactions, in addition to the direct damage of radiation, the population of *Eu. gracilis* and *T. thermophila* changed compared with controls, and did not fully recover. Thus, 500 or 1000 Gy irradiation extinguished one species and changed the populations of the other two species in the microcosm.

3.1.3. *5000 Gy irradiation.* At 5000 Gy, all species in the microcosm died out shortly after irradiation and the microcosm was completely destroyed.

The response of the microcosm was therefore dose-dependent within a high-dose range. A dose of 50 or 100 Gy was required for even temporary damage, 500 or 1000 Gy for severe damage, and 5000 Gy for complete destruction.

3.2. *Significance and problems of microcosm tests for the evaluation of radiation effects on ecosystems*

These results suggest that some species in ecosystems may respond to radiation differently from those in pure cultures. This phenomenon has been observed in natural ecosystems. For example, in the irradiated forest ecosystem the population and activity of micro-organisms decreased in spite of their radioresistance, a decrease that was thought to be the result of secondary effects of radiation, i.e. due to destruction of trees and shrubs by radiation (Poinsot-Balaguer *et al.* 1991). Populations of leaf mining insects and aphids increased in the irradiated forest ecosystem, though radiation is expected to damage those species directly. This increase was thought to be a result of radiation damage to trees (Woodwell and Brower 1967, Hinckley 1971). Microcosm tests therefore may be useful to investigate the mechanisms of ecological effects of radiation, for instance, to determine whether the effects arise directly or secondarily.

In present study, some radiation effects on the microcosm were first observed long after irradiation. At 500 Gy, the decrease of *Eu. gracilis* was first observed on the 264th day after irradiation. At 1000 Gy, *T. thermophila* temporarily increased and then began to decrease compared with that of controls on the 130th day after irradiation. These results indicate that it takes considerable periods of time to express radiation effects at the ecosystem level, and long-term studies are needed for evaluation of radiation effects on entire ecosystems.

In general there is some conceptual danger in extrapolating directly from model ecosystem data to natural ecosystems. It is, however, reported that an aquatic microcosm responded to heavy metals in a

similar manner to natural ecosystems (Shen *et al.* 1986). It is also reported that an aquatic microcosm responded to anionic surfactant in a similar manner to a model ecosystem derived from lake water, which had a greater number of species and is thought to more closely resemble natural lake ecosystems than the microcosm (Takamatsu *et al.* 1997). Microcosm tests can be applied to the prediction of the ecological impact of radiation by using an adequate safety factor. In general, 1–1/3 is adopted as the safety factor for extrapolating from model ecosystem data to natural ecosystems, but 1/100 for extrapolating from single-species assessment to natural ecosystems (OECD 1981, CEC 1993, Nabholz *et al.* 1993). This means that microcosm tests are at least better for the evaluation of ecological impacts than single-species assessment.

Acknowledgements

The authors are indebted to the staff of the Department of Environmental Conservation, Ehime University: Dr M.-G. Min, Mr N. Ishii and Ms C. Aki for valuable discussions, Ms K. Yagi for handling of the microcosm and Ms A. Yagi for technical assistance.

This work was partly supported by a Japanese Ministry of Education, Science and Culture, Grant-in-Aid for Creative Basic Research (09NP1501), 'An interactive study on biodiversity conservation under global change and bio-inventory management system'.

References

BEYERS, R. J., 1963, The metabolism of twelve aquatic laboratory microecosystems. *Ecological Monographs*, **33,** 281–306.

BEYERS, R. J. and ODUM, H. T., 1993, *Ecological Microcosms* (New York: Springer-Verlag), pp. 3–4.

BOTHWELL, M. L., SHERBOT, D. M. J. and POLLOCK, C. M., 1994, Ecosystem response to solar ultraviolet-B radiation: influence of trophic-level interactions. *Science*, **265,** 97–100.

CEC, 1993, Environmental risk assessment of new chemicals notified under directive 92/21/EEC (XI/509/93) (Brussels: Commission of the European Communities), pp. 53.

COOKE, G. D., 1967, The pattern of autotrophic succession in laboratory microecosystems. *BioScience*, **17,** 717–721.

CROW, M. E. and TAUB, F. B., 1979, Designing a microcosm bioassay to detect ecosystem level effects. *The International Journal of Environmental Studies*, **13,** 141–147.

ELLIOTT, A. M., 1959, Biology of *Tetrahymena*. *Annual Review of Microbiology*, **13,** 79–96.

GORDEN, R. W., BEYERS, R. J., ODUM, E. P. and EAGON, R. G., 1969, Studies of a simple laboratory microecosystem: bacterial activities in a heterotrophic succession. *Ecology*, **50,** 86–100.

HINCKLEY, A. D., 1971, Infestation of irradiated white oaks by the solitary oak leafminer, *Cameraria hamadryadella* (Lepidoptera: Gracilariidae). *Annals of the Entomological Society of America*, **64,** 1094–1098.

HUTCHINSON, T. C. and CZYRSKA, H., 1975, Heavy metal toxicity and synergism to floating aquatic weeds. *Verhandlungen der Internationalen Vereinigung für Theoretische und Angewandte Limnologie*, **19,** 2102–2111.

INTERNATIONAL ATOMIC ENERGY AGENCY, 1976, Effects of ionizing radiation on aquatic organisms and ecosystems. Technical Reports Series no. 172 (Vienna: IAEA).

INTERNATIONAL ATOMIC ENERGY AGENCY, 1988, Assessing the impact of deep sea disposal of low level radioactive waste on living marine resources. Technical Reports Series no. 288 (Vienna: IAEA).

INTERNATIONAL ATOMIC ENERGY AGENCY, 1992, Effects of ionizing radiation on plants and animals at levels implied by current radiation protection standards. Technical Reports Series no. 332 (Vienna: IAEA).

KAWABATA, Z., MATSUI, K., OKAZAKI, K., NASU, M., NAKANO, N. and SUGAI, T., 1995, Synthesis of a species-defined microcosm with protozoa. *Journal of Protozoological Research*, **5,** 23–26.

KOZUBOV, G. M. and TASKAEV, A. I., editors, 1990, *The Radiation Influence on the Coniferous Forests in the Region of the Catastrophe at the Chernobyl Atomic Power Station* (Siktivkar, Russia: Komi Scientific Centre).

KRIVOLUTSKY, D. A. and POKARZHEVSKY, A. D., 1990, Changes in the population of soil fauna caused by the Chernobyl nuclear power plant accident. Biological and radioecological consequences of the accident at the Chernobyl nuclear power plant. Proceedings of the 1st International Conference, Zeleny Mys, September 1990. (Moscow, The USSR Academy of Sciences) p. 78.

LÉONARD, A., DELPOUX, M., CHAMEAUD, J., DECAT, G. and LÉONARD, E. D., 1981, Biological effects observed in mammals maintained in an area of very high natural radioactivity. *Canadian Journal of Genetics and Cytology*, **23,** 321–326.

MOSSER, J. L., FISHER, N. S. and WURSTER, C. F., 1972, Polychlorinated biphenyls and DDT alter species composition in mixed cultures of algae. *Science*, **176,** 533–535.

NABHOLZ, J. V., MILLER, P. and ZEEMAN, M., 1993, Environmental risk assessment of new chemicals under the toxic substances control act (TSCA) section five. In *Environmental Toxicology and Risk Assessment*, edited by W. G. Landis, J. S. Hughes and M. A. Lewis (Philadelphia: American Society for Testing Materials), pp. 31–46.

NAKAJIMA, H. and KAWABATA, Z., 1996, Sensitivity analysis in microbial communities. In *Microbial Diversity in Time and Space*, edited by R. Colwell *et al.* (New York: Plenum Press), pp. 85–91.

NCRP, 1991, Effects of ionizing radiation on aquatic organisms. NCRP Report no. 109 (Bethesda: NCRP).

ORGANIZATION FOR ECONOMIC COOPERATION AND DEVELOPMENT, 1981, *OECD Guidelines for Testing of Chemicals* (Paris: OECD), pp. 201–209.

POINSOT-BALAGUER, N., CASTET, R. and TABONE, E., 1991, Impact of chronic gamma irradiation on a Mediterranean forest ecosystem in Cadarache (France). *Journal of Environmental Radioactivity*, **14,** 23–36.

SHEN, Y.-F., BUIKEMA, A. L., JR., YONGUE, W. H., JR., PRATT, J. R. and CAIRNS, J., JR., 1986, Use of protozoan communities to predict environmental effects of pollutants. *Journal of Protozoology*, **33,** 146–151.

SPARROW, A. H., UNDERBRINK, A. G. and SPARROW, R. C., 1967, Chromosomes and cellular radiosensitivity. I. The

relationship of D_0 to chromosome volume and complexity in seventy-nine different organisms. *Radiation Research*, **32,** 915–945.

TAKAMATSU, Y., INAMORI, Y., SUDO, R., KURIHARA, Y. and MATSUMURA, M., 1997, Ecological effects assessment of anionic surfactant on aquatic ecosystem using microcosm system. *Journal of Japan Society on Water Environment*, **20,** 710–715 (in Japanese).

TAUB, F. B., 1976, Demonstration of pollution effects in aquatic microcosm. *The International Journal of Environmental Studies*, **10,** 23–33.

TAUB, F. B. and DOLLAR, A. M., 1968, The nutritional inadequacy of *Chlorella* and *Chlamydomonas* as food for *Daphnia pulex*. *Limnology and Oceanography*, **13,** 607–617.

TEMPLETON, W. L., NAKATANI, R. E. and HELD, E. E., 1971, Radiation effects. In *Radioactivity in the Marine Environment* (Washington: National Academy of Sciences), p. 223.

WILKES, F. G., 1978, Laboratory microcosms for use in determining pollutant stress. In *Aquatic Pollutants—Transformation and Biological Effects*, edited by O. Hutzinger, L. H. V. Lelyveld and B. C. J. Zoeteman (Oxford: Pergamon), pp. 309–321.

WOODWELL, G. M., 1967, Radiation and the patterns of nature. Sensitivity of natural plant populations to ionizing radiation seems to follow known ecological patterns. *Science*, **156,** 461–470.

WOODWELL, G. M. and BROWER, J. H., 1967, An aphid population explosion induced by chronic gamma irradiation of a forest. *Ecology*, **48,** 680–683.

PERGAMON

Toxicology in Vitro 14 (2000) 309–319

Toxicology in Vitro

www.elsevier.com/locate/toxinvit

Different cytotoxic response to gadolinium between mouse and rat alveolar macrophages

Y. KUBOTA [1,*], S. TAKAHASHI [1], I. TAKAHASHI [2] and G. PATRICK [3]

[1]Environmental and Toxicological Sciences Research Group, National Institute of Radiological Sciences, Chiba, Japan, [2]Tokyo Nuclear Services Co., Ltd, Tokyo, Japan and [3]MRC Toxicology Unit, Leicester, UK

(Accepted 11 January 2000)

Abstract—The cytotoxicity of gadolinium (Gd) chloride was investigated in alveolar macrophages (AM) cultured *in vitro*. A marked difference in the cytotoxic response to Gd was found between mouse and rat AM. The viability of rat AM was decreased by exposure to Gd at doses more than 3 μM, while mouse AM appeared to be resistant even up to 1000 μM Gd exposure. The decrease in the viability of rat AM exposed to Gd at doses up to 1000 μM was mitigated by centrifugation and filtration of the culture medium containing Gd, or by the treatment of AM with lysosomotropic agents such as NH_4Cl or chloroquine, suggesting that the cytotoxic response of rat AM to Gd at doses up to 1000 μM was dependent on the intracellular uptake and subsequent dissolution of Gd present in the culture medium in colloidal form. The phagocytic activity of mouse AM, evaluated by the uptake of latex particles, was higher than that of rat AM. Furthermore, quantitative analysis of Gd with inductively coupled plasma-mass spectrometry revealed that mouse AM took up a larger amount of Gd than rat AM. Therefore, the marked difference in the cytotoxic response to Gd between mouse and rat AM could not be attributed to the phagocytic activities for the colloidal form of Gd. The cytotoxic sensitivity of AM to Gd present in non-colloidal form was almost the same between mouse and rat AM. Therefore, it is suggested that the extent to which Gd-colloid phagocytosed is dissolved in the phagolysosome or the subsequent process to exhibit the cytotoxicity may be different between mouse and rat AM.

Keywords: gadolinium; cytotoxic; macrophages; alveolar; colloid; phagocytosis; cadmium; apoptosis.

Abbreviations: AM = alveolar macrophages; DMEM = Dulbecco's modified Eagle's medium; FCS = fetal calf serum; Gd = gadolinium; HBSS = Hanks' balanced salt solution; polyHEMA = poly 2-hydroxyethyl methacrylate.

INTRODUCTION

The use of gadolinium (Gd), a lanthanide element, has recently increased with the rapid development of advanced technologies (Hirano and Suzuki, 1996). Gd combined with chelating agents has been extensively used in the field of clinical medicine as a contrast agent for magnetic resonance imaging (Rocklage *et al.*, 1991; Runge and Parker, 1997; Weinmann *et al.*, 1984). It has also been used medically and experimentally to block the reticuloendothelial system, since Lazar (1973) reported this action of rare earth metals in rats. Intravenous administration of Gd inhibited the phagocytic activity of Kupffer cells (liver macrophages) and so has been frequently used to study the role of Kupffer cells in physiological and pathological conditions. From these studies, it has been suggested that Gd affected not only the phagocytic activity of Kupffer cells (Suzuki *et al.*, 1996; Ruttinger *et al.*, 1996) but also their ability to produce interleukins (Callery *et al.*, 1990; Rai *et al.*, 1996), superoxide (Liu *et al.*, 1995), NO (Roland *et al.*, 1994, 1996) and chemoattractant (Hisama *et al.*, 1996), as well as their viability (Kohno *et al.*, 1997; O'Neill *et al.*, 1994; Sarphie *et al.*, 1996).

There have been a few studies on the effects of Gd on lung macrophages *in vivo*. The phagocytic activity of pulmonary intravascular macrophages was significantly depressed in sheep by the administration of Gd (Molina *et al.*, 1995). It was shown that O_3-induced enhancement of O_2^- and NO production by alveolar macrophages (AM) was attenuated by Gd pretreatment of rats (Pendino *et al.*, 1995), and that

*Corresponding author. Tel: 043-206-3159; fax: 043-251-4853; e-mail: y_kubota@nirs.go.jp

0887-2333/00/$ - see front matter
PII: S0887-2333(00)00027-8

lung injury after intratracheal instillation of lipopolysaccharide was alleviated by $GdCl_3$ in guinea pigs (Tasaka *et al.*, 1996). It was obvious from these studies that Gd affected lung macrophages; however, the extent of toxicity of Gd for the macrophages remained obscure. Recently Mizgerd *et al.* (1996) demonstrated the lethal effects of Gd on rat AM cultured *in vitro*. We have also studied the cytotoxic effects of Gd on mouse AM, but did not find the same lethal effect. This prompted us to compare the cytotoxicity of Gd between mouse and rat AM, and we here report a marked difference in the cytotoxic response to Gd between macrophages from the two species.

MATERIALS AND METHODS

Materials

The following items were purchased: gadolinium chloride hexahydrate ($GdCl_3 \cdot 6H_2O$) and cadmium chloride hemi pentahydrate ($CdCl_2 \cdot 2.5H_2O$) from Wako Pure Chemical Industries, Ltd (Osaka, Japan); Dulbecco's phosphate buffered saline (PBS), Dulbecco's MEM (DMEM), Hanks' balanced salt solution (HBSS), 100 bp DNA ladder and DNA MASS™ Ladder from Gibco BRL (Grand Island, NY, USA); poly 2-hydroxyethyl methacrylate (polyHEMA), NH_4Cl and chloroquine from Sigma Chemical Co. (St Louis, MO, USA); fetal calf serum (FCS) from C&C Lab (Tokyo, Japan); latex particles with 2 μM in diameter from Polysciences Inc. (Warrington, PA, USA); and ultrapure grade of HNO_3, HF and $HClO_4$ from Tama Chemicals Co., Ltd (Kawasaki, Japan). Complete culture medium consisted of DMEM supplemented with heat-inactivated FCS (10%) and 100 U penicillin/ml and 100 μg streptomycin/ml.

Alveolar macrophages

Two strains of male rats, Sprague–Dawley (SD) and Wistar, and two strains of male mice, C3H and C57Black/6 (B6) were purchased from the domestic breeder (SLC Co., Ltd, Shizuoka, Japan), and were housed in a controlled environment with access to food and water *ad lib.* All the animal experiments were carried out with permission and according to the regulations of the Institutional Committee for Animal Safety and Welfare of the National Institute of Radiological Sciences, and Regulations on Appropriate Animal Breeding and Treatment, Ministry Office of Japan. After the animals were anaesthetized by halothane and killed by exsanguination, resident AM were harvested by repeated post-mortem bronchoalveolar lavage with PBS according to the procedure described elsewhere (Kubota *et al.*, 1994). $0.5–1.0 \times 10^6$ cells per mouse and $0.5–1.0 \times 10^7$ cells per rat were collected. The proportion of AM was greater than 95% of the lung lavage cells based on morphological criteria, the remainder being lymphocytes and neutrophils. More than 98% of AM were viable according to trypan blue exclusion. The cells were then washed and suspended in the complete culture medium.

Gd and Cd preparation

$GdCl_3 \cdot 6H_2O$ and $CdCl_2 \cdot 2.5H_2O$ were dissolved in sterile saline to be a concentration of 30 mM and then each preparation was diluted serially with complete culture medium. Where the effects of the particulate (colloidal) form of Gd and Cd preparations were studied, the preparations were centrifuged at 12,000 *g* for 30 min after diluting to the designated concentrations, and the supernatants were filtered with a 0.22 μm membrane filter (Millipore MILLEX, Millipore, Bedford, MA, USA) to remove the particulate form (the resultant solutions are referred in the following as filtered Gd and Cd preparations).

Cell culture

The collected AM were plated in 24-well microculture plates (Falcon 3046, B&D Lab, NJ, USA) precoated with polyHEMA to prevent AM from adhering, at a cell density of 5×10^5 in 0.5 ml complete culture medium per well. 0.5 ml complete culture medium containing one or a combination of test agents (Gd, Cd, NH_4Cl, chloroquine) was then added to the well to reach the designated final concentrations and the incubation was started at 37°C in a humidified atmosphere of 5% CO in air (this time point was defined as 0 hr). In the experiment where filtered Gd and Cd preparations were used, 5×10^5 cells pelleted in an Eppendorf tube were resuspended in 1 ml filtered Gd or Cd preparations and cultured in 24-well microculture plates.

Determination of cell viability

At the end of culture, cells and medium were transferred to an Eppendorf tube and centrifuged. Then 0.4% of trypan blue in saline was added to the cell pellets, and the number and viability of AM were determined microscopically. To compensate for variation in experimental conditions in each series of experiments, we calculated and used a standardized viability. Thus the term "viability" in the following denotes the percentage of the viable cell number in metal-loaded culture to that in control culture at the corresponding time point. Two wells were prepared for each data point. The mean and standard error of the cell viability were calculated from three separate experiments.

Morphological study of AM

The mode of cell death induced in AM by exposure to Gd was examined by light microscopy, as described previously (Kubota *et al.*, 1994). After 48 hr of culture, the cells were collected by centrifugation, smeared on glass slides and dried in air. Then the cells were fixed with acetic acid–ethanol (1:3) for 10–20 min and stained with Giemsa. The percentage of cells showing pyknosis and/or nuclear fragmentation was calculated by observing at least 200 AM in each individual sample under the microscope.

DNA extraction and agarose gel electrophoresis

DNA was extracted by the method of Martin and Cotter (1991) with slight modification. After proteinase K and RNAse digestion of the cell lysate, the crude DNA was extracted twice using phenol–chloroform buffered with 0.1 M Tris–HCl (pH 7.8), then precipitated in the presence of 0.2 M NaCl and 70% ethanol at −20°C for 1 hr. Finally, the DNA was rinsed with 70% ethanol, and resuspended in 20–30 μl Tris-EDTA buffer. Electrophoresis of the DNA was carried out in a 1.2% agarose gel containing 0.5 μg of ethidium bromide/ml at 100 V for 1 hr in TAE buffer containing 0.5 μg of ethidium bromide/ml. As size markers, 100 bp DNA ladder and DNA MASS Ladder were used.

Phagocytic activity of AM

AM were prepared as described above. At the beginning of culture, latex particles 2 μm in diameter were loaded to reach a final concentration of 1.5×10^7 particles/ml, that is the ratio of particles to AM 30:1. The cells were fixed and stained as described above 8, 24 and 48 hr after the beginning of culture. For each sample, the number of particles phagocytosed by each cell was counted under a microscope at least in 200 individual AM. Individual AM was classified according to the number of phagocytosed particles, namely 0, 1–5, 6–10, 11–20, or >20 particles. The number of classified AM was expressed as a percentage of the total AM counted. The mean and standard error were calculated from three separate experiments.

Quantitative analysis of Gd incorporated into AM

AM were exposed to 300 μM Gd in the same culture conditions as described above, except that the incubation time was 0, 4 and 10 hr, and that the incubation temperature was 4 or 37°C. At the end of culture, 10^6 cells were recovered on the filter from two wells of the 24-well culture plates by the filtration through a 47-mm Nuclepore polycarbonate filter with 3 μm pore size (Corning Separations Division, Acton, MA, USA). In a preliminary experiment it was confirmed that Nuclepore filter with this pore size effectively trapped both mouse and rat AM by observing that no AM was found in the filtered solution. AM trapped on the filter were washed twice with 5 ml HBSS and lysed with 1 ml of 1% sodium dodecyl sulfate and 10 mM EDTA in PBS. The resultant cell lysate was digested with acids (HNO_3, HF and $HClO_4$) using a microwave digester (CEM, MDS2000). After digestion, the samples were heated on a hotplate, then redissolved in 1% HNO_3. The amount of Gd was measured by ICP-MS (Yokogawa PMS-2000, Yokogawa Analytical Systems, Tokyo, Japan) (Yoshida and Muramatsu 1997). Internal standards were used to compensate for the drift of analytical signals during the operation. A standard solution was prepared from SPEX Multi Element Plasma Standards (SPEX Industries Inc., XSTC-1,7,8 and 13) and used to make calibration curves. The amounts of Gd in serially diluted Gd preparations (Gd solution in complete culture medium) and the corresponding filtered Gd preparations were also determined by ICP-MS with the same protocol as described for the cell lysate, and the percentage of Gd existing in a non-colloidal form (amount of Gd in filtered Gd preparation) in total Gd (amount of Gd in Gd preparation) was calculated.

Statistical analysis

The mean and standard error were calculated from the data of independent samples; however, error bars were omitted in some figures because they overlapped on many data points. A two-sample Student's *t*-test was used to evaluate the critical data. The difference between means was regarded as significant if $P<0.05$

RESULTS

Figure 1 shows the viability of mouse and rat AM after 48 hr of exposure to Gd or Cd. The viability of AM was decreased by increasing exposure to Cd, although the dose–response varied with species and strain. The cytotoxicity of Cd for Wistar rat AM appeared to be slightly higher than for AM from other animals examined. The viability of AM exposed to Gd was remarkably different between mice and rats. The viability of SD rat AM decreased linearly up to 10 μM Gd, and was less than 10% at 10 μM. In contrast, the viability of B6 mouse AM was not affected at doses up to 1000 μM. At 3000 μM, Gd killed both mouse and rat AM almost completely. As the cytotoxicity of Gd for AM was similar between B6 and C3H mice and between SD and Wistar rats, B6 mouse and SD rat AM were used in the following studies.

Plate 1 shows light microscopic photographs of AM exposed to Gd for 48 hr. SD rat AM exposed to 300 and 3000 μM Gd and B6 mouse AM exposed to 3000 μM Gd contained a number of cells with condensed nuclei and/or two to three fragmented nuclei within a cell, while B6 mouse AM exposed to 300 μM Gd appeared to be intact. To obtain quantitative data, the percentage of the apoptotic cells, that is the cells with condensed nuclei and nuclear fragmentation, was determined. As shown in Fig. 2, the percentage of the apoptotic cells was markedly higher in SD rat AM exposed to 300 and 3000 μM Gd and in B6 mouse AM exposed to 3000 μM Gd, compared with those in control AM and B6 mouse AM exposed to 300 μM Gd. Plate 2 shows the migration profile of DNA extracted from AM in agarose gel electrophoresis. DNA from B6 mouse AM exposed to 3000 μM Gd and from SD rat AM exposed to 300 and 3000 μM Gd revealed a distinct ladder migration pattern (lanes 3,5 and 6, respectively), indicating

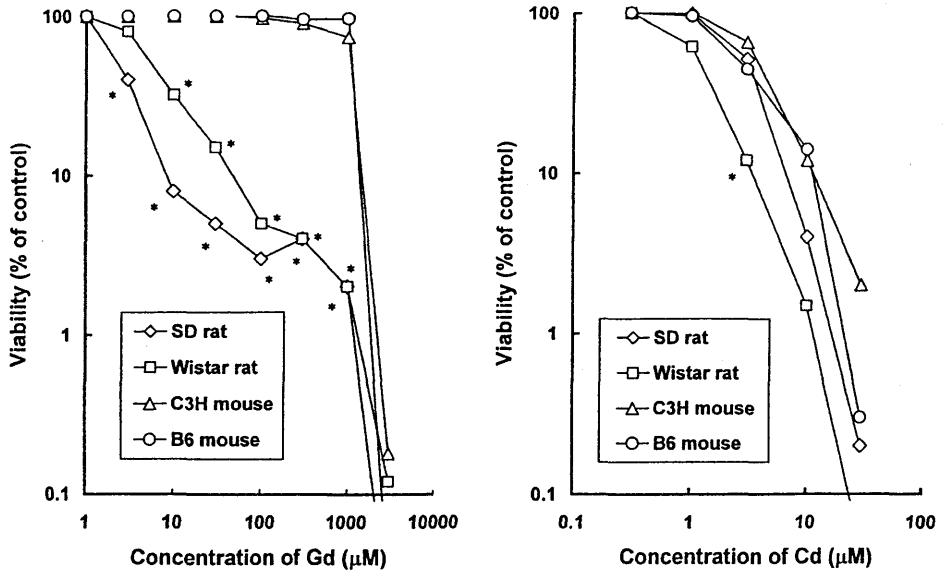

Fig. 1. The viability of muse and rat AM after 48 hr of exposure to Gd (left) and Cd (right). The viability was expressed as the percentage of the viable cell number to that in control culture. Each data point is a mean of three separate experiments. Error bars were omitted because they overlapped on many data points. Asterisks indicate the statistically significant difference from C3H and B6 mice at the corresponding concentration of Gd or Cd.

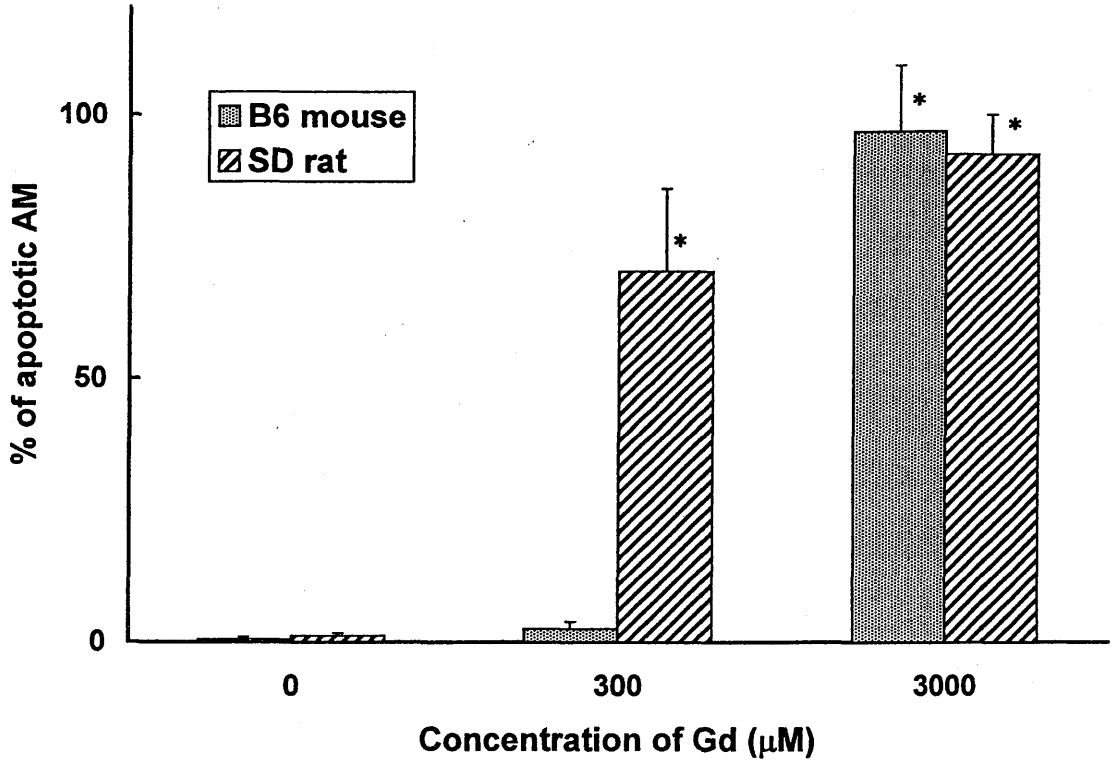

Fig. 2. The percentage of apoptotic cells showed pyknosis and/or nuclear fragmentation at 48 hr of culture. At least 200 AM were observed in each individual sample. The mean and standard error were calculated from three separate experiments. Asterisks indicate the statistically significant difference from the control (0 μM Gd) in B6 mice and SD rats, respectively.

internucleosomal DNA fragmentation that is a representative feature of apoptosis. On the other hand, as expected from the data of Plate 1 and Fig. 2, the ladder pattern of DNA migration was not observed in the control AM (lanes 1 and 4) and B6 mouse AM exposed to 300 μM Gd (lane 2).

Observations of the culture under an inverted phase-contrast microscope revealed that Gd preparations (Gd in complete culture medium) contained particulate matter, the amount of which appeared to depend on Gd concentration, suggesting that Gd might exist as a colloidal form. Cd and Gd

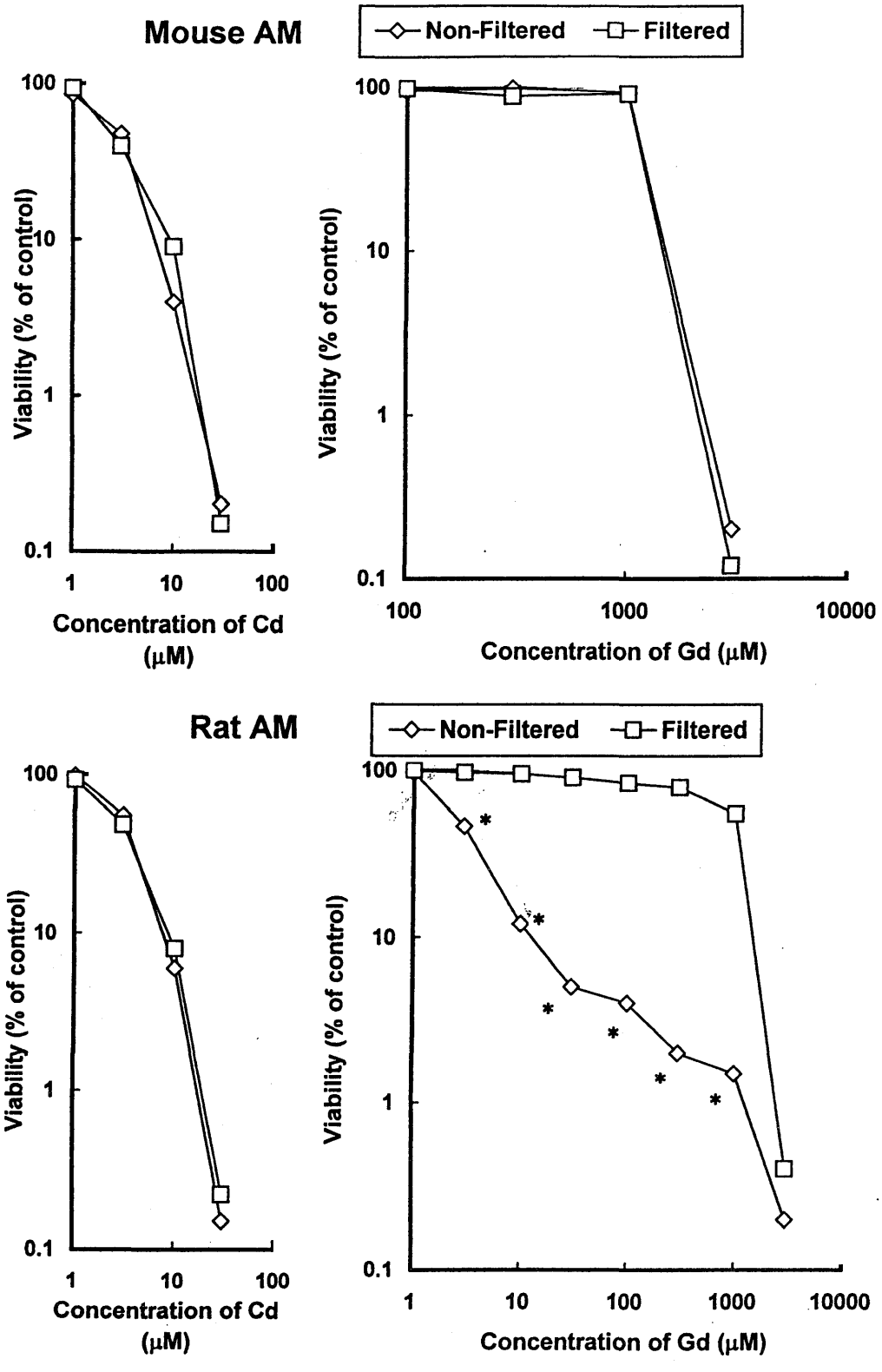

Fig. 3. Effects of filtration of Gd (right) and Cd (left) preparations on cell viability determined at 48 hr of culture in B6 mouse (upper) and SD rat (lower) AM. Each data point is a mean of three separate experiments. Error bars were omitted because they overlapped on many data points. Asterisks indicate the statistically significant difference from those exposed to filtered Gd at the corresponding concentration of Gd. Note the scale of Gd concentration is different between upper and lower graphs.

preparations were centrifuged and filtered to remove particulate matter, and then the cytotoxic effects of filtered and non-filtered preparations were compared (Fig. 3). Filtration did not alter the cytotoxicity of Cd preparations for both mouse and rat AM. In contrast, the filtered Gd preparations made by the filtration of originally 3–1000 μM Gd preparations exhibited a markedly reduced cytotoxicity for rat AM in comparison with non-filtered preparations. Filtration did not affect the cytotoxicity of

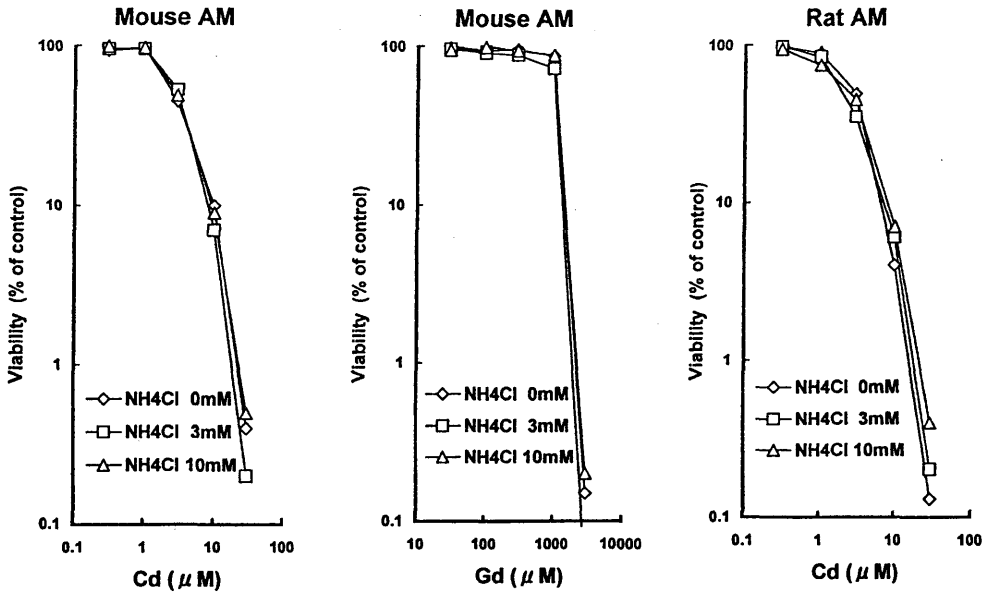

Fig. 4. The effect of NH_4Cl treatment on cytotoxicity of Gd for B6 mouse AM (center), Cd for B6 mouse (left) and SD rat (right) AM. Cell viability was determined at 48 hr of culture. Each data point is a mean of three separate experiments. Error bars were omitted because they overlapped on many data points. There was no statistically significant difference between NH_4Cl treated and non-treated samples. Note: the scale of horizontal axis (metal concentration) is different between the graphs.

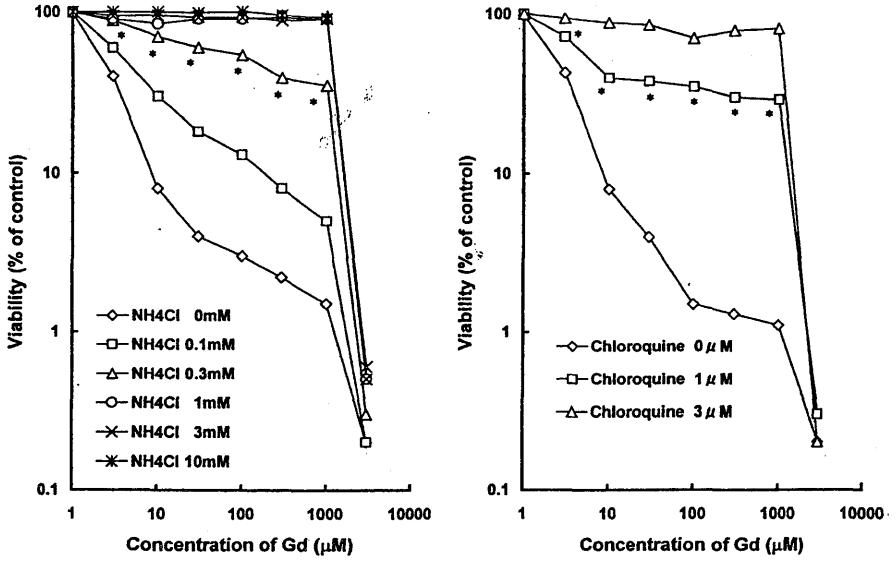

Fig. 5. The effect of NH_4Cl (left) or chloroquine (right) treatment on the cytotoxicity of Gd for SD rat AM. Cell viability was determined at 48 hr of culture. Each data point is a mean of three separate experiments. Error bars were omitted because they overlapped on many data points. Asterisks indicate the statistically significant difference from non-treated AM at the corresponding concentration of Gd.

3000 μM Gd preparation for either mouse or rat AM.

Figures 4 and 5 show the effects of NH_4Cl or chloroquine treatment on the cytotoxicity of Cd and Gd for mouse and rat AM. These are well known lysosomotropic agents which elevate pH in lysosomes and consequently suppress the acidic lysosomal enzyme activities. The treatment of NH_4Cl had no effect on the cytotoxicity of Cd for either mouse or rat AM. On the other hand, the cytotoxicity of Gd at doses up to 1000 μM for SD rat AM was greatly reduced by treatment with NH_4Cl or chloroquine at appropriate concentrations. The cytotoxicity of Gd at a dose of 3000 μM was not altered by NH_4Cl or chloroquine treatment in either mouse or rat AM.

The phagocytic activity of mouse and rat AM was evaluated by adding latex particles to the culture of AM (Fig. 6). At all time points examined, both the percentage of AM phagocytosing more than one particle, and the percentage containing a relatively large number of particles, that is more than 11, were consistently higher in B6 mouse AM, indicating that the phagocytic activity of B6 mouse AM was higher than that of SD rat AM.

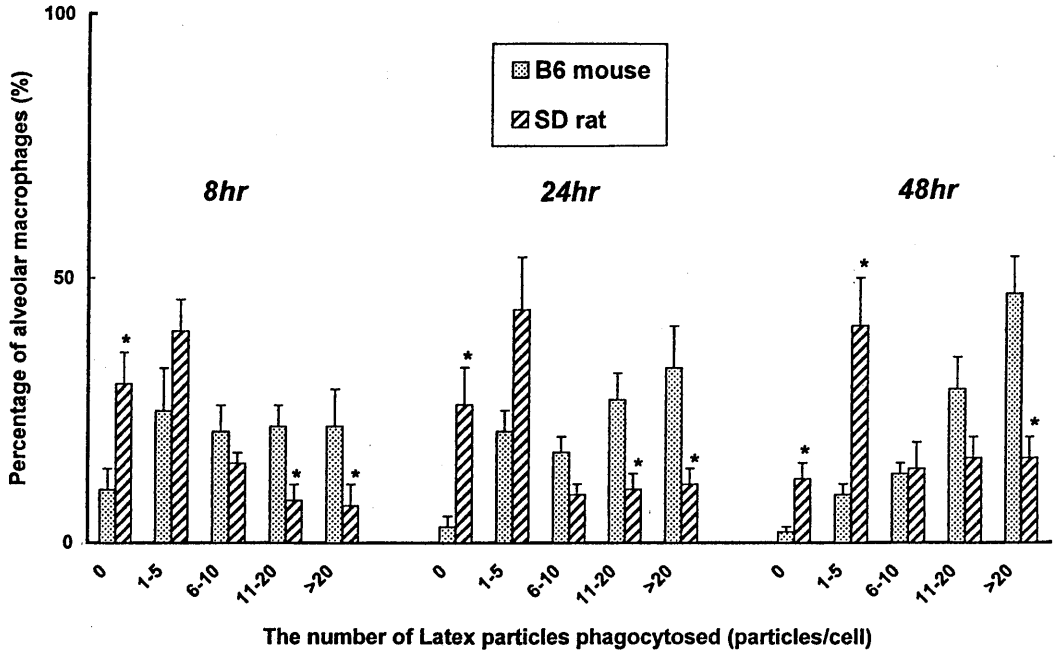

Fig. 6. The percentage of AM classified according to the number of latex particles phagocytosed by individual AM. B6 mouse and SD rat AM were exposed to latex particles for 8, 24 and 48 hr. The mean and standard error were calculated from three separate experiments. Asterisks indicate the statistically significant difference from B6 mouse AM at the corresponding data points.

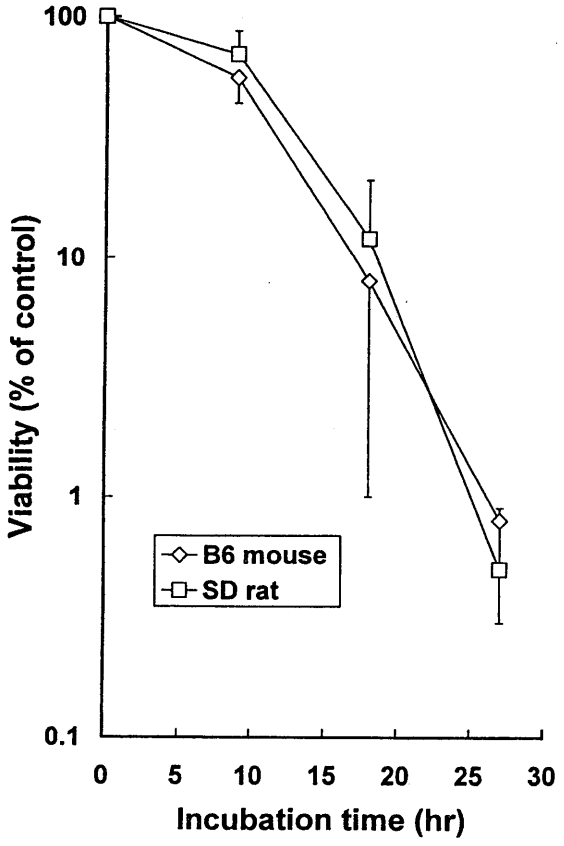

Fig. 7. The cytotoxicity of the filtered Gd preparation made by the filtration of original 3000 μM Gd preparation in B6 mouse and SD rat AM. The mean and standard error were calculated from three separate experiments. There was no statistically significant difference between B6 mouse and SD rat AM.

The amount of Gd incorporated into AM was shown in Table 1. The values at 0 hr of incubation, where 10^6 AM were suspended in 2 ml of 300 μM Gd preparation and immediately separated from the Gd preparation through the filter, were approximately 0.1% of total Gd in the preparations, validating the experimental procedure with a very small amount of non-specific Gd contamination. The values at 4°C, which might be considered as non-specific adsorption of Gd to AM because phagocytosis is suppressed at 4°C, appeared to be similar between B6 mouse and SD rat AM. The uptake of Gd by B6 mouse AM incubated at 37°C was approximately twice that by SD rat AM at both 4- and 10-hr incubations.

Finally, the cytotoxicity of filtered Gd preparation made by the filtration of original 3000 μM Gd preparation was compared between mouse and rat AM at several time points. As shown in Fig. 7, SD rat and B6 mouse AM exhibited almost the same cytotoxicity to the particulate-free Gd preparation.

DISCUSSION

Gd has been utilized extensively as a functional blocking agent of the reticuloendothelial system. However, the extent and the mechanism of toxicity of Gd for macrophages has not been fully elucidated. Mizgerd *et al.* (1996) reported in SD rats that *in vitro* exposure of AM to Gd caused cell death in both dose- and time-dependent fashions, with a significant decrease in AM viability by the exposure to more than 27 μM Gd for 24 hr of culture. In the present

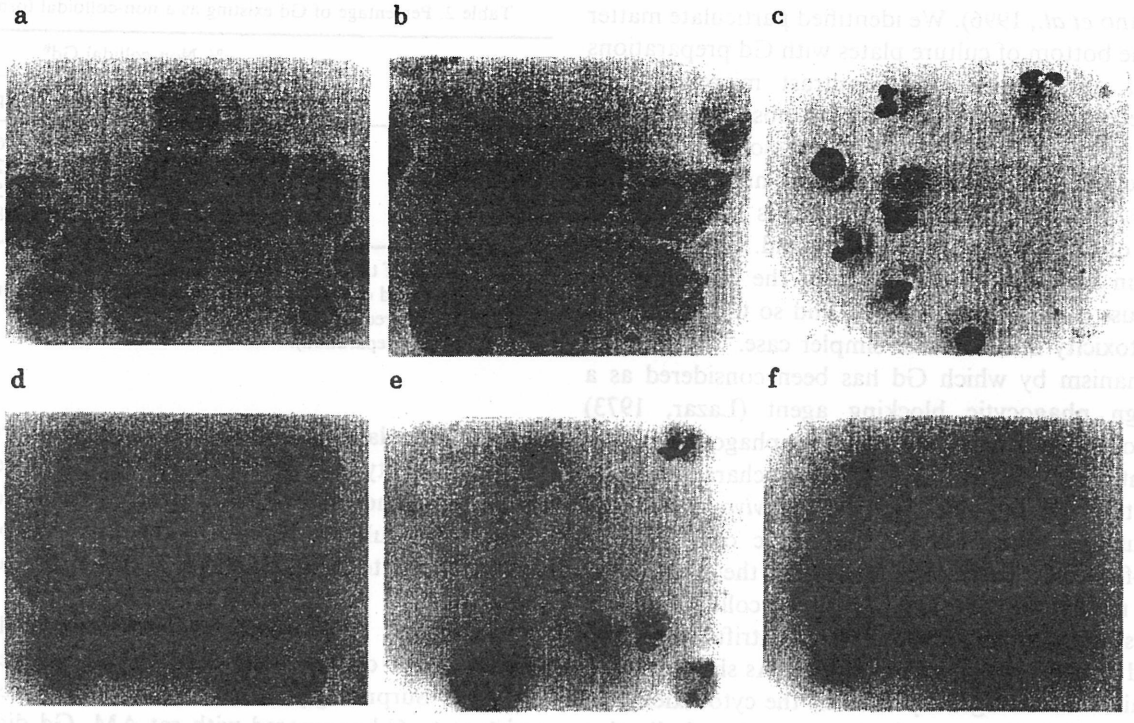

Plate 1. Light microscopic photographs of B6 mouse AM (a,b,c) and SD rat AM (d,e,f) at 48 hr of culture. (a) and (d) control AM; (b) and (e) AM exposed to 300 μM Gd; (c) and (f) AM exposed to 3000 μM Gd. All photographs were at the same magnification.

Table 1. Uptake of Gd by B6 mouse and SD rat AM after 0, 4 and 10 hr

Incubation time (hr)	Incubation temperature (°C)	AM	% Gd[a] Exp. I	% Gd[a] Exp. II
0	–	B6 mouse	0.06	n.d
0	–	SD rat	n.d	0.10
4	4	B6 mouse	0.28	0.36
4	4	SD rat	0.22	0.27
4	37	B6 mouse	1.12	0.96
4	37	SD rat	0.58	0.60
10	4	B6 mouse	0.27	0.40
10	4	SD rat	0.31	0.26
10	37	B6 mouse	1.40	2.00
10	37	SD rat	0.78	0.86

[a] Amount of Gd per 10^6 AM, expressed as a percentage of total amount of Gd added, i.e. 2 ml 300 μM Gd.

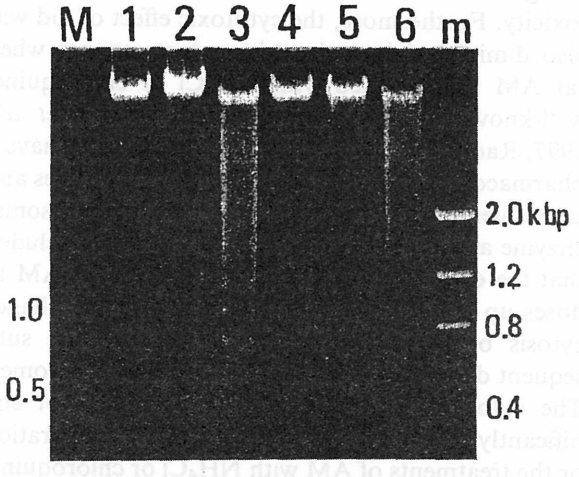

Plate 2. The migration profile of DNA extracted from AM at 48 hr of culture. Lane M, a molecular size marker of 100 bp DNA; Lane 1, control B6 mouse AM; Lane 2, B6 mouse AM exposed to 300 μM Gd; Lane 3, B6 mouse AM exposed to 3000 μM Gd; Lane 4, control SD rat AM; Lane 5, SD rat AM exposed to 300 μM Gd; Lane 6, SD rat AM exposed to 3000 μM Gd; Lane m, a molecular size marker of DNA MASS™ Ladder.

study, the viability of both SD rat and Wistar rat AM was diminished by 48 hr of exposure of 3–10 μM Gd (Fig. 1). Although direct comparison is difficult because of the different experimental protocols, the degree of Gd toxicity observed appeared to be similar to those observed in the present study.

Interphase cell death can be induced via either of two morphologically and biochemically distinct modes: necrosis or apoptosis (Kerr *et al.*, 1972; Wyllie, 1980). Apoptosis has been defined on the basis of two hallmarks: characteristic cell morphology including nuclear condensation and fragmentation; and internucleosomal DNA fragmentation revealed as a ladder migration pattern in DNA electrophoresis. All observations presented in Plates 1 and 2 and Fig. 2 consistently indicated that the interphase cell death of AM induced by Gd exposure was apoptotic in both mice and rats. Mizgerd *et al.* (1996) also identified Gd-induced apoptosis in SD rat AM, and our findings were consistent with their findings.

Rare earth metals have been known to form colloidal macromolecules as carbonate, phosphate and hydroxide complex in a physiological condition

(Hirano *et al.*, 1996). We identified particulate matter on the bottom of culture plates with Gd preparations under an inverted phase-contrast microscope. A white cloudy substance was also observed immediately after adding Gd solution dissolved in sterile saline into the culture medium at high concentrations. From these observations, it is apparent that part of the Gd might exist as colloid. Cd was included in almost all experiments of the present study because it did not precipitate, and so to compare its cytotoxicity in this rather simpler case. The primary mechanism by which Gd has been considered as a benign phagocytic blocking agent (Lazar, 1973) without adverse effects on non-phagocytic cells, might be attributed to this chemical characteristic of Gd to form colloidal particles *in vivo*, which are exclusively taken up by phagocytic cells such as Kupffer cells. To determine whether the cytotoxicity was related to the phagocytosis of colloidal Gd in this study, Gd preparations were centrifuged and filtered to remove particulate matter. As shown in Fig. 3, this treatment greatly reduced the cytotoxicity for SD rat AM. This may be interpreted as indicating that the cytotoxicity was caused by the particulate form of Gd in the non-filtered medium, and that below an initial concentration of 1000 μM there was insufficient non-particulate Gd remaining after centrifugation and filtration to cause significant cytotoxicity. Furthermore, the cytotoxic effect of Gd was also diminished in a dose-dependent manner when rat AM were treated with NH_4Cl or chloroquine, well-known lysosomotropic agents (Brazil *et al.*, 1997; Rao *et al.*, 1995). NH_4Cl or chloroquine have a pharmacologic action to elevate pH in lysosomes and consequently to suppress the acidic lysosomal enzyme activities. On this basis, it may be concluded that the expression of Gd cytotoxicity in rat AM at doses up to 1000 μM largely depends on the phagocytosis of particulate forms of Gd and the subsequent dissolution of those in the phago-lysosomes. The cytotoxicity of Gd at 3000 μM was not significantly affected by the filtration of Gd preparation or the treatments of AM with NH_4Cl or chloroquine. Therefore, it is suggested that at a dose level as high as 3000 μM, significant amounts of Gd existed in a non-colloidal form and thus damaged the AM by the mechanism independent from the phagocytosis of particulate forms of Gd and subsequent dissolution of those in the phago-lysosomes. It could be supposed that the amounts of non-particulate Gd were so different between 1000 and 3000 μM Gd preparations that mouse AM were almost alive and dead, respectively. As shown in Table 2, the percentage of Gd existing as a non-colloidal form (the amount of Gd in the filtered Gd preparation) in total Gd (the total amount of Gd in Gd preparation) was not very different between 1000 and 3000 μM Gd, indicating that non-particulate Gd concentration in 3000 μM Gd preparation was roughly threefold that in 1000 μM Gd preparation, and that this threefold difference in non-particulate Gd concentration might be crucial for the viability loss in mouse AM. In the present study, it was not elucidated in what chemical forms the non-particulate Gd existed and which form of Gd was cytotoxic to AM. These are a matter for future research.

Table 2. Percentage of Gd existing as a non-colloidal form

Dose[a]	% Non-collidal Gd[b]	
	Exp. I	Exp. II
100	23.7	26.8
300	24.0	22.5
1000	24.7	25.3
3000	32.0	28.3

[a] Concentration of total Gd (μM).
[b] Percentage of Gd existing as a non-colloidal form (the amount of Gd in the filtered Gd preparation) in total Gd (amount of Gd in original Gd preparation).

The present study demonstrates the marked difference in the cytotoxic effect of Gd on mouse and rat AM. Surprisingly, mouse AM were extremely resistant to Gd compared with rat AM. Gd did not affect the viability of mouse AM at doses up to 1000 μM, whereas the viability of rat AM was much reduced by exposure to Gd at doses more than 3 μM. Naito *et al.* (1996) reported that peritoneal macrophages from Balb/c mice were not killed for up to 48 hr by exposure to $GdCl_3$ at a dose of 5 mg/100 ml (135 μM). At this dose level, rat AM are remarkably damaged. The present study and that of Naito *et al.* (1996) suggest the consistent resistance of mouse macrophages to Gd toxicity. To explain the species difference, we hypothesized that there might be less phagocytosis of Gd-colloid by mouse AM compared with rat AM. To clarify this point, the phagocytic activity of AM was compared between mouse and rat AM. In the first experiment, the phagocytosis of latex particles was used as an indicator of phagocytic activity, since latex particles are non-toxic and often used for this purpose. As shown in Fig. 6, there was no indication that the phagocytic activity of B6 mouse AM was lower than that of SD rat AM. In the second experiment, the actual amount of Gd incorporated into AM was measured by ICP-MS. To avoid the influence of toxicity of Gd itself, the uptake was compared in relatively short incubation times of 4 and 10 hr. As shown in Table 1, the non-specific adsorption of Gd by AM, indicated by the uptake at 4°C, was similar for mice and rats. The amount of Gd taken up by AM at 37°C was larger in B6 mouse AM than SD rat AM. It thus appears that the amount of Gd incorporated into the cells by phagocytosis was not significantly less in mouse AM than in rat AM. Based on these two experiments, it could be concluded that the difference in phagocytic activity was not responsible for the species difference between mice and rats in the cytotoxicity of Gd.

Another possible explanation is that rat AM were inherently more vulnerable to Gd toxicity than

mouse AM. To examine this, the effect of the filtered Gd preparation (original Gd concentration of 3000 μM before the filtration) was compared between rat and mouse AM. As shown in Fig. 7, the viability of AM exposed to the filtered Gd preparation was almost same between mouse and rat AM at all the time points examined. Therefore, the cytotoxic sensitivity of AM to extracellular non-colloidal Gd appeared to be the same between mice and rats. Taking into account the above findings, the most plausible explanation for the species difference in Gd cytotoxicity, was that the dissolution rate or mode of Gd-colloid in the phago-lysosomes may differ between mouse and rat AM, and/or rat AM may be more easily impaired by Gd dissolved in the phago-lysosomes of AM. There are a few reports that the intracellular particle dissolution rates in AM or intraphagolysosomal pH values differed between species (Heilmann *et al.*, 1992; Kreyling *et al.*, 1990, 1992).

In conclusion, a marked difference in the cytotoxic response to Gd at doses up to 1000 μM was found between mouse and rat AM. The cytotoxicity of Gd at the dose range was dependent on the intracellular uptake and subsequent dissolution of Gd-colloid formed in the culture medium. However, the marked difference in the cytotoxic response to Gd between mouse and rat AM could not be attributed to the phagocytic activities for colloidal form of Gd. Therefore, it is suggested that the extent to which Gd-colloid phagocytosed is dissolved in the phago-lysosome or the subsequent process to exhibit the cytotoxicity may differ between mouse and rat AM. Rat AM may dissolve Gd-colloid more actively or may be more sensitive to Gd dissolved inside the phago-lysosomes with respect to the cytotoxicity.

REFERENCES

Brazil M. I., Weiss S. and Stockinger B. (1997) Excessive degradation of intracellular protein in macrophages prevents presentation in the context of major histocompatibility complex class II molecules. *European Journal of Immunology* **27,** 1506–1514.

Callery M. P., Kamei T. and Flye M. W. (1990) Kupffer cell blockade increases mortality during intra-abdominal sepsis despite improving systemic immunity. *Archives of Surgery* **125,** 36–40.

Heilmann P., Beisker W., Miaskowski U., Camner P. and Kreyling W. G. (1992) Intraphagolysosomal pH in canine and rat alveolar macrophages: flow cytometric measurements. *Environmental Health Perspectives* **97,** 115–120.

Hirano S. and Suzuki K. T. (1996) Exposure, metabolism, and toxicity of rare earth and related compounds. *Environmental Health Perspectives* **104,** 85–95.

Hisama N., Yamaguchi Y., Ishiko T., Miyanari N., Ichiguchi O., Goto M., Mori K., Watanabe K., Kawamura K., Tsurufuji S. and Ogawa M. (1996) Kupffer cell production of cytokine-induced neutrophil chemoattractant following ischemia/reperfusion injury in rats. *Hepatology* **24,** 1193–1198.

Kerr J. F. R., Wyllie A. H. and Currie A. R. (1972) Apoptosis: a basic biological phenomenon with wide ranging implications in tissue kinetics. *British Journal of Cancer* **26,** 239–257.

Kohno H., Yamamoto M., Iimuro Y., Fujii H. and Matsumoto Y. (1997) The role of splenic macrophages in plasma tumor necrosis factor levels in endotoxemia. *European Surgical Research* **29,** 176–186.

Kreyling W. G. (1992) Intracellular particle dissolution in alveolar macrophages. *Environmental Health Perspectives* **97,** 121–126.

Kreyling W. G., Godleski J. J., Kariya S. T., Rose R. M. and Brain J. D. (1990) In vitro dissolution of uniform cobalt oxide particles by human and canine alveolar macrophages. *American Journal of Respiratory Cell and Molecular Biology* **2,** 413–422.

Kubota Y., Takahashi S. and Sato H. (1994) Effect of γ-irradiation on the function and viability of alveolar macrophages in mouse and rat. *International Journal of Radiation Biology* **65,** 335–344.

Lazar G. (1973) The reticuloendothelial-blocking effect of rare earth metals in rats. *Journal of the Reticuloendothelial Society* **13,** 231–237.

Liu P., McGuire G. M., Fisher M. A., Farhood A., Smith C. W. and Jaeschke H. (1995) Activation of Kupffer cells and neutrophils for reactive oxygen formation is responsible for endotoxin-enhanced liver injury after hepatic ischemia. *Shock* **3,** 56–62.

Martin S. J. and Cotter T. G. (1991) Ultraviolet B irradiation of human leukemia HL-60 cells in vitro induces apoptosis. *International Journal of Radiation Biology* **59,** 1001–1016.

Mizgerd J. P., Molina R. M., Stearns R. C., Brain J. D. and Warner A. E. (1996) Gadolinium induces macrophage apoptosis. *Journal of Leukocyte Biology* **59,** 189–195.

Molina R. M., Warner A. E. and Brain J. D. (1995) Uptake of circulating particles by sheep pulmonary intravascular macrophages (PIMs) is significantly decreased by intravenous gadolinium chloride. *FASEB Journal* **9,** A570.

Naito M., Nagai H., Kawano S., Umezu H., Zhu H., Moriyama H., Yamamoto T., Takatsuka H. and Takei Y. (1996) Liposome-encapsulated dichloromethylene diphosphonate induces macrophage apoptosis in vivo and in vitro. *Journal of Leukocyte Biology* **60,** 337–344.

O'Neill P. J., Ayala A., Wang P., Ba Z. F., Morrison M. H., Schultze A. E., Reich S. S. and Chaudry I. H. (1994) Role of Kupffer cells in interleukin-6 release following traumahemorrhage and resuscitation. *Shock* **1,** 43–47.

Pendino K. J., Meidhof T. M., Heck D. E., Laskin J. D. and Laskin D. L. (1995) Inhibition of macrophages with gadolinium chloride abrogates ozone-induced pulmonary injury and inflammatory mediator production. *American Journal of Respiratory Cell and Molecular Biology* **13,** 125–132.

Rai R. M., Zhang J. X., Clements M. G. and Diehl A. M. (1996) Gadolinium chloride alters the acinar distribution of phagoytosis and balance between pro- and anti-inflammatory cytokines. *Shock* **6,** 243–247.

Rao M., Wassef N. M., Alving C. R. and Krzych U. (1995) Intracellular processing of liposome-encapsulated antigens by macrophages depends upon the antigen. *Infection and Immunity* **63,** 2396–2402.

Rocklage S. M., Worah D. and Kim S. H. (1991) Metal ion release from paramagnetic chelates: what is tolerable? *Magnetic Resonance in Medicine* **22,** 216–221.

Roland C. R., Walp L., Stack R. M. and Flye M. W. (1994) Outcome of Kupffer cell antigen presentation to a cloned murine Th1 lymphocyte depends on the inducibility of nitric oxide synthase by IFN-gamma. *Journal of Immunology* **153,** 5453–5464.

Roland C. R., Naziruddin B., Mohanakumar T. and Flye M. W. (1996) Gadolinium chloride inhibits Kupffer cell nitric oxide synthase (iNOS) induction. *Journal of Leukocyte Biology* **60,** 487–492.

Runge V. M. and Parker J. R. (1997) Worldwide clinical safety assessment of gadoteridol injection: an update. *European Journal of Radiology* **7,** 243–245.

Ruttinger D., Vollmar B., Wanner G. A. and Messmer K. (1996) In vivo assessment of hepatic alterations following gadolinium chloride-induced Kupffer cell blockade. *Journal of Hepatology* **25,** 960–967.

Sarphie T. G., D'Souza N. B. and Deaciuc I. V. (1996) Kupffer cell inactivation prevents lipopolysaccharide-induced structural changes in the rat liver sinusoid: an electron-microscopic study. *Hepatology* **23,** 788–796.

Suzuki S., Nakamura S., Serizawa A., Sakaguchi T., Konno H., Muro H., Kosugi I. and Baba S. (1996) Role of Kupffer cells and the spleen in modulation of endotoxin-induced liver injury after partial hepatectomy. *Hepatology* **24,** 219–225.

Tasaka S., Ishizaka A., Sayama K., Waki Y., Soejima K., Nakamura M., Matsubara H., Oguma T. and Kanazawa M. (1996) Role of inflammatory cells in the pathogenesis of acute lung injury in guinea pigs exposed to heat-killed bacteria. *Nippon Kyobu Shikkan Gakkai Zasshi* **34,** 864–869.

Yoshida S. and Muramatsu Y. (1997) Determination of major and trace elements in mushroom, plant and soil samples collected from Japanese forests. *International Journal of Environmental Analytical Chemistry* **67,** 49–58.

Weinmann H. J., Brasch R. C., Press W. R. and Wesbey G. E. (1984) Characterization of gadolinium-DTPA complex: a potential NMR contrast agent. *American Journal of Roentgenology* **142,** 619–624.

Wyllie A. H. (1980) Glucocorticoid-induced thymocyte apoptosis is associated with endogenous endonuclease activation. *Nature* **284,** 555–556.

Bull. Environ. Contam. Toxicol. (2001) 66:139–145
© 2001 Springer-Verlag New York Inc.
DOI: 10.1007/s001280000216

Bulletin of Environmental Contamination and Toxicology

Survival of Genetically Modified *Escherichia coli* Carrying Extraneous Antibiotic Resistance Gene through Microbial Interactions

K. Matsui,[1] N. Ishii,[2] Z. Kawabata[1]

[1] Center for Ecological Research, Kyoto University, Kamitanakami Hirano-cho 509-3, Otsu 520-2113, Japan
[2] Environmental and Toxicological Science Research Group, National Institute of Radiological Sciences, 9-1 Anagawa-4-chome, Inage-ku, Chiba-shi 263-8555, Japan

Received: 13 July 2000/Accepted: 11 October 2000

The advance of recombinant DNA techniques allows us to construct novel bacterial strains. The potential uses of such recombinant bacteria in the environment include biocontrol of insects, environmental remediation and waste treatment (Alexander 1981). Intended release of such genetically engineered microorganisms (GEMs) into natural environments has, however, raised questions regarding their ecological impact and many studies are being conducted to evaluate their ecological effects (e.g. Goodnow et al. 1990; Min et al. 1998; Tiedje et al. 1989). The safety of releasing GEMs is still uncertain and, in Japan, the field application of GEMs is prohibited by law to prevent possible ecological impact. Recently, much more environmental concern has been paid to the unintended release of laboratory bacterial strain, which may be recombinant, for research purposes. (Av-Gay 1999). Although we can regulate the deliberate release of GEMs into environment, we are still exposed to unintended release of recombinant bacteria.

Bacteria such as *Escherichia coli* K-12 are intensively used as laboratory microorganisms in the area of molecular biology and their genetic characteristics are frequently modified for research purposes by introducing a foreign gene. Using *E. coli* K-12 as the parental strain for genetic manipulation has been deemed safe because not only have their modified characteristics led to loss of their ability to survive in natural environments but they are also burdened with the increased metabolic demands of the maintenance and expression of the introduced foreign genes. Several studies have been conducted to evaluate the effects of releasing genetically modified *E. coli* K-12 into the environment (e.g. Chao and Feng 1990; Helling et al. 1981) but the results were inconsistent. Some support the safety of releasing them and some cast doubt on their safety (Brill 1985; Sobecky et al. 1992). To evaluate the impact of unintentionally releasing genetically modified *E. coli* K-12, it is necessary to focus on the factors, which are not site-specific, involved in its survival.

In this study, we focused on the effects of microbial interactions, which including the competition with the parental strain, and the existence of protozoa and algae, as factors which would be involved in the survival of genetically modified *E. coli* K-12. For this purpose, we used a species-defined microcosm, which consisted of the bacterium *E. coli*, a bacteria feeding protozoan *Tetrahymena thermophila* and a photosynthetic alga *Euglena gracilis* (Kawabata et al. 1995). In this system, *T.*

Correspondence to: Z. Kawabata

thermophila interact with *E. coli* directly through predation but *E. gracilis* interact with *E. coli* only through its metabolites (Matsui et al. in press). Therefore, we will be able to evaluate both direct and indirect effects of these processes on the survival of the genetically modified *E. coli* K-12 in this system. We also tried to evaluate the impact of the genetically modified *E. coli* K-12 for the population dynamics of the protozoan and the alga in this microcosm.

MATERIALS AND METHODS

E. coli K-12 DH5α (Sambrook et al. 1989), designated here as *E. coli*, is a laboratory strain commonly used for molecular biological studies and is used here as the parental strain of the genetically modified strain. Plasmid pBluescriptII SK(+) (Alting-Mees et al. 1989), encoding the antibiotics ampicillin resistance gene, is a plasmid vector widely used for DNA recombination. It was transformed into *E. coli* to construct the genetically recombinant strain, harboring the extraneous plasmid, designated here as *E. coli* (P). *E. coli* and *E. coli* (P) were maintained on Luria-Bertani (LB) agar medium (Sambrook et al. 1989) and LB with 50μg/ml ampicillin agar medium respectively.

E. coli (P) was introduced into an *E. coli* single culture to test competition with the parental strain. Half strength #36 Taub's salt solution (Taub and Doller. 1968) without $NaNO_3$ was supplemented with 500 mg/L of proteose peptone (Difco laboratory, USA) and used as a culture medium. The medium was decanted into a series of test tubes and autoclaved before inoculation with the organisms. To synchronize the condition of the cells, *E. coli* were precultured in LB medium until they reached the late-logarithmic growth phase, washed twice in half strength Taub's #36 salt solution, resuspended in the same solution and then inoculated into each test tube at 10^2 cells/mL, the initial population density. Each test tube was placed stationary, in an incubator under 2500 lx by fluorescent lamps with 12-12LD light regime at 25°C and were sacrificed for counting on each sampling day. *E. coli*(P) was introduced into *E. coli* cultures at the beginning and after 5-days of the cultivation period. The numbers of *E. coli* (P) were monitored by colony formation units (CFU) on broth-agar plate medium (extracted bonito 3.0 g, polypeptone 3.0 g, NaCl 5.0 g, and 15 g agar powder in 1 liter of distilled water; pH adjusted to 7.0) with 0.5mg/L of ampicillin. The total cell number was obtained by the CFU on nutrient agar without ampicillin. Each count was carried out for three petridishes and the mean values of three counts were used as CFU per mL.

E. coli (P) were also introduced into a simple aquatic microcosm, which was developed by Kawabata et al. (1995), to evaluate the effects of microbial interactions on the survival of the recombinant strain. The microcosm consisted of a photosynthetic alga *Euglena gracilis* (producer), a bacteria-feeding protozoan *Tetrahymena thermophila* (consumer) and bacterium *E. coli* (decomposer) and was thus, employed to represent a simplified aquatic microbial ecosystem (Kawabata et al. 1995). High reproducibility of this microcosm suggested its reliability as a model of a microbial community (Matsui et al. in press). The microcosm was constructed by inoculating the *E. gracilis*, *T. thermophila* and *E. coli* into culture medium by the same methods as used for *E. coli* single-culture except that the pre-culture of *T. thermophila* and *E. gracilis* was conducted in nutrient rich media (for *T. thermophila*; proteose peptone 2.5 g, yeast extract 2.5 g and dextrose 10 g in 1 liter of distilled water; pH adjusted to 7.0: for *E. gracilis*;

tryptone 10 g, yeast extract 1 g, dextrose 10 g and vitamin B_{12} 100μg in 1 liter of distilled water; pH adjusted to 3.0). *E. coli* (P) was inoculated into the microcosm at the beginning of cultivation (day-0) and after 5-days of cultivation. The methods used to obtain the numbers of *E. coli* (P) and the total cell numbers were as described above. The numbers of *T. thermophila* and *E. gracilis* cell were counted under a microscope according to Kawabata et al. (1995).

RESULTS AND DISCUSSION

Figure 1 shows the population changes of *E. coli* (P) in the *E. coli* single-culture system. No significant difference in growth was observed between *E. coli* and *E. coli* (P) when the latter was introduced to the *E. coli* culture at the beginning of cultivation (Fig. 1A). This indicates that *E. coli* (P) has the same growth potential as the parent *E. coli*. In contrast, *E. coli* (P) declined sharply when introduced into *E. coli* single-culture after 5-days of incubation (Fig. 1B). The disappearence of *E. coli* (P) from the culture may reflect an uncomfortable environment for its growth, such as a scarcity of nutrients because both strains have the same metabolite pathways and would compete for each others resources. Another possibility was accumulation of metabolites from *E. coli* which might negatively affect the growth for both *E. coli and E. coli* (P) (Matsui et al. in press). No significant difference was observed in the population density of the parental strain with the addition of *E. coli* (P). From these results in the *E. coli* single-culture system, it seems less possible that unintentionally released *E. coli* (P) survive at a release site, where its parental *E. coli* already existed, due to competition with the parental strain.

When *E. coli* (P) were introduced into the three species microcosm at the start of cultivation, they grew in the same manner as the parent *E. coli* (Fig. 2A). However, *E. coli* (P) were also able to maintain their population density over 20 days when introduced into a three species microcosm on day 5 of cultivation (Fig. 2B). The addition of *E. coli* (P) did not affect the population densities of the other species in the microcosm (Fig. 2).

It has been well documented that predation by protozoa is an important factor in reducing the population densities of bacteria in aquatic environments (Nakano et al. 1998) and this is supported by the decrease of the *E. coli* population densities from 10^7 cells/mL (in single culture) to 10^6 cells/mL (in three species microcosm). Here, we found additionally that the existence of algae and protozoa in the microcosm ameliorated the competition between *E. coli* and *E. coli* (P) and provided conditions which allowed the survival of *E. coli* (P) (Fig. 2B), which had disappeared from the five-day old *E. coli* single culture. The metabolites from algae and protozoa would ameliorate the self-toxicity of the *E. coli* metabolites and thus support the survival of *E. coli* (Matsui et al. in press). Although the exact mechanism by which *E. coli* (P) maintained its population in the three species microcosm is not clear. In a previous study, we found that, in addition to protozoan predation, a metabolite of the indigenous bacteria were factors affecting the decreases of both *E. coli* and *E. coli* (P) when introduced to a paddy field microcosm (Kawabata et al. 1998). The results in the present study suggest that a metabolite from the competitive *E. coli*, might be a stronger factor than protozoa in the decrease of the introduced genetically recombinant *E. coli* and that genetically recombined *E. coli* used in a laboratory have the possibility of surviving in aquatic environments through such microbial interaction.

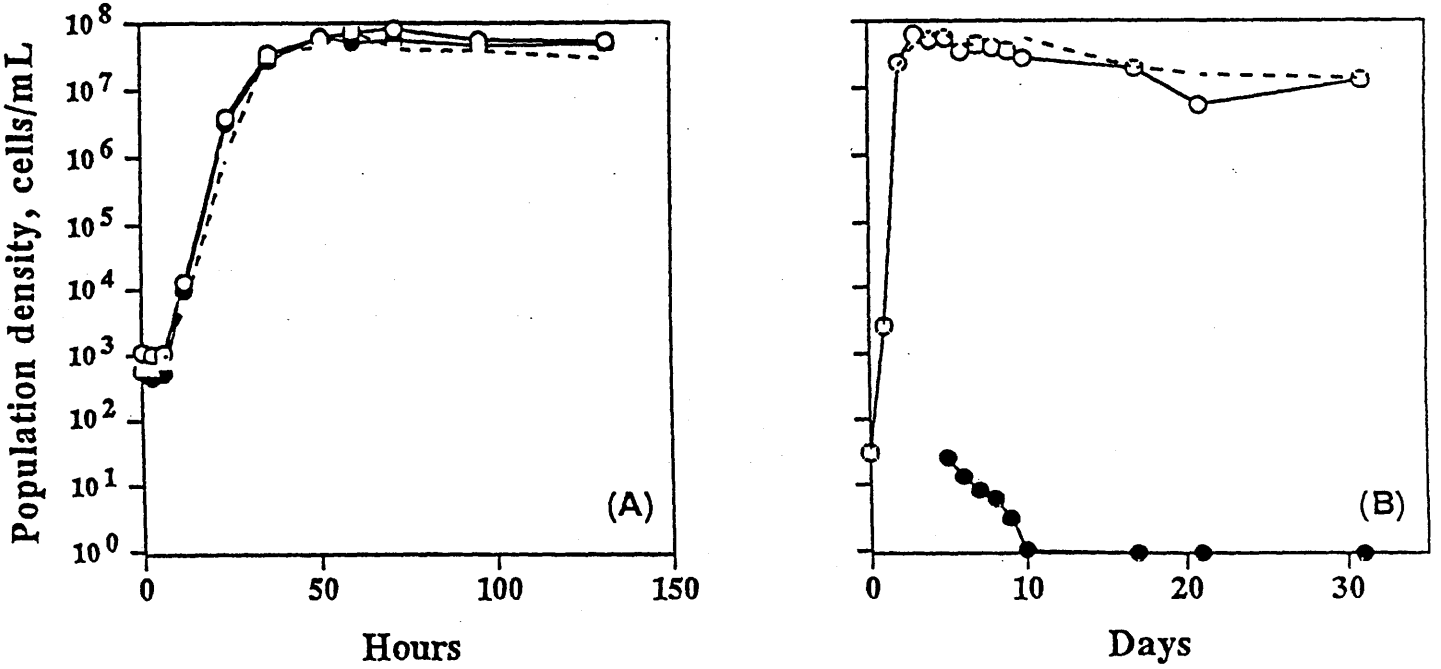

Figure 1. Population changes of *E. coli* (P)(●) introducing into *E. coli* single culture at the same time as *E. coli* (A), and after 5 days cultivation of *E. coli* (B). Population changes of *E. coli* (P) + *E. coli* (○), are also represented and broken lines indicate results of control experiments.

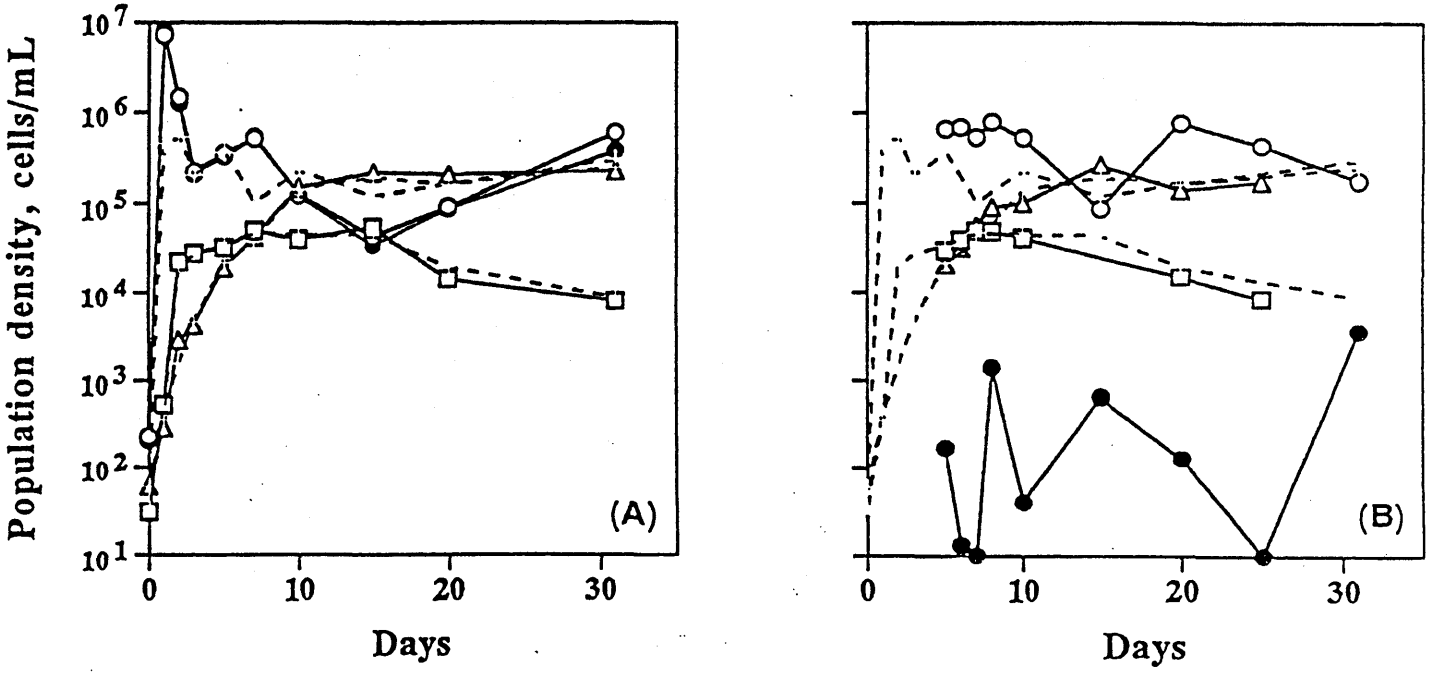

Figure 2. Population changes of *E. coli* (P)(●) introduced into a three-species microcosms at the same time as the other three species (A) and after 5 days cultivation of the other three species (B). Population changes of *E. coli* (P) + *E. coli* (○), *T. thermophila* (□), and *E. gracilis* (◇) are also represented. Broken lines represent results of control experiments.

The difference between intended and unintended release of GEMs are the genetic and physiological designs of the bacteria. With an intended environmental application the GEMs would often have as an objective their stable maintenance and function in a particular environmental niche. In contrast, the bacteria which were unintentionally released from a laboratory would originally be designed and recombined for a specific research purpose, such as cloning of a specific gene, and therefore, less attention would have been paid to its survival after experiments. In this study, we used the species defined microcosm and have demonstrated that the survival potential of a laboratory *E. coli* strain, through microbial interaction which may attenuate competition with the parental strain. Since there are several reports that *E. coli* is one component of the resident bacteria in aquatic environments (Brettar et al. 1992), our results indicate that the survival of laboratory used genetically recombined *E. coli* in aquatic environment is possible, where parental *E. coli* are resident.

Acknowledgments. This work was partly supported by a Japanese Ministry of Education, Science and Culture Grant-in-Aid for Scientific Research on Priority Areas (#319), Project "Symbiotic Biosphere: An ecological interaction network promoting the coexistence of many species" and also by a Research Fellowships of the Japan Society for the Promotion of Science for Young Scientists.

REFERENCES

Av-Gay Y (1999) Uncontrolled release of harmful microorganisms. Science 284: 1621

Alting-Mees MA, Short JM (1989) pBluescript II: gene mapping vectors. Nucleic Acids Res 17: 9494

Alexander M (1981) Biodegradation of chemicals of environmental concern Science 211: 132-138

Brettar I, Höfle MG (1992) Influence of ecosystematic factors on survival of *Escherichia coli* after large-scale release into lake water mesocosms. Appl Environ Microbiol 58: 2201-2210

Brill WJ (1985) Safety concerns and genetic engineering in agriculture. Science 227: 381-384

Chao WL, Feng RL (1990) Survival of genetically engineered *Escherichia coli* in natural soil and river water. J Appl Bacteriol 68: 319-325

Goodnow RA, Harrison MD, Morris DJ, Sweeting KB, Laduca RJ (1990) Fate of ice nucleation-active *Pseudomonas syringae* strains in alpine soils and waters and in synthetic snow samples. Appl Environ Microbiol 56: 2223-2227

Helling RB, Kinney T, Adams J (1981) The maintenance of plasmid-containing organisms in populations of *Escherichia coli*. J Gen Microbiol 123: 129-141

Kawabata Z, Matsui K, Okazaki K, Nasu M, Nakano N, Sugai T (1995) Synthesis of a species-defined microcosm with protozoa. J Protozool Res 5: 23-26

Kawabata Z, Min MG, Matsui K, Ishii N (1998) Factors affecting the survival of genetically engineered *Escherichia coli* bearing a plasmid in a paddy field microcosm. Intern J Environ Studies 55: 77-85

Matsui K, Kono S, Saeki A, Ishii N, Min MG, Kawabata Z (in press) Direct and indirect interactions for coexistence in a species defined microcosm. Hydrobiologia

Min MG, Kawabata Z, Ishii N, Takata R, Furukawa K (1998) Fate of a PCBs degrading recombinant *Pseudomonas putida* AC30 (pMFB2) and its effect on the densities of microbes in marine microcosms contaminated with PCBs. Intern J Environ Stud 55: 271-285

Nakano S, Ishii N, Manage PM, Kawabata Z (1998) Trophic roles of heterotrophic nanoflagellates and ciliates among planktonic organisms in a hypereutrophic pond. Aquat Microb Ecol 16: 153-161
Sambrook J, Fritsch EF, Maniatis T (1989) Molecular cloning, A laboratory manual. Cold Spring Harbor Press, Cold Spring Harbor, New York
Sobecky PA, Schell MA, Moran MA, Hodson RE (1992) Adaptation of model genetically engineered microorganisms to lake water: growth rate enhancements and plasmid loss. Appl Environ Microbiol 58: 3630-3637
Taub FB, Doller AM (1968) Nutritional inadequacy of *Chlorella* and *Chlamydomonas* as food for *Daphnia pulex*. Limnol Oceanogr 13: 607-617
Tiedje JM, Colwell RK, Grossman YL, Hodson RE, Renski RE, Mack RN, Regal PJ (1989) The planned introduction of genetically engineered organisms: ecological considerations and recommendations. Ecology 70: 298-315

Proceedings of the International Workshop on Comparative Evaluation of Health Effects of Environmental Toxicants Derived from Advanced Technologies, Supplement, J. Inaba & Y. Nakamura, Chiba, 127-130. 1999.

15. Effect of Acidification on the Population of Growth Stage Aquatic Microcosm

K. MIYAMOTO[1], S. FUMA[1], H. TAKEDA[1], K. YANAGISAWA[1], Y. INOUE[1], N. SATO[1], M. HIRANO[1] and Z. KAWABATA[2]

[1]Environmental and Toxicological Sciences Research Group, National Institute of Radiological Sciences, Chiba 263-8555, Japan, [2]Department of Environmental Conservation, Ehime University, Matsuyama, Ehime 790-8566, Japan

INTRODUCTION

Acidification phenomenon of natural ecosystem caused by human activity such as industrial energy production or motorization is recognized as one of the most serious ecological stress. It is necessary to establish a reasonable method to evaluate the ecological effect of acidification comparing with the other environmental toxicants, if human beings want to maintain a sustainable development. As the natural ecosystem consists of various biological species and includes the complex mutual interaction among them, it is not easy to assess any effects on ecosystem from accumulated knowledge of the effect on single species. Experimental studies on model ecosystem might have an ideal possibility, by which we can get valuable information that cannot be induced from either experiments for single species in a laboratory, or observation of complicated phenomena in natural ecosystem. In this study an aquatic microcosm system was adopted as a model ecosystem for ecological assessment of acidification effect. This system is a biological community, which has capability to demonstrate an indirect effect by any ecological stress on the species composing the ecosystem.

MATERIAL AND METHODS

The aquatic microcosm system consists of three species of microorganism in a small container like a test tube or a small plastic bottle. This system was composed by Kawabata *et al.*[1)], and the mutual interaction of materials among the three species incubated in a regular condition has been investigated. This microcosm consists of flagellate algae *Euglena gracilis Z* as a producer which has chloroplast to do photosynthesis, ciliated protozoa *Tetrahymena thermophila* B as a consumer which grazes bacteria, and bacteria *Escherichia coli* DH5 α as a decomposer which decomposes metabolite and dead bodies of the other two species. They can survive by exchanging materials each other in a closed container with limited nutrients at the start of incubation, and their population densities are kept in a steady-state for a long time, usually for more than a year.

An experiment of acidification was carried out as follows: Each microorganism was preincubated following the method of Kawabata *et al.*[1)] Then three species of microorganisms were inoculated into a culture medium (0.05 % protease peptone in half strength of modified Taub and Dollar's solution) in test tubes. The culture medium was in advance acidified to pH 4.0 by adding the volume equivalently mixed solution of 1N nitric acid and 1N sulfuric acid, while the control medium was originally pH 7-8. Population densities of each organism were determined at various time intervals after starting incubation under a 2500 lx and 12-12 hrs. LD light regime at 25 ℃. The population density of *Eu. gracilis* and *T. thermophila* were counted microscopically, and that of *E. coli* was measured by counting colonies formed in the broth-agar medium.

RESULTS AND DISCUSSION

Figs. 1-3 show the time dependent variations in the population densities of three

microorganisms after inoculation in the control microcosm and in the microcosm acidified to pH 4.0, which are compared with the changes in the population densities of each microorganism incubated in the single pure culture.

I. Acidification effect on each three microorganism in the single pure culture

Eu. gracilis (Fig. 1): *Eu. gracilis* in the pH 4.0 single pure culture increased more than that in the control. The population density of *Eu. gracilis* in the steady-state from the twentieth day after inoculated into the pH 4.0 medium reached to 10^5 cells/ml order, while that in the control is 10^4 cells/ml order. This is because *Eu. gracilis* is not stressed by acidification but promoted to increase by addition of nitric acid and sulfuric acid.

T. thermophila (Fig. 2): The population density of *T. thermophila* in the pH 4.0 single pure culture was not so much different from that in the control. Although *T. thermophila* is not stressed by acidification to pH 4.0, it was extinguished after thirty days passed from inoculation, in the same way as the control. Because it cannot survive alone with neither organic matters which were consumed during the thirty days, nor *E. coli* which plays a role of feed for *T. thermophila*.

E. coli (Fig. 3): The population density of *E. coli* in the pH 4.0 single pure culture kept the approximate same order of that at the time of inoculation, which means 10^{-3} times lower than the control in the steady-state. *E. coli* was not extinguished but could not increase in the stressed condition by acidification.

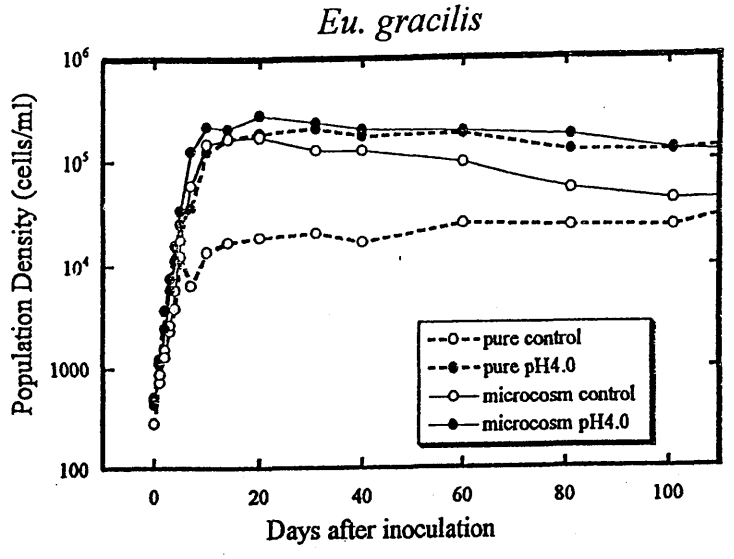

Fig. 1 The changes in the population density of Eu. gracilis in the control and the pH 4.0 single pure culture, and also in the control microcosm and in the pH 4.0 microcosm

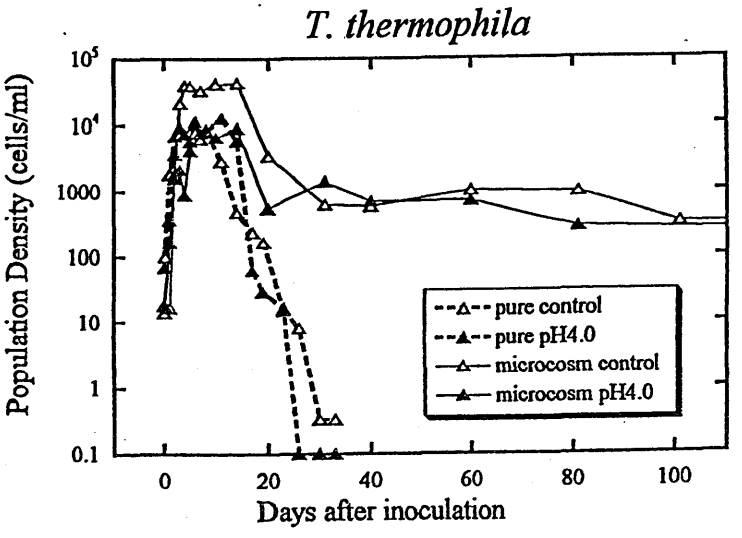

Fig. 2 The changes in the population density of T. thermophila in the control and the pH 4.0 single pure culture, and also in the control microcosm and in the pH 4.0 microcosm.

II. Acidification effect on each three microorganism in the microcosm

Eu. gracilis (Fig. 1): The population density of *Eu. gracilis* in the pH 4.0 microcosm is higher than that in the control microcosm. Consequently, the population density of *Eu. gracilis* in the steady-state was highest in both cases of single pure culture and microcosm system, when the medium was acidified to pH 4.0. It is concluded that *Eu. gracilis* is not stressed by acidification but promoted to increase. It is interesting that the control microcosm system is better condition for

Eu. gracilis to increase and to keep the high population density, compared with the control single pure culture.

T. thermophila (Fig. 2): It is clearly recognized that the population density of *T. thermophila* in the microcosm increased and kept a steady-state of 10^3 cells/ml even after thirty days from the inoculation. This is because *T. thermophila* can survive without protease pepton by grazing *E. coli*. Although the population density of *T. thermophila* was not affected by the acidification to pH 4.0 in the case of single pure culture, the population density of *T. thermophila* in the pH 4.0 microcosm is one order lower than that in the control microcosm in the growth stage until twenty days passed after inoculation. It is considered that the population density of *E. coli*, which plays a role of feed for T. thermophila was not enough during this period, compared with the control, as is described later.

E. coli (Fig. 3): The population density of *E. coli* in the pH 4.0 microcosm decreased and did not increase until seven days passed after inoculation, while in the control microcosm it increased and reached a steady-state of 10^6 cells/ml. Then the population density of *E. coli* in the pH 4.0 microcosm had increased till the tenth day and reached the same order as that of the control. As *E. coli* cannot increase in the pH 4.0 medium in the case of single pure culture, it is considered that the condition in the acidified microcosm changed to be suitable for increasing of *E. coli* until ten days passed, as is described later.

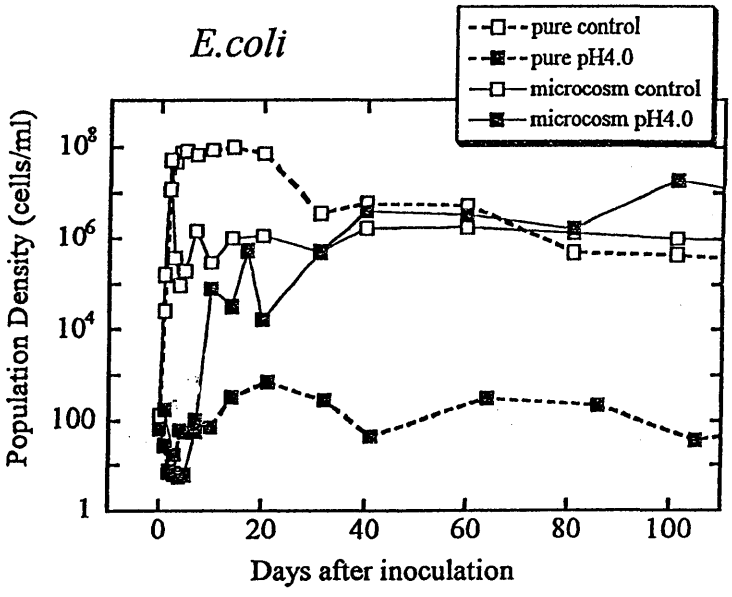

Fig. 3 The changes in the population density of E.coli in the control and the pH 4.0 single pure culture, and also in the control microcosm and in the pH 4.0 microcosm

On the other hand, as mentioned above, the population density of *T. thermophila*, the predator for *E. coli*, in the pH 4.0 microcosm was lower than that in the control in the growth stage. As *E. coli*, the feed for *T. thermophila*, did not increase during this period, *T. thermophila* was inhibited to increase by the low population density of *E. coli*. This phenomenon is recognized to be an indirect effect resulted from interspecific interaction occurred in a model ecosystem, microcosm. *T. thermophila* was affected secondarily by low population density of *E. coli*, which was directly affected by acidification.

III. The change of pH of microcosm

Fig. 4 shows the time dependent variation of pH of microcosm. The pH of the control microcosm increased from 7.8 to 8.2 until ten days passed after inoculation. The pH of the acidified microcosm also increased from 4.0 to 7.1 until ten days passed after inoculation. As the pH was changed to be suitable for increasing of *E. coli*, the population density of *E. coli* reached to the same 10^5 cells/ml order as that of the control on the tenth day after inoculation in the pH 4.0 microcosm. What worked for elevating pH of the microcosm?

Fig. 5 shows the time dependent variation of pH of single pure culture of *Eu. gracilis*. It

was also elevated from 4.0 to 6.5 until ten days passed after inoculation. It is, therefore, concluded that in the pH 4.0 microcosm the pH was elevated by *Eu. gracilis*, and as a result, *E. coli* started increasing. This is thought to be one kind of demonstration of an interspecific interaction occurred in a model ecosystem, microcosm.

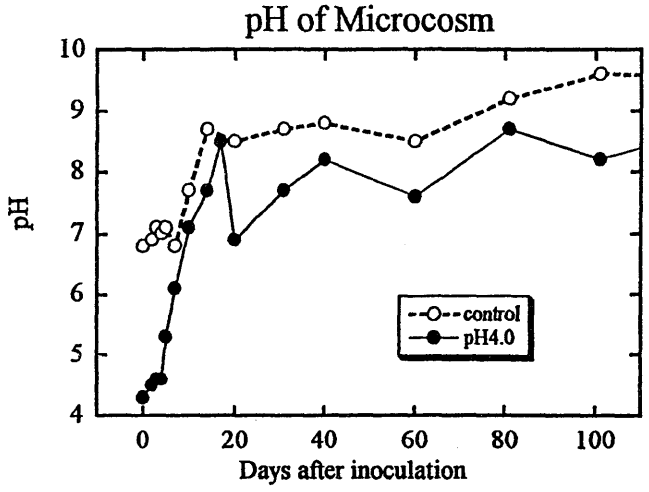

Fig. 4 The change of the pH of microcosm

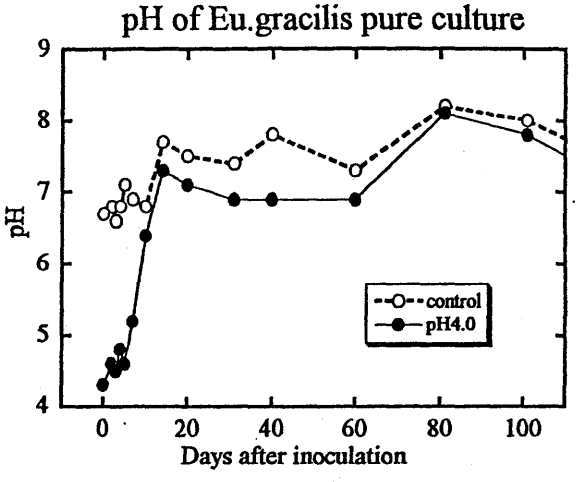

Fig. 5 The change of the pH of single pure culture of Eu. gracilis

CONCLUSION

The present study showed that acidification did not affect on the microcosm, consequently. Although one of the species was directly affected, the other contributed to remediation of the condition of microcosm system. This microcosm system could be expected to be applied to examine other various ecological toxicants, by its advantage of demonstrating indirect effects originated from mutual interaction among the organisms.

REFERENCE

1. Kawabata, Z., Matsui, K., Okazaki, K., Nasu, M., Nakano, N. and Sugai, T. : J. Protozool. Res., 5, 23-26 (1995)

Determination of plutonium concentration and its isotopic ratio in environmental materials by ICP-MS after separation using ion-exchange and extraction chromatography

JAAS
Journal of Analytical Atomic Spectrometry

Yasuyuki Muramatsu,[a] Shigeo Uchida,[a] Keiko Tagami,[a] Satoshi Yoshida[a] and Takashi Fujikawa[b]

[a]*Environmental and Toxicological Sciences Research Group, National Institute of Radiological Sciences, Anagawa 4-9-1, Inage-ku, Chiba, 263-8555 Japan*
[b]*Kansai Environmental Engineering Center Co. Ltd., Azuchi-machi 1-3-5, Chuo-ku, Osaka, 541-0052 Japan*

Received 4th January 1999, Accepted 19th March 1999

An analysis method for ^{239}Pu and ^{240}Pu in environmental samples (including four certified reference materials) by ICP-MS was studied. Two types of chromatographic resin, Dowex 1X8 and TEVA, were examined for their applicability to the separation of Pu from the matrix elements. Sufficient decontamination factors (10^4–10^5) for many matrix elements including U, which interferes with the detection of mass 239, were obtained with both resins. The detection limit of Pu by ICP-MS was about 0.02 pg ml^{-1} (0.05 mBq ml^{-1} for ^{239}Pu; 0.17 mBq ml^{-1} for ^{240}Pu) in the sample solution or 0.1 pg in the sample. Analytical results of $^{239+240}Pu$ in certified reference materials (IAEA-135, -SOIL-6, -368 and -134) indicated that the accuracy of the method was satisfactory. Data on the $^{240}Pu/^{239}Pu$ atom ratios in these reference materials, which are scarce in the literature, were also obtained, *i.e.*, 0.211 for IAEA-135, 0.191 for IAEA-SOIL-6, 0.043 for IAEA-368 and 0.200 for IAEA-134. Compared with alpha-spectrometry, the ICP-MS method has significant advantages in terms of its simple analytical procedures, prompt measurement time and capability of determining the $^{240}Pu/^{239}Pu$ ratio.

Introduction

Plutonium is one of the most important nuclides from the viewpoints of radioecology and toxicology. There are different anthropogenic sources of Pu in the environment. Atomic weapons testing introduced the major deposited fraction of Pu onto the Earth's surface. It was estimated that 10^4 TBq of $^{239+240}Pu$ have been injected into the atmosphere through weapons testing.[1] Plutonium has also been released into the environment due to accidents at nuclear facilities such as Sellafield (UK),[2] Kyshtym (Russia)[3] and Chernobyl (Ukraine).[4]

The isotopes of Pu range from ^{232}Pu to ^{246}Pu, of which ^{238}Pu (half-life: 87.7 years), ^{239}Pu (half-life: 24 110 years), ^{240}Pu (half-life: 6584 years) and ^{241}Pu (half-life: 14.35 years) are thought to be the most important in terms of environmental studies. Among them, ^{239}Pu and ^{240}Pu are the two most abundant Pu isotopes in the environment. The $^{240}Pu/^{239}Pu$ atom ratio in global fallout reported by Krey *et al.*[5] is, on average, 0.176 ± 0.014. It is known that the $^{240}Pu/^{239}Pu$ ratio is a good indicator to identify the source of the contamination.[6] However, data for the $^{240}Pu/^{239}Pu$ ratio in environmental samples are still limited. There are no values for the $^{240}Pu/^{239}Pu$ ratio in certified reference materials for environmental research, as far as we know, in a survey report prepared by the IAEA.[7]

The analytical methods usually used for Pu determination are alpha-spectrometry,[8–12] LX/-α ray measurement,[13] fission track,[14,15] TIMS (thermal ionization mass spectrometry)[16,17] and ICP-MS (inductively coupled plasma mass spectrometry).[15,18–21] The most widely used method is alpha-spectrometry. However, this method is very time consuming and it cannot resolve the ^{239}Pu and ^{240}Pu peaks because of their similar energies (5.15 and 5.16 MeV). Analytical results from alpha-spectrometry are therefore expressed as the sum of the ^{239}Pu and ^{240}Pu activity concentration (*i.e.*, $^{239+240}Pu$). TIMS provides very accurate and precise determinations of Pu isotopes at very low concentrations. However, the instrument is very expensive and its operation requires much experience. In this context, ICP-MS, which is increasingly being used in environmental analysis for the determination of several elements[22,23] and isotopes,[24] has advantages in terms of ease of operation and prompt analysis, although the precision is not as high as that in TIMS. Kim *et al.*[15] applied ICP-MS to the determination of ^{239}Pu and ^{240}Pu in soil and silt samples after chemical separation of the nuclides by solvent extraction and ion-exchange. Crain *et al.*[18] reported the determination of actinides (including Pu) in soil leachates by ICP-MS and alpha-spectrometry after separation by extraction chromatography using a resin which is known to absorb actinides.[25–27] Recently, Yamamoto *et al.*[19] successfully used ICP-MS in the determination of Pu isotopes in samples collected from the former Semipalatinsk Nuclear Site. Chiappini *et al.*[20] improved the detection limits for actinides through improvements in the interface pumping system in ICP-MS and by using a high-efficiency nebulizer system. However, there are still only a few papers dealing with the application of ICP-MS to the determination of Pu and its isotopes in environmental materials. No details of separation procedures suitable for ICP-MS or of the validation of the analytical qualities are given in these papers. Therefore, further investigations of the details of the analytical procedure are necessary in order to establish an appropriate method for ICP-MS. Because there is almost no information on the $^{240}Pu/^{239}Pu$ ratio in international certified reference materials, it is also necessary to obtain these isotopic data.

In this paper, analytical procedures for Pu in environmental samples (including certified reference materials of soil, sediment and fish flesh) by ICP-MS were studied. Particular

attention was paid to the separation procedures. Two different techniques, *viz.*, ion-exchange and extraction chromatography, were compared for their efficiency in the separation of Pu from the matrix. The following points were specifically studied: (1) chemical separation of Pu from the matrix; (2) determination of Pu by ICP-MS; and (3) determination of Pu and the $^{240}Pu/^{239}Pu$ atom ratio in international certified reference materials. Several soil samples collected in Japan with background Pu levels were also analyzed using the developed method.

Experimental

Standards, reagents and samples

Plutonium-242 (CRM 130, Plutonium Spike Assay and Isotopic Standard, New Brunswick Laboratory, USA) was used to spike the samples. The standard solution of ^{242}Pu was diluted to obtain stock solutions with a concentration of 0.2 ng ml^{-1} (29 mBq ml^{-1}) in 2 M HNO_3 solution. To check the $^{240}Pu/^{239}Pu$ ratio, a Pu isotope standard solution (NIST SRM 947) was used. Standard solutions of other elements (*e.g.*, U, Th, Ce, Fe) were prepared from Multielement Plasma Standards (SPEX Industries). As an internal standard, Bi (20 ng ml^{-1}) was used to assess any changes in analytical signals during the measurement.

The ion-exchange resin used was Dowex 1X8 (anion-exchange resin, 100–200 mesh, Dow Chemical Co.). The resin was first conditioned in a large column (*ca.* 250 ml) by passing solutions in the following order: 1 M NaOH (*ca.* 5 l), H_2O (washing), 0.5 M $(NH_4)_2SO_4$ (*ca.* 0.5 l), H_2O (washing), 3 M HCl (*ca.* 2.5 l) and H_2O (washing). After this procedure had been repeated, the conditioned resin was placed in a plastic bottle and kept in a cool, dark place. For the analysis, 2 ml of the resin were placed in a mini-column (diameter: 8 mm; length: 80 mm). The extraction chromatography resin used was TEVA-Spec (Eichrom Industries). This resin consisted of methyloctyldidecylammonium ion sorbed on an inert polymeric support (Amberline XAD-7). A ready-to-use mini-column (diameter: 7 mm; length: 80 mm) packed with 2 ml of TEVA resin was applied for the analysis. Both resins, Dowex 1X8 and TEVA, retain only the tetravalent form of Pu quantitatively.

All reagents used were of analytical-reagent grade. Nitric acid used in the final solution for ICP-MS was of super-pure grade (AA-100, Tama Chemicals).

The certified reference materials analyzed were IAEA-135 (sediment from the Irish Sea),[28] IAEA-SOIL-6 (soil from Austria),[29] IAEA-368 (ocean sediment from Mururoa Atoll)[30] and IAEA-134 (fish flesh from the Irish Sea).[31] Two soil samples were collected from a forest in Ohmagari (Akita Prefecture, Japan) and from a rice paddy field in Hitachinaka (Ibaraki Prefecture, Japan). They were air-dried and sieved through a 1 mm sieve.

Sample pre-treatment

A known amount of ^{242}Pu (0.1–0.5 ml of a 0.2 ng ml^{-1} stock solution) was added to samples (2–50 g, depending on the concentration level) as a spike. The sample was ashed at 500 °C for 4–6 h in a muffle furnace to decompose organic matter. (If the sample amount is low, less than 5 g, the ashing procedure can be omitted.) The ashed sample was placed in a Pyrex beaker and 8 M HNO_3 (more than five times the sample weight) was added. The mixture was boiled on a hot-plate (180–200 °C) for at least 3 h. During heating, the beaker was covered with a watch-glass to prevent significant evaporation, and the sample was stirred occasionally with a glass rod. The warm supernatant (leachate) was filtered through a glass-fibre filter (Whatman GF/F). The residue in the beaker was boiled again with 8 M HNO_3 (about twice the sample volume) for about 20 min, then filtered. This leaching procedure was usually repeated twice. Samples with a large volume had to be centrifuged prior to filtration so that the procedure could be completed rapidly. The residue, as obtained after centrifugation, was again boiled with 8 M HNO_3 (about twice the sample volume), then filtered. This procedure was repeated twice.

All the filtrates were collected in a beaker, and heated on a hot-plate until a thick wet paste was obtained. (If the paste was completely dried, it could not easily be dissolved in HNO_3 in the following processes.) The wet paste was dissolved by adding HNO_3 while warming on the hot-plate. The sample solution was diluted with de-ionized water to adjust the acidity of the solution to 8 M HNO_3 (for Dowex 1X8) or 2 M HNO_3 (for TEVA). The solution volume should be maintained at 40–200 ml; the actual volume depended on the amount of sample. Any residue appearing was removed by filtration. In order to select an appropriate reagent for converting Pu to Pu(IV), which is the only retainable form in the chromatography columns (both for Dowex 1X8 and TEVA), $NaNO_2$ was added to the filtered leachate. (For comparison tests, reagents such as $NH_2OH{\cdot}HCl$ and H_2O_2 were also used instead of $NaNO_2$; see under Results and discussion.)

Separation by resins

Anion-exchange resin (Dowex 1X8). The sample solution (8 M HNO_3) was loaded onto a column containing 2 ml of Dowex 1X8 at a rate of <2 ml min^{-1}. The resin was washed with 8 M HNO_3 (40 ml), then with 10 M HCl (40 ml). Tetravalent Pu should be retained on the resin and most of the U and matrix elements should pass through the column. Finally, NH_4I (5%)–10 M HCl solution (40 ml, <2 ml min^{-1}) was added to reduce Pu(IV) to Pu(III). Since Pu(III) is not retained on the resin, Pu was eluted from the column. HNO_3 (4 ml) and $HClO_4$ (0.2 ml) were added to the eluate which was heated on a hot-plate to decompose any organic material (*e.g.*, fine resin particles) and to expel the excess of iodine. In order to remove iodine completely from the beaker, H_2O_2 (1 ml) was also added to convert iodide to I_2 and volatilize it. After the solution had been taken to dryness, the residue was dissolved in HNO_3.

Extraction chromatography (TEVA). The sample solution (2 M HNO_3) was loaded onto a column containing 2 ml of TEVA resin at a rate of <2 ml min^{-1}. The resin was washed with 2 M HNO_3 (40 ml), then with 9 M HCl (40 ml). Tetravalent Pu should be retained on the resin and most of the U and matrix elements should pass through the column. Finally, hydroquinone (0.1 M)–9 M HCl solution (40 ml, <2 ml min^{-1}) was added to reduce Pu(IV) to Pu(III) and to elute Pu from the column. The separation chemistry using TEVA was based on the procedure recommended in the information sheet provided by Eichrom Industries[32] for this resin. To the eluate, HNO_3 (4 ml) and $HClO_4$ (0.2 ml) were added and the solution was heated on a hot-plate to decompose any hydroquinone that remained. After the solution had been taken to dryness, the residue was dissolved in HNO_3.

Decontamination factor. The decontamination factor, defined as 'the number of atoms in the initial solution' divided by 'the number of atoms in the final solution', was determined for selected elements (U, Th, Ce, Zn, Fe, Mn, Ca, Al, Mg and Na) in solutions which were passed through the two different resins.

Determinations by ICP-MS

The sample solution separated by the above-mentioned procedure was adjusted to an acid concentration of 4% m/m HNO_3. The total volume of the final solution was usually 5 ml. As an internal standard, Bi was added (20 ng ml^{-1}) to the sample and standard solutions. (The concentration of Bi can be reduced, if necessary.) Concentrations of Pu and other elements were determined by ICP-MS using a quadrupole-type mass spectrometer (Yokogawa PMS-2000) with a conventional liquid nebulizer (Meinhard type). Measurement conditions are shown in Table 1. The total counting time was selected after due consideration of the isotope concentrations as follows: 50–100 s for ^{239}Pu, 100–200 s for ^{240}Pu, 20–40 s for ^{242}Pu, 1–5 s for other elements. From the results of isotopic ratios to the spike (^{242}Pu), concentrations of ^{239}Pu and ^{240}Pu were calculated (isotope dilution method). A Pu isotope standard solution (NIST SRM 947) with a known $^{240}Pu/^{239}Pu$ ratio was used to check the accuracy. The abundance sensitivity based on ^{238}U measurement (masses 237 and 238) was about 1×10^6. Mass bias per unit mass, as determined for a U standard (natural) and a Pu isotope standard solution (NIST SRM 947), was usually $<0.5\%$.

Results and discussion

Separation procedures

Chemical yields in the chromatographic separation. The major chemical forms of Pu extracted from the samples by HNO_3 on heating are expected to be the oxidized forms, Pu(VI) and/or Pu(V). Since both resins, Dowex 1X8 and TEVA, retain only tetravalent Pu quantitatively, the chemical species of Pu should be converted to Pu(IV) by adding appropriate reagents. Three reagents, $NaNO_2$, $NH_2OH{\cdot}HCl$ and H_2O_2, were examined. The results obtained for the chemical yields in the chromatographic separation by using these reagents are shown in Table 2. The highest chemical yields in the separation procedures were found by using $NaNO_2$, followed by $NH_2OH{\cdot}HCl$. Use of H_2O_2 led to a poor chemical yield, although this reagent is recommended for use in some literature.[33] From these results it was decided to use $NaNO_2$ (0.2 M) to convert Pu to Pu(IV) in the sample solution prior to loading it onto the columns.

Table 1 Instrumental parameters for ICP-MS

Plasma:	
Frequency/MHz	27.12
Rf power/kW	1.2
Argon flow/l min^{-1}:	
Plasma	14
Auxiliary	1.2
Carrier	0.83
Sampling distance/mm	4.8
Sampling uptake rate/ml min^{-1}	0.2
Data acquisition:	
Mode	Peak jumping mode
No. of points per peak	3
No. of sweeps	200–800
No. of replicates	3

Table 2 Chemical yields in the separation by using Dowex 1X8 and TEVA. Three reagents were compared for their ability to convert Pu to Pu(IV)[a]

Reagent added to the sample solution	Concentration/ M	Chemical yield (%)[b]	
		Dowex 1X8	TEVA
H_2O_2	0.05	62±8	19±6
H_2O_2	0.2	64±4	23±10
$NH_2OH{\cdot}HCl$	0.05	84±4	62±19
$NH_2OH{\cdot}HCl$	0.2	93±2	66±17
$NaNO_2$	0.05	93±5	86±11
$NaNO_2$	0.2	97±2	89±12

[a]Sample: forest soil from Akita. [b] ±: standard deviation of 2–3 samples.

Decontamination factors using two different resins. Total cation concentrations in the final solution for ICP-MS should be less than 1000 ppm (μg ml^{-1}) to avoid matrix suppression and/or interface cloaking. Therefore, it is necessary to reduce the element concentrations in the sample solution without losing the Pu content. In addition to the separation of major matrix elements, the element U should also be eliminated to avoid peak overlap on ^{239}Pu due to polyatomic ion production (uranium hydride ion: $^{238}UH^+$) and/or to the effect of up-mass tailing during the ICP-MS measurement. The results for the decontamination factors for ion-exchange chromatography (Dowex 1X8) and extraction chromatography (TEVA) obtained from soil samples [Akita-soil (Japan) and IAEA-SOIL-6 (Austria)] are shown in Fig. 1. Elements showing high concentrations in the initial solutions (soil leachates) were usually Fe (10^3–10^4 μg ml^{-1}) and Al, Mg, Na and Ca (10^2–10^3 μg ml^{-1}). In the final solution (after the separation procedures), the element showing the highest concentration was usually Na (up to 5 μg ml^{-1}) and the total concentrations of the measured cations were significantly less than 20 μg ml^{-1} with both resins. The decontamination factors for many elements (including U) were of the order of 10^4–10^5. Concentrations of U in the final solution were, in many cases, 0.04–0.2 ppb (0.4–2×10^{-4} μg ml^{-1}). These results indicated that the matrix elements and also U were successfully separated by both resins. Comparison of the two resins showed that the decontamination factor for U was better with Dowex 1X8 than with TEVA for the samples studied here.

The influence of U concentrations on ^{239}Pu determination by ICP-MS was assessed. A solution containing U (100 ng ml^{-1}) was used and the increase in the 239 mass peak was measured. During normal operation, the influence of U on mass 239 was about 3×10^{-5}. If it is assumed that the maximum U concentration in the final solution is 1 ppb

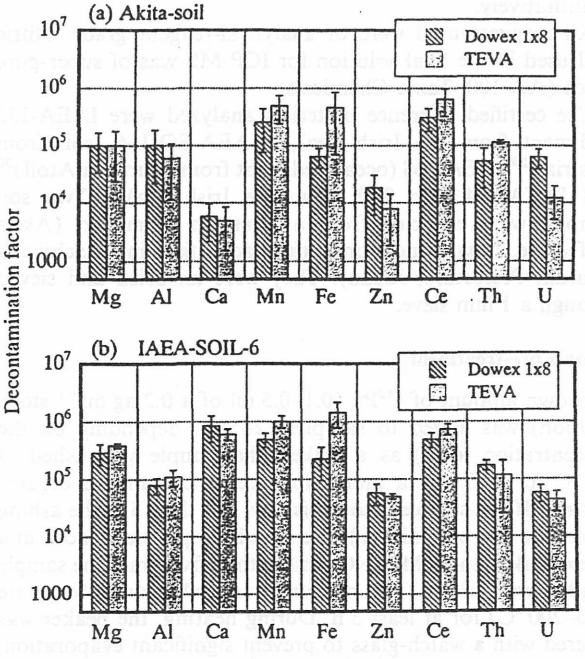

Fig. 1 Decontamination factors of selected elements with Dowex 1X8 and TEVA for (a) Akita-soil and (b) IAEA-SOIL-6. (Error bars: standard deviations of 2–5 separate runs.)

(ng ml^{-1}), the expected influence is calculated to be only about 0.03 pg ml^{-1}, which is almost the same as the detection limit. Because the U concentration in the final solution was usually much less than 1 ng ml^{-1}, there would be almost no effect due to U.

Using a sample (50 g) collected from a deeper soil layer, in which the Pu level should be very low, no Pu peaks (^{239}Pu, ^{240}Pu, ^{242}Pu) were found after the separation procedure, indicating that there were no influences due to blanks from the reagents used and from soil substances.

These results suggested that our separation procedure was appropriate and applicable to the determination of environmental levels of Pu.

Measurements by ICP-MS

The sample solution separated by the above-mentioned procedure was subjected to ICP-MS measurements of Pu. The measurement time for one sample was 10–20 min. For alpha-spectrometry, the counting time is normally 1–5 d. ICP-MS has a significant advantage in terms of analytical time.

The sensitivity, in counts per second per ng ml^{-1} of ^{242}Pu, was about 3×10^4 cps under normal operating conditions. Background counts on the mass were 2–4 cps. The detection limit, defined as three times the standard deviation of the blank solution (4% HNO_3), was about 0.02 pg ml^{-1} (ppt) Pu (or ^{239}Pu: 0.05 mBq ml^{-1}; ^{240}Pu: 0.17 mBq ml^{-1}) for a counting time of 100 s. Since the volume of the final solution was 5 ml, the absolute detection limit (in pg) was calculated to be about 0.1 pg. Using a 50 g sample, the concentration factor of Pu in the final solution (usually 5 ml) would be 10, which would result in detection limits of about 0.005 Bq kg^{-1} for ^{239}Pu and 0.017 Bq kg^{-1} for ^{240}Pu. In this study, Pu was measured by ICP-MS with a normal nebulizer. However, if other types of nebulizer such as ultrasonic or micro-concentric nebulizers or electrothermal vaporization were used, much better sensitivities might be obtained. Chiappini *et al.*[20] detected down to 35 fg of Pu in environmental samples by using a high-efficiency nebulizer system (Mistral) together with an improved interface pumping system.

The relative standard deviation (RSD) for three analyses of the same sample solution was usually 1–5% for a Pu concentration of >2 pg ml^{-1}. The RSD obtained from the measurements of the isotopic ratio to the spike (*i.e.*, ^{239}Pu/^{242}Pu and ^{240}Pu/^{242}Pu) was better than the above-mentioned value, *i.e.*, usually 0.5–2%. The ratios to ^{242}Pu were used and the concentrations of ^{239}Pu and ^{240}Pu in the samples were calculated on the basis of the isotope dilution method. These data indicated that the precision of the ICP-MS measurements was reasonable in the determination of Pu in environmental samples.

Analysis of certified reference materials

In order to validate the analytical method and to obtain data on the Pu isotopic composition, four international certified reference materials (2 sediments, 1 soil and 1 fish flesh) having recommended values for $^{239+240}$Pu (but no data on ^{240}Pu/^{239}Pu ratios) were analyzed. The analytical method finally used is summarized in Fig. 2. Results obtained for ^{239}Pu and ^{240}Pu in certified reference materials are shown in Tables 3–6, together with information on the resin types, chemical yields and sample weights. The ^{240}Pu/^{239}Pu atom ratios were also calculated and are also given in Tables 3–6.

Table 3 shows the results obtained for IAEA-135 (Irish Sea sediment). Only about 2 g of the sample were used because of its high Pu concentration due to contamination from the Sellafield nuclear facility. Six analyses were performed on this material: three analyses were by Dowex 1X8 and three were by TEVA. There were no significant differences between the analytical data obtained by the two resins. The sum of ^{239}Pu and ^{240}Pu concentrations ($^{239+240}$Pu) was calculated for comparison with the value recommended by the IAEA. Our analytical results for $^{239+240}$Pu (mean value: 210 ± 12 Bq kg^{-1}) agreed well with the recommended value (213 Bq kg^{-1}).[28] The ^{240}Pu/^{239}Pu atom ratio was calculated as 0.211 ± 0.004. Since there is no IAEA information on the ^{240}Pu/^{239}Pu ratio for the reference materials, it was not possible to make a comparison. Our value was comparable to the ratio (0.20) reported by Yamamoto *et al.*[19] in a sediment sample originating from the Sellafield area.

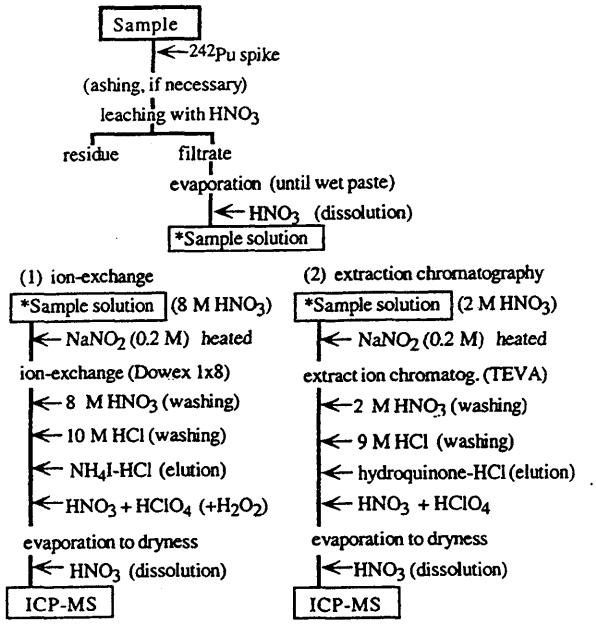

Fig. 2 Analytical procedures for the determination of Pu by ICP-MS: (1) separation procedure by ion-exchange (Dowex 1X8) and (2) separation procedure by extraction chromatography (TEVA).

Table 4 shows analytical results for IAEA-SOIL-6 (surface soil collected from Austria). The value obtained for the $^{239+240}$Pu concentration (1.00 ± 0.04 Bq kg^{-1}) agreed well with the recommended value (1.04 Bq kg^{-1}) given by the IAEA.[29] A comparison of the results obtained with Dowex 1X8 and with TEVA showed that there were no marked differences between the analytical results obtained. The mean ^{240}Pu/^{239}Pu atom ratio obtained for IAEA-SOIL-6 was 0.191 ± 0.005, which was comparable to the global fallout value of 0.176 ± 0.014 reported by Krey *et al.*[5]

Table 5 shows the results for IAEA-368 (ocean sediment from Mururoa Atoll). The mean $^{239+240}$Pu value of the eight analyses, 29.7 ± 3.0 Bq kg^{-1}, agreed with the recommended value (31 Bq kg^{-1}).[30] There were also no significant differences between the mean values obtained with Dowex 1X8 and TEVA. The standard deviation for the eight analyses was larger than that of the previous two samples (IAEA-135 and SOIL-6). This sample had a high calcium carbonate content and was derived from ocean sediments (coral rich) near a nuclear weapons test site. The homogeneity of the sample might not be as good as that of the other two samples. It was noted that the ^{240}Pu/^{239}Pu atom ratio obtained for IAEA-368 was very low, *i.e.*, 0.043 ± 0.008. This suggests that the Pu was derived from the testing of a Pu-bomb in which ^{239}Pu was enriched.

Table 6 shows the results for IAEA-134 (fish flesh from the Irish Sea). The mean value for the $^{239+240}$Pu concentration for the four analyses (15.4 ± 0.5 Bq kg^{-1}) agreed well with the IAEA recommended value (15 Bq kg^{-1}).[31] This indicated that the present method is also applicable to biological materials, which are ashed prior to analysis. The ^{240}Pu/^{239}Pu atom ratio

Table 3 Analytical results for ^{239}Pu, ^{240}Pu and their atom ratios in IAEA-135 (Irish Sea sediment)[a]

Resin	Sample weight/g	Yield (%)	^{239}Pu/ Bq kg^{-1}	^{249}Pu/ Bq kg^{-1}	$^{239+240}Pu$/ Bq kg^{-1}	$^{249}Pu/^{239}Pu$ (atom ratio)
Dowex 1X8	1.7	97	124±5	99±2	224±5	0.217±0.004
Dowex 1X8	2.2	94	111±8	86±5	197±9	0.212±0.002
Dowex 1X8	2.2	82	114±6	88±6	201±8	0.210±0.005
TEVA	1.7	53	120±3	91±2	210±4	0.207±0.004
TEVA	2.2	72	114±5	87±5	201±7	0.209±0.006
TEVA	2.2	80	126±6	98±4	224±7	0.213±0.004
Mean (Dowex)		91	116±8	91±6	208±13	0.213±0.004
Mean (TEVA)		68	120±6	92±6	212±11	0.210±0.003
Mean (total)		80	118±7	92±6	210±12	0.211±0.004
IAEA recommended					213	

[a] ±: standard deviation.

Table 4 Analytical results for ^{239}Pu, ^{240}Pu and their atom ratios in IAEA-SOIL-6 (Austrian soil)[a]

Resin	Sample weight/g	Yield (%)	^{239}Pu/ Bq kg^{-1}	^{240}Pu/ Bq kg^{-1}	$^{239+240}Pu$/ Bq kg^{-1}	$^{240}Pu/^{239}Pu$ (atom ratio)
Dowex 1X8	25	90	0.58±0.01	0.41±0.02	0.99±0.02	0.196±0.004
Dowex 1X8	25	89	0.56±0.02	0.40±0.01	0.96±0.02	0.192±0.002
Dowex 1X8	50	87	0.58±0.03	0.40±0.02	0.98±0.03	0.190±0.006
Dowex 1X8	50	92	0.59±0.02	0.41±0.01	1.00±0.02	0.186±0.004
TEVA	25	69	0.62±0.02	0.46±0.03	1.08±0.03	0.198±0.006
TEVA	25	69	0.58±0.02	0.39±0.01	0.97±0.02	0.184±0.006
Mean (Dowex)		89	0.58±0.01	0.41±0.01	0.98±0.02	0.191±0.004
Mean (TEVA)		69	0.60±0.03	0.43±0.05	1.03±0.06	0.191±0.010
Mean (total)		83	0.59±0.02	0.41±0.03	1.00±0.04	0.191±0.005
IAEA recommended					1.04[b]	

[a] ±: standard deviation. [b]The IAEA recommended value was originally described as 28 pCi (or 1.04 Bq kg^{-1}) for '^{239}Pu' on the information sheet and related publication (IAEA 1984). However, we confirmed with IAEA that the value should be for '$^{239+240}Pu$'.

Table 5 Analytical results for ^{239}Pu, ^{240}Pu and their atom ratios in IAEA-368 (Ocean sediment, Mururoa Atoll)[a]

Resin	Sample weight/g	Yield (%)	^{239}Pu/ Bq kg^{-1}	^{240}Pu/ Bq kg^{-1}	$^{239+240}Pu$/ Bq kg^{-1}	$^{240}Pu/^{239}Pu$ (atom ratio)
Dowex 1X8	5.4	86	27.3±0.9	3.7±0.1	31.0±0.9	0.037±0.002
Dowex 1X8	5.4	54	28.3±1.1	5.5±0.2	33.8±1.1	0.053±0.001
Dowex 1X8	5.0	92	23.9±0.6	3.4±0.1	27.3±0.6	0.039±0.001
Dowex 1X8	5.0	88	21.8±0.6	3.3±0.1	25.1±0.6	0.042±0.001
Dowex 1X8	5.0	93	27.6±0.8	3.9±0.1	31.5±0.9	0.039±0.002
Dowex 1X8	5.0	86	28.4±0.9	3.9±0.1	32.3±0.9	0.038±0.001
TEVA	5.4	46	26.4±0.7	3.4±0.2	29.7±0.7	0.036±0.002
TEVA	5.4	47	22.1±0.6	4.5±0.2	26.6±0.6	0.056±0.002
Mean (Dowex)		83	26.2±2.7	4.0±0.8	30.2±3.3	0.041±0.006
Mean (TEVA)		47	24.3±3.1	4.0±0.8	28.2±2.2	0.046±0.014
Mean (Total)		74	25.7±2.7	4.0±0.7	29.7±3.0	0.043±0.008
IAEA recommended					31	

[a] ±: standard deviation.

Table 6 Analytical results for ^{239}Pu, ^{240}Pu and their atom ratios in IAEA-134 (fish flesh, Irish Sea)[a]

Resin	Sample weight/g	Yield (%)	^{239}Pu/ Bq kg^{-1}	^{240}Pu/ Bq kg^{-1}	$^{239+240}Pu$/ Bq kg^{-1}	$^{240}Pu/^{239}Pu$ (atom ratio)
Dowex 1X8	5	69	9.6±0.3	6.5±0.1	16.1±0.3	0.185±0.009
Dowex 1X8	5	96	8.6±0.2	6.4±0.2	15.0±0.3	0.203±0.003
Dowex 1X8	10	87	8.6±0.1	6.5±0.2	15.1±0.2	0.204±0.004
Dowex 1X8	10	89	8.7±0.2	6.6±0.2	15.3±0.3	0.207±0.006
Mean (Dowex)		85	8.9±0.5	6.5±0.1	15.4±0.5	0.200±0.010
IAEA recommended					15	

[a] ±: standard deviation.

for this material was 0.200±0.010. This value was almost the same as the ratio obtained for the Irish Sea sediment sample (IAEA-135), suggesting that the origin of the contamination was the same.

As mentioned above, good agreements were found between the present results for $^{239+240}Pu$ concentrations in the certified reference materials and the recommended values. This indicated that the accuracy of the method was reasonable and also suggested that Pu in the sample was almost completely extracted from the matrix by boiling the sample with HNO_3 for at least 3 h. However, further tests on the extraction procedure for other matrices might be necessary to confirm

the applicability of the method to a variety of samples and Pu forms.

A comparison of the two resins showed that the chemical yields using Dowex 1X8 (24 analyses) were 54–99% (mean: 89%) and using TEVA (eight analyses) 46–80% (mean: 64%). The decontamination factor for U with Dowex 1X8 was also better than that with TEVA. The concentrations of HNO_3 used in the column separation were 2 M for TEVA and 8 M for Dowex 1X8; hence, if it is desirable to reduce acid consumption, the method using TEVA is more appropriate. However, the solubility of Pu should be better in concentrated acid (*i.e.*, 8 M). Samples with certain matrices (*e.g.*, high Fe, Mn, Ce) might be effective for TEVA.

Application of the method to the analysis of common soil

The method was applied to the determination of Pu in soil samples in ordinary natural environments. Samples were collected from a forest in Akita Prefecture and from a rice paddy field in Ibaraki Prefecture. The results are shown in Table 7. For the Akita-soil, six analyses were performed. The mean value of the $^{239+240}Pu$ concentration for this sample was 1.37 ± 0.04 Bq kg^{-1}. The RSD (*i.e.*, precision) of the six determinations was about 3%. The concentration of $^{239+240}Pu$ in the rice field soil from Ibaraki was 0.39 ± 0.01 Bq kg^{-1}, which was markedly lower than that in the forest soil from Akita. The $^{240}Pu/^{239}Pu$ ratios in the Akita-soil (0.168 ± 0.06) and Ibaraki-soil (0.171 ± 0.03) were almost identical and were comparable to the global fallout value[5] mentioned above.

Comparison with other methods

Compared with alpha-spectrometry, the present method using ICP-MS has significant advantages in the determination of the Pu isotopic composition (*i.e.*, $^{240}Pu/^{239}Pu$ ratio). The separation procedure for ICP-MS is fairly simple and the analytical time is considerably shorter than for the method using the alpha-spectrometer. For example, the presence of iron and lanthanides resulted in thick deposits which gave poor resolution of alpha spectra.[1] Incomplete chemical separation of a nuclide having a similar alpha energy (*e.g.*, U, Th) interferes with the measurements. More time is also necessary for the electrodeposition procedure and measurement with an alpha-counter. A typical detection limit by alpha-spectrometry with a 4000 min counting time is of the order of 10^{-4} Bq,[20] which corresponds to about 0.05 pg of ^{239}Pu. This value is similar to the detection limit by ICP-MS with a conventional nebulizer obtained in this study. If another type of nebulizer were used, as mentioned above, the detection limit should be improved. If high resolution ICP-MS (HR-ICP-MS), which is known to have a higher mass resolution and better detection limits for many elements,[34] were used, a better sensitivity for Pu would also be expected. For the TIMS method, the separation procedure is also critical to achieve a precise analysis, *i.e.*, the separation procedure by column chromatography should be repeated 2 or 3 times to separate Pu as cleanly as possible. For ICP-MS, the chemical separation required is not so severe in comparison with the procedures for alpha-spectrometry and TIMS. This method has the advantages of simple separation chemistry, shorter analytical time, lower costs and easier operation. However, the detection limit and precision of the isotopic measurement are better in the TIMS method.

Conclusion

From the above-mentioned results for the certified reference materials and also field samples, it was found that the use of ICP-MS after a chemical separation with Dowex 1X8 or TEVA is applicable to the determination of both ^{239}Pu and ^{240}Pu in environmental samples. Compared with alpha-spectrometry, the ICP-MS method has significant advantages in terms of its simple analytical procedures, prompt measurement time and capability of determining the $^{240}Pu/^{239}Pu$ ratio.

Because there are almost no data on the $^{240}Pu/^{239}Pu$ ratios in the certified reference materials, the analytical results obtained for IAEA-135 (0.211), IAEA-SOIL-6 (0.191), IAEA-368 (0.043) and IAEA-134 (0.200) may contribute to the acquisition of information on the isotopic compositions of Pu in these materials. The determination of the $^{240}Pu/^{239}Pu$ ratio is important in understanding the source of the contamination.

Acknowledgements

We thank Professor M. Yamamoto (Kanazawa University) for his valuable comments on the separation chemistry and Dr. Y. Igarashi (Meteorological Research Institute) for his advice on the use of ICP-MS in the determination of long-lived nuclides. We also thank Dr. K. Gunji (JAERI) and Dr. M. Yamada (NIRS) for their useful comments on Pu standards, Mr. Y. Ito and Mr. H. Sato (NIRS) for their help in

Table 7 Analytical results for ^{239}Pu, ^{240}Pu and their atom ratios in soil samples collected in Japan[a]

(A) *Forest soil from Ohmagari/Akita (O-41)*—

Resin	Sample weight/g	Yield (%)	^{239}Pu/ Bq kg^{-1}	^{240}Pu/ Bq kg^{-1}	$^{239+240}Pu$/ Bq kg^{-1}	$^{240}Pu/^{239}Pu$ (atom ratio)
Dowex 1X8	24	97	0.82 ± 0.06	0.51 ± 0.04	1.33 ± 0.07	0.170 ± 0.009
Dowex 1X8	24	96	0.83 ± 0.04	0.53 ± 0.03	1.36 ± 0.05	0.174 ± 0.002
Dowex 1X8	24	92	0.83 ± 0.05	0.52 ± 0.02	1.34 ± 0.05	0.170 ± 0.003
Dowex 1X8	24	96	0.83 ± 0.04	0.52 ± 0.05	1.36 ± 0.06	0.172 ± 0.005
Dowex 1X8	50	99	0.86 ± 0.08	0.50 ± 0.02	1.36 ± 0.08	0.157 ± 0.008
TEVA	24	75	0.89 ± 0.02	0.54 ± 0.02	1.44 ± 0.03	0.166 ± 0.005
Mean (Dowex)		96	0.83 ± 0.02	0.52 ± 0.01	1.35 ± 0.01	0.169 ± 0.007
Mean (total)		93	0.84 ± 0.03	0.52 ± 0.01	1.37 ± 0.04	0.168 ± 0.006

(B) *Paddy soil from Hitachinaka/Ibaraki (P-53)*—

Resin	Sample weight/g	Yield (%)	^{239}Pu/ Bq kg^{-1}	^{240}Pu/ Bq kg^{-1}	$^{239+240}Pu$/ Bq kg^{-1}	$^{240}Pu/^{239}Pu$ (atom ratio)
Dowex 1X8	50	95	0.24 ± 0.01	0.16 ± 0.01	0.40 ± 0.01	0.173 ± 0.003
Dowex 1X8	50	93	0.23 ± 0.00	0.15 ± 0.01	0.38 ± 0.01	0.169 ± 0.005
Mean (total)	50	94	0.24 ± 0.01	0.16 ± 0.01	0.39 ± 0.01	0.171 ± 0.003

[a] ±: standard deviation.

obtaining authorization for the use of Pu isotopes for the analysis, and Mr. A. Tanaka (Kaken Co.) and Ms. K. Ebine for their technical assistance.

References

1 R. J. Pentreath, *Appl. Radiat. Isot.*, 1995, **46**, 1279.
2 A. C. Chamberlain, *Sci. Total Environ.*, 1987, **63**, 139.
3 A. Aarkrog, H. Dahlgaard, S. P. Nielsen, A. V. Trapeznikov, I. V. Molchanova, V. N. Pozolotina, E. N. Karavaeva, P. I. Yushkov and G. G. Polikarpov, *Sci. Total Environ.*, 1997, **201**, 137.
4 D. Lux, L. Kammerer, W. Rühm and E. Wirth, *Sci. Total Environ.*, 1995, **173/174**, 375.
5 P. W. Krey, E. P. Hardy, C. Pachucki, F. Rourke, J. Coluzza and W. K. Benson, *Proceedings of a Symposium on Transuranium Nuclides in the Environment*, IAEA-SM-199-39, 1976, pp. 671–678.
6 M. Koide, K. K. Bertine, T. J. Chow and E. D. Goldberg, *Earth Planet. Sci. Lett.*, 1985, **72**, 1.
7 IAEA, *Survey of Reference Materials*, IAEA-TECDOC-854, IAEA, Vienna, 1995, vol. 1.
8 K. Bunzl, W. Kracke and W. Schimmack, *Analyst*, 1992, **117**, 469.
9 M. Yamamoto, S. Igarashi, K. Chatani, K. Komura and K. Ueno, *J. Radioanal. Nucl. Chem.*, 1990, **138**, 365.
10 A. Kudo, Y. Mahara, D. C. Santry, T. Suzuki, S. Miyahara, M. Sugahara, J. Zheng and J.-P. Garrec, *Appl. Radiat. Isot.*, 1995, **46**, 1089.
11 M. Sakanoue and T. Tsuji, *Nature (London)*, 1971, **234**, 92.
12 F. D. Hindman, *Anal. Chem.*, 1986, **58**, 1238.
13 K. Komura, M. Sakanoue and M. Yamamoto, *Health Phys.*, 1984, **46**, 1213.
14 A. R. Moorthy, C. J. Schopfer and S. Banerjee, *Anal. Chem.*, 1988, **60**, 857A.
15 C. K. Kim, Y. Oura, Y. Takaku, H. Nitta, Y. Igarashi and N. Ikeda, *J. Radioanal. Nucl. Chem. Lett.*, 1989, **136**, 353.
16 W. McCarthy and T. M. Nicholls, *J. Environ. Radioact.*, 1990, **12**, 1.
17 K. O. Buesseler and J. E. Halverson, *J. Environ. Radioact.*, 1987, **5**, 425.
18 J. S. Crain, L. L. Smith, J. S. Yaeger and J. A. Alvarado, *J. Radioanal. Nucl. Chem., Articles*, 1995, **194**, 133.
19 M. Yamamoto, A. Tsumura, Y. Katayama and T. Tsukatani, *Radiochim. Acta*, 1996, **72**, 209.
20 R. Chiappini, J. M. Taillade and S. Brébion, *J. Anal. At. Spectrom.*, 1996, **11**, 497.
21 R. Chiappini, J. M. Taillade and F. Pointurier, in *ESARDA Proceedings, 25–27 Feb. 1997, Geel, Belgium*, pp. 129–137.
22 Y. Igarashi, C. K. Kim, Y. Takaku, K. Shiraishi, M. Yamamoto and N. Ikeda, *Anal. Sci.*, 1990, **6**, 157.
23 S. Yoshida, Y. Muramatsu, K. Tagami and S. Uchida, *Int. J. Environ. Anal. Chem.*, 1996, **63**, 195.
24 K. G. Heumann, S. M. Gallus, G. Rädinger and J. Vogl, *J. Anal. At. Spectrom.*, 1998, **13**, 1001.
25 E. P. Horwitz, R. Chiarizia, M. L. Dietz, H. Diamond and D. M. Nelson, *Anal. Chim. Acta*, 1993, **281**, 361.
26 L. L. Smith, J. S. Crain, J. S. Yaeger, E. P. Horwitz, H. Diamond and R. Chiarizia, *J. Radioanal. Nucl. Chem., Articles*, 1995, **194**, 151.
27 K. Bunzl and W. Kracke, *J. Radioanal. Nucl. Chem., Lett.*, 1994, **186**, 401.
28 IAEA, *Report on the Intercomparison Run IAEA-135*, IAEA/AL/063, IAEA, Vienna, 1993.
29 IAEA, *Report on the Intercomparison Run IAEA-SOIL-6*, IAEA/RL/111, IAEA, Vienna, 1984.
30 IAEA, *Report on the Intercomparison Run IAEA-368*, IAEA/AL/047, IAEA, Vienna, 1991.
31 IAEA, *Report on the Intercomparison Run IAEA-134*, IAEA/AL/062, IAEA, Vienna, 1993.
32 Eichrom Industries, *Extraction Chromatographic Material for Rapid Separation of Tetravalent Actinides*, Information Sheet on TEVA-Spec, Eichrom Industries, Darien, IL, 1996.
33 Japan Chemical Analysis Center, *Analysis of Pu* (in Japanese), *Radioactivity Measurement Series No. 12*, Science and Technology Agency Japan, Tokyo, Japan, 1991, p. 73.
34 S. Yamazaki, A. Tsumura and Y. Takaku, *Microchem. J.*, 1994, **49**, 305.

Paper 9/00071B

宇宙と地球の放射線環境
－その未来予測への挑戦－

人間活動と地球放射線環境

中　村　裕　二
なかむら　ゆうじ

編集部
筆者：放射線医学総合研究所第4研究グループ
総合研究官

人類が受ける放射線の主たるものは，宇宙線，自然放射性核種など地球環境自体に由来する．しかし，原子力利用，医療用放射線利用など，人間活動がもたらす新たな放射線場も増加している．

1. はじめに

地球の放射線環境を作り出している放射線はそのsourceから見ると，

a. 宇宙線（太陽からの紫外線も含む）
b. 自然・人工放射性核種からの放射線
c. 人為的に作り出される放射線

に大別される．一方，人の放射線被曝の場という側面からは，

1）人間の活動に依存しない放射線場
a. 宇宙線場（主に陽子，中性子）
b. 宇宙線誘導放射性核種による線源場
：内部被ばく・外部被ばく
c. 自然放射性核種による線源場
：内部被ばく・外部被ばく
2）人間活動に由来する放射線場
a. 人為的に作り出される放射線場
・医療放射線
・核技術による放射線
・原子力利用に伴う放射性核種
：内部被ばく・外部被ばく
b. 人為的に高められた自然放射線場

に分類される．

これらの放射線場，放射線環境が現在どのような大きさであるか，また人間活動に伴いどのように変化してきたか，また今後どのような変化が予想されるか概観してみる．

2. 現在の放射線環境

2-1. 自然放射線の線量

自然放射線による成人一人当たりの実効線量は，世界平均で年間約2.4mSvと推定される（表1）．このうち約1.1mSvは，宇宙線，地殻γ線，人体内の放射性核種（^{40}K等）に由来するものである．また約1.3mSvはラドン及びその崩壊生成核種による寄与である．

表1　自然放射線による成人の年間実効線量.

線源	年間実効線量 (mSv) 平均値	高い値
宇宙線	0.39	2.0
地殻起源のγ線	0.46	4.3
体内放射性核種	0.22	0.6
ラドン及び崩壊生成物	1.3	10

(UNSCEAR1993年報告から)[1]

宇宙線による寄与は，人が居住する緯度・高度により変動し，また地殻γ線寄与は地質による自然放射性核種の量によって変動する．また，自然放射性核種の体内量は食習慣に依存し，ラドンによる寄与は居住地域の地質とともに，家屋の材質・構造に強く依存している．このため自然放射線による線量は，局所的に変動することになる．

2-2. 人工放射線の線量

1) 医療被ばく

医療に伴う放射線被ばくは，診断・治療を受ける患者と非患者，国ごとの医療レベルによって大きく異なっている．放射線治療による被ばく線量は，患者一人当たりでは診断に係わる放射線被ばく線量に比べ遙かに大きいが，患者数が少ないため平均的被ばく線量としての寄与は小さい．表2に，先進工業国（レベルI）における医療放射線

表2　医療放射線被ばく線量の年平均推定値 (診断).

	平均年実効線量 (mSv) レベルI	平均値	レベルII, III	世界平均値
X線診断	0.3～2.2	1.0	0.02～0.2	0.3
放射性薬剤		0.09		0.03
全放射線診断		1.1		0.3

(UNSCEAR1993年報告から)[1]

表3　原子力発電から公衆への被ばく線量寄与.

線源 (行為) 地球規模成分	寄与 (%)
採鉱・精錬	75
原子炉運転・廃棄物処理	0.25
再処理・個体廃棄物	25
処分による地球規模拡散	
合計	100 (0.00015mSv)

(UNSCEAR1993年報告から)[1]

(診断) 被ばく線量の推定値を示す．

医療放射線被ばくは，人工放射線源からの被ばくのうち最も大きな線量寄与を与えるものである．

2) 原子力利用に伴う放射線被ばく

原子力利用に伴う放射線被ばくの主たるものは，i) 大気圏内核実験と核兵器製造及び，ii) 原

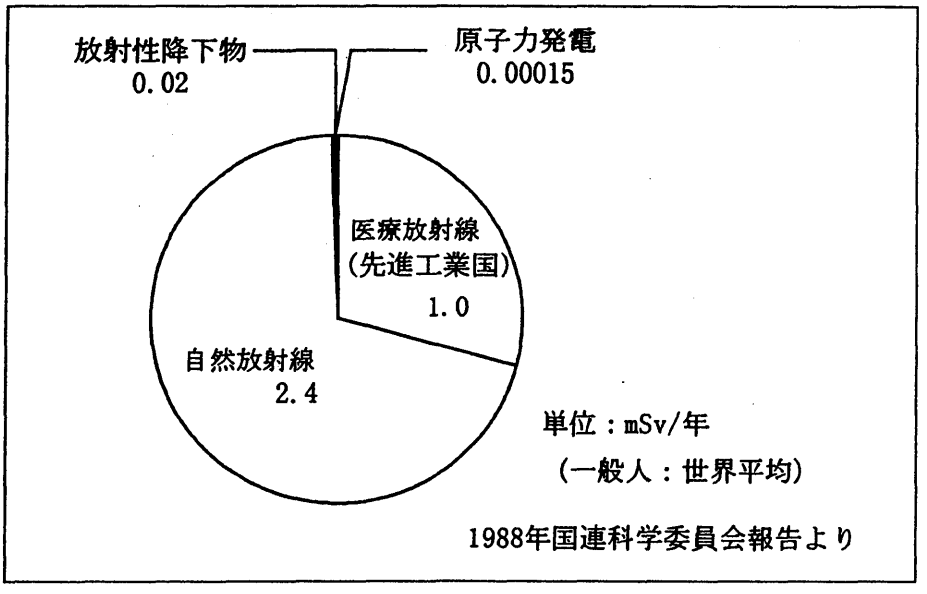

図1　平均年実効線量.

子力発電からの被ばくである．

現在では大気圏内核実験は行われておらず，フォールアウトの量も過去に比べ低下している．しかし実験開始以来，2200年までに世界全人口に与えられる平均線量は，約1.4mSvと見積もられている．この積算線量（預託）は，年平均線量にすると約0.02mSvに対応する．

一方，原子力発電に伴う放射線被ばくは，採鉱・精錬－燃料製造－原子炉運転－廃棄物処理等様々のプロセスで発生する．原子力利用に伴う放射線被ばくは，事故等の突発的事象の危険性のため，広く懸念されることが多い．しかし，このリスクは，潜在的リスクであり，その線量寄与そのものは極めて小さく，世界平均で年間約0.00015mSv程度と見積もられている．表3に，原子力発電に伴う被ばく線量寄与を示す．

図1に，自然放射線・人工放射線源からの年実効線量寄与を示す．

3. 放射線環境の変遷

前節のように，人間を取り巻く放射線場（環境）は，当然の事ながら自然放射線の寄与が最も大きい．人間の活動が与える影響は，極近年になってからである．

3-1. 放射線技術利用以前

人類が，放射線あるいは核技術を獲得する以前においては，人類を取り巻く放射線場は，宇宙線と自然放射性核種による放射線場のみである．これらの放射線源のうち，地殻に含まれる放射性核種の量は人類の歴史程度の時間では，大きな変動はない．宇宙線強度の時間変化に関しても，大きな宇宙線強度の変動は認められていないが，地球磁場の変動などによる宇宙線強度の変動が指摘されている．宇宙線強度の変動の可能性を示す1，2の例を示す．

図2は，レースベックらによる海洋堆積物中のBe-10のプロファイル[2]である．Be-10は，高エネルギー宇宙線による大気中の酸素及び窒素の核破砕反応で生成される．通常，大気中の放射能モニタリング等で検出されるBe-7と似た生成過程により，定常的に生成されている．この核種は，半減期が長く通常の放射能測定では検出が困難であるが，加速器質量分析法などによって測定されている．この実験では，ほぼ1500万年にわたり比較的一定のBe-10降下量が得られている．即ち，過去1500万年にわたっては，それほど大きな宇宙線強度変動は認められない．しかし，著者らは，1500万年以前には降下量即ち生成量が大きかった可能性があると推論している．最も，1500万年前では，人類発生以前ということになる．

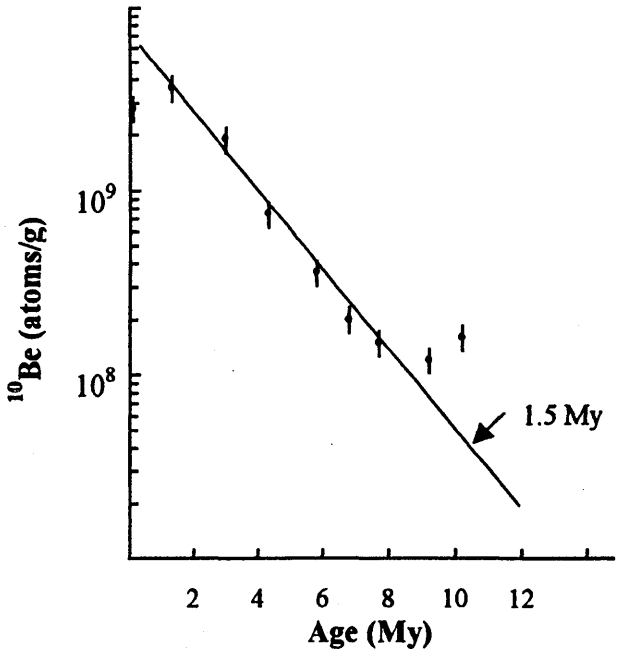

図2　海洋堆積物中の^{10}Be濃度分布．

一方，より最近にBe-10降下量の異常が認められた例もある．図3は，氷中のBe-10濃度[3]を示す．上が試料中のBe-10濃度，下は酸素同位体比であり，相互に良く同期していることがわかる．酸素同位体比の変動は，平均気温（海水温）の変化による同位体効果を示す．つまり，この同期性は，氷の堆積速度（平均気温）の違い即ち氷期と間氷期を示している．ところが，36,000年ほど前に，Be-10濃度異常が認められる．この原因については，一時的な堆積（氷積）速度の違いという解釈もなされているが，Be-10の生成速度が上昇した可能性も指摘される．この原因の一つに「地

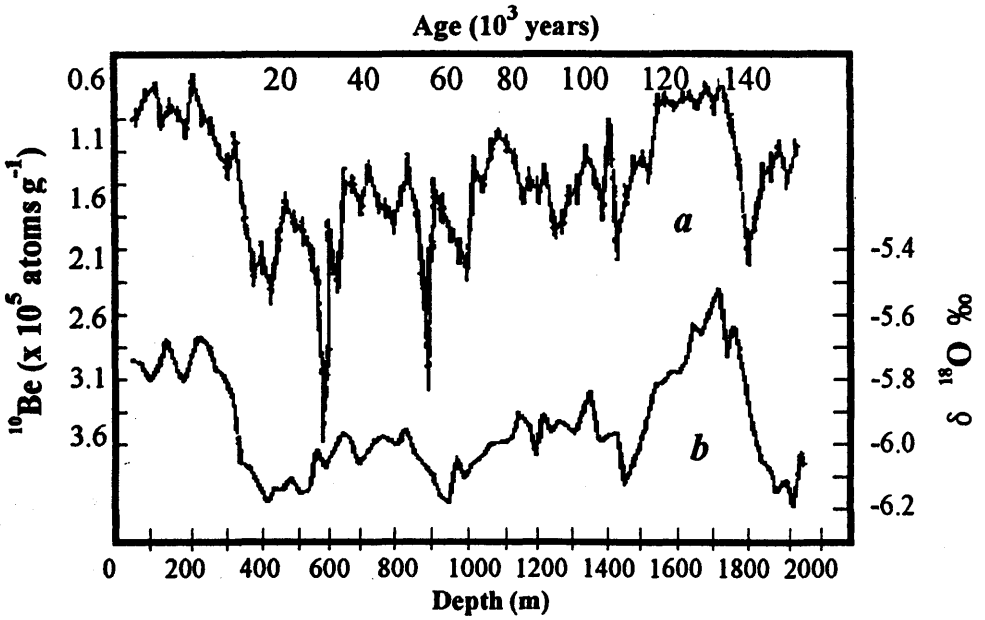

図3　氷柱中の^{10}Be濃度と酸素同位体比の変化.

球近傍でのSuper-Nova」の可能性が論じられている．もしそうであるなら，地球上での宇宙線強度が2～3倍に上昇した可能性を示すものといえよう．

Enhanced radiation（高められた自然放射線場）の1例が，「鉱山労働者の肺癌問題」である．これは，鉱山労働という閉鎖された場で，空気中のラドン濃度が高められる事により，高濃度ラドンの吸入による発癌の発生の例である．

しかしながら，おしなべて見ると核技術時代以前には，非常な高地に住む集団や特殊な地中活動をする集団という極限られた集団以外，地球上の放射線環境は当然の事ながら，かなり定常的であったと考えられる．

3-2. 核技術時代の放射線環境

1）医療被曝

X線の発見以来，人間は放射線を利用することを始めまた．放射線の医学利用は，急速に普及しそれとともに，放射線障害も発生している（表4）．現在では，これらの障害発生の経験から放射線発生装置の改良が進み，被ばく線量は以前に比べ低下している．

前節で述べたように，一人当たりの平均的な医療被ばく線量は，年平均1mSvと評価されています．これは，自然放射線被曝の1/2程度であり，

表4　放射線障害の歴史.

1895年	Roentgen	X線の発見
1896年	Grubbe	X線管の製作とX線の実験
		手の皮膚炎：手指の一部切断
	Edison	X線透視実験：眼痛
	Daniel	X線による頭髪の脱毛
1902年		X線による発癌報告（慢性潰瘍）
その他，		放射線の精巣への影響（Albers-Schonberg）
		小児の甲状腺癌（放射線による胸腺治療）
		ショウジョウバエを用いた放射線による突然変異発生の確認

他の人工放射線源（原子炉事故等の特別な被ばくを除いて）より大きい．医療被ばくは，直接的なbenefitを伴っており，また診断・治療を受ける特定個人の被ばくという側面を持っているため，他の放射線源と同様には論じられないが，前述したレベルIの国について放射線場としての一応の評価をしてみよう．

X線検査においては，上部消化管（平均実効線量：7.2mSv），血管造影（同：6.8mSv），CT撮影（4.3mSv），下部消化管（4.1mSv）等が高く，これに対してより一般的に行われる胸部直接撮影（0.25mSv）や，同間接撮影（0.52mSv）などは従来に比べ，かなり低減されている．

2）人工的に高められた自然放射線被ばく

放射線，核エネルギーの利用は，人をとりまく放射線環境を大きく変化させた．これらの人間活動はいずれも，本来の地球環境には存在していない新たな放射線場を作りだし，個々の特異な集団における放射線場の変化にとどまらず，人類全体の放射線被ばく線量の増大，あるいは増大の可能性（潜在的被ばく）をもたらしている．また，活動域の拡大（高地・極地の居住，大気圏航行，地下深部利用など）は，自然放射線場を高めている．

人間活動による放射線環境で，医療放射線とともに重要な要素は原子力利用による放射線場である．この放射線場は，前述したように線量寄与としては極めて小さいが，原子力施設における事故等に見られるように，潜在的かつ極めて局所的には高い放射線場を作り出しうる可能性をもっている．また，鉱工業における放射線利用，核技術利用による放射線場等もあるが，極めて限られた空間・対象（人）に対する放射線場であり，一般公衆に対する放射線場としての寄与は小さい．

このような放射線場以外に，人間活動に伴って人為的に高められた自然放射線場がある．

エネルギー生産における石炭・石油・天然ガス・地熱等の利用に伴う放射線場・被ばく線量寄与は，原子力発電による線量寄与のそれぞれ10，0.25，0.015，1％程度と評価されている．

また，航空機の利用がより一般的になるとともに，一般公衆の宇宙線被ばく線量の増加も起こっている．大気圏内飛行に伴う宇宙線被ばくは，飛行高度・コース・時間により様々である（表5）．

表5　大気圏飛行による宇宙線被ばく線量推定値．

宇宙線	約380μ Sv/年	
航空機	2.8μ Sv/h	平均1人当たり2μ Sv 北米で10μ Sv
超音速機(15kmH)	平均10μ Sv/h	最大40μ Sv/h

3-3．将来の地球放射線環境

地球規模での放射線環境は，本質的には自然放射線場である．この自然放射線場自体は今後相当長期間にわたって定常的であろうと予想される．これに比して，人間活動が与える放射線場は，極めて局所的であろう．原子力利用は，局所的に人間生活に壊滅的な打撃をもたらすほどの放射線環境を作り出す可能性が潜んでおり，十分な防御措置を講じる必要がある事は当然である．しかしながら平常的には，地球規模で見ると必ずしも大きな線量寄与は寄与を与えない．

むしろ今後の放射線場の変化は，生活空間の拡大によって引き起こされるであろう．大気圏外活動が目前となっている現在，人はこれまで経験していない高エネルギー粒子の空間に出ていくことになる．宇宙線場については，本号の他の記事を参照してほしい．

また，将来行われるであろう大深度地下利用に伴う地殻γ線・ラドン等による被ばく線量増加の可能性は，宇宙線被ばくの減少を伴っており，必ずしも放射線環境の増加をもたらすとは限らない．

地球規模での放射線環境の変化は，産業活動に由来する環境破壊がもたらすであろう．事実，オゾン層破壊に伴う紫外線強度の増大は確実に進行しており，放射線（非電離放射線）環境の増大をもたらすであろう．非電離放射線の生物影響に関しては，未だ不明な点も残されている．今後の研究が必要である．

参考文献

[1] UNSCEAR 1993年報告書：放射線の線源と影響．放射線医学総合研究所監修．実業広報社 (1995).

[2] G. M. Raisbeck and F. Yiou : Production of long-lived cosmogenic nuclei and their applications. Nucl. Instr. Methods in Phys. Res., **B5**, 91-99 (1984).

[3] G. M. Raisbeck *et al.* : Evidence for two intervals of enhanced ^{10}Be deposition in Antarctic ice during the last glacial period. Nature, **376**, 273-277 (1987).

保健物理，33(2)，232～237（1998）

話　題

先端技術に由来する有害物質の比較影響評価に関するワークショップ

中　村　裕　二[*1]

1. はじめに

近年の科学技術の進展とともに，従来自然環境中にはない，あるいは極めてまれにしか存在しない様々の物質が，自然環境中に負荷される可能性が増大している。エネルギー産業から放出される各種の放射性物質による人・生態系への影響に関する研究は，これまで多くの成果を上げてきた。放射線による影響では，その負荷量(dose)概念が比較的明瞭であり，因果関係解析が有効に機能してきた。しかしながら人・生態系へ影響を及ぼす環境負荷因子は，放射性物質だけではない。むしろ，人の健康や自然環境の保全という観点からは，これまで自然界には存在しなかった化学物質や，自然界に存在するものの局在化により極度に濃縮された重金属等，様々の環境負荷因子の影響を適切に評価する必要がある。

放射線医学総合研究所は，日本保健物理学会，日本放射線影響学会の共催の下，科学技術庁及び科学技術国際交流センターの後援をうけ，平成10年1月28日から30日までの3日間にわたり幕張プリンスホテル・プリンスホールにおいて，「先端技術に由来する有害物質の比較影響評価に関する国際ワークショップ」を開催した。このワークショップは，エネルギー生産及び先端科学技術の発展に伴って排出される様々な有害因子(放射性物質，重金属，レアーメタル等）に関して，環境中での分布や挙動（環境研究），人及び生物への影響（毒性学的研究），生態系への影響（生態学研究）において先導的な研究を行っている研究者を一堂に会し，境界領域を含めた総合研究への発展，将来展望について議論することを目的としたものである。

2. 国際ワークショップ

ワークショップでは，佐々木康人放射線医学総合研究所所長による開会挨拶に引き続き，国外から招聘した7名及び国内から招聘した14名，計21名の専門家による講演が行われた。ワークショップのプログラムを第1表に示す。

（基調講演及び特別講演）

ワークショップ初日には，ウクライナから招聘したG.G. POLIKARPOV教授及び大阪大学医学部の森本兼曩教授による基調講演が行われた。

G.G. POLIKARPOV教授（Academy of Science, Ukraine）は，「放射生態学研究の生物学的側面：現状と将来展望」と題して，放射生態学研究の枠組みと非放射性有害物質の影響評価への適用について，広範なレビューを行った。放射生態学研究は，原子力利用が進んでいる現代において基礎研究・応用研究の両側面においてより一層重要性が増していること，生物影響研究から得られてきた電離放射線の定量的「線量-効果」関係を基本とする影響評価の方法論は，非放射性有害物質の影響評価のモデルとなり得ること，また，生態系影響評価においても有用な手段となり得ることが述べられた。

森本兼曩教授（大阪大学医学部）は，「ライフスタイルと健康：健康指標としての染色体変化と免疫学的変化について」と題して，「不健康な」ライフスタイルが及ぼす影響について，種々の疾患に対する分子生物学的，細胞学的，疫学的研究の実例を示し，影響評価における重要性を強調した。喫煙の有無，過度の飲酒，定期的な運動，睡眠時間，食事の栄養バランス，過度の労働時間，朝食，ストレスの有無の8項目を，「健康」・「不健康」なライフスタイルの指標として，染色体異常，免疫能など様々な指標との相関が示された。

同日午後には，R. SEITZ博士（IAEA）による「放射性廃棄物及び化学毒性物質からの健康・環境影響アセスメントについて」と題する特別講演が行われた。この中で，原子力発電やその他の発電システムに伴う放射性及び非放射性廃棄物の環境・健康影響の比較評価を行うための戦略・方法論について紹介された。この講演では，放射性物質（線）と化学毒性物質の人の健康及び環境への影響を評価するための共通の尺度（基盤）を確立すること，廃棄物の量的評価，毒性評価，物理的・化学的特性，再利用の可能性，廃棄物処分の方式等についての評価が重要であることが指摘された。

3. 一般講演

特別講演に引き続き，3日間にわたり一般講演が行わ

Yuji NAKAMURA：International Workshop on Comparative Evaluation of Health Effects of Environmental Toxicants Derived from Advanced Technologies.

[*1] 放射線医学総合研究所第4研究グループ；千葉市稲毛区穴川 4-9-1（〒263-8555）
Department of Environmental and Toxicological Sciences, National Institute of Radiological Sciences；4-9-1, Anagawa, Inage-ku, Chiba 263-8555, Japan.

第 1 表 ワークショップ・プログラム

International Workshop on Comparative Evaluation of Health Effects of Environmental Toxicants Derived from Advanced Technologies

Wednesday, January 28, 1998

I. Opening Session

1. Opening remarks
   Yasuto SASAKI (or Jiro INABA), Director General, NIRS, Japan

II. Key-note Address

Chairpersons : A. HSIE (USA), Y. OHMOMO (IES)

1. G. POLIKARPOV (Ukraine)
   Biological Aspect of Radioecology : Objective and Perspective
2. K. MORIMOTO (Osaka Univ.)
   Life Style and Health : Chromosome Alterations and Immunological Potentials as Health Indices of Overall Lifestyles

III. Special Lecture

Chairpersons : G. POLIKARPOV (Ukraine), S. TAKAHASHI (NIRS), R. SEITZ (IAEA)
Assessment of Health and Environmental Effects from Radioactive and Chemically Toxic Waste

IV. Session A : Environmental Behavior of Toxicants

Chairpersons : W.R. SCHELL (USA), Y. MURAMATSU (NIRS)

1. S. YOSHIDA and Y. MURAMATSU (NIRS)
   Behavior of Trace Elements and Radionuclides in Soil-Plant Systems
2. W.R. SCHELL (USA)
   Behavior and Modeling of Radionuclide and Non-Radionuclide Toxicants in the Environment
3. S. HISAMATSU (IES)
   Behavior of Tritium in the Environment—Tritium in the Food and Human Body—
4. A. KUDO (Kyoto Univ.)
   Fate of Nagasaki $^{239+240}$Pu and Interaction of ^{239}Pu and ^{237}Np with Bentonite and Sulfate Reducing Anaerobic Bacteria
5. Y. SHIBATA (NIES)
   Chemodynamics of Arsenic in Marine Environment

Thursday, January 29, 1998

V. Session B: Effects on Eco-system

Chairpersons : H. JONES (UK), K. KOMURA (Kanazawa Univ.)

1. Z. KAWABATA (Ehime Univ.)
   Evaluation of the Effects of Biological Perturbations on an Ecosystem Using Aquatic Microcosms
2. H. JONES (UK)
   The Ecotron Controlled Environment Facility : Microcosm Studies on the Effects of Elevated CO_2 on Terrestrial Communities
3. I. AOYAMA (Okayama Univ.)
   Ecotoxicity Assessment and Bioassay of Chemicals
4. S. FUMA (NIRS)
   Ecological Effects of Radiation and Other Environmental Stress on Aquatic Microcosm

VI. Session C : Modeling and Methodology in Environmental Risk Studies

Chairpersons : H. MAUBERT (IPSN), Y. NAKAMURA (NIRS)

7. 地球規模のフォールアウトに由来する ^{137}Cs 摂取量に基づく線量評価と日本人集団におけるリスク評価（京都大学地球環境工学：島田洋子他）
8. 食品及び食事標本の多元素分析に基づく一般公衆の健康影響比較評価(放射線医学総合研究所：白石久二雄他)
9. 3種の土壌型におけるキュウリによる ^{137}Cs 及び ^{90}Sr の吸収（理化学研究所：S. GOUTHU 他）
10. 必須元素及び微量元素の土壌から農作物への移行（環境科学技術研究所：塚田祥文）
11. 放射性核種の土壌から野菜への移行に関する研究（放射線医学総合研究所：坂内忠明他）
12. テクネチウムの水田土壌から米粒への移行(放射線医学総合研究所：柳澤啓他)
13. 水田土壌における ^{99}Tc の挙動に関する考察（放射線医学総合研究所：田上恵子他）
14. 水性マイクロコズムを用いた γ 線及び紫外線の生態学的影響に関する比較評価(放射線医学総合研究所：武田洋他)
15. 酸性化による成長期の水性マイクロコズムの集団密度に対する影響(放射線医学総合研究所：宮本霧子他)
16. マイクロコズム系を用いた水性生態系に対する表面活性剤の毒性評価（筑波大学：高松良江他）
17. 複雑系の自己保存システムとしてのマイクロコズムに関する計算機シミュレーション(放射線医学総合研究所：土居雅広他)
18. ラドン誘発肺ガンは実在するか？(放射線医学総合研究所—スウェーデン国立放射線防護研究所：Anita Enflo)
19. 肺マクロファージにおけるガドリニウムの細胞毒性に関する研究(放射線医学総合研究所：久保田善久他)
20. *Rhodeus ocellatus ocellatus* の胚細胞を用いた突然変異性試験（宇都宮大学：上田高嘉他）
21. MSTO-211H セルラインにおけるアスベストと γ 線の細胞毒性の比較（東京理科大学：沖永希世他）
22. ヒトの皮膚線維芽細胞の HPRT 遺伝子座における放射線誘発突然変異の分子生物学的解析(放射線医学総合研究所：山田裕他)
23. 多環芳香族炭化水素の光化学反応毒性(食品薬品安全センター：中川ゆずき他)
24. ウニを用いた水質汚染の発生毒性モニタリングシステム（横浜市立大学：早乙女京子他）

3.5 セッション D（環境毒性学研究）

1月30日には，午前から午後にわたり生物影響・環境毒性研究に関するセッションが開かれた。

古谷圭一教授（東京理科大学理学部）は「粒子状物質の化学特性とその細胞毒性」と題し，酸化ニッケルの塩類溶液やラットの培養肺マクロファージ，C3H マウスの呼吸器系などにおける溶解性，石炭フライアッシュの物理化学的特性とラットの肺マクロファージに対する細胞毒性などについて詳しい報告を行った。

A.W. HSIE 教授（The University of Texas Medical Branch, USA）による「哺乳動物細胞における電離放射線及び化学物質によって誘発される遺伝子突然変異の分子マーカー」と題する講演では，突然変異を誘発する反応性酸素分子（ROS）による HPRT 遺伝子座の突然変異スペクトラムが詳細に報告された。放射線による ROS がもたらす突然変異誘発の機構は，ブレオマイシン，アドリアマイシン等の化学物質による変異発現機構と同一と考えられ，比較影響評価の方法論を確立する上できわめて重要な情報である。

高橋千太郎博士（放射線医学総合研究所）による「放射線と環境汚染物質の毒性影響の比較：トランスジェニックマウス，培養肺マクロファージ，DNA 二重鎖切断解析」と題する講演では，*in vivo* における突然変異検出のためのトランスジェニックマウスモデルの有効性，培養肺マクロファージを用いた細胞毒性試験法，マウス肺マクロファージや MSTO 細胞における DNA 二重鎖切断の誘発など，新しい生物毒性評価法・試験法について，極めて興味深い報告がなされた。

G. PATRICK 教授（MRC Toxicology Unit, UK）による「肺マクロファージ初代培養を用いた吸入物質の毒性影響の予見法」と題する講演では，吸入物質の毒性影響試験法について，広範なレビューが行われた。さらに，粒子状テルビウムやコバルトの肺マクロファージによる溶解性と毒性，アスベスト曝露による呼吸器細胞の免疫学的反応，呼吸器障害の誘発メカニズムとの関連等について詳しい報告がなされた。

平野靖史郎博士（国立環境研究所）による「肺に及ぼす塩化イットリウムの影響」と題する講演では，先端科学技術工業に伴う環境有害物質として希土類元素，特にイットリウムの毒性について報告された。^{90}Y は β 線放出核種であり臨床応用されているが，イットリウム自体の体内代謝，毒性についての情報は少ない。講演では，塩化イットリウムの呼吸器毒性について，SPF ウィスターラットを用いた豊富な実験データが紹介された。

荻生俊昭博士（放射線医学総合研究所）による「実験

動物における化学物質及び放射線による発癌」と題する講演では，ラットを用いた化学物質及び放射線（X線）の発ガン性の比較が紹介された。*N*-ニトロソ化合物は，強い発ガン性を持ち，かつその前駆物質は自然環境中に存在しているため，環境安全評価上重要である。講演では，MNU, ENU, PNU, BNUなどの*N*-ニトロソ化合物による発癌性，発癌部位，放射線による発癌との対比が詳しく述べられた。

4. 総合討論

1月30日午後からは，「比較影響評価研究の今後の展開」に関する総合討論が行われた。国立水俣病総合研究センター長滝澤行雄博士から，水俣病からチェルノブイル事故にまでわたる広範な環境毒性物質に関する講演が行われ，引き続いてW.A. SCHELL教授，G.G. POLIKARPOV教授，A.W. HSIE教授，R. SEITZ博士その他のワークショップ参加者から，今後の研究動向に関する提言，コメントなどが提起された。これらの提言に関しての熱心な討論が行われた。

最後に，本ワークショップ企画運営委員長である稲葉次郎放射線医学総合研究所研究総務官より，閉会の辞が述べられ盛会のうちに閉幕した。

5. おわりに

このワークショップでは，放射線・環境放射能のみならず，種々の環境有害物質に関して，環境研究から生物毒性研究にわたる様々な分野の研究者による講演・議論が行われた。講演内容のプロシーデイングは，近々刊行される予定である。

共催していただいた日本保健物理学会及び日本放射線影響学会，また後援していただいた科学技術庁，科学技術国際交流センターの諸機関に謝意を表す。

(1998年3月9日受付)

Journal of NUCLEAR SCIENCE and TECHNOLOGY, Vol. 34, No. 1, p. 63–72 (January 1997)

Effects of Atmospheric Transport on Temporal Variations of ^{222}Rn and Its Progeny Concentration in the Atmosphere

Tetsuya SAKASHITA†, Akihiko SUZUKI, Takao IIDA, Yukimasa IKEBE,

*Department of Nuclear Engineering, School of Engineering, Nagoya University**

Masamichi CHINO

*Environmental Physics Laboratory, Department of Environmental Safety Research, Japan Atomic Energy Research Institute***

(Received January 16, 1996), (Revised October 29, 1996)

The purpose of this study was to estimate the effects of atmospheric transport on temporal variations in the concentration of ^{222}Rn and its progeny in the air by using a three dimensional atmospheric dispersion model. The objective region for this study was the Chubu district in Japan and the objective period was from November 1 to 20, 1991. It is well known that the diurnal variation of concentration is due to the diurnal cycle of the growth and decay of the mixed layer. In addition, this study led to the following conclusions:

(1) Comparing the observed results with one- and three- dimensional models showed that the atmospheric transport of ^{222}Rn and its progeny affects the temporal variation of concentrations for limited area sources like the islands of Japan.

(2) Time series analyses of observed and calculated results revealed that a periodicity of several days was included in the variation of the concentration of ^{222}Rn from a remote source. Moreover, it suggested that it is dependant on the long-range transport of ^{222}Rn by the air-flow caused by the changing high and low pressure systems.

KEYWORDS: ***radon 222, progeny, atmospheric transport, advection, time series analysis, seasonal adjustment model, remote source, exhalation rate, equilibrium factor, atmospheric diffusion***

I. Introduction

In the UNSCEAR 1988 Report[1], it was estimated that the inhalation of ^{222}Rn progeny accounts for about one half of the effective dose equivalent from all natural sources of radiation. Therefore, to estimate the radiation dose to the public, it is important to study ^{222}Rn progeny's behavior in the atmosphere.

For several decades, many field studies have been carried out, in which the variations of the outdoor atmospheric concentration of ^{222}Rn and its progeny have been cleared with local time, season, altitude and location, quantitatively. Moreover, numerical analysis were performed by several investigators to reveal diurnal variations and vertical diffusion theoretically[2]-[4].

However, their studies using one dimensional model have concentrated on the variation caused by vertical diffusion, although atmospheric transport could also greatly contribute to the variation of the ^{222}Rn and its progeny concentration at sites adjacent to large bodies of water, like Japan. This study therefore aims at estimating the effects of atmospheric transport on the temporal variation of ^{222}Rn and its progeny concentration by using a three-dimensional numerical atmospheric dispersion model. In particular, the effects of advection in local and synoptic areas were investigated.

* *Furo-cho, Chikusa-ku, Nagoya 464-01.*
** *Tokai-mura, Naka-gun, Ibaraki-ken 319-11.*
† Corresponding author, Tel. +81-43-251-2111(ext.453), Fax. +81-43-251-4853, E-mail: tetsuya@nirs.go.jp

II. Model

In general, Atmospheric dispersion models are divided into two types; the Eulerian model which solves in advection and diffusion equations, and the Lagrangian model in which the transportation of materials is expressed by the movement of a large number of marker particles. One of the advantages of the Lagrangian model is that it is free from the numerical diffusion which occurs in the Eulerian model[5]. However, if the Lagrangian model is applied to an area source like ^{222}Rn, a very large number of maker particles would be needed to keep the statistical error small. Therefore, an Eulerian model that included a highly accurate finite differencing scheme for numerical diffusion was used in this study.

1. Coordinates

Rectangular coordinates were used for the horizontal plane, and a uniformly spaced computational grid was employed. For the vertical direction, we used a terrain-

following-coordinate (z^*-coordinate) in order to take the effect of terrain in the calculational area into consideration. The z^*-coordinate is represented by

$$z^* = \frac{H(z - z_g)}{(H - z_g)}, \quad (h = H - z_g), \tag{1}$$

where $z_g(x, y)$ is the terrain height and H the reference altitude for the upper boundary. The reference altitude was set at 3 km. In the vertical direction, a variable spacing grid was employed.

2. Wind Field Model

We used a mass-consistent wind field model (WSYNOP) that was developed by Ishikawa[6]. Firstly, the model wind components for each section of grid are calculated by the simple interpolation of the surface and aerological data. The wind field used in the transport calculation needs to satisfy the equation of continuity,

$$\frac{\partial(hu)}{\partial x} + \frac{\partial(hv)}{\partial y} + \frac{\partial(hw^*)}{\partial z^*} = 0, \tag{2a}$$

where u, v and w^*;

$$w^* = \frac{1}{(H - z_g)} \left\{ (z^* - H) \left(u\frac{\partial z_g}{\partial x} + v\frac{\partial z_g}{\partial y} \right) + Hw \right\} \tag{2b}$$

are components of wind velocity along the x, y and z^* axes. The interpolated wind field is adjusted by the variational method so that it satisfies Eq.(2a). (See detail in Ishikawa[6])

3. Atmospheric Transport Model

We solved advection and diffusion equations which included horizontal and vertical advection, vertical diffusion, sink and source. Equations for the transport-model for ^{222}Rn, ^{218}Po, ^{214}Pb and ^{214}Bi are

$$\frac{\partial hC_i}{\partial t} + \frac{\partial huC_i}{\partial x} + \frac{\partial hvC_i}{\partial y} + \frac{\partial hw^*C_i}{\partial z^*} = \frac{\partial}{\partial z^*}\left(\frac{H^2}{(H - z_g)^2} K \frac{\partial hC_i}{\partial z^*} \right) - h\lambda_i C_i + h\lambda_{i-1} C_{i-1}, \quad (i = 1, \cdots, 4), \tag{3}$$

where C_i is the concentration of the i-th member of the decay chain (i=1 for ^{222}Rn, i=2 for ^{218}Po, i=3 for ^{214}Pb, and i=4 for ^{214}Bi) and λ_i the corresponding radioactive decay constant. The second term, $-h\lambda_i C_i$, is the sink to radioactive decay. The third term, $h\lambda_{i-1}C_{i-1}$, is the generation, due to the decay of the (i-1)th nuclide in the decay chain. For ^{222}Rn when i=1, instead of this term, we used the following boundary conditions to consider the exhalation of ^{222}Rn from the ground;

$$-\frac{H^2}{(H - z_g)^2} K \frac{\partial hC_1}{\partial z^*} = hE \quad \text{at} \quad z = z_g, \tag{4}$$

where E corresponds to the ^{222}Rn exhalation rate and K the vertical diffusion coefficient. As for deposition, we assumed that the ^{218}Po, ^{214}Pb and ^{214}Bi, which reached the ground surface by molecular diffusion would never be resuspended. This assumption gives the following boundary conditions:

$$C_i = 0 \quad \text{at} \quad z = 0 \quad i > 1. \tag{5}$$

In this model, advection and diffusion equations for ^{222}Rn progeny were transformed to similar form to ^{222}Rn by using the numerical technique introduced by Beck so that computations can be easily performed (See detail in Ref.(3)).

The advection term was solved using the NIC scheme[7]. In this method, the flux at the grid-interval boundary x_i was calculated assuming the local density in the whole integration-domain had a continuous-first-derivative. The local density can be represented by a parabolic curve within a mesh width, Δx. Integral variables, when normalized to a unit grid interval, are

$$\Phi^t_{i-1/2} = \frac{1}{\Delta x}\int_{x_{i-1}}^{x_i} \phi(x, t)dx = \frac{1}{\Delta x}[\Psi(x_i) - \Psi(x_{i-1})], \tag{6}$$

where ϕ is the local density, Ψ the primitive function of ϕ and the subscript i the mesh number. Cubic spline interpolation is applied to Ψ to obtain ϕ. As a result, the flux at the grid-interval boundary is

$$F_i = a\frac{\Delta x}{\Delta t}[\phi_i c + (3\Phi_{i-a/2} - 2\phi_i - \phi_{i-a})c^2 + (\phi_i + \phi_{i-a} - 2\Phi_{i-a/2})c^3], \tag{7}$$

where a=$sgn(u_i)$ governs the direction of the fluxes, and c the Courant number. The average ϕ within the integral grid interval for the next time step is calculated using the following equation,

$$\Phi^{t+\Delta t}_{i-1/2} = \Phi^t_{i-1/2} - \frac{\Delta t}{\Delta x}(F_i - F_{i-1}), \tag{8}$$

where Δt is the time step. The time step used in the transport model was set to 60 s. The wind field was calculated every 3 h and linearly interpolated to the time step of the transport model.

The diffusion term was solved using the Crank Nicolson method[8]. Diffusion coefficients were calculated with the turbulence closure model (Level 2) of Mellor and Yamada[9]. The Level 2 model reduces the entire turbulence model to the algebraic relation of turbulent quantities and can be cast in a traditional eddy coefficient format modified by Richardson-number-dependent functions. The diffusion coefficient on the surface was set to the molecular diffusion constant of 5.4×10^{-6}m^2/s[3]. An upper limit (70 m^2/s) for the diffusion coefficient was imposed to avoid unlikely strong vertical diffusion in unstable conditions. A lower limit was also introduced as seen in **Fig. 1**.

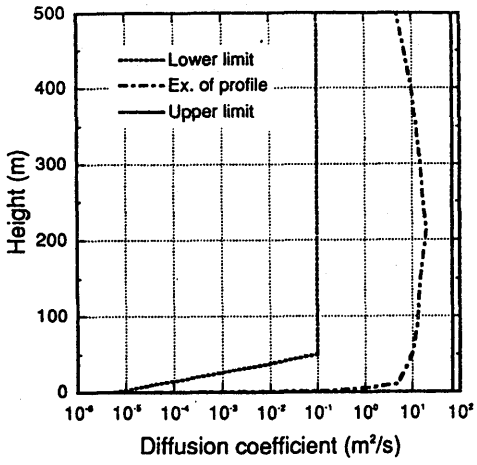

Fig. 1 Vertical profiles of the lower and upper limit of the eddy diffusion coefficient

4. Computational Area

Figure 2 shows the computational area. This area is centered at Nagoya city, and covers the Chubu-district. The grid size for the simulation was 51×51×21 with a horizontal interval of 4 km. In the vertical, the variable mesh width was used, in which the depth of the lowest layer was 2 m.

5. Meteorological Data and Calculational Period

To estimate the diffusion coefficients, we used wind and air temperature data from Chukyo-TV monitoring station of the Aichi Prefectural Office (15, 17, 135 and 137 m), the electric power plant at Hamaoka (20 and 100 m) and Environmental Science Research Center of Fukui prefecture (7.5 and 185 m).

Aerological wind and air temperature data from Hamamatsu, Wazima and Shionomisaki stations of the Japan Meteorological Agency were used to estimate the upper wind-field above about 1,500 m (850 hPa). Furthermore, wind data from the Japan Meteorological Agency's Automated Meteorological Data Acquisition System (AMeDAS) were used to calculate horizontal wind field near the surface.

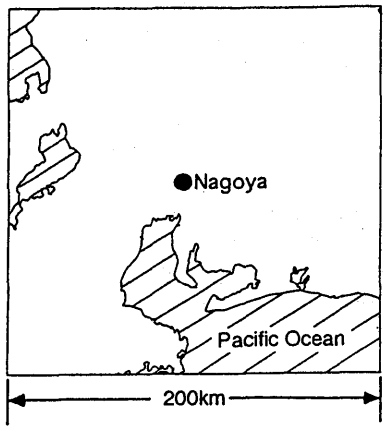

Fig. 2 Computational area

The calculations were done for the period from November 1 to 20, 1991.

6. Boundary Conditions

The inflow of ^{222}Rn and its progeny at the lateral boundary was assumed to be zero in this simulation. However, the measured concentrations of ^{222}Rn are the summation of ^{222}Rn emanating in the computational area and ^{222}Rn flowing into the computational area from the outside of the area. Therefore, the value of 2.3 Bq/m^3[10] was added to calculated concentrations to account for ^{222}Rn flowing into the area. As for the radon progeny, the concentration balancing to 2.3 Bq/m^3 of ^{222}Rn was added to the computed value to account for the contribution from remote sources.

Ⅲ. Results

1. Analysis of Observations

Outdoor ^{222}Rn concentration, which was averaged for 1 h, was measured with an electrostatic radon monitor (ERM)[11] at a height of 1 m above the ground every hour. Polonium-218, ^{214}Pb and ^{214}Bi concentrations, which were averaged for 7 min after evaluation time, were measured using a filter method monitor (MGR)[12] at the same height every 3 h.

Calculated results for all the objective nuclides were averaged for 1 h.

Since there was little rain over the calculational period in Nagoya, it was supposed that the contribution of the precipitation to the observed concentration was minor.

In order to eliminate short term fluctuations from observed ^{222}Rn and its progeny concentrations, and to estimate the distribution of observations, a trend model was used.

The trend model[13] assumes that time series of observation Y_n, which is the ^{222}Rn concentration measured in outdoors, consists of the trend-component-model in Eq.(9) and the observational-model in Eq.(10). The trend model is written as

$$\Delta^k t_n = v_n, \tag{9}$$

$$Y_n = t_n + w_n, \tag{10}$$

where t_n is the trend at the n-th time step, Δ^k the k-th order of the finite difference, and v_n the white noise whose standard deviation is τ (system noise) and the average is zero. w_n is the white noise of which the standard deviation is σ (observational noise) and its average is zero. This represents the observational error. For k, we used a value of 2. When k=2, Eq.(9) is t_n=2t_{n-1}−t_{n-2}+v_n. This allows the trend component to vary linearly in a local aspect. The trend was calculated using Kalman filtering and smoothing. σ was calculated using the max-

imum likelihood method. **Figure 3** shows the results applied trend model analysis to ^{222}Rn concentration. Most of the observed points are within $\pm 3\sigma$ of the trend component.

2. Comparison of Three Simulations with Observed Data

The trend of the observed data were compared with those of the following three simulations: (1) one-dimensional ^{222}Rn simulation (1D); (2) three-dimensional ^{222}Rn simulation assuming a constant-exhalation-rate (3D(CE)); (3) three-dimensional ^{222}Rn simulation taking the exhalation-rate map into consideration (3D(ME)).

To clarify the effects of advection, 1D was compared to 3D(CE). While the one-dimensional model assumes essentially an infinite plane source, the three-dimensional model must consider the source distribution on land and sea. Thus, in 1D and the land areas of 3D(CE), the ^{222}Rn exhalation rate was set to 0.48 atom/cm^2·s[14]. Since the oceanic emission was 100-1,000 times smaller[15] than the emission from the land areas, the flux of ^{222}Rn from the ocean was assumed to be zero in 3D(CE). Furthermore, a constant value of 2.3 Bq/m^3 was added to the calculated value of the 3D(CE) to sum up the inflow from the outside of the area. As shown in **Fig. 4**(a) and (b), it is clear that the variations in 3D(CE) are closer to the trend of observed than those of 1D. The trend of the observed results was not shown from 0:30 13th November to 9:30 14th November, because of the lack of observed data.

The radon exhalation rate varies widely according to the soil, atmospheric conditions, and so on[16]. Although, in 3D(CE), the radon exhalation rate was assumed to be constant at 0.48 atom/cm^2·s, the geographical distribution of the source was also considered in 3D(ME). The source was estimated by the following equation introduced by Ikebe *et al.*[10]:

$$Q = 0.48E + 2.3, \tag{11}$$

where Q is the annual average of ^{222}Rn concentration (Bq/m^3) and E the exhalation rate (Bq/m^2·s) depending on the geographical location. From observed data at some sites in the objective region[17], Q was estimated at each grid point by simple interpolation with the weight of the reverse square of the distance between the site and grid. The second term on the right hand of the equation, 2.3 Bq/m^3, corresponds to the remote source component. **Figure 5** is a map of ^{222}Rn exhalation rate.

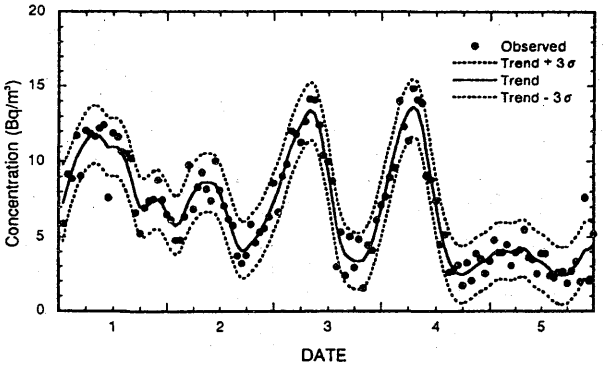

Fig. 3 Trend and errors of observed ^{222}Rn concentration with the trend model

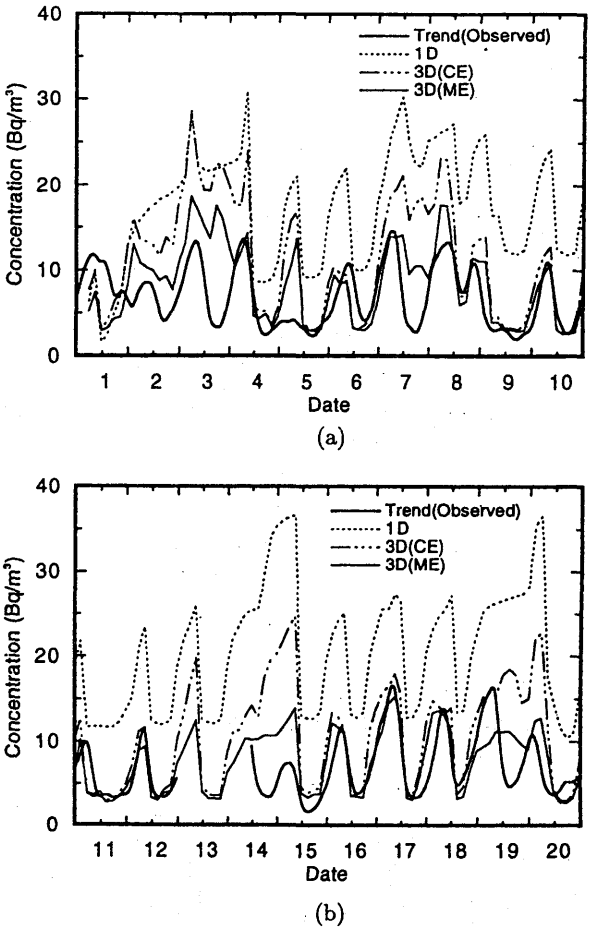

Fig. 4 Comparison of three following simulations with the trend of the observed on (a) November 1-10, 1991 and (b) November 11-20, 1991
(1) 1D represents one-dimensional simulation; (2) 3D(CE) represents the 3-dimensional simulation assuming a constant exhalation rate; (3) 3D(ME) is the 3-dimensional simulation taking the exhalation-rate map into consideration.

The result of the three-dimensional simulation that takes the exhalation rate map into consideration (3D(ME)) is shown in Fig. 4. In Fig. 4, it can be seen that 3D(ME) showed better agreement with the trend of observed than 3D(CE).

3. Comparison of Observed and Simulated Concentrations for ^{222}Rn, ^{218}Po, ^{214}Pb and ^{214}Bi

Comparisons of observed concentrations of ^{222}Rn,

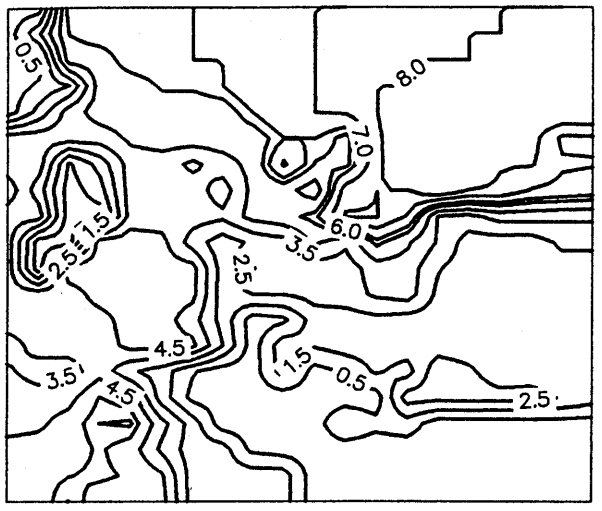

Fig. 5 Radon-222 exhalation rate distribution map ($\times 10^{-1}$ atom/cm^2·s=2.1 mBq/m^2·s)

^{218}Po, ^{214}Pb and ^{214}Bi with calculated ones in 3D(ME) are shown in **Figs. 6-9**, respectively. In each figure, calculated results, observed results, Trend $+3\sigma$ and Trend -3σ are presented. However, in Fig. 7, "Trend" in place of "Trend $+3\sigma$" and "Trend -3σ" was presented because fluctuations in the observed results were very large. The observed and calculated concentration averages over the calculational period (1991.11.1-11.20) are shown in **Table 1**. As can be seen in Table 1, the average calculated concentration for each nuclide is approximately the same as what was observed. This means that our calculational model worked well.

Table 2 shows the observed and calculated equilibrium factors. The calculated equilibrium factor was very close to the observed one. Both are also close to the value

Table 1 Average observed and calculated concentration for the calculational period (1991.11.1-11.20)

	Observed (Bq/m^3)	Calculated (Bq/m^3)
^{222}Rn	6.93	8.06
^{218}Po	5.25	7.90
^{214}Pb	6.39	7.20
^{214}Bi	5.74	6.77

Table 2 Equilibrium factor

Term	Observed	Calculated
1991.11.1-11.20	0.87	0.89

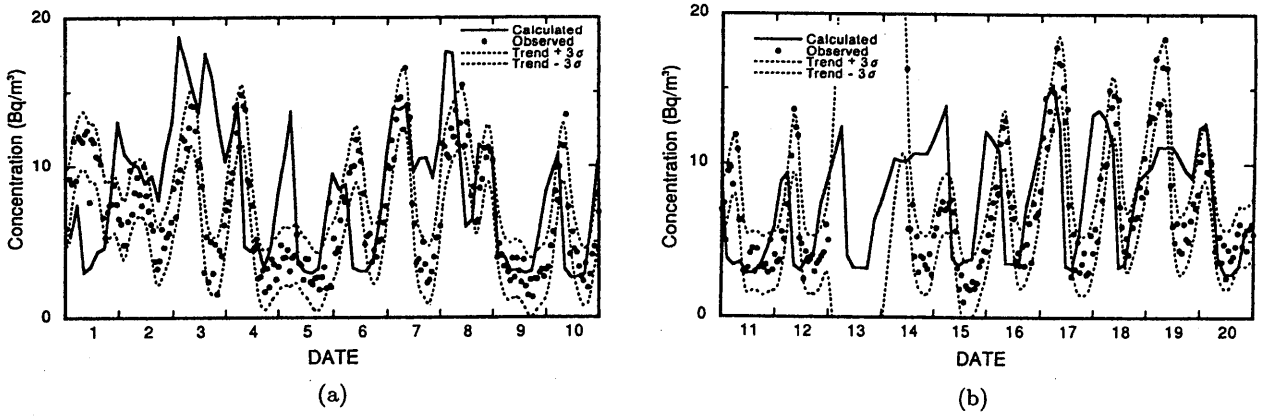

Fig. 6 Comparison of observed and calculated ^{222}Rn concentration on (a) November 1-10, 1991 and (b) November 11-20, 1991

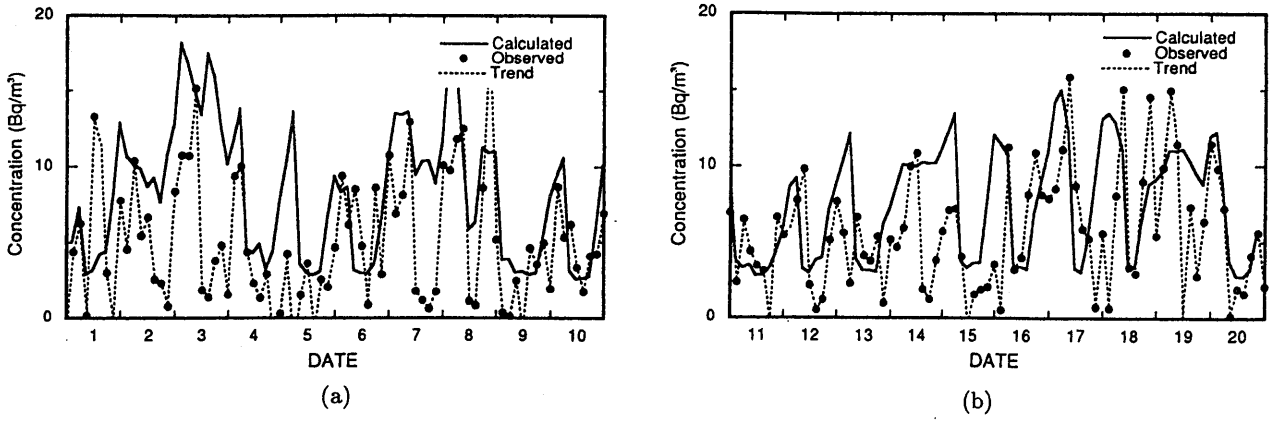

Fig. 7 The same as Fig. 7, except for ^{218}Po

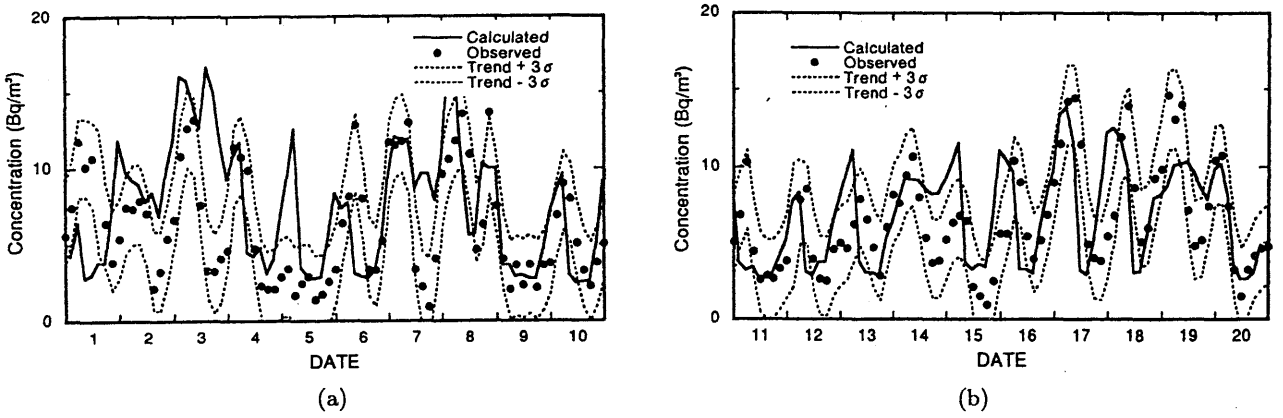

Fig. 8 The same as Fig. 7, except for ^{214}Pb

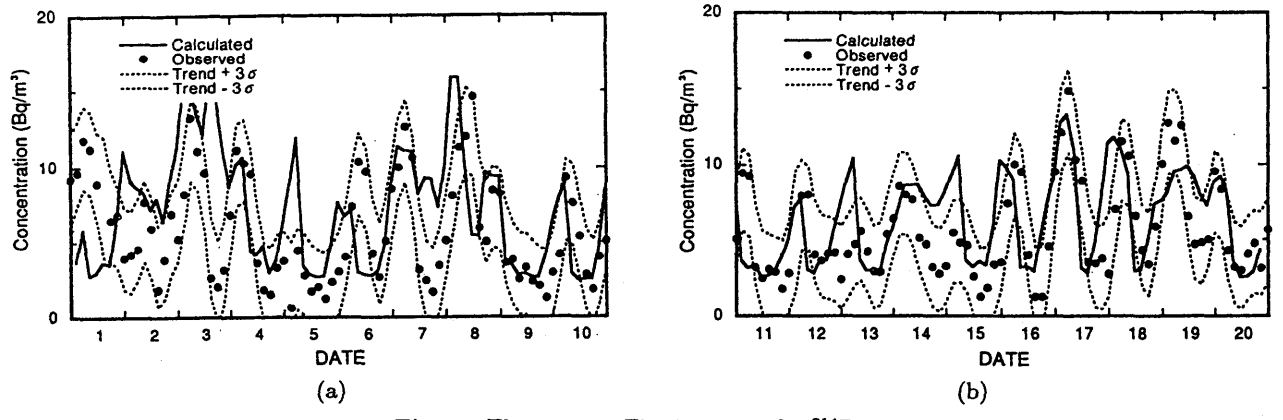

Fig. 9 The same as Fig. 7, except for ^{214}Bi

reported in UNSCEAR 1988[1] Report.

Although the calculated concentrations agreed well with the measurements on average, there are still some discrepancies between the calculated concentrations and the observed range from Trend $+3\sigma$ to Trend -3σ in Figs. 6-9. In the following section, the discrepancy between the observed and calculated ^{222}Rn concentrations will be investigated with time series analyses of the observed and calculated results, because the variation of ^{222}Rn progeny are just like that of ^{222}Rn.

IV. Discussion

In this chapter, the causes of the discrepancies of ^{222}Rn concentrations found in Figs. 6 is investigated by using the following time series analysis: (1) Autocorrelation function and power spectrum of observed and calculated ^{222}Rn concentration; (2) Application of seasonal adjustment model[13] to observed and three calculated concentrations; (3) Correlation between observed ^{222}Rn concentration and atmospheric pressure; (4) Scale analysis of a variation of ^{222}Rn concentration.

1. Autocorrelation Function and Power Spectra

As the first step to clarify the reasons of the discrepancies, the autocorrelation function between the observed and the calculated concentrations were evaluated for ^{222}Rn. We used the data with the interval of 3 h by the following reasons: (1) The data with the interval of 3 h had almost the same correlation and the power spectrum as those of 1 h data; (2) The variation with in longer cycles than 3 h was discussed, because the input interval of meteorological data was 3 h in the calculation.

Figures 10(a) and (b) shows the autocorrelation functions of the observed and calculated ^{222}Rn concentrations. Time-lag (in days) was represented by the abscissa. As shown in Figs. 10(a) and (b), both have the strong correlation with the time lag of 1 day. In addition, the correlation with the time lag of about 5 days, shown by the dotted line in Fig. 10(b), overlapped daily correlation in the calculated result, whereas observed result did not show the correlation with such a time-lag. To inspect this difference in more detail, power spectra of the variations of the observed and calculated concentrations was evaluated.

The power spectra of the observed and calculated ^{222}Rn concentrations, which represent the magnitude of various periodical components included in the variations, are shown in **Fig. 11**. The shapes of both spectra were basically similar. In the spectrum of the observed result,

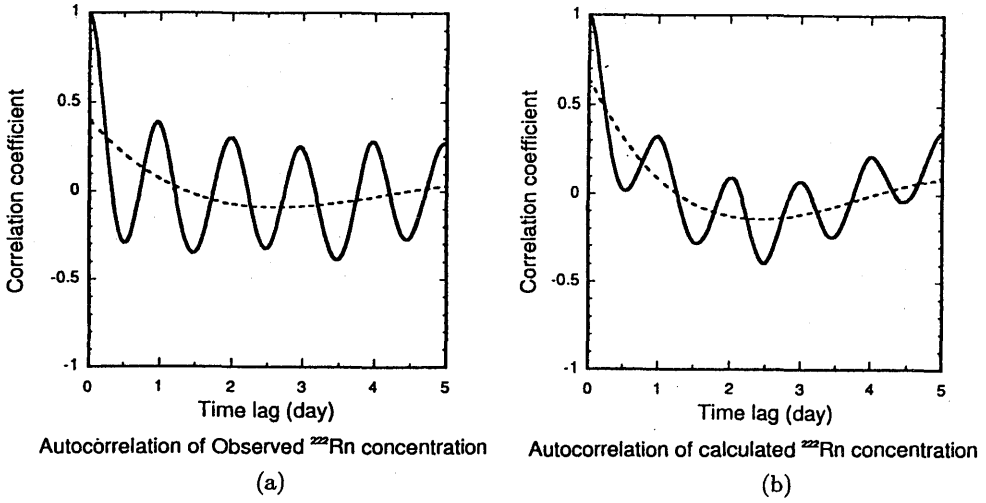

Fig. 10 Autocorrelation function of the observed and calculated ^{222}Rn concentration

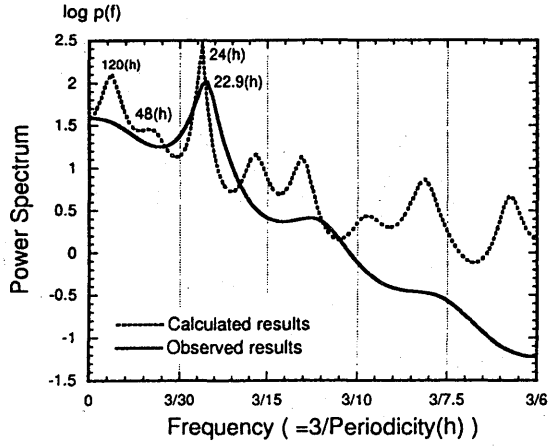

Fig. 11 Observed and calculated power spectra

there was the distinguished peak of 22.9 (h). The rest of peaks were also higher harmonics of 22.9 (h). In contrast, many peaks at 120, 48 and 24 (h) were appeared in the calculated spectrum. The first two spectral peaks were not appeared in the observed spectrum. From these results, it is concluded that the variation of the calculated concentration had conspicuous long-term cycles, including 5-day appeared in Fig. 10(b), whereas the effect of such a cycle was not shown in that of the observed. The reason of this discrepancy was studied by using the seasonal adjustment model which could decompose a variation into some components with the characteristic cycle.

2. Application of the Seasonal Adjustment Model

To estimate components of a variation and investigate the effects of diffusion, advection and the geographical distribution of the source on the components, we applied the seasonal adjustment model to observed and three calculated variations, 1D, 3D(CE) and 3D(ME) (See detail in Sec.III-2). This model is almost similar to the trend model. Observations Y_n are written as

$$\begin{aligned} Y_n &= t_n + d_n + p_n + w_n \\ t_n &= t_{n-1} + \sigma_t \qquad (n = 1, \cdots, m), \\ d_n &= d_{n-8} + \sigma_d \\ p_n &= \sum_{k=1}^{2} a_{n-k} C_{n-k} + \sigma_p, \end{aligned} \tag{12}$$

where t_n, d_n, p_n and w_n are a trend component (TC), a daily component (DC), a stationary autoregressive component (AR) and an observational noise component at a time step n, respectively. σ_t, σ_d and σ_p are white noises. m is the total number of the time steps. A daily component represents a daily variation. A stationary AR component represents a variation dominantly affected by concentrations within 6 h before an evaluating time. In addition, it represents a variation with a short-term cycle. A trend component is different from that of the trend model mentioned in the Sec.III-1. It is a variation except daily and AR components from a variation, and represents a variation with a long-term cycle.

The power spectra of components, DC, AR and TC and variations of them were investigated.

(1) Daily Component

Figure 12(a) shows power spectra of daily components of observed, 1D, 3D(CE) and 3D(ME). All the spectral shapes were almost the same. However, by looking into the daily variations of the observed and three calculated concentrations, the discrepancies between them became apparent as shown in **Fig. 12**(b). The variation of 3D(ME) was the closest one to that of observed, and the concentrations of 3D(ME) are almost the same value as observed ones. This result shows that 3D(ME) can simulate the daily variation of observed concentrations and it is important to consider the effects of advection and source's distribution.

(2) Autoregression Component

Figure 13(a) shows the power spectra of autoregression components. Power spectra of calculated results,

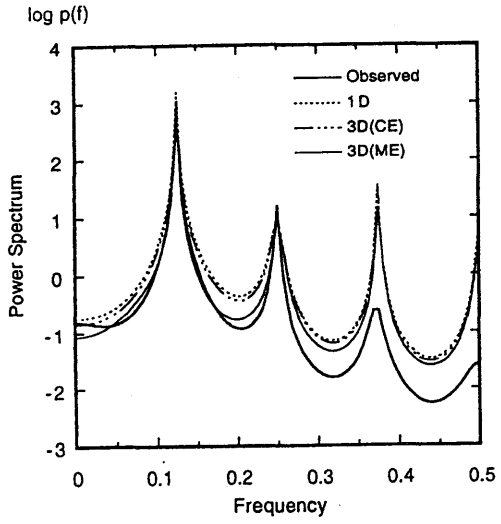

Fig. 12(a) Power spectra of daily components of observed, 1D, 3D(CE) and 3D(ME)

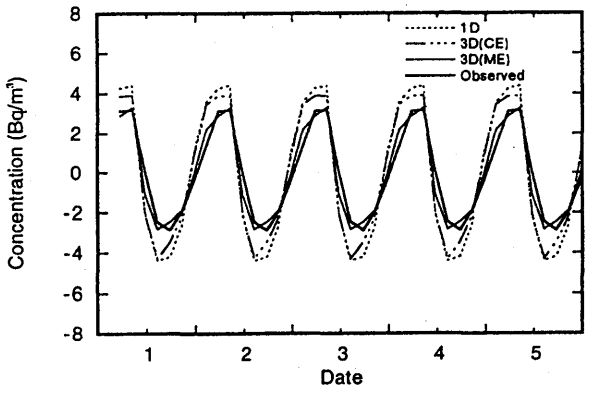

Fig. 12(b) Variations of daily components of observed, 1D, 3D(CE) and 3D(ME)

1D, 3D(CE) and 3D(ME) had almost the same shape. In the region of the long-term cycles, the considerable discrepancies between observed and calculated results were appeared. This discrepancy is more apparent in the variation of autoregression components shown in **Fig. 13**(b). As shown Fig. 13(b), all calculated results had basically similar patterns in the variation. In addition, every several days, the overestimations of the calculated concentrations happened to all calculated results.

This means that the calculated variations have the several-days cycle. Thus, the several-days cycle of calculated results shown in Fig. 13(a) was caused by this overestimations. Moreover, it seemed that the discrepancies on several-days cycle in Fig. 11 (See detail in Sec.IV-1) was caused by the same reason. The root of the problem that the calculated variations had the several-days cycle was the insufficient modeling. However, as shown by the arrows, the discrepancies became small by the improvement of the model. Introducing a more realistic model is proper. Nevertheless, a little discrepancies were left in these term. In addition, there was no improvement in

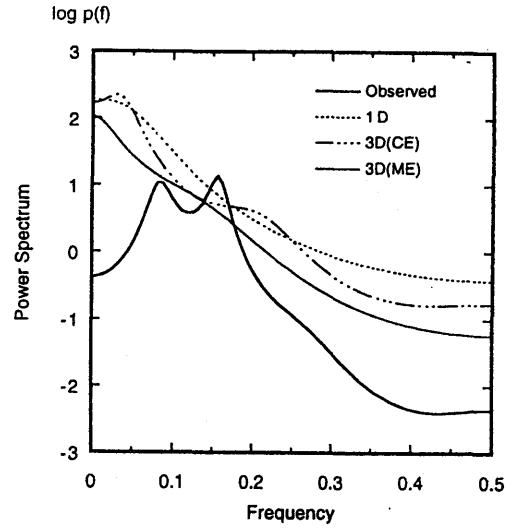

Fig. 13(a) Power spectra of autoregression components of observed, 1D, 3D(CE) and 3D(ME)

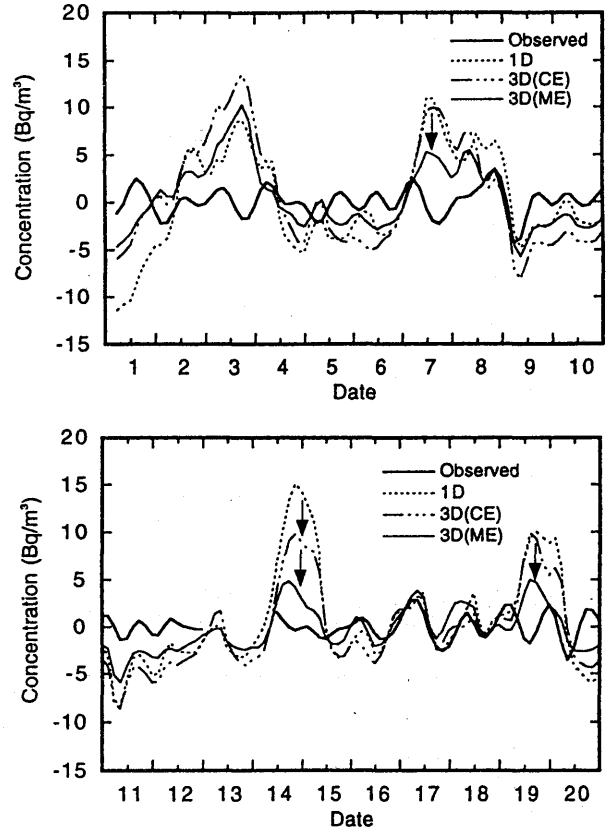

Fig. 13(b) Variations of autoregression components of observed, 1D, 3D(CE) and 3D(ME)

the term from 2nd to 4th November. As for these discrepancies, although Level 2.0 would be probably one of causes on these problems, they need to be investigated in detail.

(3) Trend Component

Figure 14(a) shows power spectra of trend compo-

nents of observed, 1D, 3D(CE) and 3D(ME). The spectrum of observed results had the distinguished peak at several-days cycle. The spectrum of 1D's results was also shown.

The variations of the trend components are shown in **Fig. 14**(b). The trend component of 1D's result gradually increased. It was caused by a transition to a steady state, because of the initial condition that ^{222}Rn concentrations were equal to zero in the whole domain. The trend component of observed results varied with a several-days cycle. However, the trend components of 3D(CE) and 3D(ME) were constant. Thus, the trend components seems important to explain the discrepancies between the observed and calculated variations. Two explanations are possible. One reason of the discrepancy is the changes in meteorological conditions in the local area, affecting the exhalation rate of ^{222}Rn. It will be discussed in the next section. Second is a contribution of ^{222}Rn (remote source component) migrating from the outside of the calculational area, which is not considered in the calculation.

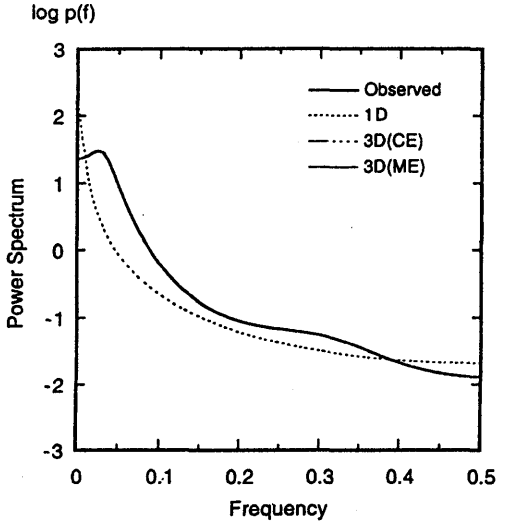

Fig. 14(a) Power spectra of trend components of observed, 1D, 3D(CE) and 3D(ME)

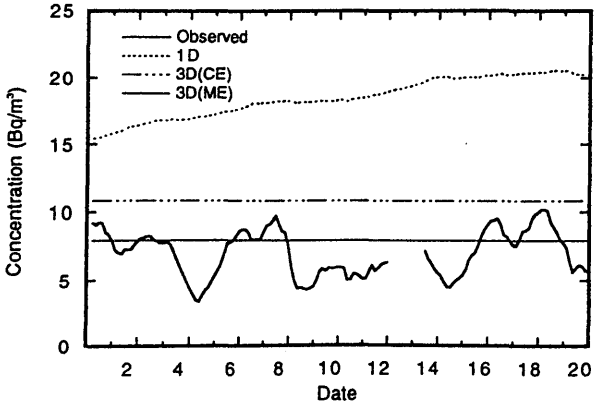

Fig. 14(b) Variations of trend components of observed, 1D, 3D(CE) and 3D(ME)

3. Correlation between Observed ^{222}Rn and Atmospheric Pressure

For changes of atmospheric pressure, it is possible that ^{222}Rn exhalation changes over a few days. To investigate the effect, the cross-correlation function between observed ^{222}Rn and the atmospheric pressure were evaluated. **Figure 15** shows the result of it.

In the previous section, it was pointed out that the trend component of ^{222}Rn concentration varied with several days cycle. In relation to this, it should be noted that the ^{222}Rn exhalation rate increases with the low atmospheric pressure. However, since the cross-correlation between the local atmospheric pressure and observed ^{222}Rn concentration is positive, as seen in Fig. 15, there is no evidence of such influence. Therefore, the time variation of observed ^{222}Rn concentration, like the trend component in Fig. 14(b), must be due to variations on the remote source component.

4. Scale Analysis

A simple analysis was performed in order to relate the time scale of the periodical variation, *i.e.* ^{222}Rn concentration, to the geographical scale.

If the effect of eddy diffusion on long-range transport is smaller than that of advection, the transport equation can be approximated as

$$\frac{\partial C}{\partial t} = -u\frac{\partial C}{\partial x}, \tag{13}$$

where C is the concentration and u the wind velocity along the x-axis. One of the solutions of Eq.(13) is

$$C = A\cos\left\{\frac{2\Pi}{\lambda}(x - ut)\right\}, \tag{14}$$

where A is a constant and λ the wave length. The dispersion relation is

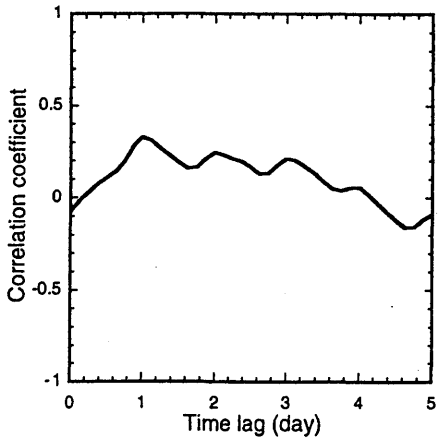

Fig. 15 Cross-correlation functions between ^{222}Rn and atmospheric pressure

$$\lambda = uT, \tag{15}$$

where T is the periodicity. This relation is shown in **Fig. 16**. This means that a cycle of several days corresponds to a wave length of several hundred to several thousand km. This scale coincides with the scale of an ordinary high or low pressure system. It suggests that the time variation of the remote-source component of ^{222}Rn concentration depends on the change in air-flow due to high or low pressure systems and long-range transport that accompanies the change.

V. Conclusion

The effects of atmospheric transport on temporal variations of ^{222}Rn and its progeny concentration in the atmosphere were estimated using a numerical model. The major findings are as follows:

(1) Advection and geographical variations in ^{222}Rn exhalation rate affect a variation of ^{222}Rn concentration.
(2) The daily component of the observed variation were simulated well by our model.
(3) The long-term cycle of the observed variation could not be simulated by a local calculational model. The calculation for a nuclide with a half-life time like ^{222}Rn needs the regional calculational area.

Furthermore, time series analyses suggested that the time variation of the remote-source component of ^{222}Rn concentration depends on the change of air-flow due to high or low pressure systems and the long-range transport accompanied with these changes.

Decomposing an original variation into some components with the characteristic cycle, the discrepancies between observed and calculated variations became more apparent. On each components, if the causes of the discrepancies would be investigated in more detail, simulating the observed variation by the computational model will be possible.

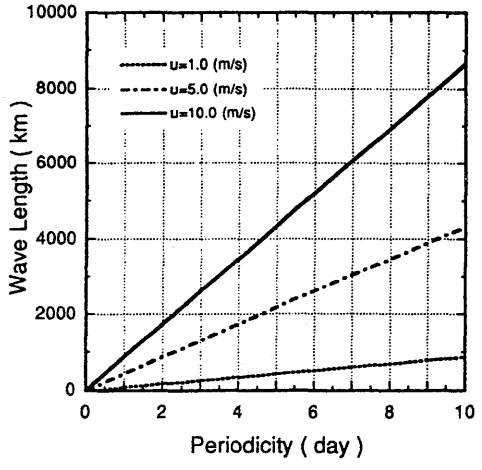

Fig. 16 Dispersion relation

In addition, the eddy diffusion coefficient should be improved as the limitations of the level 2 model under unstable and extremely stable conditions were pointed out by Takagi *et al.*[18]. The influences of meteorological factors must be also studied in detail.

Numerical simulations of this study provide detailed information on the source, diffusion, deposition and equilibrium factors, which are useful for clarifying the behavior of ^{222}Rn and its progeny in the environment.

Acknowledgment

The authors wish to thank the Environmental Radiation Physics Lab. at the Japan Atomic Energy Research Institute (JAERI), and Ikebe's Lab. at Nagoya University. Special thanks are due to Dr. K. Fujitaka and Dr. Y. Nakamura for his suggestions, The National Institute of Radiological Sciences (NIRS), and lastly Dr. T. Yamasaki of the Electric Power Research and Development Center in Chubu Electric Power Co., Inc, for his MGR measurements.

—References—

(1) UNSCEAR: United Nations, New York, Annex A, (1988).
(2) Jacobi, W., Andre, K.: *J. Geophys. Res.*, **68**, 3799 (1963).
(3) Beck, H.L., Gogolak, C.V.: *J. Geophys. Res.*, **84**, 3139 (1979).
(4) Liu, S.C., *et al.*: *J. Geophys. Res.*, **89**, 7291 (1984).
(5) Maekawa, I.: *Nihon-Genshiryoku-Gakkai Shi* (*J. At. Energy Soc. Jpn.*), **29**, 823 (1987), [in Japanese].
(6) Ishikawa, H.: *J. Nucl. Sci. Technol.*, **31**, 969 (1994).
(7) Emde, K.V.D.: *Mon. Wea. Rev.*, **120**, 482 (1992).
(8) Smith, G.D.: "*Numerical Solution of Partial Differential Equations*", Oxford Univ. Press, **17** (1965).
(9) Mellor, G., Yamada, T.: *J. Atmos. Sci.*, **31**, 1791 (1974).
(10) Ikebe, Y., *et al.*: *Nihon-Genshiryoku-Gakkai Shi*, (*J. At. Energy Soc. Jpn.*), **35**, 735 (1993), [in Japanese].
(11) Iida, T., *et al.*: *Res. Lett. Atmos. Electr.*, **11**, 55 (1991).
(12) Yamasaki, T., *et al.*: *J. Jpn. Health Phys. Soc.*, **30**, 149 (1995), [in Japanese].
(13) Kitagawa, G.: "*Programming of Time Series Analysis*", Iwanami Press, 245 (1993), [in Japanese].
(14) Tojo, K.: *Nagoya Univ. M. Paper*, (1989), [in Japanese].
(15) Wilkening, M.H., Clements, W.E.: *J. Geophys. Res.*, **80**, 3828 (1975).
(16) Tanner, A.B.: "*Natural Radiation Environment III*", (Gesell, T.F., Lowder, W.M., Eds.), 5 (1978).
(17) Yamanishi, H., *et al.*: *J. Nucl. Sci. Technol.*, **28**, 331 (1991).
(18) Takagi, H., Kitada, T.: *Tenki*, **41**, 827 (1994), [in Japanese].

EFFECTS OF GADOLINIUM ON THE RETENTION AND TRANSLOCATION OF ^{239}Pu-HYDROXIDE

H. Sato, S. Takahashi, and Y. Kubota*

Abstract—**The effect of gadolinium on the lung retention, excretion, and translocation of plutonium was studied in rats instilled intratracheally with plutonium hydroxide with and without gadolinium. Three types of plutonium hydroxide were prepared: pure ^{239}Pu-hydroxide colloid, that containing a high concentration of gadolinium, and that containing a low concentration of gadolinium. The lung retention of ^{239}Pu was higher and the fecal excretion was lower in the rats administered ^{239}Pu-hydroxide containing a high concentration of gadolinium than those administered pure ^{239}Pu-hydroxide colloid. The translocation of ^{239}Pu from lung to other organs including the liver, spleen, femur, and kidney was not affected by gadolinium. The cytological examination of bronchoalveolar lavage cells showed that the administration of ^{239}Pu-hydroxide containing a high concentration of gadolinium induced the inflammatory reactions in the lung. The delayed alveolar clearance of plutonium in the rats administered ^{239}Pu-hydroxide colloid containing a high concentration of gadolinium may be attributable to the change in physicochemical characteristics of colloid and the inflammation induced in the lung by gadolinium.**

Health Phys. 80(2):164–169; 2001

Key words: plutonium; rat; lungs, rodent; biokinetics

INTRODUCTION

GADOLINIUM (Gd), one of the rare earth elements, is used as a material in semiconductor and magnetic substances in industry, and as a contrast agent for magnetic resonance imaging in clinical medicine (Hirano and Suzuki 1996; Weinmann et al. 1984; Runge and Parker 1997). Gadolinium is also used as a neutron absorber in the nuclear industry. In a newly developed facility for reprocessing of nuclear fuel in Japan, gadolinium nitrate is added to the nitric acid solution as a neutron absorber during the fuel-dissolution process. There is concern, therefore, that workers could be simultaneously exposed to gadolinium and radioactive nuclides in an accident. Gadolinium is a toxic element, especially for reticuloendothelial cells such as alveolar macrophages (O'Neill et al. 1994; Yoneda et al. 1995; Suzuki et al. 1996; Ruttinger et al. 1996), and thus may affect the metabolism of radionuclides in the human body. However, little is known about the effects of gadolinium on the retention and metabolism of radionuclides in the human body.

Inhalation may be a possible route for the accidental contamination by gadolinium and radionuclides. In such a case, plutonium would be one of the important radionuclides. In the present study, therefore, an animal experiment was carried out to elucidate whether or not the co-existence of gadolinium may affect the retention and translocation of plutonium in the lung. Plutonium hydroxide with and without gadolinium was instilled into the rat lung, and the lung retention and translocation of plutonium were compared.

MATERIALS AND METHODS

$^{239}PuO_2$ was obtained from the Japan Atomic Energy Research Institute† and converted to ^{239}Pu nitrate by a procedure described elsewhere (Black and Drummond 1965). Then gadolinium nitrate, $Gd(NO_3)_3$, was added to the plutonium nitrate solution, and the pH of the solution was adjusted to 7.2 with 0.1 M sodium hydroxide under vigorous agitation. By this neutralization, a colloidal form of plutonium hydroxide containing gadolinium was formed. The resultant hydroxide colloids were stabilized with 0.2% gelatin and made isotonic with 0.25 M glucose. Two types of ^{239}Pu-hydroxide colloid containing gadolinium were prepared. One was ^{239}Pu-hydroxide containing a high level of gadolinium (0.9 mg Gd mL^{-1} in the final solution, referred to as Pu-Gd-H in the following), and another containing a low level of gadolinium (0.22 mg Gd mL^{-1}, referred to as Pu-Gd-L). ^{239}Pu-hydroxide colloid was also prepared by the same procedures described above without addition of gadolinium. The radioactive concentration of ^{239}Pu in the final colloidal solutions was 15 kBq mL^{-1} in all three solutions. The reagents used for these procedures were analytical grade (Wako Pure Chemical Industries‡).

* The 4th Research Group, National Institute of Radiological Sciences, 9-1, Anagawa 4-chome, Inage-ku, Chiba-shi, Chiba 263-8555, Japan.

For correspondence or reprints contact H. Sato at the above address, or email at hi_sato@nirs.go.jp.

(*Manuscript received* 23 *November* 1999; *revised manuscript received* 18 *May* 2000, *accepted* 22 *September* 2000)

0017-9078/01/0

† Japan Atomic Energy Research Institute, 2-4, Shirane, Shirakata, Tokai-mura, Ibaraki 319-1195, Japan.

‡ Wako Pure Chemical Industries, Ltd., 5-13, Honcho 4-chome, Nihonbashi, Chuo-ku, Tokyo 103-0023, Japan.

Nine-week-old male Sprague-Dawley rats, weighing about 300 g, were obtained from a domestic breeder.[§] All animals were kept in an air-conditioned room (22±2°C), and given a commercial rat chow[‖] and drinking water *ad libitum*. The animals were divided into three groups consisting of fourteen rats each, and the colloidal solution of Pu and Gd was administered into lung with intratracheal instillation. The detail of the procedure has been described elsewhere (Sato et al. 1994). In brief, the animals were anesthetized with pentobarbital, and 0.3 mL of ^{239}Pu-hydroxide, Pu-Gd-H, or Pu-Gd-L was administered with a single and rapid instillation via an intratracheal cannula. It has been previously found that this dose of Pu-hydroxide colloidal solutions induces no significant inflammatory reactions in the lung (Sato et al. 1994; Takahashi and Sato 1991).

Four weeks after instillation, three rats of each group were sacrificed to determine the lung retention and translocation of ^{239}Pu. The lung, liver, kidney, spleen, and right femur were dissected. Feces and urine were collected 4 d, 1 wk, 2 wk, 3 wk, and 4 wk after instillation. The activity of ^{239}Pu was measured by liquid scintillation counting as described by Keough and Powers (1970). In brief, the tissue samples and feces were ashed at 550°C for 12 h, and the residues were dissolved in 0.2 mL of 7 M nitric acid containing a small amount of concentrated hydrogen fluoride. Then 3.6 mL of scintillation cocktail was added to the sample solution, and the activity was measured using a liquid scintillation counter.[¶] The activity of ^{239}Pu in urine was measured directly with a liquid scintillation counter after filtering through a 0.22 μm membrane filter.[#] The lung retention, excretion, and translocation of ^{239}Pu were represented as a percent of the initial alveolar deposition. The initial alveolar deposition (IAD) was defined as the whole body retention of ^{239}Pu on the third day after administration (i.e., the administered ^{239}Pu minus that excreted up to the third day). This value did not exactly represent the actual retention of ^{239}Pu in the lung, since the activity of ^{239}Pu in organs other than the lung is also included. However, this value could be used for IAD, since the activity of ^{239}Pu in organs other than the lung is assumed to be negligible (Ishigure et al. 1994; Oghiso et al. 1994).

To monitor the occurrence of inflammation in the lung, the remaining animals were serially killed, and bronchoalveolar lavage cells were collected by lung lavage with sterilized Dulbecco's phosphate-buffered saline. The total number of cells collected was determined with a hematocytometer, and differential cell counts were performed on smeared cells after Giemsa staining.

Means of the groups were compared by single-tailed *t*-tests to determine the level of significance. An observed difference was considered statistically significant if $p < 0.05$.

[§] Japan SLC Inc., 3371-8, Koto, Hamamatsu-shi, Shizuoka 431-1103, Japan.

[‖] MB-1, Funabashi Farms, 2-465, Kamiyama, Funabashi-shi, Chiba 273-0046, Japan.

[¶] LS 1214, Wallac Oy, P.O. Box 10, SF-20101, Turku, Finland.

[#] Japan Millipore Ltd., 3-12, Kitashinagawa 1-chome, Shinagawa-ku, Tokyo 140-0001, Japan.

RESULTS

As shown in Table 1, the ratios of IAD to instilled activity were 0.30±0.15, 0.38±0.13, and 0.41±0.19 in the rats administered ^{239}Pu-hydroxide, Pu-Gd-L, and Pu-Gd-H, respectively. There was no statistically significant difference among the 3 groups.

Whole-body retention and total excretion of ^{239}Pu are shown in Fig. 1. The retention of ^{239}Pu in the lungs and the fecal and urinary excretions are shown in Fig. 2. In the rats administered ^{239}Pu-hydroxide, the lung retention of ^{239}Pu was 25.8±2.5% IAD 4 wk after administration. In contrast, the lung retention of ^{239}Pu in the rats administered Pu-Gd-H was 43.2±4.4% IAD. The difference between the groups was statistically significant ($p < 0.05$). The lung retention of ^{239}Pu in the Pu-Gd-L group was similar to that in the ^{239}Pu-hydroxide group. The fecal excretions of ^{239}Pu decreased with the increase in gadolinium contents: 51.9±5.9, 40.9±6.4, and 28.2±0.6% IAD in the ^{239}Pu-hydroxide, Pu-Gd-L, and Pu-Gd-H groups, respectively. The urinary excretion of ^{239}Pu in the Pu-Gd-L group was significantly higher than in the other groups ($p < 0.005$). Figs. 3 and 4 show the daily and cumulative excretion of ^{239}Pu in feces and urine. The daily fecal excretion was significantly lower in the Pu-Gd-H group than the ^{239}Pu-hydroxide group throughout the experimental period (4 d to 4 wk after the administration, $p < 0.05$). In the Pu-Gd-L group, the daily fecal excretion was significantly lower than the ^{239}Pu-hydroxide group only 3 wk after administration ($p < 0.01$). Cumulative fecal excretion was similar to that in the ^{239}Pu-hydroxide group. As shown in Fig. 4, the daily urinary excretion was significantly higher in the Pu-Gd-L group than the ^{239}Pu-hydroxide group 4 d, 1 wk, 2 wk, and 4 wk after administration ($p < 0.05$). Interestingly, there was no significant difference between Pu-hydroxide and Pu-Gd-H groups for the daily and cumulative excretion in urine.

Fig. 5 shows the translocations of ^{239}Pu to the major organs, expressed as % IAD per organ. The amounts of ^{239}Pu in the liver of rats administered ^{239}Pu-hydroxide, Pu-Gd-L, and Pu-Gd-H were 3.16±0.29, 3.38±1.14, and 2.89±0.42%, respectively. The amounts of ^{239}Pu translocated from lung to kidney, spleen, and femur were less than 1% in all groups. In all the organs examined, no

Table 1. Instilled activity and initial alveolar deposition (IAD) of ^{239}Pu and the ratio of IAD to instilled activity in 3 groups.[a]

	Instilled activity[b]	IAD[b]	IAD/Instilled
Pu-hydroxide	4289 ± 306	1242 ± 572	0.30 ± 0.15
Pu-Gd-L	1757 ± 357	647 ± 219	0.38 ± 0.13
Pu-Gd-H	2961 ± 457	1163 ± 439	0.41 ± 0.19

[a] All values are expressed as mean ± SD ($N = 3$).
[b] The values are expressed as Bq.

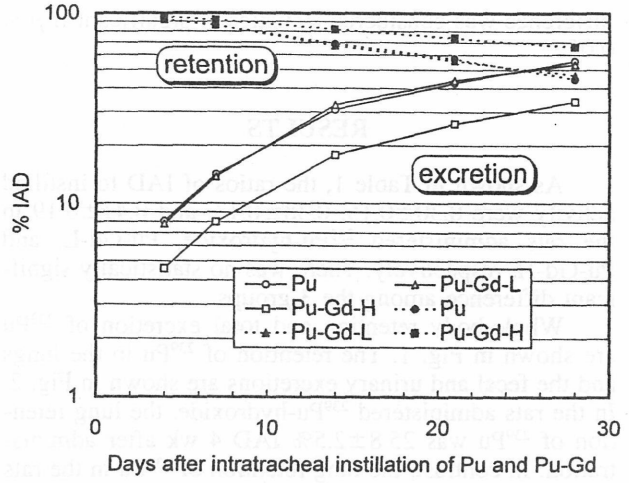

Fig. 1. Whole body retention and cumulative excretion of ^{239}Pu in rats following intratracheal instillation of ^{239}Pu-hydroxide, Pu-Gd-L, and Pu-Gd-H. Each point is the mean of three rats.

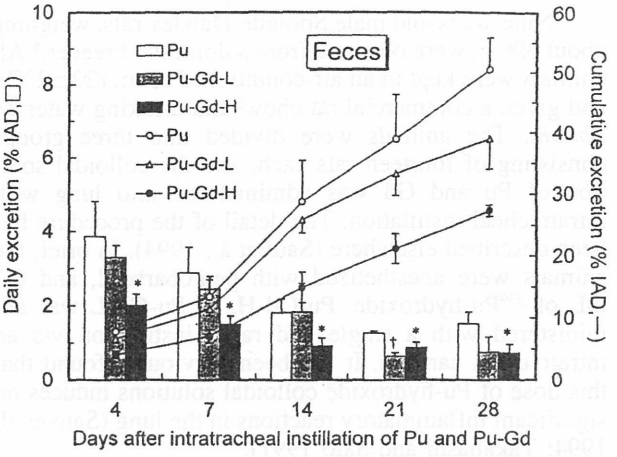

Fig. 3. Daily and cumulative excretion of ^{239}Pu in feces following intratracheal instillation of ^{239}Pu-hydroxide, Pu-Gd-L, and Pu-Gd-H. Vertical bar shows SD of three rats. * denotes significant difference from ^{239}Pu-hydroxide group at $p < 0.05$; † $p < 0.01$.

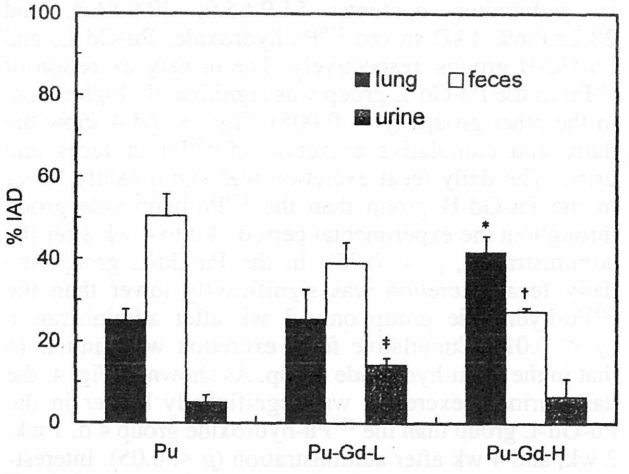

Fig. 2. Lung retention and cumulative excretion of ^{239}Pu in feces and urine 4 wk after intratracheal instillation of ^{239}Pu-hydroxide, Pu-Gd-L, and Pu-Gd-H. Vertical bar shows SD of three rats. * denotes significant difference from ^{239}Pu-hydroxide group at $p < 0.05$.; † $p < 0.01$; ‡ $p < 0.005$.

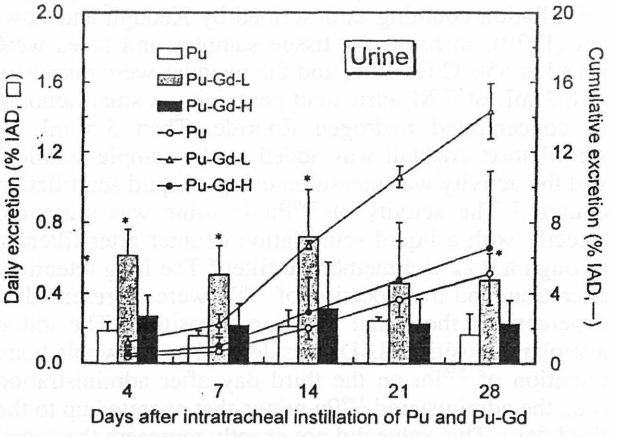

Fig. 4. Daily and cumulative excretion of ^{239}Pu in urine following intratracheal instillation of ^{239}Pu-hydroxide, Pu-Gd-L, and Pu-Gd-H. Vertical bar shows SD of three rats. * denotes significant difference from ^{239}Pu-hydroxide group at $p < 0.05$.

statistically significant differences in the ^{239}Pu translocation were observed between these groups.

Fig. 6 shows time-course changes in the numbers of alveolar macrophages and neutrophils in bronchoalveolar lavage cells of the rats administered Pu-Gd-H. Neutrophils appeared 1 d after administration, increased with time, and reached a maximum level 4 d after the instillation. The number of alveolar macrophages decreased during the first 2 d and then recovered to the control value. In the rats administered Pu-Gd-L, the number of neutrophils was low, but did not significantly increase during the first 2 d (data are not shown). Neutorophil number did not change in the rats administered ^{239}Pu-hydroxide. No changes in the number of macrophages were observed in the rats administered Pu-Gd-L and ^{239}Pu-hydroxide.

DISCUSSION

In the respiratory tract model, the clearance of ^{239}Pu from the lung following acute intake of ^{239}Pu-hydroxide is about 50% a month after intake. The daily excretion of plutonium into feces reaches a maximum 2 d after intake and then declines. The level of daily fecal excretion declines slowly from about 10 d after intake. The daily excretion of plutonium into urine reaches a maximum 1 d after intake and then declines continuously (ICRP 1988). In this study, the clearance of plutonium from the lung of rats was faster than the ICRP model and 75% IAD was cleared 4 wk after administration. The daily excretion of

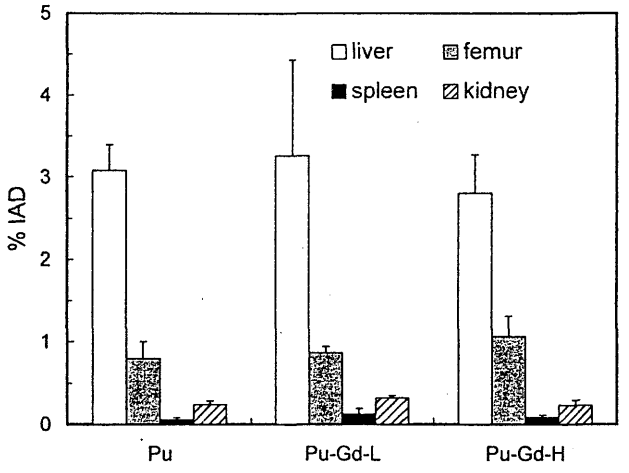

Fig. 5. Translocation of ^{239}Pu from lung to other organs following intratracheal instillation of ^{239}Pu-hydroxide, Pu-Gd-L, and Pu-Gd-H. Vertical bar shows SD of three rats.

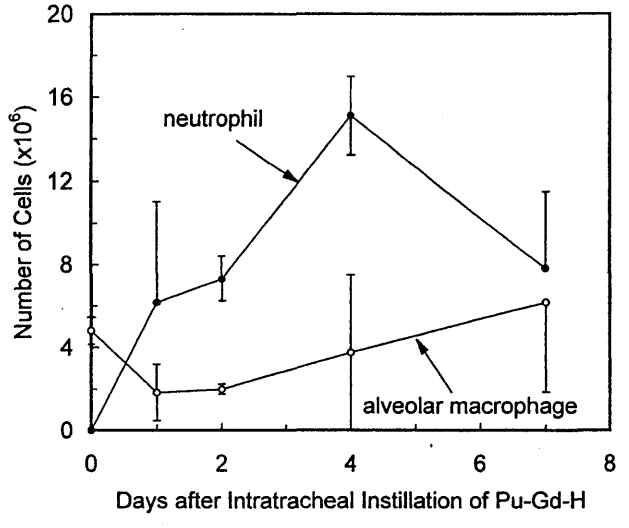

Fig. 6. Time-course changes in the number of alveolar macrophages and neutrophils in the bronchoalveolar lavage cells following intratracheal instillation of Pu-Gd-H. Data represent mean±SD of three rats. The data at day 0 represent the number of cells in non-treated rats.

plutonium in feces from 2 to 4 wk after administration was a constant to very little in variation. This excretion pattern is very similar to the ICRP model. The differences in the daily excretion of plutonium into urine was small; that is, the level of daily excretion was similar throughout the experimental period.

The alveolar clearance of inhaled particles depends on many factors, including the physicochemical characteristics of particles such as size and solubility, as well as the physiological and pathological conditions of the animals (ICRP 1994). The present study demonstrated that the clearance of ^{239}Pu from the lung was slower in the rats instilled with ^{239}Pu-hydroxide containing a high level of gadolinium (Pu-Gd-H) than those instilled with pure ^{239}Pu-hydroxide. It is well known that plutonium nitrate forms hydroxide colloids at near neutral pH, and the physicochemical properties of the resultant colloid particles are affected by reaction conditions including pH, concentration of plutonium, co-existing substances and ionic strength of the solution (Ockenden and Welch 1956; Lindenbaum and Westfall 1965). Therefore, it is likely that the physicochemical properties were different between the Pu-Gd-H and pure ^{239}Pu-hydroxide and that this difference was responsible for the different clearance rate of plutonium from the lung.

Another possible cause of the slower clearance of ^{239}Pu in the rats administered Pu-Gd-H colloids may be the gadolinium-induced inflammation in the lung. There are a few reports indicating that gadolinium is toxic for respiratory cells, especially for alveolar macrophages, and induces acute inflammatory pneumonia (Yoneda et al. 1995; Mizgerd et al. 1996). The number of alveolar macrophages decreased during the first 2 d after the instillation, and then gradually increased in the Pu-Gd-H group (Fig. 6). This pattern of change in the number of alveolar macrophages was a similar finding observed in the pulmonary inflammation after gadolinium administration (Yoneda et al. 1995). The increase in the number of neutrophils in bronchoalveolar lavage apparently indicated that an acute lung inflammation was induced in the Pu-Gd-H group in the present study.

A number of studies have demonstrated that inflammatory reactions in the lung retarded the alveolar clearance of inhaled particles (Sanders et al. 1975; Kubota et al. 1988; Slauson et al. 1989; Benson et al. 1995). For example, Sanders et al. (1975) have reported that the clearance of plutonium from the lungs of rats was decreased to 60% of the normal rate in animals with acute pneumonia induced by beryllium oxides. The authors have also shown that delayed type-hypersensitive pneumonia impaired the alveolar clearance mechanisms of inhaled ^{198}Au-colloid particles in rats (Kubota et al. 1988). Initial pulmonary deposition of ^{198}Au-colloid was decreased in DTH rats, but in this study IAD/instilled ratio was not different among the 3 groups; that is, the initial deposition of Pu-hydroxide was not affected by Gd. The clearance of particles is impaired not only in acute but also chronic inflammation. It has been reported that clearance of particles from the lung is delayed in chronic airway disease, chronic bronchitis or pulmonary fibrosis (Camner et al. 1973; Bohning et al. 1982).

In the human respiratory tract model, the clearance rate of particles from bronchial and bronchiolar regions of the lungs in asthma, chronic bronchitis, and *mycoplasma pneumonia* are assumed 70, 50, and 30% of normal, respectively (ICRP 1994). Therefore, it appears that inflammatory reactions induced in the lung by gadolinium may be, at least in part, responsible for the delayed clearance of ^{239}Pu from the lung. Neither the lung retention of ^{239}Pu nor the population of bronchoalveolar lavage cells changed significantly in the rats

administered ^{239}Pu-hydroxide containing a low level of gadolinium (Pu-Gd-L group). This may indirectly indicate the relationship between the inflammation and delayed alveolar clearance of plutonium by gadolinium.

The urinary excretion of ^{239}Pu only increased in this Pu-Gd-L group. This may suggest the occurrence of some metabolic disturbance in the respiratory tract, but the detailed mechanisms of such a phenomenon are unclear.

The doses of gadolinium used here were 0.9 and 0.22 mg kg^{-1} body weight for Pu-Gd-H and Pu-Gd-L groups, respectively. These doses are deemed to be relevant to those exposed in a practical setting under the following conditions. The solution in nuclear fuel reprocessing in the Japanese facility contains 0.7% of gadolinium, and it is supposed that this solution is released as aerosol into the environment, it would contain 5 g water m^{-3} air, which corresponds to a dense fog (Green and Lane 1964). If the reference man breathing under a working physiological condition is exposed to the gadolinium aerosol, he will inhale 0.9 and 0.22 mg kg^{-1} body weight in 40 min and 10 min, respectively. This indicates that in the case of accidental exposure, there is a possibility that workers may be exposed to levels of gadolinium used in this study.

CONCLUSION

The present study demonstrates that the coexistence of gadolinium may influence the alveolar clearance of plutonium administered as a hydroxide colloid, although the exact mechanisms remain unclear. This indicates that when plutonium is inhaled accidentally with gadolinium and the inhaled amount of gadolinium is so high that an inflammatory reaction is induced and the physicochemical properties of plutonium hydroxide is changed, the lung retention of plutonium and thus the radiation dose in lung may become larger than in ordinary cases.

REFERENCES

Benson, J. M.; Chang, I-Y.; Cheng, Y. S.; Hahn, F. F.; Kennedy, C. H.; Barr, E. B.; Maples, K. R.; Snipes, M. B. Particle clearance and histopathology in lungs of F344/N rats and B6C3F$_1$ mice inhaling nickel oxide or nickel sulfate. Fundam. Appl. Toxicol. 28:232–244; 1995.

Black, R. M.; Drummond, J. L. A comparison of procedures for dissolving ignited plutonium oxides for analysis. Warrington, U.K.: The Reactor Group; TRG report 1072(D):1–9; 1965.

Bohning, D. E.; Atkins, H. L.; Cohn, S. H. Long-term particle clearance in man: Normal and impaired. Ann. Occup. Hyg. 26:259–271; 1982.

Camner, P.; Mossberg, B.; Philipson, K. Tracheobronchial clearance and chronic obstructive lung disease. Scand. J. Respir. Dis. 54:272–281; 1973.

Green, H. L.; Lane, W. R. Aerosol in nature. In: Particulate clouds: Dusts, smokes and mists, 2nd Ed. London: E & F. N. Spon Ltd.; 1964: 410–439.

Hirano, S.; Suzuki, K. T. Exposure, metabolism, and toxicity of rare earth and related compounds. Environ. Health Perspect. 104:85–95; 1996.

International Commission on Radiological Protection. Monitoring data for individual radionuclides: Plutonium. In: Individual monitoring for intakes of radionuclides by workers: Design and interpretation. Oxford: Pergamon Press; ICRP Publication 54, Appendix; Ann. ICRP 19(1–3); 1988: 237–273.

International Commission on Radiological Protection. Clearance of particles from the respiratory tract. In: Human respiratory tract model for radiological protection. Oxford: Pergamon Press; ICRP Publication 66, Annex E; Ann. ICRP 24(1–3); 1994: 301–413.

Ishigure, N.; Nakano, T.; Enomoto, H.; Fukuda, S.; Iida, H.; Oghiso, Y.; Sato, H.; Takahashi, S.; Yamada, Y.; Koizumi, A.; Yamada, Y.; Miyamoto, K.; Inaba, J. Lung retention of Pu following inhalation of PuO_2 in rats measured using whole body counter. J. Radiat. Res. 35:16–25; 1994.

Keough, R. F.; Powers, G. J. Determination of plutonium in biological materials by extraction and liquid scintillation counting. Anal. Chem. 42:419–421; 1970.

Kubota, Y.; Takahashi, S.; Sato, H.; Yamada, Y.; Matsuoka, O. Pulmonary deposition and clearance of inhaled or instilled ^{198}Au-colloid in the rat after the induction of pulmonary delayed type sensitivity reactions. Hoken Butsuri 23:295–302; 1988.

Lindenbaum, A.; Westfall, W. Colloidal properties of plutonium in dilute aqueous solution. Int. J. Appl. Rad. Isotopes 16:545–553; 1965.

Mizgerd, J. P.; Molina, R. M.; Stearns, R. C.; Brain, J. D.; Warner, A. E. Gadolinium induces macrophage apoptosis. J. Leukoc. Biol. 59:189–195; 1996.

Ockenden, D. W.; Welch, G. A. The preparation and properties of some plutonium compounds. Part V. Colloidal quadrivalent plutonium. J. Chem. Soc. 3358–3363; 1956.

Oghiso, Y.; Yamada, Y.; Ishigure, N.; Fukuda, S.; Iida, H.; Yamada, Y.; Sato, H.; Koizumi, A.; Inaba, J. High incidence of malignant lung carcinomas in rats after inhalation of $^{239}PuO_2$ aerosol. J. Radiat. Res. 35:222–235; 1994.

O'Neill, P. J.; Ayala, A.; Wang, P.; Ba, Z. F.; Morrison, M. H.; Schultze, A. E.; Reich, S.; Chaudry, I. H. Role of Kupffer cells in interleukin-6 release following trauma-hemorrhage and resuscitation. Shock 1:43–47; 1994.

Runge, V. M.; Parker, J. R. Worldwide clinical safety assessment of gadoteridol injection: an update. Eur. J. Radiol. 7:243–245; 1997.

Ruttinger, D.; Vollmar, B.; Wanner, G. A.; Messmer, K. *In vivo* assessment of hepatic alterations following gadolinium chloride-induced Kupffer cell blockade. J. Hepatol. 25:960–967; 1996.

Sanders, C. W.; Cannon, W. C.; Powers, G. J.; Adee, R. R.; Meier, D. M. Toxicology of high-fired beryllium oxide inhaled by rodents I. Metabolism and early effects. Arch. Environ. Health 30:546–551; 1975.

Sato, H.; Bulman, R. A.; Takahashi, S.; Kubota, Y. Effects of macromolecular chelating agents on the release of ^{239}Pu and ^{59}Fe from rat alveolar macrophages after phagocytic uptake of ^{239}Pu-^{59}Fe-iron hydroxide colloid. Health Phys. 66:545–549; 1994.

Slauson, D. O.; Lay, J. C.; Castleman, W. L.; Neilsen, N. R. Acute inflammatory lung injury retards pulmonary particle clearance. Inflammation 13:185–199; 1989.

Suzuki, S.; Nakamura, S.; Serizawa, A.; Sakaguchi, T.; Konno, H.; Muro, H.; Kosugi, I.; Baba, S. Role of Kupffer cells and

the spleen in modulation of endotoxin-induced liver injury after partial hepatectomy. Hepatology 24:219–225; 1996.

Takahashi, S.; Sato, H. New method to estimate the solubility of radioactive particles in the respiratory tract: Comparison of solubility between ^{59}Fe- ^{239}Pu-hydroxide colloid particles. Hoken Butsuri 26:351–353; 1991.

Weinmann, H. J.; Brasch, R. C.; Press, W. R.; Wesbey, G. E. Characterization of gadolinium-DTPA complex: a potential NMR contrast agent. Am. J. Roentgenol. 142:619–624; 1984.

Yoneda, S.; Yoneda, N.; Emi, Y.; Fujita, M.; Ohmichi, S.; Hirano, S.; Suzuki, K. T. Effects of gadolinium chloride on the rat lung following intratracheal instillation. Fundam. Appl. Toxicol. 28:65–70; 1995.

■ ■

ELSEVIER

Developmental Brain Research 114 (1999) 99–108

DEVELOPMENTAL BRAIN RESEARCH

Research report

Different patterns of abnormal neuronal migration in the cerebral cortex of mice prenatally exposed to irradiation

Xue-Zhi Sun [a,*], Sentaro Takahashi [a], Yoshihiro Fukui [b], Setsuji Hisano [c], Yoshihisa Kuboda [a], Hiroshi Sato [a], Minoru Inouye [d]

[a] *The 4th Research Group, National Institute of Radiological Sciences, Chiba 263-8555, Japan*
[b] *Department of Anatomy, School of Medicine, Tokushima University, Tokushima 770-8503, Japan*
[c] *Department of Anatomy, Institute of Basic Medical Sciences, University of Tsukuba, Tsukuba, Ibaraki 305-8575, Japan*
[d] *Department of Teratology and Genetics, Division of Molecular and Cellular Adaptation, Research Institute of Environmental Medicine, Nagoya University, Nagoya 464-01, Japan*

Accepted 9 February 1999

Abstract

A characteristic abnormal cortical architecture in the adult brain was produced in mice subjected to 1.5 Gy of X-irradiation on embryonic day 14. Neurons in the lateral regions were organized into an essentially six-layered structure, while neurons in the dorsal regions formed a unique four-layered cortex. The patterns of neuronal migration in these different cortical regions were examined with immunohistochemistry for anti-bromodeoxyuridine (BrdU), anti-midkine (MK), and anti-glial fibrillary acidic protein (GFAP) antibodies. In the cortical lateral region, BrdU-labeled cells in the upper layers were fewer, and those in lower layers more numerous in prenatally irradiated mice than in control, while in the dorsal region (four-layered region), BrdU-labeled cells were very few in layer 2, and a large number of labeled-cells remained in layer 4. These results indicated that some neuroblasts in the lateral cortical region could not migrate to the upper layers, and that most neuroblasts in the dorsal cortical region failed to pass through the earlier migration zone. MK- and GFAP-stained radial glial fibers showed that the radial fibers were consistently oriented in the direction of neuronal migration in the control brains. However, in the irradiated brain, such radial fibers were crumpled in the lateral region, or were reduced markedly in number in some parts of the dorsal region. These results revealed that neuronal migratory pathways (radial glial fibers) were destroyed differently in different regions, and that X-rays killed some cells including radial glial cells or their precursors during the embryonic stage. These effects of radiation on the developing brain may result from the possibility that neurogenetic time is different or there are cellular mechanisms involved in the radiosensitivity among different regions.

Keywords: Bromodeoxyuridine; Disorder of neuronal migration; Glial fibrillary acidic protein; Midkine; Neuroblast; Radial glial fiber

1. Introduction

The developing brain is known to be one of the fetal structures most susceptible to radiation. This high vulnerability of the fetal brain is a distinctive teratological characteristic commonly recognized in all mammalian species including human beings [15,16]. A characteristic brain malformation may be the result of many developmental processes, depending on when the fetus was exposed to radiation, the amount of radiation, and the type of species. We have examined the patterns of brain malformation in 6-week old mice prenatally exposed to doses of X-irradiation ranging from 0.5 to 2.0 Gy on day 1 from embryonic days 12 to 19 (E12–E19) and found that different types of cortical malformation were induced at different doses or different periods of cortical neurogenesis. Among these different types of cortical malformation, a characteristic abnormal cortical architecture was found in mice subjected to 1.5 Gy on E14: (a) a four-layered cortex appeared in the dorsal region but not in the lateral cortex; (b) the cellular structure of the cortex in the lateral region showed minor changes but the lamination was essentially normal; (c) groups of ectopic cells forming ectopic gray matter were located below the subcortical white matter. These biological effects of irradiation on the developing brain might be responsible for cell death and abnormal neuronal migration

* Corresponding author. Fax: +81-43-251-4853; E-mail: sun_s@nirs.go.jp

0165-3806/99/$ - see front matter
PII: S0165-3806(99)00029-2

[40]. We were interested to know the histogenesis of brain malformations of this type, especially for the four-layered cortical pattern, because a similar brain malformation can also be found in human lissencephaly type I, in which it is suspected that neurons destined for the upper cortical layers fail to migrate to their normal position and accumulate below the external cellular layer [2,5,10,41].

In order to study the cytokinetics occurring in the course of histogenesis of the neocortex, 5-bromo-2-deoxyuridine (BrdU) was chosen as a marker to label migrating cells [14,38,46]. Like ^{3}H thymidine, BrdU is incorporated into nuclear DNA, but it is neither radioactive or myelotoxic at the doses used [8,12,25,37]. To study the possibility that abnormalities in migration could be related to the abnormal guidance of neuroblasts, glial fibrillary acidic protein (GFAP) was chosen as a mark to analyze radial glial cells in the developing brain [3,31,39,48]. In view of the fact that the GFAP-immunoreactive glial fibers were observed markedly only after birth in the mouse cerebrum [44], radial glial fibers were also examined by means of midkine (MK) immunocytochemistry in the present study. MK is a new heparin-binding growth/differentiation factor specified by a retinoic acid-responsive gene [17,28]. It is the first number of a new protein family of developmentally regulated cytokines with diverse biological activities. MK is mitogenic for certain fibroblastic cell lines, and enhances both neurite outgrowth and the survival of various embryonic neuron types [26,27,43,49]. Increased expression of MK was detected on the processes of radial glial cells in the developing mouse and rat cerebral cortex [18,20,29]. Such radial glial fibers stained with anti-MK antibody were similar to those fibers stained with anti-vimentin (Vim) antibody in a distinct fashion during the embryonic stage [44]. Therefore, MK may be useful for the analysis of gliogenesis in the early stages of the developing central nervous system.

2. Materials and methods

2.1. Animals

A closed colony of Slc:ICR mice obtained from the Shizuoka Laboratory Animals Center (Shizuoka, Japan) was kept in a controlled atmosphere of 23 ± °C with 55 ± 5°C humidity under a 12-h dark/light cycle. They were given commercial laboratory food, CA-2, and tap water ad libitum. Eight-week old nulliparous females were paired with potent males in cages overnight and checked for vaginal plugs the next morning. The day on which a vaginal plug appeared was regarded as day 0 of pregnancy.

2.2. Treatment

Pregnant mice were subjected to a single whole-body exposure of X-irradiation at a dose of 1.5 Gy on E14. Pregnant control mice were sham-treated. The pregnant mice of both groups were then injected intraperitoneally (i.p.) with the thymidine analog BrdU (30 mg/kg b.wt; Becton Dickinson, USA) at E16 in order to label neurons normally committed to the upper cortical layers [22,32]. Some mice were allowed to give birth and rear their litters. Two mice were randomly selected for evaluation at each experimental stage when about five fetuses and pups were examined. Between 6 h after exposure and postnatal day 28 (P28), the brains from fetuses and pups were extracted and removed for study as follows.

2.3. Experimental techniques

For histological examination, brains were fixed in Bouin's solution, dehydrated, embedded in paraffin, and

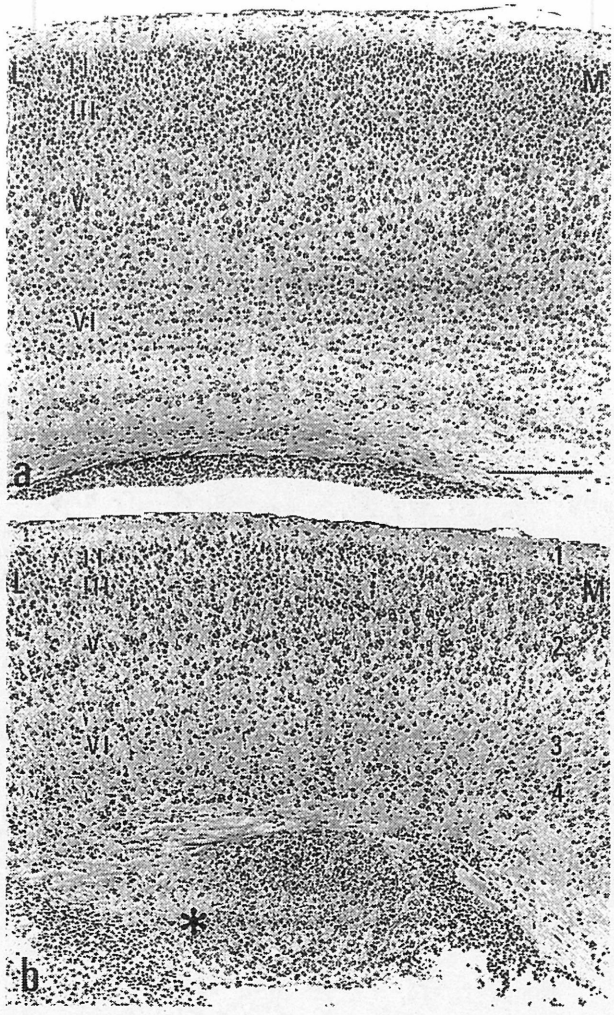

Fig. 1. Cerebral cortex of 1-week old mice. (a) In control cortex, a laminar pattern of six layers (from I to VI) can be observed clearly. (b) In the irradiated cerebral cortex, a basic cellular structure of six layers can be recognized in the lateral cortex, but not in the dorsal region. Layers II, III and IV from the lateral cortical region to the dorsal cortical region become progressively thinner and unclear, and neurons in the dorsal cortex form a unique four-layered cortex. Between the two specific laminar patters, no specific layers can be defined because of the disarranged cytoarchitecture. Ectopic cell mass (asterisk) is situated beneath layer VI and is separated from layer VI by a thin band of fibers. L: Lateral, M: medial. HE stain. Scale bar = 150 μm.

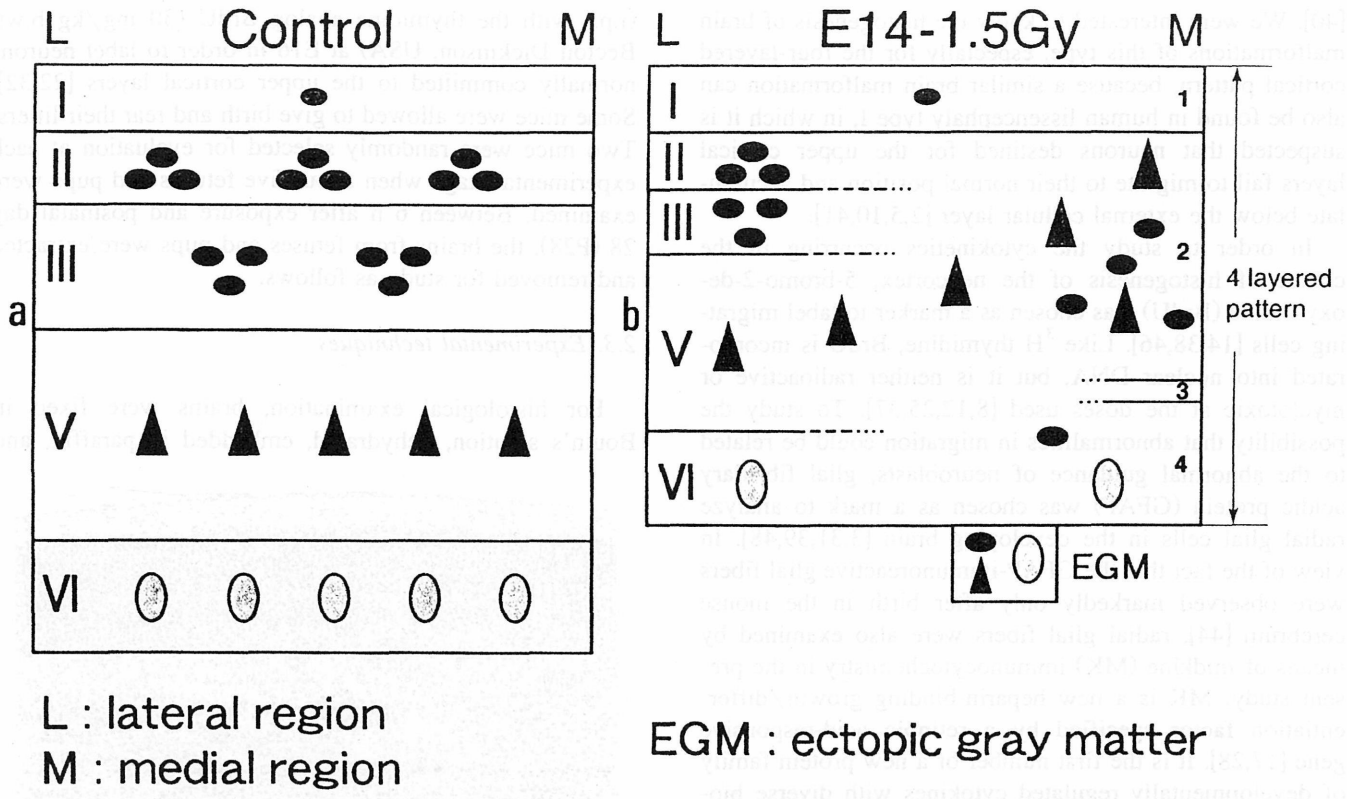

Fig. 2. Schematic drawings summarizing the laminar patterns of cerebral cortex in 4-week old mice.

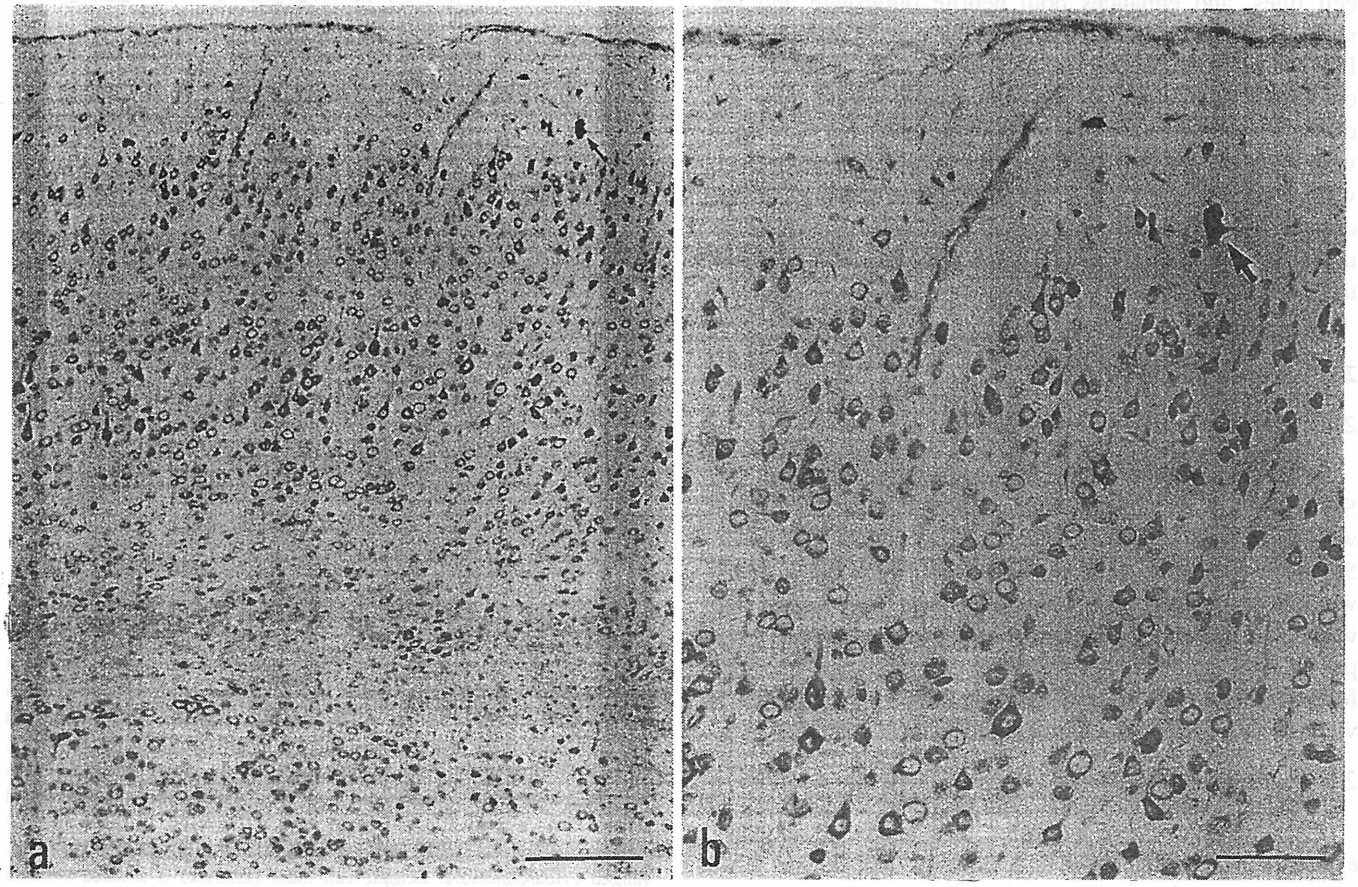

Fig. 3. Cerebral cortex of 4-week old mice irradiated on E14. (a) The large pyramidal cell is aberrantly located below the molecular layer (arrow). (b) Higher magnification of the same photomicrograph showing the abnormal orientation of the large pyramidal cell (arrow). Luxol fast blue stain. Scale bar: $a = 250$ μm; $b = 50$ μm.

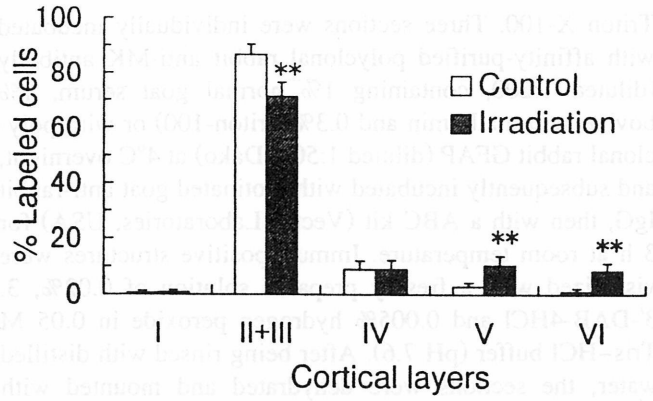

Fig. 4. Histogram showing the distribution of BrdU-labeled cells in the lateral regions of field 3 of cerebral cortex in 4-week old mice (mean ± S.D.; $n = 5$ in each group). **Significantly different from the control group at $P < 0.01$ (Student's t-test).

serially sectioned in a frontal plane at 5 μm. The sections were stained with hematoxylin and eosin (HE) or Luxol fast blue. Because field 3 of Caviness [4] and Krieg [19] is the most completely stratified of all the cortical areas, the histological sections through field 3 in the adult brain or parietal areas in immature cerebral mantle from the fetuses and litters that corresponded to the adult field 3 were selected from each brain for the following examinations.

For BrdU immunohistochemical examination, samples were fixed with 5% acetic acid in 80% ethanol at 4°C overnight, then dehydrated in graded ethanol. Brains were embedded in paraffin and sectioned at 5 μm in the frontal plane. For each brain, three sections were selected and mounted on glass slides that had been previously coated with a mixture of equal amounts of glycerol and 10% albumin. These sections were deparaffinized with xylene, rehydrated in graded ethanol, and rinsed with 0.1 M phosphate buffered saline (PBS, pH 7.4). Following 8 min in 1 N HCl at 60°C to partially hydrolyze the double-stranded DNA into single strands, the sections were neutralized with 0.1 M sodium borate (pH 8.5) for 5 min, and washed with 0.1 M PBS containing 0.3% Triton X-100 for 30 min. The sections were incubated with anti-BrdU monoclonal antibody (diluted 1:100 in PBS with 1 mg/ml bovine serum albumin, pH 7.4; mouse IgG heavy chain and kappa light chain, Becton Dickinson) at 37°C for 60 min. These sections were sequentially incubated with goat

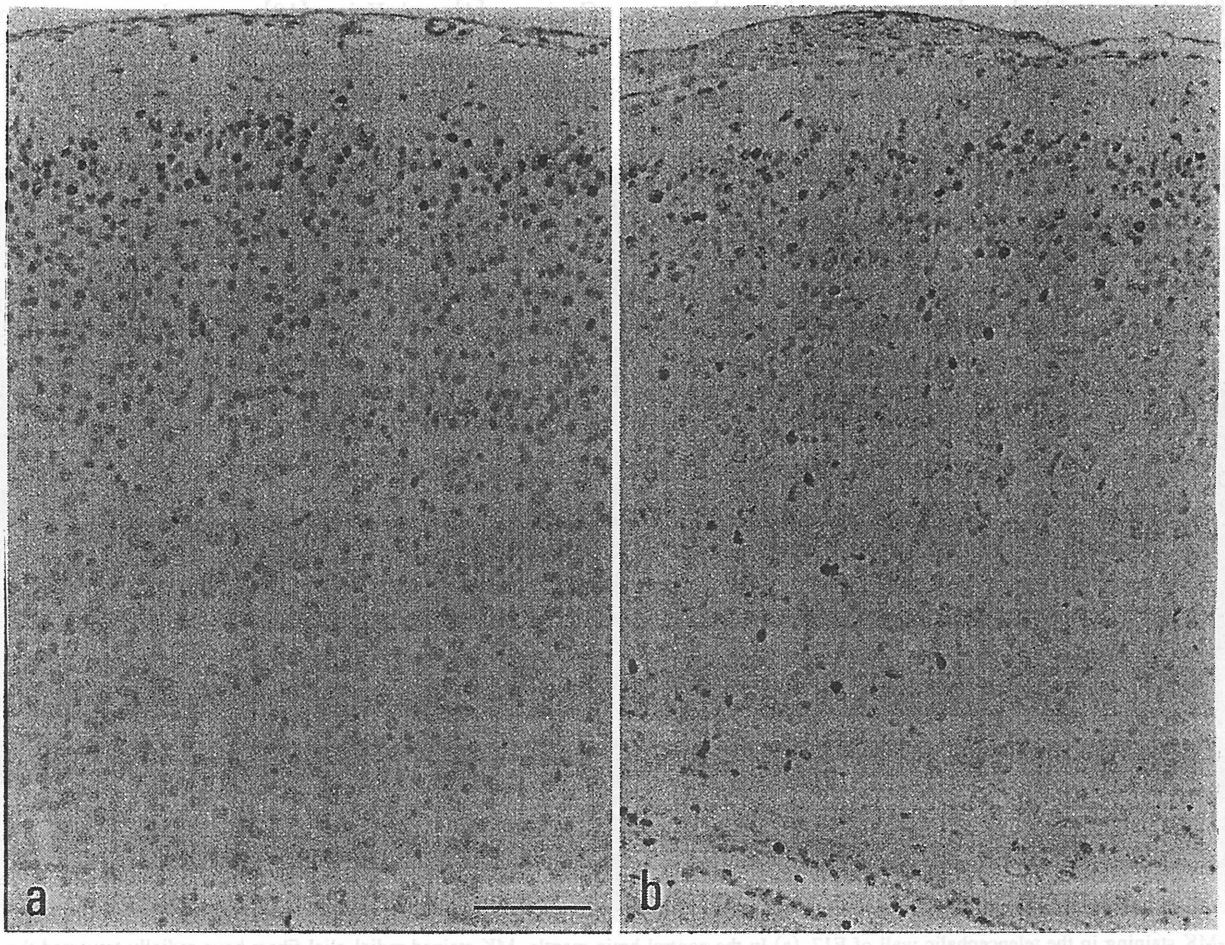

Fig. 5. Anti-BrdU staining in the dorsal region of the cerebral cortex of 1-week old mice. (a) In the control cortex, most labeled cells are located in the upper layers, whereas few labeled cells can be observed in the lower layers. (b) In the irradiated cortex (four-layered region), labeled cells are deficient in layer 2, but numerous in layer 4. Scale bar = 100 μm.

anti-mouse IgG (H + L) biotinylated secondary antibody (diluted 1:220, CALTAG) at 37°C for 30 min, and then in an avidin–biotin–horseradish peroxidase complex (diluted 1:800) for 60 min, followed by development of the reaction product with 3,3′-diaminobenzidine (DAB, Sigma) and hydrogen peroxide, resulting in the formation of a brown precipitate in the nuclei of BrdU-labeled cells. They were then counter-stained with HE and examined under a light microscope.

For MK and GFAP immunohistochemical examination, samples were fixed with Zamboni's solution (4% formaldehyde and 0.2% picric acid in 0.1 M PMS, pH 7.4) at 4°C overnight. The brains were immersed in 20% sucrose at 4°C for 1 day and embedded in 10% gelatin at 4°C for 2 days, then snap-frozen by carbon dioxide gas, cut in the frontal plane (5–15 μm thickness) through the entire cerebrum by cryostat (CM 1800, Leica, Germany), and thaw-mounted onto poly-L-lysine-treated glass slides. The dissection and orientation of the tissue blocks were given special attention. The tissue blocks through the full thickness of the cerebral cortex were dissected as nearly as possible perpendicular to the longitudinal axis of the cerebral hemisphere. For each brain, six sections were selected for treatment with 0.6% hydrogen peroxide in 80% methanol for 5 min to block endogenous peroxide activity, then rinsed three times with 0.1 M PBS containing 0.3% Triton X-100. Three sections were individually incubated with affinity-purified polyclonal rabbit anti-MK antibody (diluted 1:200, containing 1% normal goat serum, 1% bovine serum albumin and 0.3% Triton-100) or with polyclonal rabbit GFAP (diluted 1:500, Dako) at 4°C overnight, and subsequently incubated with biotinated goat anti-rabbit IgG, then with a ABC kit (Vector Laboratories, USA) for 3 h at room temperature. Immunopositive structures were visualized with a freshly prepared solution of 0.02%, 3, 3′-DAB-4HCl and 0.005% hydrogen peroxide in 0.05 M Tris–HCl buffer (pH 7.6). After being rinsed with distilled water, the sections were dehydrated and mounted with resin.

The control mice were processed in the same manner as the treated animals.

2.4. Quantitative study

Histological examination showed that the cellular structure of the cortex in the lateral region was essentially normal. In order to know whether neuronal migration was affected by irradiation in this region, a quantitative study was performed in 4-week old mice. As mentioned above, histological sections which corresponded to field 3 of Caviness [4] and Krieg [19] were chosen to count the number of BrdU-labeled cells in the cortical layers of the

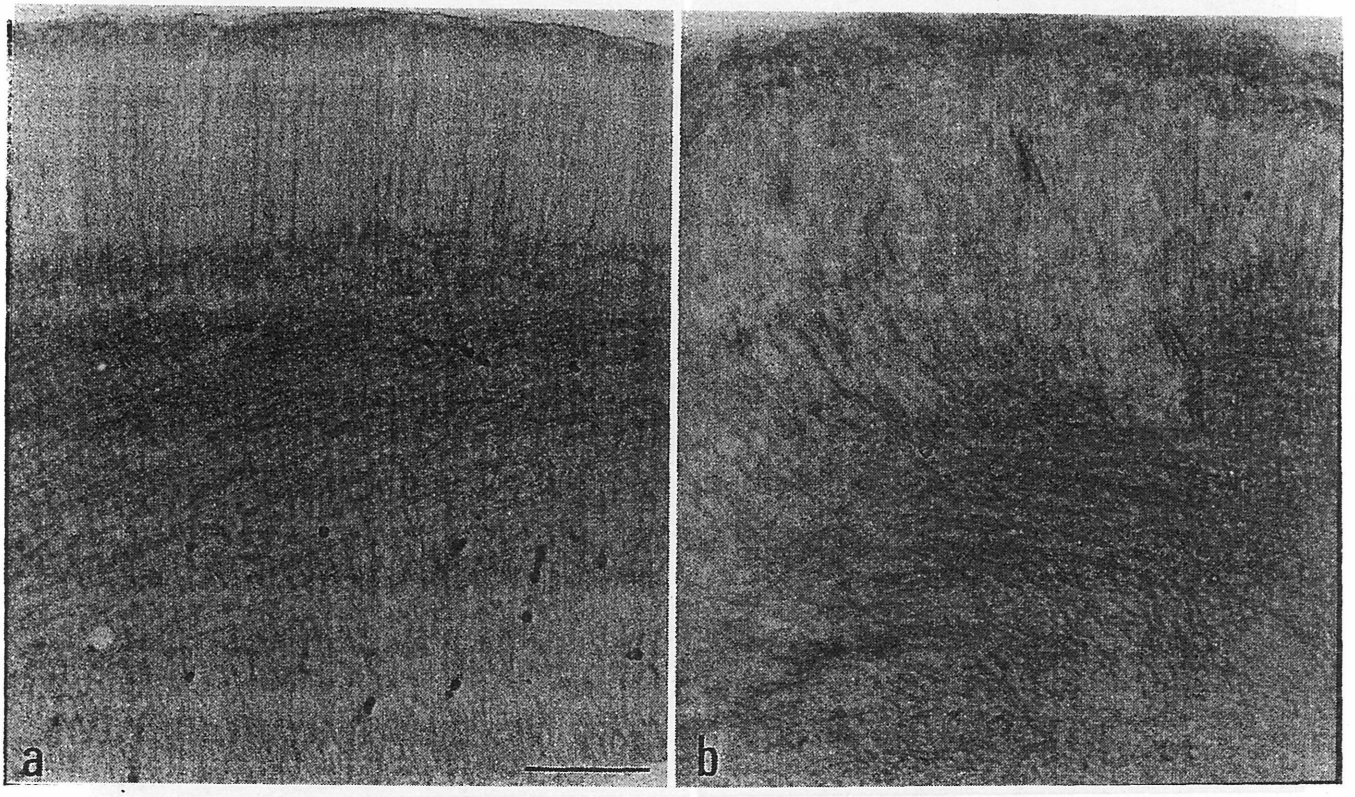

Fig. 6. Anti-MK staining in the telencephalic wall of E17. (a) In the control brain mantle, MK-stained radial glial fibers have radially traversed the entire distance from the ventricular zone to the pial surface, and their orientation is always consistent with the direction of neuronal migration. (b) In the irradiated brain mantle, radial glial fibers are disorganized, and their courses have taken a different direction. Some of them are no longer perpendicular to the surface of the cortex. MK-immunoreactive fibers cannot be found in some parts of the dorsal region. Scale bar = 100 μm.

lateral region. BrdU-labeled cells were counted in the lateral regions bounded by two parallel lines of the same length, and the labeled cells in different layers were compared by Student's *t*-test between irradiated mice and controls. *P*-values of less than 0.05 were considered significant.

3. Results

Extensive cell death occurred 6 h after exposure (E14), and dead cells disappeared by 48 h after exposure. Following cellular remodelling, some bizarre cellular structures appeared temporarily in the irradiated brain during the embryonic period. The cortical abnormality could be defined in more detail as maturation processed. In postnatal mice, a laminar pattern of cortical neurons (six layers) was observed only in the lateral region of the brains irradiated at E14 (Figs. 1b and 2b). Layer I was readily detected, and the inner layers (layers V and VI) were recognized through the presence of large pyramidal cells. Layers II, III and IV formed bands of different densely packed cells. However, layers II, III and IV from the lateral cortical region to the dorsal cortical region became progressively thinner and unclear. In the mid-dorsal region, a four-layered cortical organization had formed (Figs. 1b and 2b). The four-layered sequence consisted of layer 1, corresponding to the molecular layer, layer 2 located in the upper cellular layer, layer 3 which was a sparsely cellular zone, and layer 4 which contained heterotopic neurons. Layer 2 harbored an external lamina of large cells that connected with layer V in the lateral cortex. The large pyramidal cells located just below the molecular layer could also be found in the mid-dorsal region. The primary dendrites of these large pyramidal cells appeared not to be normally oriented towards the cortical surface (Fig. 3). Another obvious malformation was the ectopic cell masses that formed beneath layer VI and were separated from layer VI by a thin band of fibers; no specific cell layers could be identified in these ectopic cell masses (Fig. 1b, Fig. 2b).

After 24 h of BrdU injection, BrdU-labeled cells were observed only in the ventricular zone of normal cortex or in the partially preserved ventricular zone of irradiated brain. Migration of labeled cells to the cortical plate, the future neocortex, started from here in a radially centrifugal fashion. From P7 onwards, almost all labeled cells seemed to finish complete their migration, and the distributive pattern of labeled cells was no longer changed. These

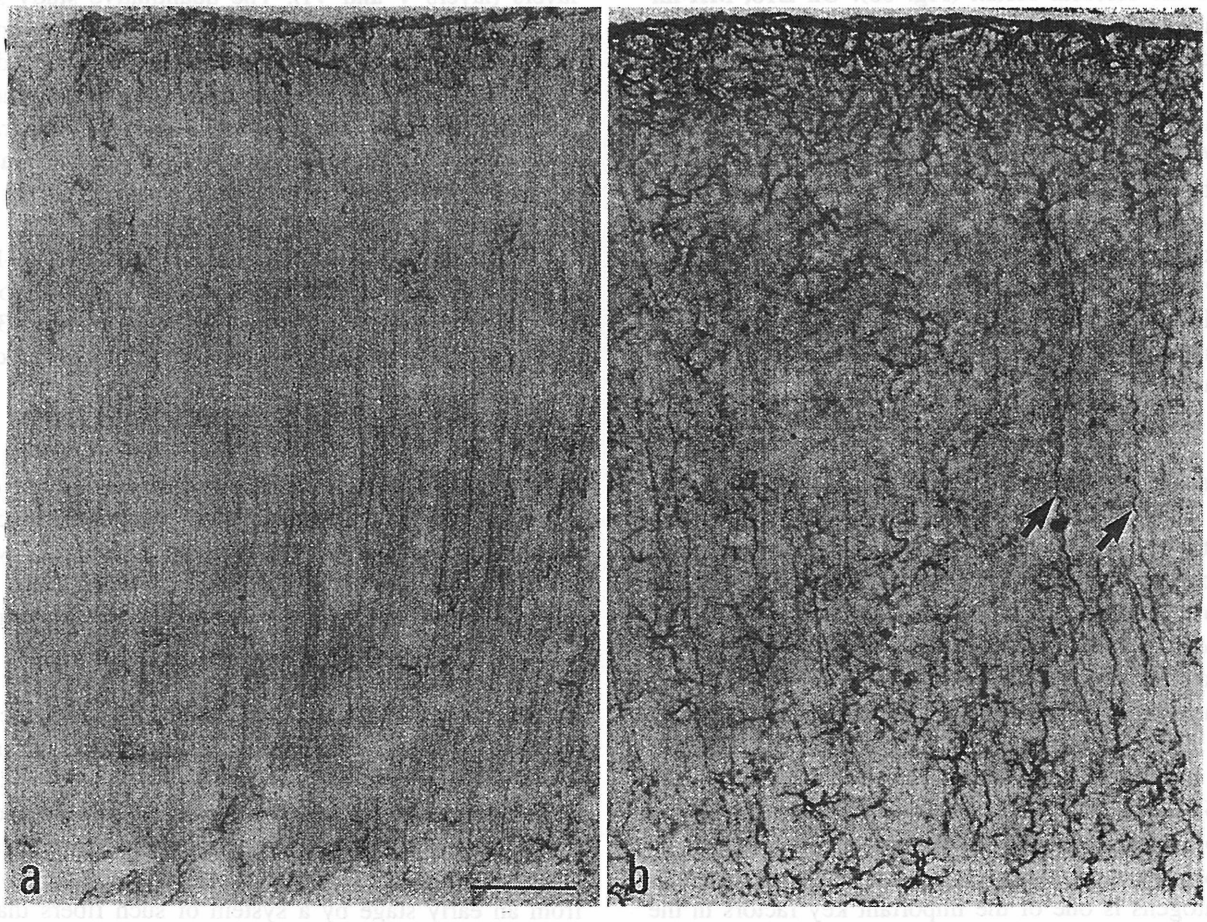

Fig. 7. Anti-GFAP staining in the cerebral cortex of P4. (a) In the control cortex, radial glial fibers are straight and perpendicular to the pial surface. (b) In the irradiated cortex, radial glial fibers are crumpled (arrows) and many astrocytes appear. Scale bar = 100 μm.

labeled cells in normal cortex were distributed widely in layers II and III, and continued to form an immunoreactive cell zone, with few labeled cells found in layers V and VI. A similar distribution of BrdU-labeled cells was observed in the lateral cortex region of irradiated mice, but quantitative study revealed significantly different distribution patterns in the lateral region between the irradiated animals and controls. The labeled cells in layers II to IV were fewer, and those in layers V and VI more numerous in irradiated mice than in controls (Fig. 4). In the region of the four-layered cortex, BrdU-labeled cells were so scarce in the upper layers that the immunoreactive cell zone was interrupted in layer 2, and a large number of labeled cells appeared in layer 4 (Fig. 5b).

MK-immunoreactive radial glial fibers in the brain mantle were detected during the embryonic period but could be not observed in the postnatal cerebral cortex. On E17, the radial glial fibers had radially traversed the entire distance from the ventricular zone to the pial surface in the control brain, and their courses were initially parallel to each other and perpendicular to the pial surface which was oriented in the direction of neuronal migration (Fig. 6a). In the irradiated brain, the MK-immunoreactive fibers formed several fascicles which changed their course in different directions, and could not be found in some parts of the dorsal region of the cerebral cortex (Fig. 6b). On E18, MK-immunoreactive fibers had decreased dramatically in number as had the intensity of staining for MK both in the control and the irradiated brain. At the same time, GFAP-immunoreactive fibers in the brain mantle first appeared. By P4, GFAP-stained fibers became more evident. In the control brain, these fibers were regularly distributed and perpendicular to the pial surface (Fig. 7a), while in the irradiated brain the fibers were crumpled and a number of fibrillary astrocytes appeared (Fig. 7b). In the following postnatal days, the radial glial fibers became progressively fewer, and disappeared completely about P21 both in control and irradiated groups.

4. Discussion

Prenatal exposure to several neuroteratogens during different embryonic stages, such as ionizing radiation, ethanol, and cytotoxic drugs (e.g., methylazoxymethanol acetate, MAM), can induce cortical laminar disorganization with varied patterns and formation of ectopic neurons. These biological effects of neuroteratogens have been presumed to result from cell death and interference with normal neuronal migration, presumably via effects on radial glia [23,24,45,50,51]. Numerous studies have revealed that a pattern of cortical laminar disorganization is decided by many developmental processes, but the time of exposure to neuroteratogens is one of the important key factors in the development of a lamina-specific pattern. Treatment of pregnant mice with MAM at E13 resulted in cortical hypoplasia that affected all but the first cortical layer, treatment at E15 caused a statistically significant reduction in cell density in the superficial layers, whereas treatment at E17 caused an alterable arrangement of the cortical layers, which were not easily separable, since MAM in perhaps limiting glial cell proliferation, modified the subsequent migration mechanisms [6,7]. Similar results also have been reported in the study of lamina-specific deletion of neurons in the monkey brain by irradiation at selected prenatal stages [1].

In our study, different distributive patterns of neurons were observed in different regions of the neocortex in mice prenatally irradiated at E14. Neurons in the lateral region were organized into an essential six-layered structure, while neurons in the dorsal regions formed a unique four-layered cortex.

In the lateral cortical region of irradiated brain, histological examination showed that the normal sequence of different layers was preserved, despite the thickness of each layer being less than that of control. However, BrdU-immunocytochemical study indicated that the migration of cortical neuroblasts in the lateral region of the animals irradiated was not really 'normal.' A high proportion of the labeled cells migrated to the upper cortical layers (layers II and III), but some remained in the lower cortical layers (layers V and VI). The quantitative study showed statistically significant differences in the distribution of the labeled cells between irradiated and sham-exposed mice. The labeled cells in the upper layers were fewer, and those in the lower layers more numerous in prenatally irradiated mice than in controls. These results suggested that some neuroblasts failed to migrate to the upper layers in the lateral cortical region.

On the other hand, in the dorsal region, a four-layered cytoarchitecture was identified; layer 1 was the molecular layer, layer 2 was the external cellular layer, layer 3 was a sparsely cellular zone, and layer 4 was the internal cellular layer. Because layer 2 was formed by an external lamina of large cells which continued to layer V and VI of the lateral region, layer 4 consisted of neurons which would have migrated to the upper layers in the normal cortex. BrdU-immunocytochemical study demonstrated that BrdU-labeled cells were very few in layer 2, whereas numerous labeled-cells appeared in layer 4. These results confirmed that the labeled cells in layer 4 were generated at the same time as those in layers II and III in the lateral cortex. These cells failed to pass through the earlier migration zone, so that large pyramidal neuron (a characteristic of layer V which formed earlier than layers II and III) appeared in layer 2.

The abnormal neuronal migration could be responsible for radial glial fibers injured by X-irradiation because it is well known that the migration of neuroblasts is guided from an early stage by a system of such fibers that span the width of the thickening telencephalon [30,33–35]. Therefore, the radial glial fibers were detected with a

technique combining MK- and GFAP-immunocytochemistry. MK-stained radial glial fibers were observed from the embryonic stage and disappeared after birth. The appearance of MK-stained radial glial fibers was consistent with the developmental stage of the brain when proliferated ventricular neuroblasts start to migrate to the cortical area [43]. During an earlier embryonic period (from E13 to E17), MK-stained radial glial fibers could be observed clearly. These fibers, spanning the cerebral wall from the ventricular zone to the pial surface, were consistently oriented in the direction of neuronal migration and traversed the cortical plate itself in a straight line in the control brains. However, such fibers were crumpled in the lateral region of brains following 1.5 Gy irradiation. Obviously, to travel such a disoriented pathway, some neuroblasts could not migrate to their proper position. Moreover, one notable finding of the present study was that MK-stained radial glial fibers were markedly reduced in number in the some parts of the dorsal region. Radial glial fibers which ordinarily projected radially from the ventricular zone to the surface of the cerebral mantel were seldom found there. These results revealed that neuronal migratory pathways (radial glial fibers) were almost destroyed in some parts of the dorsal region and that X-rays might have killed some cells including radial glia cells or their precursors.

Similar feature of radial glia cells stained with anti-GFAP antibody were observed in the postnatal brains. About P4, clearly immunoreactive radial glial cells with anti-GFAP became evident in both control and irradiated brains. In the control brains, such fibers projected radially from the ventricular zone to the upper wall of the cerebral mantle, while in the irradiated brains they were disorganized, and numerous astrocytes appeared. The fact that numerous protoplasmic transitional forms were displaced by astrocytes indicated the presence of reactive gliosis as the response of a brain exposed to irradiation.

It was of importance to inquire why different types of cerebral malformations produced in the same cerebral cortex appeared after irradiation, and why a four-layered pattern was found only in the dorsal region but not in the lateral region. To answer such questions, the possibility of 'proliferative units' was considered. Studies of neurogenesis and neurogenetic gradients have indicated that neurons produced within individual proliferative units align themselves along a radial glial fascicle and enter the developing cortical plate where they form ontogenetic columns [36,47]. If the generation of cortical neuroblasts was not synchronous and uniform throughout the periventricular germinal layer, irradiation could only destroy proliferative units which were susceptible at the time of exposure to X-irradiation. Therefore, some ontogenetic columns might become normally developing units, and the migratory pathway could be preserved, whereas others might be completely destroyed. Such destroyed proliferative unites occurring in the dorsal region but not in the lateral region may demonstrate that the neurogenetic time is different or that there are cellular mechanisms possibly involved in the radiosensitivity among different regions. Further studies are need to clarify these points.

A four-layered pattern of cortical malformation can also be found in human lissencephaly type I [9–11]. It has been identified as the eponymous, the Miller–Dieker and Norman–Roberts syndromes in recognition of the first authors [21]. A number of studies on human lissencephaly type I have shown that neurons destined for the upper cortical layers fail to migrate to their normal positions and remain below the external cellular layer [5,41]. Although the phenotype of brain malformation in humans was similar to animal models in this experiment, the agents inducing a four-layered cortex were different. Patients with Miller–Dieker syndrome often present combined with the anomaly of a short arm of chromosome 17 [9,11,42].

Another evident malformation in the neocortex of prenatally irradiated mice was the formation of groups of ectopic cells located below the subcortical white matter. Previous descriptions of the recovery of the germinal neuroepithelium from prenatal irradiation indicated that migrating cells detained along the migratory pathway (within the cortex) might result from an aberrant or partially broken migratory pathway, while the formation of the ectopic masses might result from a complete failure of migrating neuroblasts [45]. The neuroblasts which failed completely to migrate curled up and continued to proliferate to form the ectopic masses. Such ectopic masses may be produced at some time during cortical neurogenesis by irradiation, with larger masses forming at an earlier stage of brain development, and smaller ones at a later stage [13]. The size of these ectopic masses resulting from irradiation at different stages may depend on how severely the migratory pathways (radial glial fibers) were disturbed and how many neuroblasts failed to migrate. In the present study, the finding that a large number of MK-stained radial glial fibers appeared around E14 of mice may suggest that E14 is the time when neuronal migration waves reached their peak. Thus, ectopic masses in mice exposed at E14 caused the larger ectopic cell masses.

In addition, the present observations showed that the orientations of the apical dendrites of some large pyramidal neurons were changed so as not to be normally oriented towards the cortical surface in the irradiated animals. It is thus conceivable that the neuronal pathway might be affected due to an alteration in the dendrites of large pyramidal neurons. To study the structural disorders of neuronal pathways following irradiation may be a valuable subject for future study.

Acknowledgements

We wish to thank Mr. I. Shimada for his preparation of the photographs.

References

[1] O. Algan, P. Pakic, Radiation-induced, lamina-specific deletion of neurons in the primate visual cortex, J. Comp. Neurol. 381 (1997) 335–352.

[2] P.G. Barth, Disorders of neuronal migration, Can. J. Neurol. Sci. 14 (1987) 1–16.

[3] A. Bignami, T. Raju, D. Dahl, Localization of vimentin, the non-specific intermediate filament protein, in embryonic glia and in early differentiating neurons, Dev. Biol. 91 (1983) 286–295.

[4] V.S. Caviness, Architectonic map of neocortex of the normal mouse, J. Comp. Neurol. 164 (1975) 247–264.

[5] V.S. Caviness, R.S. Williams, Cellular Pathology of the Human Cortex. Congenital and Acquired Cognitive Disorders, Raven Press, New York, 1979, 69–89.

[6] S. Ciaroni, T. Cecchini, P. Ambrogini, G. Minelli, P. Del Grande, Nerve cell rearrangement in neocortical layers of MAM treated fetal mice, J. Hirnforsch. 33 (1992) 303–310.

[7] S. Ciaroni, T. Cecchini, G. Gazzanelli, P. Del Grande, Methylazoxymethanol acetate (MAM ac) effects on the ontogenesis of the mouse neocortex, J. Hirnforsch. 30 (1989) 699–705.

[8] P.N. Dean, F. Dolbeare, H.G. Gratzner, G.C. Rice, J.W. Gray, Cell cycle analysis using a monoclonal antibody to BrdUrd, Cell Tissue Kinet. 17 (1984) 427.

[9] W.B. Dobyns, The neurogenetics of lissencephaly, Neurogen. Dis. 7 (1989) 89–105.

[10] W.B. Dobyns, F.R. Stratton, F. Greenberg, Syndromes with lissencephaly: I. Miller–Dieker and Norman Roberts syndromes and isolated lissencephaly, Am. J. Med. Genet. 18 (1984) 509–526.

[11] W.B. Dobyns, R.F. Stratton, J. Parke, Miller–Dieker syndrome: lissencephaly and monosomy 17p, J. Pediatr. 102 (1983) 552–558.

[12] F.A. Dolbeare, H.G. Gratzner, M.G. Pallavicini, J.W. Gray, Flow cytometric measurement of total DNA content and incorporated bromodeoxyuridine, Proc. Natl. Acad. Sci. USA 80 (1983) 5573.

[13] I. Ferrer, Experimentally-induced cortical malformations in rats, Child's Nerv. Syst. 9 (1993) 403–407.

[14] H.G. Gratzner, Monoclonal antibody to 5-bromo and 5-iododeoxyuridine: a new reagent for detection of DNA replication, Science 218 (1982) 474–475.

[15] Y. Kameyama, High vulnerability of the developing fetal brain to ionizing radiation and hyperthermia, Environ. Med. 33 (1989) 1–17.

[16] Y. Kameyama, M. Inouye, Irradiation injury to the developing nervous system: mechanisms of neuronal injury, Neurol. Toxicol. 15 (1994) 75–80.

[17] I. Kovesdi, J.L. Fairhurst, P.J. Kretschmer, P. Bhlen, Heparin-binding neurotrophic factor (HBNF) and MK, members of a new family of homologous, developmentally regulated proteins, Biochem. Biophy. Res. Commun. 172 (1990) 850–854.

[18] P.J. Kretschmer, J.L. Fairhurst, M.M. Decker, C.P. Chan, Y. Gluzman, P. Bhlen, I. Kovesdi, Cloning, characterization and developmental regulation of two members of a novel human gene family of neurite outgrowth-promoting proteins, Growth Factors 5 (1991) 99–114.

[19] W.J.S. Krieg, Connections of the cerebral cortex: I. The albino rat. A. Topography of the cortical areas, J. Comp. Neurol. 84 (1946) 221–275.

[20] K. Matsumoto, A. Wanaka, K. Takatsuji, H. Muramatsu, T. Muramatsu, M. Tohyama, A novel family of heparin-binding growth factors, pleiotrophin and midkine, is expressed in the developing rat cerebral cortex, Dev. Brain Res. 79 (1994) 229–241.

[21] J.Q. Miller, Lissencephaly in 2 siblings, Neurology 13 (1963) 841–850.

[22] M.W. Miller, Development of projection and local circuit neurons in neocortex, Development and Maturation of the Cerebral Cortex, Vol. 17, Plenum, New York, 1988, 133–175.

[23] M.W. Miller, Migration of cortical neurons is altered by gestational exposure to ethanol, Alcohol. Clin. Exp. Res. 17 (1993) 304–314.

[24] M.W. Miller, S. Robertson, Prenatal exposure to ethanol alters the postnatal development and transformation of radial glia to astrocytes in the cortex, J. Comp. Neurol. 337 (1993) 253–266.

[25] R. Moscan, A. Darzynkiewicz, L. Staiano-Coico, M.R. Melamed, Detection of 5-bromodeoxyuridine (BrdUrd) incorporation by monoclonal antibodies: role of the DNA denaturation step, J. Histochem. Cytochem. 33 (1985) 821.

[26] H. Muramatsu, T. Inui, T. Kimura, S. Sakakibara, X. Song, H. Murata, T. Muramatsu, Localization of heparin-binding, neurite outgrowth and antigenic regions in midkine molecule, Biochem. Biophys. Res. Commun. 203 (1994) 1131–1139.

[27] H. Muramatsu, T. Muramatsu, Purification of recombinant midkine and examination of its biological activities: functional comparison of new heparin binding factors, Biochem. Biophys. Res. Commun. 177 (1991) 652–658.

[28] H. Muramatsu, H. Shirahama, S. Yonezawa, H. Maruta, T. Muramatsu, Midkine (MK), a retinoic acid-inducible growth/differentiation factor: immunochemical evidence for the function and distribution, Dev. Biol. 159 (1993) 392–402.

[29] T. Muramatsu, The midkine family of growth differentiation factors, Dev. Growth Differ. 36 (1994) 1–8.

[30] R.S. Nowakowski, P. Rakic, Mode of migration of neurons to the hippocampus: a Golgi and electron microscopic analysis in fetal rhesus monkey, J. Neurocytol. 8 (1979) 697–718.

[31] B. Onteniente, H. Kimura, T. Maeda, Comparative study of the glial fibrillary acidic protein in vertebrates by PAP immunohistochemistry, J. Comp. Neurol. 215 (1983) 427–436.

[32] E. Raedler, A. Raedler, Autoradiographic study of early neurogenesis on rat neocortex, Anat. Embryol. 154 (1988) 267–284.

[33] P. Rakic, Guidance of neurons migrating to the fetal monkey neocortex, Brain Res. 33 (1971) 471–476.

[34] P. Rakic, Mode of cell migration to the superficial layers of fetal monkey neocortex, J. Comp. Neurol. 145 (1972) 61–84.

[35] P. Rakic, Genesis of the dorsal lateral geniculate nucleus in the rhesus monkey: site and time of origin, kinetics of proliferation, routes of migration, J. Comp. Neurol. 176 (1977) 23–52.

[36] P. Rakic, Specification of cerebral cortical areas: the radial unit hypothesis, Science 241 (1988) 170–176.

[37] A. Raza, C. Spiridamidis, K. Ucar, G. Mayers, R. Bankert, H.D. Preisler, Double labeling of S-phase murine cells with bromodeoxyuridine and a specific DNA probe, Cancer Res. 45 (1985) 2283.

[38] A. Raza, K. Ucar, R. Bhayana, M. Kempski, H.D. Preisler, Utility and sensitivity of BrdUrd antibodies in assessing S-phase cells compared to autoradiography, Cell Biochem. Funct. 3 (1985) 149.

[39] M. Sancho-Tello, S. Valles, C. Montoliu, J. Renau-Piqueras, C. Guerri, Developmental pattern of GFAP and vimentin gene expression in rat brain and in radial glial cultures, Glia 15 (1995) 157–166.

[40] W.J. Schull, S. Norton, R.P. Jensh, Ionizing radiation and the developing brain, Neurotoxicol. Teratol. 12 (1990) 249–260.

[41] R.M. Stewart, D.P. Richman, V.S. Caviness, Lissencephaly and packygyria: an architectonic and topographical analysis, Acta Neuropathol. 31 (1975) 1–12.

[42] R.F. Stratton, W.B. Dobyns, S.D. Airhart, New chromosomal syndrome: Miller–Dieker syndrome and monosomy 17p13, Hum. Genet. 67 (1984) 193–200.

[43] X.Z. Sun, Y. Fukui, Midkine, a new heparin-binding growth/differentiation factor: expression and distribution during embryogenesis and pathological status, Cong. Anom. 38 (1998) 25–38.

[44] X.Z. Sun, M. Inouye, Y. Fukui, S. Hisano, K. Sawada, H. Muramatsu, T. Muramatsu, An immunohistochemical study of radial glial cells in the mouse brain prenatally exposed to γ-irradiation, J. Neuropathol. Exp. Neurol. 56 (1997) 1339–1348.

[45] X.Z. Sun, M. Inouye, Y. Takagishi, S. Hayasaka, H. Yamamura, Follow-up study on histogenesis of microcephaly associated with ectopic gray matter induced by prenatal γ-irradiation in the mouse, J. Neuropathol. Exp. Neurol. 55 (1996) 357–365.

[46] T. Takahashi, R.S. Nowakowski, V.S. Caviness, BrdU as an S-phase

marker for quantitative studies of cytokinetic behaviour in the murine cerebral ventricular zone, J. Neurocytol. 21 (1992) 185–197.
[47] S.S. Tan, M. Kalloniatis, K. Sturm, P.P. Tam, B.E. Reese, B. Faulkner-Jones, Separate progenitors for radial and tangential cell dispersion during development of the cerebral neocortex, Neuron 21 (1998) 295–304.
[48] M. Tardy, C. Fages, H. Riol, G. Leprince, P. Rataboul, C. Charrière-Bertrand, J. Nuñez, Developmental expression of the glial fibrillary acidic protein mRNA in the central nervous system and in cultured astrocytes, J. Neurochem. 52 (1989) 162–167.
[49] J. Tsutsui, K. Uehara, K. Kadomatsu, S. Matsubara, T. Muramatsu, A new family of heparin-binding factors: strong conservation of midkine (MK) sequences between the human and the mouse, Biochem. Biophys. Res. Commun. 176 (1991) 792–797.
[50] S.R. Vincent, K. Semba, J.M. Radke, A. Jakubovic, H.C. Fibiger, Loss of striatal somatostatin neurons following prenatal methylazoxymethanol, Exp. Neurol. 110 (1990) 194–200.
[51] L.L. Zhang, P.A. Collier, K.W. Ashwell, Mechanisms in the induction of neuronal heterotopiae following prenatal cytotoxic brain damage, Neurotoxicol. Teratol. 17 (1995) 297–311.

ELSEVIER

PII: S0269-7491(96)00124-8

Environmental Pollution, Vol. 95, No. 2, pp. 151–154, 1997

0269-7491/97 $17.00+0.00

CONCENTRATION OF GLOBAL FALLOUT ^{99}Tc IN RICE PADDY SOILS COLLECTED IN JAPAN

K. Tagami & S. Uchida

Environmental and Toxicological Sciences Research Group, National Institute of Radiological Sciences, 3609 Isozaki, Hitachinaka-shi, Ibaraki, 311-12 Japan

(Received 5 May 1996; accepted 3 October 1996)

Abstract

Analysis of global fallout ^{99}Tc in environmental samples should provide useful information for predicting the nuclide behaviour under natural conditions which is important from the viewpoint of radioecology. Concentrations of ^{99}Tc in rice paddy soils collected in Japan have been studied. After chemical separation, ^{99}Tc in the final solution was measured by ICP-MS. The activity ratio of ^{99}Tc/^{137}Cs was used to understand the ^{99}Tc behaviour in the environment because the fission yields of ^{99}Tc and ^{137}Cs from ^{235}U or ^{239}Pu are almost the same. The theoretical activity ratio from fission which is calculated now is about 3.0×10^{-4}. Our results showed that the range of activity ratios of ^{99}Tc/^{137}Cs in the soil samples was $(2.0–5.2)\times10^{-3}$; these ratios were one order of magnitude higher than the theoretical one. ^{99}Tc has been accumulating in rice paddy soil like ^{137}Cs has, although their mechanisms might differ. One of the reasons for the high ratio in the surface soil might be the ratios in the atmospheric samples, which have increased from the order of 10^{-3} to 10^{-2} (García-León et al., *1993).* © *1997 Elsevier Science Ltd. All rights reserved*

Keywords: Technetium-99, paddy field soil, anaerobic condition, activity ratio, accumulation.

INTRODUCTION

Technetium-99 in the environment has been accumulating because of its long half-life of 2.1×10^5 years. ^{99}Tc is a pure beta emitter ($E_{max}=294$ keV) and it is produced in the fission of ^{235}U or ^{239}Pu with a relatively high fission yield of *ca* 6% which is similar to the values for ^{137}Cs and ^{90}Sr. The radionuclide is released to the environment via nuclear weapons tests and nuclear industries. Nuclear medical use of ^{99m}Tc (half-life: 6.01h) which decays directly to ^{99}Tc is another source though the ^{99}Tc introduced into the environment via this route is negligible. Generally, Tc is expected to be mobile in the surface soil environment because of its chemical form, TcO_4^-. The negative surface charge of soil particles makes for this mobility and plants can absorb it easily. For this reason, a knowledge of Tc behaviour in the environment is important for dose assessment. However, clarification is not easy using results of laboratory tracer experiments because the behaviour of Tc is dependent upon its chemical form; the most stable chemical form in the surface soil is pertechnetate, TcO_4^-, but, under reducing conditions, it could be an insoluble form (Bondietti & Garten, 1985; Sheppard *et al.*, 1990; Yanagisawa & Muramatsu, 1995; Tagami & Uchida, 1996*a*).

Analysis data of global fallout ^{99}Tc in environmental samples should give useful information for predicting the nuclide behaviour. But due to its very low concentration and analytical difficulties with environmental samples, there are not many data.

In this study, we focused on determination of ^{99}Tc in paddy field soil samples. ^{137}Cs concentration in the sample was also measured, then the activity ratio of ^{99}Tc/^{137}Cs was calculated to understand Tc mobility in the paddy soil environment. Paddy field soil is one of the environmental samples in which the nuclide could be accumulated because of the relatively low redox conditions. Besides, the soil-rice plant system is an important path for transfer of ^{99}Tc to humans in Japan and other Asian countries because rice is the main crop in these areas (The Times Atlas of the World, 1994).

MATERIALS AND METHODS

Soil preparation

Five soil samples were collected from the surface layer (< 20 cm) of paddy fields in Japan (Fig. 1). The soil properties are listed in Table 1. The samples were air-dried and passed through a 2 mm mesh sieve. They were incinerated for 8 h at 450°C to decompose organic matter.

Chemical separation

The experimental method for soil sample was reported previously (Tagami & Uchida, 1993*b*, 1996*b*). The scheme is shown in Fig. 2 and only a brief explanation is given here.

1. Technetium was separated from the incinerated soil sample by volatilization, i.e. by combustion of the sample at 950°C and trapping of the gaseous element in a potassium carbonate solution.

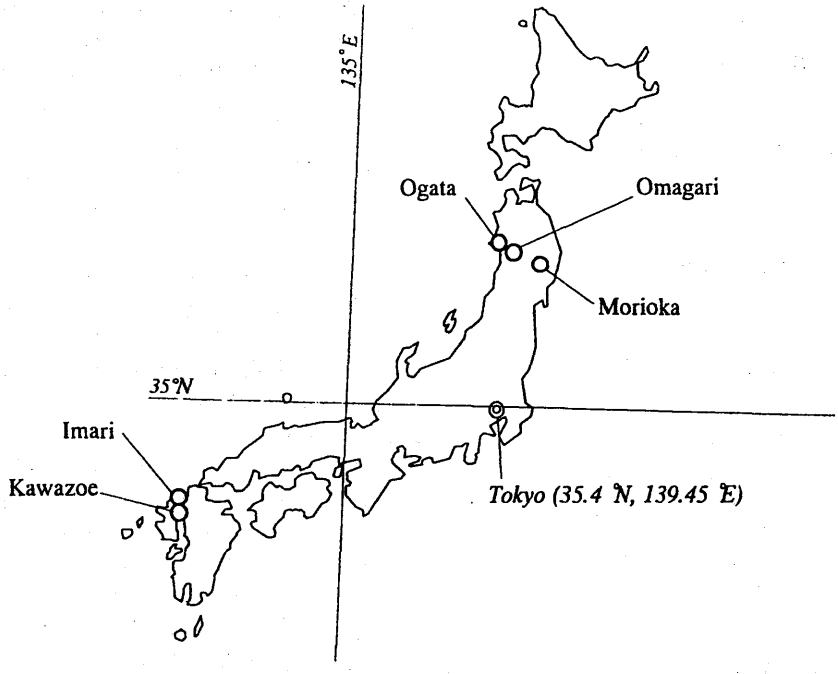

Fig. 1. Soil collection sites in Japan.

2. The solution was shaken with cyclohexanone to extract its Tc and to remove ruthenium which has an isotopic abundance of 12.7% at mass 99 (Morita *et al.*, 1991). Then Tc in the organic layer was back-extracted into deionized water by the addition of carbon tetrachloride.
3. The aqueous phase was adjusted to 2% nitric acid with super-analytical grade reagent (Tama Chemicals, AA-100). Then, the ^{99}Tc concentration in the solution was measured by ICP-MS (Yokogawa, PMS-2000).

For the ICP-MS measurement, ^{99}Tc standard solution (Japan Radioisotope Association, NH_4TcO_4 form in 0.1% ammonia solution) was used. Measurement time was approximately 10 min per solution. The detection limit for ICP-MS was 0.05 ppt (0.03 mBq ml^{-1}). During the measurement, mass numbers 101 and 102 were also detected for Ru in the samples.

Recovery of Tc was determined with ^{95m}Tc (DuPont, $NaTcO_4$ in H_2O). A paddy field soil contaminated for one month was used for the determination of the yield. The area of the gamma peak of 204 keV of ^{95m}Tc was measured with a NaI(Tl) well-type scintillation counting system (Aloka, ARC-300).

^{137}Cs measurement

The activities in the soil samples were measured by a Ge detector (Seiko EG&G Ortec) coupled with a multi channel analyzer (Seiko EG&G, Model 7800). 100 ml of each soil sample were transferred into a plastic vessel and measured for 80 000 s. The same volume standard solution (a mixed radionuclide γ-ray reference standard in solution, Amersham, QCY.46) was used for the ^{137}Cs determination. The method was applicable because a preliminary experiment showed that there was no remarkable difference in efficiencies between the liquid standard and a reference soil (IAEA Soil-6).

RESULTS AND DISCUSSION

For the determination, 300 to 500 g of incinerated soil samples were used. The soil incineration was carried out at 450°C to decompose organic matter because its

Table 1. Properties of the soil samples

Sampling place	Ogata Village (Akita Prefecture)	Omagari City (Akita Prefecture)	Morioka City (Iwate Prefecture)	Imari City (Saga Prefecture)	Kawazoe Town (Saga Prefecture)
Depth (cm)	0–15	0–18	0–14	0–20	0–17
Classification	Gray lowland soils	Gray lowland soils	Andosols	Yellow soils	Gray lowland soils
Soil properties					
CEC (meq/100 g dry)	—	18.4	27.4	16.0	0.85
AEC (meq/100 g dry)	—	(<0.05)	0.17	(<0.05)	(<0.05)
Active Al (mg/100 g dry)	—	223	6510	236	158
Active Fe (mg/100 g dry)	—	420	3600	741	600
Organic C (% dry)	—	1.84	6.64	2.06	2.00
Total N (% dry)	—	0.16	0.56	0.23	0.19

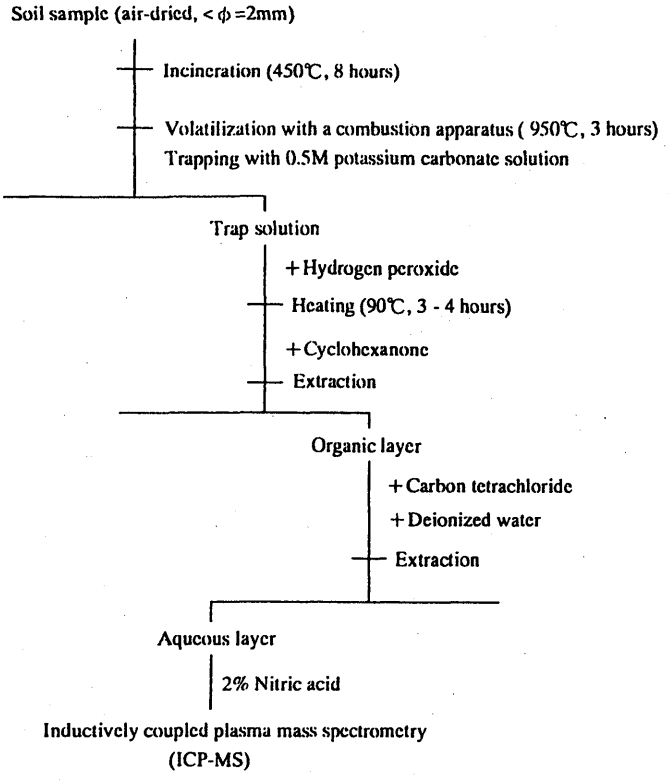

Fig. 2. Separation procedure for ^{99}Tc in soil.

presence in samples interfered with Tc separation. Previously, we reported (Tagami & Uchida, 1993*a*, 1996*b*) that soil samples including Andosol and Gray lowland soil could be incinerated without any loss of Tc despite a difference in organic matter content among soil samples. In this experiment, the soil sample which had been contaminated with ^{95m}Tc for one month was used in parallel for determination of the chemical recovery of the five soil samples. ^{95m}Tc was not added as a tracer to the soil samples because there is a possibility that ^{95m}Tc solution includes an interfering element at mass of 99 introduced during its production procedure (Tagami & Uchida, 1996*b*). In order to identify the separation of Ru from the solution, the counts for mass numbers 101 and 102 were measured with ICP-MS. Both counts were almost the same as those of blank sample. It was assumed that there was no evidence of Ru existing in the sample solutions. The average recovery of ^{95m}Tc from the contaminated soil sample was 58 ± 6%.

Table 2 shows the results of ^{99}Tc and ^{137}Cs measurements. The ranges of ^{99}Tc and ^{137}Cs concentrations are 0.02–0.11 Bq kg^{-1} dry and 4.9–16.9 Bq kg^{-1} dry, respectively. The activity ratios of $^{99}Tc/^{137}Cs$ are in the last column, $(2.0–5.2)\times10^{-3}$. The activity ratio of $^{99}Tc/^{137}Cs$ from fission is now calculated as 3.0×10^{-4} with correction of decay out. The measured ratios in the paddy field soil samples were one order of magnitude higher than the theoretical one from fission.

The higher $^{99}Tc/^{137}Cs$ activity ratio in soil is presumably influenced by that of depositions containing rain and dry fallout. Ehrhardt and Attrep (1978) reported that the range of the activity ratio of $^{99}Tc/^{137}Cs$ in rain samples which were collected in the USA was $(0.11–2.5)\times10^{-2}$ during 1961–1974. In Spain, García-León *et al.* (1993) measured similar values of $(0.3–12.3)\times10^{-2}$ in rain samples collected during 1984–1987. These ratios in rain samples were almost the same as those of soils. It seems that the $^{99}Tc/^{137}Cs$ in soil was affected by that in deposition on the soil. However, it is still difficult to understand the ^{99}Tc behaviour in the atmosphere and terrestrial environments because of the limited numbers of ^{99}Tc data in deposition samples. Our results, at least, lead to a tentative conclusion that more Tc might be fixed on the soil we had expected before.

The mechanisms of Tc accumulation in paddy fields can be explained by the changes of Tc's chemical form in soil under the waterlogged condition. Generally, during the planting period, the paddy field soils are waterlogged and subsequently the redox potentials decrease, so that relatively low redox conditions are generated in the soils. Although the nuclide is expected to be in a soluble form as pertechnetate (TcO_4^-) under an aerobic condition like that in surface soils, this changes through a combination of factors such as the redox condition and microbial activity (Tagami & Uchida, 1996*a*, 1996*c*). Probably, Tc is transformed from its soluble TcO_4^- form to a lower oxidation form such as TcO_2, $TcO(OH)_2$ or TcS_2 under a relatively low redox condition (Lieser & Bausher, 1987; Brookins, 1988). The sulfide might occur because H_2S gas can be produced in waterlogged soil when rice plants are growing. These lower oxidation forms have lower solubility and Tc in these forms would be sorbed onto soil. The activity ratio of $^{99}Tc/^{137}Cs$ in unploughed soil

Table 2. Concentrations of ^{99}Tc and ^{137}Cs in paddy field soils in Japan on a dry weight basis and activity ratios of ^{99}Tc to ^{137}Cs

Collection place and type of the soil	Collection year	^{99}Tc (Bq kg^{-1})	^{137}Cs (Bq kg^{-1})	$^{99}Tc/^{137}Cs$ ($\times10^{-3}$)
Ogata Village, Akita Prefecture Paddy soil	1991	0.11 ± 0.03	28.2 ± 0.8	3.9 ± 1.0
Omagari City, Akita Prefecture Paddy soil	1992	0.034 ± 0.005	16.92 ± 0.64	2.0 ± 0.3
Morioka City, Iwate Prefecture Paddy soil	1992	0.052 ± 0.01	10.13 ± 0.63	5.1 ± 0.1
Kawazoe Town, Saga Prefecture Paddy soil	1991	0.022 ± 0.003	4.94 ± 0.47	4.5 ± 0.8
Imari City, Saga Prefecture Paddy soil	1991	0.088 ± 0.015	16.84 ± 0.66	5.2 ± 0.9

±: Counting errors in the measurements or statistical errors in calculation.

in Japan was $(1.2–39)\times10^{-3}$ (Otsuji, 1989; Matsuoka *et al.*, 1990; Morita *et al.*, 1993). These values were one to two orders of magnitude higher than the theoretical one. Since these soil conditions were aerobic conditions, it is expected that the chemical form of Tc is TcO_4^- has only a small possibility of changing to a lower oxidation form. Although local reduction conditions could be seen even in the surface soil, the mechanisms of Tc sorption onto the soil should not be explained only by this. Further studies are needed to clarify the phenomena of ^{99}Tc accumulation in the surface soil layer including upland field.

ACKNOWLEDGEMENT

We are pleased to acknowledge the valuable comments of Dr G. M. Milton, Chalk River Laboratory, Atomic Energy of Canada Limited.

REFERENCES

Bondietti, E. A. & Garten, C. T. (1985). Speciation of ^{99}Tc and ^{60}Co: Correlation of laboratory and field observations. In *Speciation of Fission and Activation Products in the Environment*, ed. R. A. Bulman & J. R. Cooper. Elsevier Appl. Sci. Pub., London, pp. 79–92.

Brookins, D. G. (1988). *Eh-pH Diagrams for Geochemistry*. Springer-Verlag, Berlin, pp. 97–99.

Ehrhardt, K. C. & Attrep, M. (1978). Technetium-99 in the atmosphere. *Environ. Sci. Technol.*, **12**, 55–57.

Garcia-León, M., Manjón, G. & Sánchez-Angulo, C. I. (1993). $^{99}Tc/^{137}Cs$ activity ratios in rainwater samples collected in the south of Spain. *J. Environ. Radioact.*, **20**, 49–61.

Lieser, K. H. & Bausher, C. (1987). Technetium in the hydrosphere and in the geosphere 1. Chemistry of technetium and iron in natural waters and influence of redox potential on the sorption of technetium. *Radiochim. Acta*, **42**, 205–213.

Matsuoka, N., Umata, T., Okamura, M., Shiraishi, N., Momoshima, N. & Takashima, Y. (1990). Determination of technetium-99 from the aspect of environmental radioactivity. *J. Radioanal. Nucl. Chem., Articles*, **140**, 57–73.

Morita, S., Kim, C. K., Takaku, Y., Seki, R. & Ikeda, N. (1991). Determination of technetium-99 in environmental samples by inductively coupled plasma mass spectrometry. *Intl. J. Appl. Radiat. Isot.*, **42**, 531–534.

Morita, S., Tobita, K. & Kurabayashi, M. (1993). Determination of technetium-99 in environmental samples by inductively coupled plasma mass spectrometry. *Radiochim. Acta*, **63**, 63–67.

Otsuji, M. (1989). Development of a new method for the determination of Tc-99 in environmental samples. Master's Thesis. Tsukuba Univ. (in Japanese).

Sheppard, S. C., Sheppard, M. I. & Evenden, W. G. (1990). A novel method used to examine variation in Tc sorption among 34 soils, aerated and anoxic. *J. Environ. Radioact.*, **11**, 215–233.

Tagami, K. & Uchida, S. (1993*a*). Investigation of pre-treatment of soil for ^{99}Tc analysis—Loss of Tc by incineration in relation to aging effect (abstract in English). *Radioisotopes*, **42**, 89–92.

Tagami, K. & Uchida, S. (1993*b*). Separation procedure for the determination of technetium-99 in soil by ICP-MS. *Radiochim. Acta*, **63**, 69–72.

Tagami, K. & Uchida, S. (1996*a*). Microbial role in immobilization of technetium in soil under waterlogged conditions. *Chemosphere*, **33**, 217–225.

Tagami, K. & Uchida, S. (1996*b*). Analysis of technetium-99 in soil and deposition samples by inductively coupled plasma mass spectrometry. *Appl. Radiat. Isot.*, **47**, 1057–1060.

Tagami, K. & Uchida, S. (1996*c*). Aging effect on technetium behaviour in soil under aerobic and anaerobic conditions. *Toxicol. Environ. Chem.*, **56**, 235–247.

The Times Atlas of the World, 9th comprehensive edition (1994). Times Books, London.

Yanagisawa, K. & Muramatsu, Y. (1995). Transfer of technetium from soil to paddy and upland rice. *J. Radiat. Res.*, **36**, 171–178.

RADIATION RESEARCH 154, 686–691 (2000)
0033-7587/00 $5.00

Inhibition of Repair of Radiation-Induced DNA Double-Strand Breaks by Nickel and Arsenite

Sentaro Takahashi,[a,1] Eriko Takeda,[b] Yoshihisa Kubota[a] and Ryuichi Okayasu[c]

[a] *Environmental and Toxicological Research Group, National Institute of Radiological Sciences, Chiba, Japan;*
[b] *Department of Chemistry, Science University of Tokyo, Tokyo, Japan; and*
[c] *Department of Radiological Health Sciences, Colorado State University, Fort Collins, Colorado 80523-1673*

Takahashi, S., Takeda, E., Kubota, Y. and Okayasu, R. Inhibition of Repair of Radiation-Induced DNA Double-Strand Breaks by Nickel and Arsenite. *Radiat. Res.* 154, 686–691 (2000).

The effect of arsenite or nickel on the repair of DNA double-strand breaks (DSBs) was studied in γ-irradiated Chinese hamster ovary cells using pulsed-field gel electrophoresis. After treatment with nickel chloride or arsenite for 2 h, cells were irradiated with γ rays at a dose of 40 Gy, and the numbers of DNA DSBs were measured immediately after irradiation as well as at 30 min postirradiation. Both arsenite and nickel(II) inhibited repair of DNA DSBs in a concentration-dependent manner; 0.08 m*M* arsenite significantly inhibited the rejoining of DSBs, while 76 m*M* nickel was necessary to observe a clear inhibition. The mean lethal concentrations for the arsenite and nickel(II) treatments were approximately 0.12 and 13 m*M*, respectively. This indicates that the inhibition of repair by arsenite occurred at a concentration at which appreciable cell survival occurred, but that nickel(II) inhibited repair only at cytotoxic concentrations at which the cells lost their proliferative ability. These novel observations provide insight into the mechanisms underlying the effects of combined exposure to arsenite and ionizing radiation in our environment. © 2000 by Radiation Research Society

INTRODUCTION

Recent advances in science and technology involve the potential release of various toxic agents into the environment that might have adverse effects on human health. Since simultaneous exposure to multiple toxicants frequently occurs in the environment, studies of the combined and/or competitive effects of toxicants are of great importance. In the field of radiation protection, the combined effects of radiation and other toxic agents are recognized as an important research area, but data for use in providing accurate risk assessment are limited. Thus elucidation of the basic mechanisms involved in combined effects is crucial.

It has been shown that exposure to some heavy metals or to arsenic results in supra- or subadditive effects when they are combined with ionizing or nonionizing radiation including X rays and UV light (for reviews, see refs. *1–3*). Although the underlying mechanisms are not clearly understood, the interference with DNA repair as well as the enhancement of radical formation are possible explanations for the combined effects of these metals and radiation. Many metals or metalloids including nickel (*1–14*), arsenite (*4, 5, 8, 15–19*), cadmium (*4, 6, 11, 12, 14, 17, 20*), mercury (*4, 5, 21, 22*), cobalt (*4, 23*), lead (*20*), and copper (*4, 5*) have been shown to interfere with the process of repair of DNA damage induced by a variety of genotoxic substances.

The inhibitory potential of a specific metal may depend on the nature of the DNA damage. For instance, nickel(II) inhibited the repair of DNA damage induced by X rays and UV light but not the damage induced by methyl methanesulfonate (*7, 8*). In contrast, mercury(II) interfered with the repair of DNA damage induced by X rays but not the repair of damage induced by UV light (*21, 22*). There are many kinds of DNA damage, including double-strand breaks (DSBs), single-strand breaks (SSBs), and base modifications. Of these, the DNA DSB is known to be a very destructive lesion in which both strands of the DNA double helix are sheared at the same time by chemical or physical actions. The misrepaired DSBs or DSBs that remain when repair has been completed can lead to cell death, mutation or neoplastic transformation (*24*). Although an inhibitory effect on the repair of X-ray-induced DNA SSBs has been demonstrated (*4, 5, 9, 21, 22*), there has been no study of the effect of metals or metalloids on DNA DSB repair. Thus we investigated the effects of arsenite and nickel on the repair of DSBs induced by γ radiation. These compounds were selected because of the increased interest in their inhibitory effects on various forms of DNA repair (*4–19*). Our data demonstrate that arsenite at subtoxic concentrations has a strong inhibitory effect on the repair of radiation-induced DSBs.

[1] Author to whom correspondence should be addressed at Environmental and Toxicological Research Group, National Institute of Radiological Sciences, 4-9-1 Anagawa, Inage-ku, Chiba 263-8555, Japan.

MATERIALS AND METHODS

Chemicals

The medium, serum and antibiotics used for the cell culture are products of Gibco (Gaithersburg, MD). Nickel chloride and sodium arsenite are analytical-grade reagents produced by Wako Chemical (Tokyo, Japan), and chemicals used for electrophoresis are analytical-grade reagents from Sigma (St. Louis, MO) unless otherwise specified.

Cell Culture

Chinese hamster ovary cells (CHO-K1) were obtained from Riken Cell Bank (Ibaraki, Japan) and were maintained in Ham's F-12 medium supplemented with 10% FBS, 100 μg/ml streptomycin, and 100 U/ml penicillin at 37°C in an atmosphere of 5% CO_2 and 95% air. Plateau-phase cells were obtained by growing 3–4 × 10^5 cells in a 60-mm tissue culture dish (5 ml medium) for 4 days without a change of medium. Subsequently 1.5 × 10^5 cells were inoculated in a 35-mm tissue culture dish in 2 ml of the above medium and labeled with 0.74 kBq/ml [^{14}C]thymidine plus 5 μ*M* cold thymidine added at the time of culture preparation. Cells were used for the experiment 24–28 h after incubation, when approximately 5 × 10^5 cells had accumulated. Thus the experiments were performed with exponentially growing cells. This culture protocol gave consistent results regarding the amount of DNA DSBs measured, and the cell cycle distribution of the population used was similar in all of the experiments.

Exposure to Chemicals and γ Radiation

At the beginning of the experiments, the culture medium was replaced with 1 ml of fresh medium, and then 0.1 ml of chemical solution was added. The chemicals used were nickel chloride and sodium arsenite; they were dissolved in freshly prepared Hanks' balanced salt solution. The cells were exposed to various concentrations of chemicals for 2 h and then irradiated on ice using a ^{137}Cs irradiator at a dose of 40 Gy (dose rate: 10.2 Gy/min). Subsequently, in some cultures (non-repair group), the cells were washed once with cold medium, trypsinized at room temperature for 1.5–2 min, and collected in a test tube on ice for further analysis of DNA DSBs. In other cultures (repair groups), cell incubation continued at 37°C for 30 min to allow DSB repair, and then the cells were prepared for analysis of DSBs with the same procedure used for the non-repair groups. In the non-repair group, there is a possibility that a few DSBs might be rejoined since the cells were maintained at room temperature during the trypsin-EDTA treatment. If we assume that DSBs were repaired during the trypsin-EDTA treatment at the same rate as at 37°C, about 7% of DSBs were repaired before the assay. However, our procedures were very consistent from experiment to experiment, so no serious deviation in the data was expected.

Analysis of DNA DSBs

The assay of DSBs was carried out by pulsed-field gel electrophoresis as described elsewhere (*25, 26*). In brief, the recovered cells were mixed with melted 0.5% agarose solution, pipetted into plastic molds, and cooled on ice until they had solidified. These agarose samples were immersed in an ice-cold lysis solution containing 0.5 *M* EDTA, 0.01 *M* Tris, 2% sarcosyl, and 0.2 mg/ml proteinase K for 1 h and then incubated overnight at 50°C. After lysis, samples were washed and treated with 0.1 mg/ml ribonuclease A for 1 h. Sample plugs were electrophoresed in 0.5× TBE buffer (45 m*M* Tris, 45 m*M* boric acid, 1.5 m*M* EDTA, pH 8.2) in a clamped homogeneous electric-field gel box (Bio-Rad, Tokyo, Japan), on 0.8% agarose gel (CHEF grade, Bio-Rad) at 14°C. The voltage applied was 200 V with a 60-s pulse time for the first 9 h followed by a 120-s pulse time for the last 14 h (total run time, 23 h). After electrophoresis, the gels were stained with ethidium bromide, photographed under UV light, and cut to separate the plug from the lane of each sample. The ^{14}C activity of each piece was measured in a scintillation counter and the fraction of activity released (FAR) was calculated as the disintegrations per minute (dpm) for a lane divided by the total dpm (lane + plug) per sample. Background FAR values, obtained from the lanes containing unirradiated DNA, were typically between 2 and 5% and were subtracted from the FAR values of treated samples.

Cell Viability and Colony-Forming Ability

The proliferative ability of the cells was determined by a colony-forming assay. The cells were prepared and exposed to each chemical for 2.5 h, which corresponded to the sum of the preincubation time with the chemicals (2 h) and the repair incubation time (0.5 h). Then they were trypsinized, counted and replated onto 35-mm tissue culture dishes in triplicate to yield 100–500 colonies per dish 8–9 days later. The colonies were stained with Giemsa solution and counted. In some experiments, the toxicities of nickel and arsenite were also determined by trypan blue dye exclusion. After exposure to chemicals for 2.5 h, the culture medium was recovered, and the dish was rinsed to remove nonadherent cells. The recovered medium and rinsed solutions were centrifuged to collect the nonadherent cells. The number and viability of the nonadherent cells recovered and the adherent cells on the dish were determined by a dye exclusion test with 0.5% trypan blue. The cytotoxicity and DNA DSB assays were performed in duplicate or triplicate in at least three independent experiments. Statistical analysis was carried out with the Student's *t* test (n = 6–12).

RESULTS

The Effect of Chemicals on Cell Adherence and Viability

Figure 1A and B shows the cell viability determined by trypan blue dye exclusion and the percentage of cells that adhered to the culture dish at the end of 2.5 h exposure. The viability was greater than 90% in cells exposed to arsenite at all the concentrations used. In cells exposed to Ni(II), the viability was greater than 90% for concentrations of 20 m*M* or less and decreased to 84 and 20% at 76 and 200 m*M*, respectively. The percentages of adherent cells were greater than 95% except for the cells exposed to the highest concentration of arsenite, where approximately 20% of the cells were detached from the culture dish (Fig. 1A). These results indicate that most cells adhered to culture dishes after exposure and were processed for the subsequent DNA DSB assay. The plating efficiencies of the cells after 2.5 h exposure to arsenite and Ni(II) are shown in Fig. 2A and B, respectively. The survival data fit a log-linear curve well, and the lack of a shoulder in the dose–response curves is consistent with previous reports (*7, 27*). The mean lethal concentrations for the arsenite and Ni(II) treatments were approximately 0.121 and 13.3 m*M*, respectively.

Induction of DNA DSBs by γ Radiation and their Repair

To examine the kinetics of DSB repair, the repair incubation was extended up to 120 min after irradiation, and DSB repair was assayed 30, 45, 60 and 120 min postirradiation. As shown in Fig. 3, there was a rapid decrease in the FAR in the first hour. By 120 min, the FAR value had almost reached the background level. This decrease in FAR is attributable to the rejoining of DSBs as reported in previous studies (*28, 29*). In the following study, the inhibitory effects of Ni(II) and arsenite on DSB rejoining were inves-

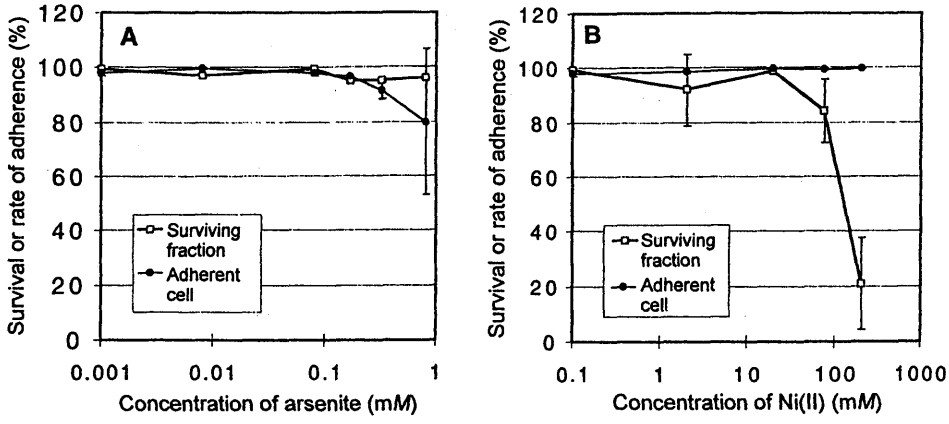

FIG. 1. Cell viability determined by the trypan blue dye exclusion test and the percentage of adherent cells after 2.5 h exposure to arsenite (panel A) or Ni(II) (panel B). Vertical bars indicate the SD for 6 to 12 cultures obtained from at least three independent experiments.

tigated at 0 (no repair) and 30 min postirradiation, since the most rapid and significant repair occurred during this period.

Inhibition of DNA DSB Repair by Ni(II) and Arsenite

Cells were preincubated with chemicals for 2 h and irradiated with 40 Gy γ rays. Some cultures were then assayed for DSBs immediately and the others were incubated for a further 30 min to allow repair. Figure 4A shows the FAR values for the cells exposed to arsenite. Up to 0.12 m*M* arsenite, the FAR for cells assayed immediately after irradiation (no repair) were at levels similar to those in untreated (0 m*M*) cells and then increased gradually with increasing arsenite concentration. The FAR values at 30 min postirradiation were significantly increased due to the exposure to arsenite at 0.08 m*M* or more, indicating a strong inhibitory effect on repair by arsenite in this concentration range. The arsenite concentration dependence of the inhibition of DSB repair is clearly shown in Fig. 4A. In this figure, the repair fraction (fraction of repaired DSBs) was calculated by the following equation:

$$\text{Repair fraction} = \frac{[\text{FAR}(0) - \text{FAR}(\text{BL})] - [\text{FAR}(30) - \text{FAR}(\text{BL})]}{\text{FAR}(0) - \text{FAR}(\text{BL})},$$

where FAR(0) and FAR(30) denote the FAR values at 0 and 30 min after irradiation, respectively, and FAR(BL) is the blank FAR values in the cells that received neither γ irradiation nor chemical exposure. Since it has been shown that FAR is proportional to the number of DSBs in a linear manner in these ranges (*28, 30*), the above equation indicates the actual fraction of DSBs repaired.

The data in Fig. 5A indicate that the repair inhibition occurred in the biologically significant concentration range of arsenite. For Ni(II), as shown in Fig. 4B, no significant changes in the FAR values were observed up to 20 m*M* for the initial induction of DSBs (0 min). Then the initial damage gradually increased and the FAR at 30 min also increased at concentrations higher than 40 m*M* Ni(II). These results indicate that Ni(II) also inhibits the repair of DSBs at concentrations of more than 40 m*M*, and that 76 m*M* nickel was necessary to observe a clear inhibition (Fig. 5B).

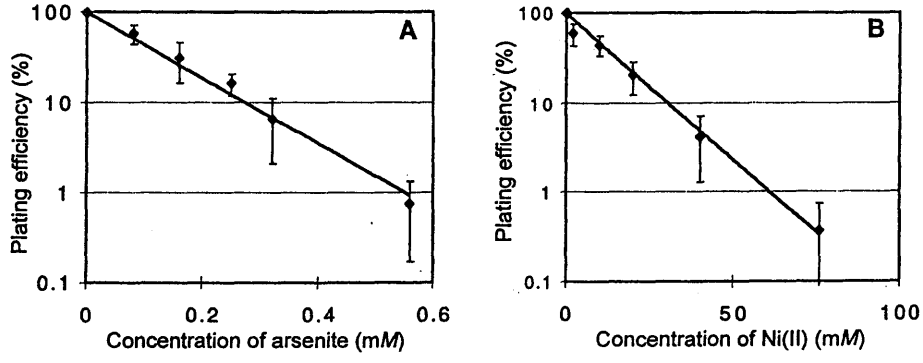

FIG. 2. Cell survival as determined by the colony-forming assay after 2.5 h exposure to arsenite (panel A) or Ni(II) (panel B). Vertical bars indicate the SD for six to nine cultures obtained from at least three independent experiments.

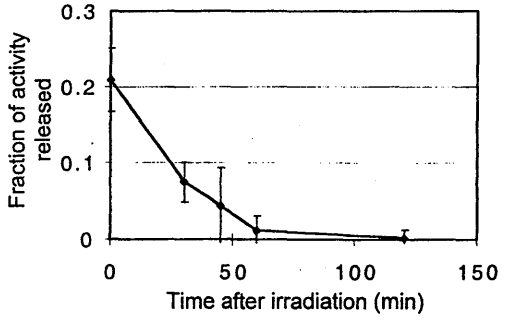

FIG. 3. Change in FAR values with time (or kinetics of DSB rejoining as a function of postirradiation time) after 40 Gy γ irradiation. Background values have been subtracted from individual data points. Vertical bars indicate SD for six to nine cultures obtained from at least three independent experiments.

However, these concentrations are much higher than the biologically significant concentration range for Ni(II).

It has been reported that rejoining of DSBs has a fast and a slow component (*28*). To show how arsenite affects these phases, data for rejoining kinetics up to 120 min postirradiation are presented in Fig. 6. The inhibition of repair by arsenite is very distinct in the first 60 min after irradiation, and this appears to lead to a substantial number of unrejoined DSBs (~40% of initial breaks) at 2 h postirradiation. Such unrejoined breaks could well be the cause of the sensitization by arsenite and could be more important than the repair effects on the rate of each component.

DISCUSSION

In this study, we have shown the inhibitory effects of arsenite and Ni(II) on the repair of DSBs induced by γ radiation. Although a high concentration of Ni(II) (>40 m*M*) was necessary to inhibit repair of DSBs, a low concentration of arsenite (0.08 m*M*) inhibited DSB repair. This arsenite concentration is significant since it allowed more than 50% of the cells to survive. To the best of our knowledge, this is the first direct evidence that arsenite inhibits the repair of DSBs. It has been reported that arsenite enhances the accumulation of DSBs in cells exposed to methyl methanesulfonate (*16*). The presence of DSBs in that study may be the result of effects on the repair of the lesions induced by methyl methanesulfonate.

There are a number of reports demonstrating that both Ni(II) and arsenite inhibit the repair of X-ray- or UV-radiation-induced DNA damage measured using alkaline elution, alkaline unwinding, or the nucleoid sedimentation assay (*4–11, 13–15*). The concentrations of compounds used in those studies were relatively low and resulted in little or no cytotoxicity. In the present study, however, only arsenite interfered with the repair of DSBs at relatively low concentrations, while Ni(II) inhibited repair only at high concentrations. Interestingly, the repair of DNA damage induced by methyl methanesulfonate was inhibited by nontoxic levels of arsenite, but not by Ni(II) (*8*).

The initial yield of DSBs after irradiation was higher at greater concentrations of Ni(II) or arsenite (Fig. 4A and B). Since DSBs were induced after the exposure to high concentrations of nickel or arsenite alone (without radiation), the increase may be attributable to the direct induction of DNA damage by Ni(II) or arsenite. An interaction between metals and scavengers such as thiols may not be the case in this situation.

Although the mechanism of inhibition of DSB repair by these compounds is not fully understood, the ligation step may be affected by these compounds, as has been suggested in the inhibition of repair of other types of DNA damage (*2, 8, 11, 18, 19*). Unique effects of arsenite on mutagenesis have been reported and may be relevant to the inhibitory effects of arsenite on DSB repair demonstrated in the present study. Arsenite was believed to be a weak mutagen in standard mutation assays using cultured mammalian cells (for reviews, see refs. *2* and *31*). However, Hei *et al.* (*27*) recently demonstrated that arsenite is a strong mutagen and that it induced mostly large deletion mutations. Not only the direct effect on DNA strands but also the inhibition of DSB repair by arsenite may be responsible for the large deletions observed.

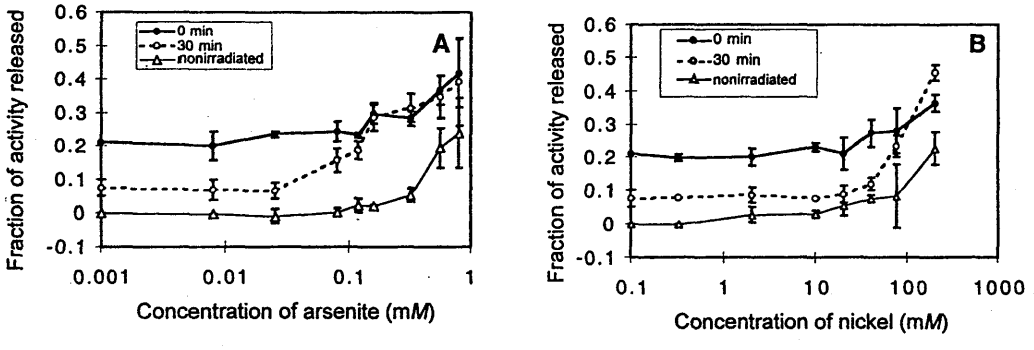

FIG. 4. FAR values assayed immediately after irradiation (closed circles with solid line) or 30 min after the repair incubation with arsenite (panel A) or Ni(II) (panel B) (open circles with broken line). FAR values for the nonirradiated cells are also shown (open triangles). Vertical bars indicate the SD for 6 to 12 cultures obtained from at least three independent experiments.

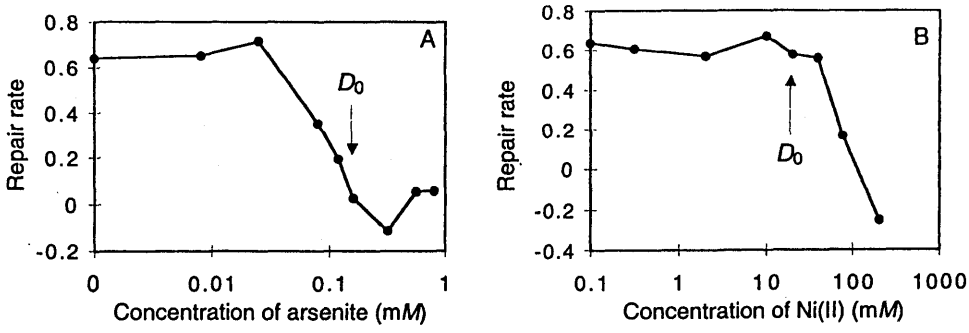

FIG. 5. Repair fractions calculated from the FAR values presented in Fig. 4A for cells exposed to arsenite (panel A) and in Fig. 4B for cells exposed to Ni(II) (panel B). The arrow in each panel indicates the mean lethal concentration for the respective treatments.

As described above, 0.08 m*M* of arsenite inhibited the repair of DSBs. This concentration is not much higher than the levels of arsenic found in the environment (as reviewed in ref. *32*). For example, in some regions, the concentration of arsenic in natural well water (not artificially contaminated) reaches 1 ppm (0.014 m*M*). In artificially contaminated areas, concentrations that were 10 to 100 times higher were observed. In human blood and soft tissues, the arsenic concentration is usually less than 0.3 ppm (0.004 m*M*), which is $^1/_{20}$ of the effective concentration in the present study. However, in human tissues accidentally treated with arsenic or exposed to an environment with a higher level of arsenic, the tissue concentrations could become more than 10 ppm (0.14 m*M*), which is greater than those found to inhibit DSB repair in the present study.

The International Agency for Research on Cancer (IARC) categorizes both nickel and arsenic as group 1 human carcinogens (*33, 34*). Nickel induces lung and sinonasal cancer, and its carcinogenic action has been demonstrated in human epidemiological studies as well as in animal experiments (*33, 35, 36*). Exposure to arsenic compounds leads to skin and lung cancer in humans, although animal studies failed to detect a carcinogenic potential (*31, 34, 36*). Therefore, several studies indicated that the interaction with DNA repair processes might be the predominant mechanism in arsenic-induced carcinogenicity compared to direct DNA damage (as reviewed in refs. *1–3* and *36*). The present results, which demonstrate that arsenite inhibits the repair of DSBs induced by γ radiation, may clarify and give new insight into the mechanism(s) underlying the carcinogenic potential of arsenic compounds.

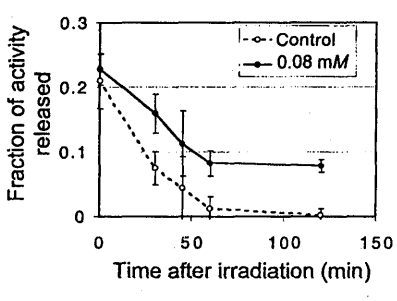

FIG. 6. Time-dependent changes in FAR value (repair of DSBs) after 40 Gy irradiation with or without 0.08 m*M* arsenite. Values are mean ± SD of eight cultures obtained from four independent experiments.

In conclusion, it is apparent that arsenite inhibits the repair of DSBs induced by γ radiation. The observed inhibitory effect of arsenite on DSB repair may have important implications for the combined effects of arsenite and ionizing radiation, since this kind of combined exposure is possible in the environment. In the case of Ni(II), this metal ion interfered with the rejoining of DSBs only at highly cytotoxic concentrations under the present experimental conditions. Since Ni(II) is known to cause inhibition of repair of other types of DNA damage at low concentrations (*4–14*), a longer incubation period (e.g. >4 h) may be needed to observe the effect (*10, 12*), and further studies may be necessary to elucidate a clear effect of nickel on DSB repair.

Received: October 7, 1999; accepted: July 11, 2000

REFERENCES

1. A. Hartwig, I. Kruger and D. Beyersmann, Mechanisms in nickel genotoxicity: The significance of interactions with DNA repair. *Toxicol. Lett.* **72**, 353–358 (1994).
2. A. Hartwig, Current aspects in metal genotoxicity. *BioMetals* **8**, 3–11 (1995).
3. A. Hartwig, Carcinogenicity of metal compounds: Possible role of DNA repair inhibition. *Toxicol. Lett.* **102–103**, 235–239 (1998).
4. R. D. Snyder, G. F. Davis and P. J. Lachmann, Inhibition by metals of X-ray and ultraviolet-induced DNA repair in human cells. *Biol. Trace Element Res.* **21**, 389–398 (1989).
5. R. D. Snyder and P. J. Lachmann, Thiol involvement in the inhibition of DNA repair by metals in mammalian cells. *J. Mol. Toxicol.* **2**, 117–128 (1989).
6. A. Hartwig and D. Beyersmann, Comutagenicity and inhibition of DNA repair by metal ions in mammalian cells. *Biol. Trace Element Res.* **21**, 359–365 (1989).
7. S. F. Lee-Chen, M. C. Wang, C. T. Yu, D. R. Wu and K. Y. Jan, Nickel chloride inhibits the DNA repair of UV-treated but not methyl methanesulfonate-treated Chinese hamster ovary cells. *Biol. Trace Element Res.* **37**, 39–50 (1993).
8. S. F. Lee-Chen, C. T. Yu, D. R. Wu and K. Y. Jan, Differential effects of luminol, nickel, and arsenite on the rejoining of ultraviolet light and alkylation-induced DNA breaks. *Environ. Mol. Mutagen.* **23**, 116–120 (1994).

9. W. W. Au, M-Y. Heo and T. Chiewchanwit, Toxicological interactions between nickel and radiation on chromosome damage and repair. *Environ. Health Perspect.* **102**, 73–77 (1994).
10. A. Hartwig, L. H. Mullenders, R. Schlepegrell, U. Kasten and D. Beyersmann, Nickel(II) interferes with the incision step in nucleotide excision repair in mammalian cells. *Cancer Res.* **54**, 4045–4051 (1994).
11. A. Hartwig, R. Schlepegrell, H. Dally and M. Hartmann, Interaction of carcinogenic metal compounds with deoxyribonucleic acid repair processes. *Ann. Clin. Lab. Sci.* **26**, 31–38 (1996).
12. H. Dally and A. Hartwig, Induction and repair inhibition of oxidative DNA damage by nickel(II) and cadmium(II) in mammalian cells. *Carcinogenesis* **18**, 1021–1026 (1997).
13. S. Lynn, F. H. Yew, K. S. Chen and K. Y. Jan, Reactive oxygen species are involved in nickel inhibition of DNA repair. *Environ. Mol. Mutagen.* **29**, 208–216 (1997).
14. M. Hartmann and A. Hartwig, Disturbance of DNA damage recognition after UV-irradiation by nickel(II) and cadmium(II) in mammalian cells. *Carcinogenesis* **19**, 617–621 (1998).
15. T. Okui and Y. Fujiwara, Inhibition of human excision DNA repair by inorganic arsenic and the co-mutagenic effect in V79 Chinese hamster cells. *Mutat. Res.* **172**, 69–76 (1986).
16. S. F. Lee-Chen, J. R. Gurr, I. B. Lin and K. Y. Jan, Arsenite enhances DNA double-strand breaks and cell killing of methyl methanesulfonate-treated cells by inhibiting the excision of alkali-labile sites. *Mutat. Res.* **294**, 21–28 (1993).
17. A. Hartmann and G. Speit, Effect of arsenic and cadmium on the persistence of mutagen-induced DNA lesions in human cells. *Environ. Mol. Mutagen.* **27**, 98–104 (1996).
18. S. Lynn, H-T. Lai, J-R. Gurr and K. Y. Jan, Arsenite retards DNA break rejoining by inhibiting DNA ligation. *Mutagenesis* **12**, 353–358 (1997).
19. Y. Hu, L. Su and E. T. Snow, Arsenic toxicity is enzyme specific and its affects on ligation are not caused by the direct inhibit. *Mutat. Res.* **408**, 203–218 (1998).
20. A. Hartwig, Role of DNA repair inhibition in lead- and cadmium-induced genotoxicity: A review. *Environ. Health Perspect.* **102**, 45–50 (1994).
21. O. Cantoni, R. M. Evans and M. Costa, Similarity in the acute cytotoxic response of mammalian cells to mercury(II) and X-rays: DNA damage and glutathione depletion. *Biochem. Biophys. Res. Commun.* **108**, 614–619 (1982).
22. N. T. Christie, O. Cantoni, M. Sugiyama, F. Cattabeni and M. Costa, Differences in the effects of Hg(II) on DNA repair induced in Chinese hamster ovary cells by ultraviolet or X-rays. *Mol. Pharmacol.* **29**, 173–178 (1985).
23. U. Kasten, L. H. Mullenders and A. Hartwig, Cobalt(II) inhibits the incision and the polymerization step of nucleotide excision repair in human fibroblasts. *Mutat. Res.* **383**, 81–89 (1997).
24. G. Chu, Double strand break repair. *J. Biol. Chem.* **272**, 24097–24100 (1997).
25. Y. Kinashi, R. Okayasu, G. E. Iliakis, H. Nagasawa and J. B. Little, Induction of DNA double-strand breaks by restriction enzymes in X-ray-sensitive mutant Chinese hamster ovary cells measured by pulsed-field gel electrophoresis. *Radiat. Res.* **141**, 153–159 (1995).
26. R. Okayasu, K. Suetomi and R. L. Ullrich, Wortmannin inhibits repair of DNA double-strand breaks in irradiated normal human cells. *Radiat. Res.* **149**, 440–445 (1998).
27. T. K. Hei, S. X. Liu and C. Waldren, Mutagenicity of arsenic in mammalian cell: Role of reactive oxygen species. *Proc. Natl. Acad. Sci. USA* **95**, 8103–8107 (1998).
28. G. E. Iliakis, D. Blocher, L. Metzger and G. Pantelias, Comparison of DNA double-strand break rejoining as measured by pulsed field gel electrophoresis, neutral sucrose gradient centrifugation and non-unwinding filter elution in irradiated plateau-phase CHO cells. *Int. J. Radiat. Biol.* **59**, 927–939 (1991).
29. R. Okayasu, S. Takahashi, S. Yamada, T. K. Hei. and R. L. Ullrich, Asbestos and DNA double strand breaks. *Cancer Res.* **59**, 298–300 (1999).
30. G. E. Iliakis, O. Cicilioni and Metzger, Measurement of DNA double-strand breaks in CHO cells at various stages of the cell cycle using pulsed field gel electrophoresis: calibration by means of ^{125}I decay. *Int. J. Radiat. Biol.* **59**, 343–357 (1991).
31. M. Goldman and J. C. Dacre, Inorganic arsenite compounds: Are they carcinogenic, mutagenic, teratogenic? *Environ. Geochem. Health* **13**, 179–191 (1991).
32. National Research Council, Committee on Medical and Biological Effects of Environmental Pollutants, *Arsenic*. National Academy Press, Washington, DC, 1977.
33. IARC. *Chromium, Nickel and Welding*. Vol. 49, IARC Monographs on the Evaluation of Carcinogenic Risks in Humans, IARC, Lyon, 1990.
34. IARC, *Overall Evaluation of Carcinogenicity: An Updating of IARC Monographs Volumes 1–42*. IARC, Lyon, 1987.
35. J. K. Dunnick, M. R. Elwell and A. E. Radvsky, Comparative carcinogenic effects on nickel subsulfide, nickel oxide, or nickel sulfate hexahydrate chronic exposures in the lung. *Cancer Res.* **55**, 5251–5256 (1995).
36. R. B. Hayes, The carcinogenicity of metals in humans. *Cancer Causes Control* **8**, 371–385 (1997).

INT. J. RADIAT. BIOL 2001, VOL. 77, NO. 3, 375–381

Comparative biokinetics of tritium in rats during continuous ingestion of tritiated water and tritium-labeled food

H. TAKEDA*†, H. M. LU‡, K. MIYAMOTO†, S. FUMA†, K. YANAGISAWA†, N. ISHII† and N. KURODA†

(Received 5 July 2000; accepted 20 October 2000)

Abstract.
Purpose: The biokinetics of tritium during continuous ingestion of tritiated water and tritiated wheat were investigated to estimate the radiation dose rates at the end of two modes of chronic exposure.
Materials and methods: Wistar strain male rats continuously ingested tritiated water as drinking water and tritiated wheat as food for 14 weeks. Urine and tissue samples were obtained and total tritium in the fresh wet samples and organically bound tritium (OBT) in the freeze-dried samples were determined.
Results: The biokinetics of tritium was different between the two modes of exposure. The concentration of total tritium in the tissues exposed to tritiated water attained a steady-state condition by 2–3 weeks. The steady-state condition in the case of exposure to tritiated wheat was not observed for 10 weeks after the start of exposure in the majority of tissues. The relatively efficient and prolonged OBT formation during chronic exposure to tritiated wheat resulted in relatively high incorporation and retention of tritium in the tissues compared with those for exposure to the same activity of tritiated water.
Conclusion: Radiation dose rates estimated at the end of continuous ingestion showed that tritiated wheat gave higher dose rates than tritiated water by a factor of 1.3 to 4.5, but the factors were within 2.0 in the majority of tissues except for small intestine and adipose tissue.

1. Introduction

A considerable amount of tritium is currently produced in fission reactors and in future a significant amount of this isotope will be used as fuel in fusion reactors. Tritium is released from these nuclear facilities mainly in the form of water. In this form, it is widely distributed in the biosphere and easily enters not only environmental water but also the bodies of plants and animals. This radionuclide is incorporated into the organic constituents of organisms, more efficiently in plants by photosynthetic processes. Thus, tritium transformed into organic form may be ingested by man as food as well as tritium in the form of water.

*Author for correspondence; e-mail: h_takeda@nirs.go.jp
†Environmental and Toxicological Sciences Research Group, National Institute of Radiological Sciences, 9-1 Anagawa-4-chome, Inage-ku, Chiba-shi 263-8555, Japan.
‡Institute of Industrial Hygiene, Ministry of Public Health, Beijing 100088, China.

It is well known that tritium in organic form is more efficiently incorporated into mammalian tissues than tritium as water. Some investigators have already reported a greater tritium incorporation from tritiated organic molecules (Vennart 1969, Mewissen *et al.* 1977, Takeda 1982) and from tritiated foods (Kirchmann *et al.* 1977, Rochalska and Szot 1977, Pietrzak-Flis *et al.* 1978, Takeda *et al.* 1985). However, there are few experimental studies of tritium dynamics in mammals under the condition of chronic exposure to tritiated water or tritiated food. For chronic exposure to tritium, especially in the form of food, few long-term data are available on tritium dynamics in mammalian tissues. Rodgers (1992) reported on tritium dynamics in mice chronically exposed to tritiated water and diet, but the duration of chronic exposure (56 days) was not enough to ensure that a steady-state condition had been attained. Tritiated food used in the experiments was prepared by mixing tritiated amino acid mixture with powdered commercial diet.

In the present study, rats were continuously exposed to tritiated water as drinking water or tritiated wheat as food for about 100 days. During chronic exposure, the biokinetics of tritium was investigated to elucidate the dynamics into a steady-state condition and to estimate the radiation dose rates under the steady-state condition. The results will be useful for comparative evaluation of the potential risk between the two modes of exposure.

2. Materials and methods

Wistar male rats weighing about 450 g were used in this study. Sixty rats were separated into two groups receiving chronic exposure either to tritiated water or tritiated wheat. Throughout the experiments, rats were housed in metabolic cages (Metabolica, Sugiyama-gen Co.) in order to measure consumption of water and food, and to collect daily samples of urine from each animal. The daily ingested amounts of drinking water and food averaged over all the present experiments were 36 ml

International Journal of Radiation Biology ISSN 0955-3002 print/ISSN 1362-3095 online © 2001 Taylor & Francis Ltd
http://www.tandf.co.uk/journals
DOI: 10.1080/09553000010017117

and 24 g, respectively. The daily excreted amount of urine averaged 17 ml.

Tritiated water (purchased from NEN) was diluted to an appropriate concentration with distilled water to prepare tritiated drinking water and tritiated food. The concentration of tritium in drinking water was adjusted to 6.3 kBq/ml. For preparation of tritiated food, wheat was grown in a 0.02 m^2 plastic Wagner's pot and after flowering the plant was sometimes irrigated with tritiated water in a phytotron with controlled temperature and natural light. At the time of ripening, the plants were harvested and the edible part was fed to the rats; it was first pulverized, freeze-dried and mixed with the powdered standard chow. The concentration of tritium in the food including tritiated wheat was 0.18 kBq/g.

Urine samples collected daily during these experiments were assayed for radioactivity. The rats were sacrificed by decapitation under ether anesthesia from weeks 1–14 after start of ingestion. Tissue samples were taken and the total tritium activity in the fresh wet tissues was determined. Part of each tissue sample was lyophilized for determination of organically bound tritium (OBT). Lyophilization was repeated twice with addition of distilled water to remove water-bound tritium and easily exchangeable OBT. Samples were combusted in an oxidizer (Model 306 Tri-Carb, Packard Instrument Co.) and tritium radioactivity in the combustion water was measured with a liquid scintillation counter.

Data were presented as a percentage of the concentration of tritium in the ingested water or food, and also as a percentage of tritium ingested per gram of wet or dry tissue. The former was expressed in terms of relative concentration and the latter was in terms of relative integrated activity. They were respectively calculated as follows

$$\text{Relative concentration} = \frac{\text{Radioactivity per g of wet or dry sample}}{\text{Radioactivity per g of ingested drinking water or food}} \times 100$$

$$\text{Relative integrated activity} = \frac{\text{Radioactivity per g of wet or dry sample}}{\text{Radioactivity ingested per g of tissue}} \times 100$$

Data values show the average of determinations on three or five animals.

The R-value, defined as the ratio of specific activity (T/H) of tritium in dry tissues to specific activity (T/H) of tritium in daily ingested drinking water or food, was also calculated for rat tissues at the end of 98 days of chronic exposure to tritiated water or tritiated wheat. For this calculation, the values used were for the hydrogen content for the organic component of various tissues given by Pietrzak-Flis *et al.* (1978). The hydrogen content of drinking water or tritiated food was calculated on the basis of their chemical composition to be 11.1% and 7.0%, respectively.

All experimental animals were treated and handled according to the 'Recommendations for handling of laboratory animals for biomedical research', compiled by the Committee on the Safety and Handling Regulations for Laboratory Animal Experiments, NIRS.

3. Results

Time variations in the relative concentration of tritium in urine collected daily during continuous ingestion of tritiated water or tritiated food are shown in figure 1. Concentrations of tritium in urine rapidly increased after the start of ingestion, and attained a steady-state condition by about day 10 after the start of tritiated water ingestion and day 20 after the start of tritiated food ingestion. The steady-state concentrations were approximately 64% of the concentration of tritium in drinking water and approximately 37% of that of tritium in the food. These values at steady-state seemed to be an index of contribution to body water tritium from drinking water and food, respectively. It was apparent in the preliminary experiments that the presence of OBT in urine could be ignored due to the low content of organic materials (about 3%), even after exposure to tritiated organic compounds including foods.

Time variations in the relative concentrations of total tritium and OBT in the selected tissues are shown in figure 2 and figure 3. In the case of exposure to tritiated water, the concentrations of total tritium increased rapidly and attained steady-state by 2–3 weeks. The steady-state concentrations of total tritium for the majority of tissues, including the tissues not shown in this figure, ranged from 40% to 50% of the concentration of tritium in drinking water. The steady-state concentration in blood was somewhat higher than that for other tissues, at about 60%. In adipose tissue, the steady-state condition was not clearly observed. The steady-state concentration of OBT in rats exposed to tritiated water was observed at about 4 weeks after the start of chronic exposure, although the steady-state concentrations for all the examined tissues were within 20% of the concentration of the ingested tritiated water. In the case of chronic exposure to tritiated food, a steady-state for both total tritium and OBT was not so clearly observed for 10 weeks after the start of chronic exposure for the majority of the examined tissues except for liver, in which the steady-state seemed to be attained at about 4 weeks. At the steady-state, the

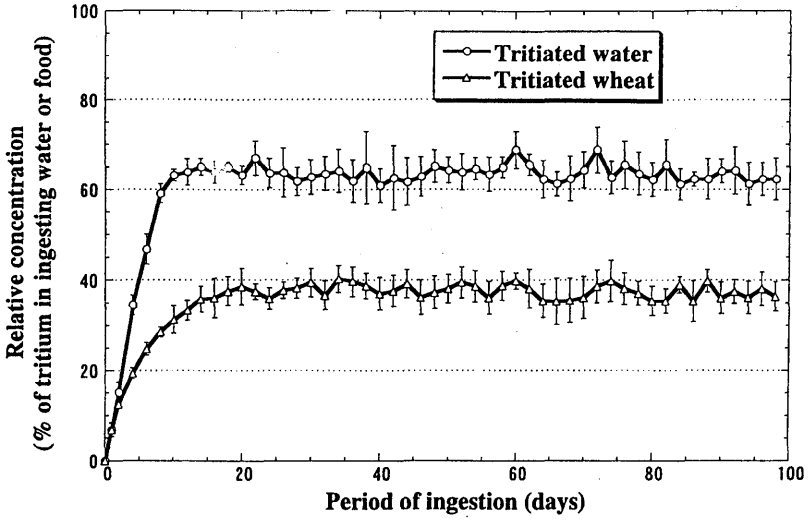

Figure 1. Time variations in the relative concentration of total tritium in urine.

concentrations of total tritium ranged from 39% to 56%, and those of OBT ranged from 47% to 71% of the concentration of tritium in the ingested food.

Table 1 shows the amount of total tritium and OBT retained in the tissues of rat at the end of chronic exposure, expressed in terms of the relative integrated activity, which enables the comparison of the amount of tritium incorporated and retained in the tissues between the two modes of exposure. It was evident that the amount of total tritium or OBT in the tissues of rats exposed to tritiated wheat was higher than that in rats exposed to tritiated water, the difference being more significant for OBT than for total tritium. The ratios of the relative integrated activity of OBT after exposure to tritiated wheat to that after exposure to tritiated water ranged from 5.6 in adipose tissue to 10.4 in heart.

The R-value, as defined above, is a useful factor for evaluating the extent of tritium incorporation into organic constituents of tissues. The R-values calculated for different tissues of rats at the termination of 98 days of chronic exposure to tritiated water or tritiated wheat are shown in table 2: they ranged from 0.13 for adipose tissue to 0.24 for testis (for tritiated water ingestion), and for tritiated wheat exposure the range was 0.36 for brain and adipose tissue and 0.78 for lung.

On the basis of the biokinetics data, the radiation dose rates at the end of chronic exposures were calculated. The following formula was used

$$D = 1.38 \times 10^{-2} (A \times E)$$

where D is the dose-rate in Gy/day, A is the tritium concentration in kBq/g, and E is the average energy of tritium β-rays (5.7×10^{-3} MeV). In this calculation, it was assumed that total radioactivity ingested during the chronic exposures was 3.7 MBq/g bodyweight in order to enable a comparative evaluation of the dose rates from the exposures to tritiated water and tritiated wheat. The dose calculation was performed not only for total tritium but also for OBT. For the calculation of the OBT contribution, the values of water content for individual tissues of rats determined in a previous study (Takeda and Kasida 1979) were used. The results are shown in table 3. In this table, the ratios of the dose rates from tritiated wheat ingestion to those from tritiated water ingestion are also given. The results show that the total dose rates from exposure to tritiated wheat were higher than those from exposure to tritiated water by a factor of 1.3 to 4.5, but the factors did not exceed 2.0 in the majority of tissues, except for small intestine and adipose tissue.

4. Discussion

The results of the present study showed a difference in tritium dynamics in rats chronically exposed to tritiated wheat as a food compared with rats exposed to tritiated water as a drinking water. The time taken to attain a steady-state concentration of total tritium in urine was longer in rats exposed to tritiated food than in rats exposed to tritiated water. With regard to the contribution of tritium in drinking water to body water tritium, the result was similar to that previously reported (Thompson and Ballou 1956, Hatch and Mazrimas 1972, Takeda 1991).

The steady-state condition for total tritium in the tissues was observed at 2–3 weeks in rats exposed to tritiated water, while that in rats exposed to tritiated wheat was not observed for 10 weeks in the majority of tissues. The differences in the dynamics of tritiated

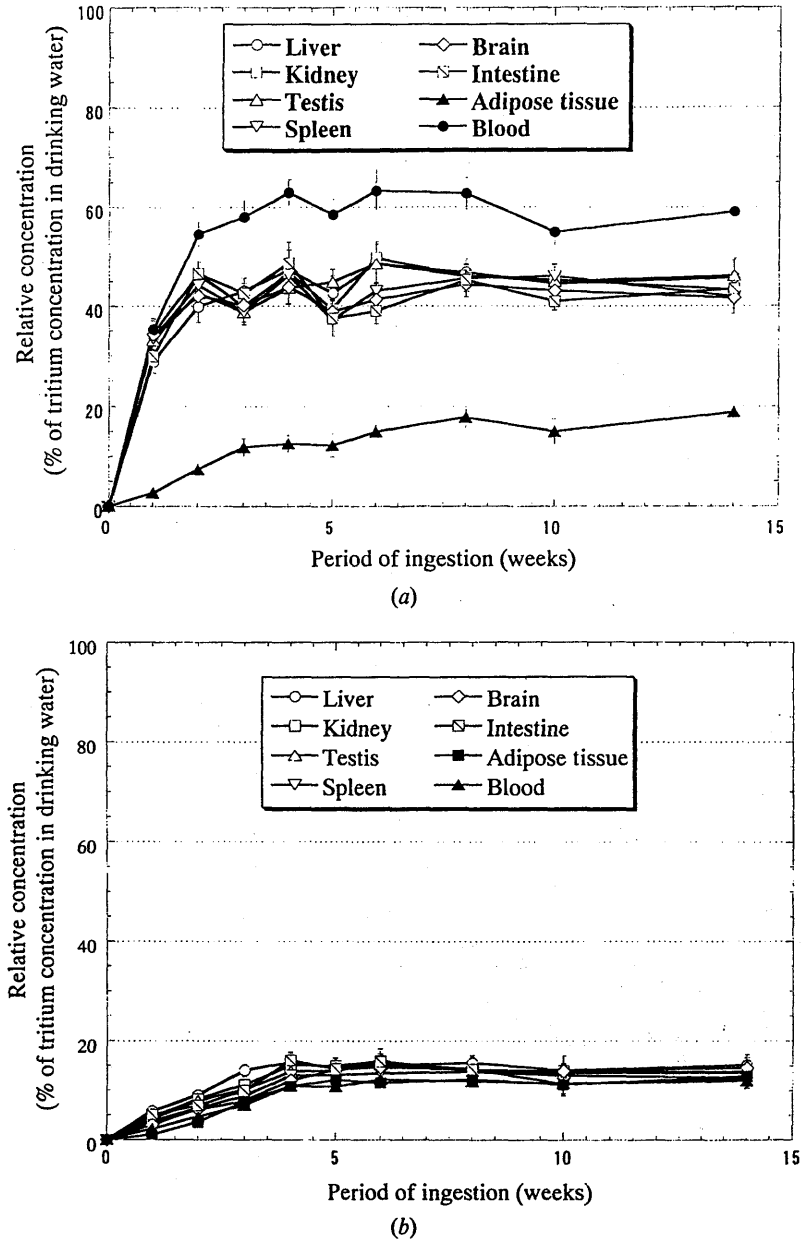

Figure 2. Relative concentration of (a) total tritium and (b) OBT in tissues during chronic exposure to tritiated water.

water and tritiated wheat were mostly due to the rate and duration of OBT formation. Because of the relatively efficient and prolonged OBT formation during the exposure to tritiated wheat, the relative integrated activity of tritium incorporated and retained in the tissues at the end of exposure was greater in rats exposed to tritiated wheat than those in rats exposed to tritiated water (table 1). As described previously, there are a few comparative studies on tritium incorporation into the tissue organic constituents from tritiated food and from tritiated water (Kirchmann *et al.* 1977, Rochalska and Szot 1977, Pietrzak-Flis *et al.* 1978). Comparing the results of these reports with those of present study, the relative integrated activity of OBT after the chronic exposure to tritiated water was almost the same level irrespective of the different duration of chronic exposure; in contrast, the integrated activity after exposure to tritiated food showed differences that may have been due to differences in the types of food used in individual experiments.

R-values estimated at the end of chronic exposure were higher for tritiated wheat than for tritiated water. In a previous study (Takeda *et al.* 1985), the R-values in tissues of rats continuously exposed for 22 days were also estimated. Compared with the

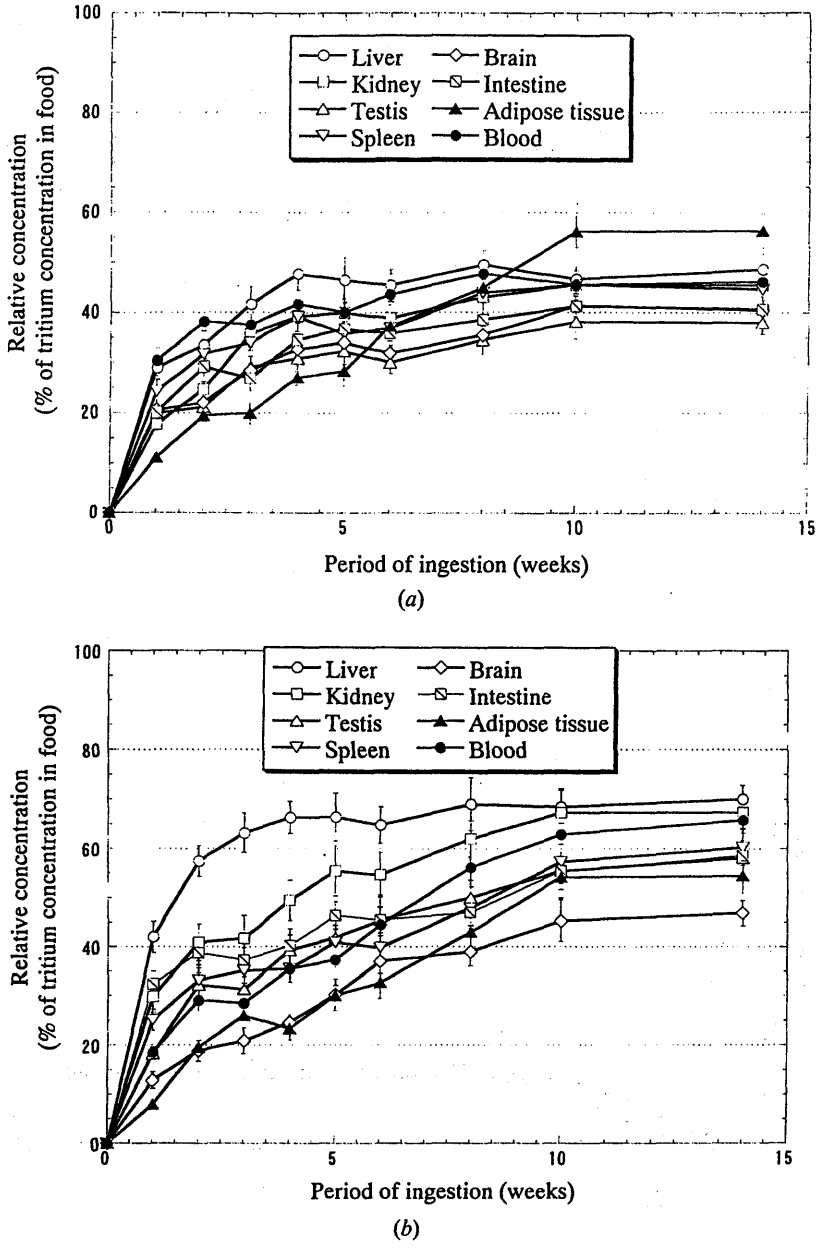

Figure 3. Relative concentration of (a) total tritium and (b) OBT in tissues during chronic exposure to tritiated wheat.

previous result, the present R-values for the exposure to tritiated water did not differ significantly, but those for the exposure to tritiated wheat were greater in tissues other than liver. Nevertheless, values never exceeded 1.0, indicating that the specific activity of tritium in the tissue organic constituents did not exceed the specific activity of tritium in the food as well as that in the drinking water.

Estimation of radiation dose rates at the end of chronic exposure showed that the total dose rates from exposure to tritiated wheat were 1.3–4.5 times higher than those from exposure to tritiated water. In the previous study, in which tritiated water and tritiated wheat were continuously ingested for about 3 weeks, it was reported that the dose rates from tritiated food were higher than those from tritiated water by a factor of 2.1 to 4.8. The results of the present study therefore indicate that the difference in the dose rates between tritiated water and tritiated food would not increase by lengthening the period of chronic exposure.

The differences in the tritium biokinetics observed

Table 1. Relative integrated activity of total tritium and OBT in the tissues of rats at the end of chronic exposure to tritiated water or tritiated wheat.

Tissue	Relative integrated activity[a] (percentage of activity ingested per gram of wet or dry tissue)			
	Total tritium		OBT	
	Tritiated water	Tritiated wheat	Tritiated water	Tritiated wheat
Liver	6.3±0.2	12.2±1.3	2.3±0.2	19.4±0.7
Kidney	6.7±0.3	11.6±1.1	1.9±0.2	17.1±0.8
Testis	7.7±0.3	9.7±0.5	2.2±0.2	15.7±0.7
Spleen	6.7±0.4	10.6±0.4	1.7±0.3	15.3±1.1
Brain	5.9±0.3	10.2±0.3	2.1±0.2	12.0±1.7
Muscle	6.4±0.4	10.3±0.3	1.6±0.2	13.4±1.0
Small intestine	5.9±0.6	15.1±1.1	1.8±0.3	16.2±1.5
Lung	6.4±0.3	10.2±0.4	1.8±0.2	15.7±2.1
Heart	6.6±0.5	10.5±0.6	1.7±0.3	17.6±2.5
Adipose tissue	3.2±0.2	14.4±0.9	2.5±0.3	13.9±0.7
Blood	9.4±0.4	13.4±0.7	1.7±0.2	16.7±1.2

[a] Each value is the mean±SD of five rats for tritiated water and three rats for tritiated wheat.

Table 2. Ratio of specific activity of tritium in dry tissue to specific activity in the daily ingested tritiated water or tritiated food, estimated at the end of chronic exposure.

Tissue	Hydrogen content (%)	R-value	
		Tritiated water	Tritiated food
Liver	7.11	0.23	0.70
Kidney	7.62	0.20	0.62
Testis	6.32	0.24	0.68
Spleen	6.12	0.19	0.69
Brain	9.26	0.16	0.36
Muscle	5.93	0.21	0.67
Small intestine	7.95	0.17	0.56
Lung	5.61	0.23	0.78
Heart	8.15	0.15	0.59
Adipose tissue	11.69	0.13	0.36

Table 3. Radiation dose rates from total tritium and OBT contribution to dose rates at the end of chronic exposure.

Tissues	Dose rate (mGy/day)[a] and OBT contribution[b]		Rate of dose rate
	Tritiated water	Tritiated wheat	tritiated wheat / tritiated water
Liver	18 (11.3)	36 (49.3)	2.0
Kidney	20 (7.7)	34 (39.8)	1.7
Testis	22 (4.3)	28 (24.3)	1.3
Spleen	20 (6.6)	31 (37.5)	1.6
Brain	17 (8.9)	30 (29.4)	1.8
Muscle	19 (7.0)	30 (36.8)	1.6
Small intestine	17 (8.5)	44 (30.0)	2.6
Lung	19 (6.8)	30 (36.9)	1.6
Heart	19 (7.0)	31 (45.3)	1.6
Adipose tissue	9 (66.4)	42 (82.0)	4.5
Blood	27 (3.6)	39 (24.9)	1.4

[a] The dose rates were calculated assuming tritium exposure to be 3.7 MBq/g body weight.
[b] OBT contribution is expressed as a percentage of total dose rate in parentheses.

at the chronic exposures to tritiated drinking water and tritiated food may be explained ultimately on the basis of the physiology and metabolism of water and organic materials in the body of mammals, although it is too intricate to permit an explanation of the detailed mechanism.

The dose coefficients (Sv/Bq) for organic tritium, currently presented by ICRP (1995), are higher than those for tritiated water by a factor of 1.9 to 2.5. The results of the present study support the ICRP recommendation as an average value. In a previous study (Takeda 1995), it was shown that the cumulative doses from a single intake of various tritiated organic compounds were 1.3–5.2 times higher than that from the intake of tritiated water, and it was proposed that the annual limit on intake (ALI) for organic tritium should be five times smaller than that for tritiated water. The results of present study support this proposal.

Acknowledgements

This study was supported by a special grant from the Science and Technology Agency and in part by a Grant-in-Aid from the Ministry of Education, Science and Culture, Japan. The authors wish to thank Dr Iwakura for his suggestions during this study and his comment on dose calculations.

References

HATCH, F. T. and MAZRIMAS, J. A., 1972, Tritiation of animals from tritiated water. *Radiation Research*, **50,** 339–357.

ICRP, 1995, *Age-dependent doses to members of the public from intake of radionuclides: Part 5, Compilation of ingestion and inhalation dose coefficients.* Publication 72 (Oxford: Pergamon Press).

KIRCHMANN, R., CHARLES, P., VAN BRUWAENE, R., REMY, J., KOCH, G. and VAN DEN HOEK, J., 1977, Distribution of tritium in the different organs of calves and pigs after ingestion of various tritiated feeds. *Current Topics in Radiation Research Quarterly*, **12,** 291–312.

MEWISSEN, D. J., FUREDI, M., UGARTE, A. and RUST, J. H., 1977, Comparative incorporation of tritium from tritiated water versus tritiated thymidine, uridine or leucine. *Current Topics in Radiation Research Quarterly*, **12,** 225–254.

PIETRZAK-FLIS, Z., RADWAN, I. and INDEKA, L., 1978, Tritium in rabbits after ingestion of freeze-dried tritiated food and tritiated water. *Radiation Research*, **76,** 420–428.

ROCHALSKA, M. and SZOT, Z., 1977, The incorporation of organically-bound tritium of food into some organs of the rat. *International Journal of Radiation Biology*, **31,** 391–395.

RODGERS, D. W., 1992, Tritium dynamics in mice exposed to tritiated water and diet. *Health Physics*, **63,** 331–337.

TAKEDA, H., 1982, Comparative metabolism of tritium in rat after a single ingestion of some tritiated organic compounds versus tritiated water. *Journal of Radiation Research*, **23,** 345–357.

TAKEDA, H., 1991, Incorporation and distribution of tritium in rats after chronic exposure to various tritiated compounds. *International Journal of Radiation Biology*, **59,** 843–853.

TAKEDA, H., 1995, Metabolic and dosimetric study to estimate an annual limit on intake for organic tritium. *Fusion Technology*, **28,** 964–969.

TAKEDA, H. and IWAKURA, T., 1992, Incorporation and distribution of tritium in rats exposed to tritiated rice or tritiated soybean. *Journal of Radiation Research*, **33,** 309–318.

TAKEDA, H. and KASIDA, Y., 1979, Biological behavior of tritium after administration of tritiated water in the rat. *Journal of Radiation Research*, **20**, 174–185.

TAKEDA, H., ARAI, K. and IWAKURA, T., 1985, Comparison of tritium metabolism in rat following single or continuous ingestion of tritium labeled wheat versus tritiated water. *Journal of Radiation Research*, **26,** 131–139.

THOMPSON, R. C. and BALLOU, J. E., 1956, Studies of metabolic turnover with tritium as a tracer. V. The predominantly non-dynamic state of body constituents in the rat. *Journal of Biological Chemistry*, **223,** 795–809.

VENNART, J., 1969, Radiotoxicology of tritium and ^{14}C compounds. *Health Physics*, **16,** 429–440.

Pergamon

Chemosphere, Vol. 39, No. 15, pp. 2757-2766, 1999

0045-6535/99/ $ - see front matter

PII: S0045-6535(99)00210-6

DETERMINATION OF ^{99}Tc DEPOSITED ON THE GROUND WITHIN THE 30-km ZONE AROUND THE CHERNOBYL REACTOR AND ESTIMATION OF ^{99}Tc RELEASED INTO ATMOSPHERE BY THE ACCIDENT

S. Uchida, K. Tagami, W. Rühm[†] and E. Wirth[††]

Environmental and Toxicological Sciences Research Group, National Institute of Radiological Sciences
4-9-1 Anagawa, Inage-ku, Chiba-shi, 263-8555 JAPAN
[†]Institute for Radiation Biology, Ludwig Maximilians Universität München
Schillerstr. 42, D-80336 München, GERMANY
[††]Federal Office for Radiation Protection, Institute of Radiation Hygiene,
Ingolstädter Landstr. 1, D-85762 Oberschleißheim, GERMANY

(Received in Germany 15 March 1999; accepted 3 May 1999)

ABSTRACT- Technetium-99 was determined in samples from the 30-km zone around the Chernobyl reactor. Concentrations of ^{99}Tc in soil samples taken from three forest sites ranged from 1.1 to 14.1 Bq kg^{-1} dry weight for the organic soil layers, and from 0.13 to 0.83 Bq kg^{-1} dry weight for the mineral soil layers. In particular, for the organic layers, the measured ^{99}Tc concentrations were one or two orders of magnitude higher than those due to global fallout ^{99}Tc. The ^{99}Tc depositions (Bq m^{-2}), based on the sum of the depositions measured in organic and mineral layers, ranged from 130 Bq m^{-2} within the 10-km zone to about 20 Bq m^{-2} close to the border of the 30-km zone. Taking the corresponding measured ^{137}Cs depositions into account, it was found that the activity ratio of ^{99}Tc/^{137}Cs ranged from 6 x 10^{-5} to 1.2 x 10^{-4}. It was estimated that about 970 GBq of ^{99}Tc had been released by the Chernobyl accident. This figure corresponded to 2% - 3% of the total ^{99}Tc inventory in the core.

Key words: *Technetium-99; Chernobyl accident; Forest soil; Deposition; Cesium-137; Migration*

INTRODUCTION

There have been many reports concerning radionuclides' concentrations in environmental samples due to the accident in Unit 4 of the Chernobyl Nuclear Power Station (CNPS). Some reports have shown ^{99}Mo concentrations in environmental samples[1-6]. This radioisotope decays to ^{99}Tc [^{99}Mo ($t_{1/2}$: 65.9 h)--> ^{99m}Tc ($t_{1/2}$: 6.0 h)--> ^{99}Tc], but the amount may be negligible compared to the deposited ^{99}Tc released directly into the atmosphere with other radionuclides at the time of the accident. Because ^{99}Tc has a high

fission yield of about 6% and a long half-life of 2.1 x 10^5 y and Tc has a high absorbability by plants[7-8], a survey of the contamination levels in environmental samples is of interest to estimate the long term ^{99}Tc exposure to humans. At present, however, there are almost no data on ^{99}Tc contamination of environmental samples and consequently, limited information on the ^{99}Tc activity released by the Chernobyl accident is available.

In this paper, results of ^{99}Tc and ^{137}Cs measurements in samples taken from three forest sites within the 30-km zone around the CNPS are presented. ^{99}Tc and ^{137}Cs concentrations [Bq kg^{-1} dry weight (DW)] and depositions [Bq m^{-2}] are given for the organic soil layers and for the first 6 to 9 cm of mineral soil. The results are discussed with respect to expected values and different characteristics of ^{99}Tc and ^{137}Cs. In addition, the amount of ^{99}Tc released from the reactor into the environment is estimated using data from this paper, and results reported previously by Aarkrog and others[9-10].

MATERIALS AND METHODS

Soil Samples

For the present analysis, soil samples collected within three forest sites around Chernobyl were used. The sites D1 (mixed forest: 50% oak, 30% pine, 20% birch; 55-60 years old) and D3 (mixed forest: 50% alder, 40% birch, 10% pine; 50-75 years old) are located 28.5 km and 26.0 km to the south of the CNPS, respectively, while K2 (pine forest; about 50 years old) is located 6.0 km to the southeast of the CNPS. Soils at D1 and K2 are podsol on sandy fluvio-glacial deposits and at D3, peat-gley on sandy fluvio-glacial deposits. D1 and K2 are so-called dry forests, whereas D3 can be characterized as wet forest, since the groundwater level at this site is at a depth of about 45 cm from the top of the soil surface[11]. Samples were collected by the Federal Office for Radiation Protection, Germany, in 1994 and 1995, assisted by the Moscow State University, Russia, and the Research and Industrial Association 'Pripyat', Ukraine. Nine profiles of undisturbed soil per site and year were randomly collected within an area of about 100 x 100 m^2.

In order to produce representative organic soil samples, materials from the organic layers (L, Of, Oh horizons) gathered at the same site and in the same year, were combined to one mixed sample. The same procedure was used in order to get representative mixed mineral samples using materials from the Ah horizon and from the first 6 cm of the B horizon. At D3, no Ah-horizon could be identified and the first 9 cm of the B horizon were used. For the present analysis, D1 samples from 1994 and 1995 were combined.

Reagents

Prepacked columns of Tc-selective chromatographic resin (EIChroM Industries Inc., TEVA · Spec resin) were used for the chemical separation. Nitric acid was ultrapure-analytical grade (Tama Chemicals, AA-100). Deionized water (>17MΩ) was used throughout the work. A radiotracer of ^{95m}Tc, which was obtained from a Nb foil using the reaction ^{93}Nb (α, 2n) ^{95m}Tc[12], was applied to determine the recovery of ^{99}Tc in the samples during the chemical separation procedure.

Chemical Separation and Measurements

In all samples, ^{99}Tc and ^{137}Cs concentrations were determined. The ^{137}Cs activities were measured by use of a Ge detector system (Seiko EG&G, Ortec) without any chemical separations. For the ^{99}Tc determination, chemical separation was necessary. The separation method used was a revised form of the method reported previously[13,14]. Only a brief explanation is given here.

1) The soil sample was incinerated at 450°C in an electrical oven for one night. 2) After addition of ^{95m}Tc, the sample was placed in a combustion apparatus. 3) Tc was volatilized from the sample at 1000°C under O_2 gas stream and the element was collected in a trap solution (deionized water). 4) After adjusting to 0.1 M HNO_3, the trap solution was introduced into a TEVA · Spec resin column to extract Tc onto the resin. Then 40 mL of 2 M HNO_3 solution were passed through the column to elute co-existing elements. 5) In order to desorb the Tc from the resin, 5 mL of 8 M HNO_3 solution were pipetted onto the column. 6) The strip solution of 8 M HNO_3 from the resin was put in a glass beaker and evaporated to dryness at 70°C on a hot plate. 7) The residue was dissolved with 5 mL of 2% HNO_3 solution. 8) The ^{95m}Tc activity in each 2% HNO_3 solution was measured with a NaI (Tl) scintillation counter (Aloka, ARC-380) to obtain chemical recoveries. Total recoveries of ^{95m}Tc during the chemical separation process ranged from 39 to 93%.

After the chemical separation, ^{99}Tc concentrations in each 2% HNO_3 solution were determined by inductively coupled plasma mass spectrometry (ICP-MS; Yokogawa PMS-2000). Counting time at mass 99 was 10 min, or 200 s for three times. The concentrations of stable Mo and stable Ru in the solution were also measured. Because Ru, which has an isotopic abundance of 12.7% at mass of 99, interferes with ^{99}Tc measurement by ICP-MS and there is a possibility of a molecular peak from ^{98}MoH at mass of 99. For the ICP-MS measurement, ^{99}Tc standard solution (Japan Isotopes Association, NH_4TcO_4 form in 0.1% ammonia solution) was used.

For concentrations (Bq kg^{-1} DW), uncertainties are given with respect to statistical one-sigma errors of the measurements, throughout the paper. For given depositions (Bq m^{-2}), standard errors for the area-related densities (kg DW m^{-2}) are also taken into account. It is not possible to give standard errors arising due to the heterogeneous horizontal deposition pattern in natural ecosystems directly, since only mixed samples were analyzed in this study. From earlier measurements of ^{137}Cs at the investigated sites it is estimated, however, that this contribution to the overall one-sigma standard error of mean concentration values is less than 10% for the combined L/Of/Oh samples, and less than 20% for the combined Ah/B samples.

RESULTS AND DISCUSSION

Deposition of ^{99}Tc and ^{137}Cs within the 30-km Zone

Table 1 shows the results of ^{99}Tc and ^{137}Cs concentrations in the investigated soil samples. In the case of ^{137}Cs, the concentrations range from (0.84 ± 0.02) kBq kg^{-1} DW (D1, '94 &'95, Ah/B) to (230 ±

Table 1 Concentrations of ^{99}Tc and ^{137}Cs in Bq kg^{-1} DW with statistical one-sigma measurement error; corresponding area-related deposition in Bq m^{-2}, and $^{99}Tc/^{137}Cs$ ratios on 26 April 1986, in soil samples collected in the 30-km zone around Chernobyl. Area-related densities are based on 5 soil profiles, taken in 1993 at each site. The corresponding errors are one-sigma standard errors. Additional uncertainties to mean concentration values due to the inhomogenous deposition are estimated to be less than 10% (L/Of/Oh) and less than 20% (Ah/B).

Soil sample	Tc recovery	^{99}Tc	^{137}Cs	Area-related density	^{99}Tc	^{137}Cs	Activity Ratios
	^{95m}Tc (%)	Bq kg^{-1} DW	Bq kg^{-1} DW	kg DW m^{-2}	Bq m^{-2}	kBq m^{-2}	$^{99}Tc/^{137}Cs$ x 10^{-4}
D1 ('94 & '95), L/Of/Oh	87	1.11 ± 0.02	19 ± 0.02	4.4 ± 0.4	4.9 ± 0.4	83.6 ± 7.3	0.58 ± 0.01
D1 ('94 & '95), Ah/B	73	0.13 ± 0.03	0.84 ± 0.02	86.9 ± 1.9	11.6 ± 0.3	72.4 ± 2.5	1.60 ± 0.05
D3 ('94), L/Of/Oh	93	2.43 ± 0.01	19.5 ± 0.04	4.4 ± 0.7	10.6 ± 1.6	85.2 ± 12.8	1.24 ± 0.01
D3 ('95), L/Of/Oh	88	1.72 ± 0.05	19.9 ± 0.4	4.4 ± 0.7	7.5 ± 1.1	86.9 ± 13.2	0.86 ± 0.03
D3 ('94 & '95), B	62	0.36 ± 0.01	1.8 ± 0.03	37.1 ± 2	13.4 ± 0.8	68.2 ± 3.8	1.97 ± 0.04
K2 ('94), L/Of/Oh	77	8.58 ± 0.26	230 ± 2.1	5.2 ± 0.5	44.8 ± 4.3	1200 ± 111	0.37 ± 0.01
K2 ('95), L/Of/Oh	73	13.4 ± 0.16	178 ± 2.7	5.2 ± 0.5	70.1 ± 6.5	928 ± 87	0.76 ± 0.01
K2 ('94 & '95), Ah/B	39	0.83 ± 0.02	11.4 ± 0.1	86.5 ± 1.7	72.1 ± 2.1	982 ± 23	0.72 ± 0.02

2.1) kBq kg^{-1} DW (K2, '94, L/Of/Oh). Expressed on a kBq m^{-2} basis, ^{137}Cs contamination levels of the organic samples and the mineral samples are similar at each site, i.e. between 70 and 90 kBq m^{-2} for D1 and D3, and about 1000 kBq m^{-2} for K2. A total deposition was calculated for each site by adding the depositions of the corresponding organic and mineral layers, averaged over 1994 and 1995. The results are (156 ± 8) kBq m^{-2}, (154 ± 10) kBq m^{-2} and (2046 ± 74) kBq m^{-2}, for D1, D3 and K2, respectively (Table 2). These results are in close agreement to values published previously for the same sites[11]. This shows that the samples chosen for this study are representative with respect to the measured ^{137}Cs deposition, and it is therefore assumed that the same is true for the measured ^{99}Tc deposition.

The ^{99}Tc concentrations range from (1.11 ± 0.02) to (13.4 ± 0.2) Bq kg^{-1} DW for the organic samples, and from (0.13 ± 0.03) to (0.83 ± 0.02) Bq kg^{-1} DW for the mineral samples. Expressed on a Bq m^{-2} basis, the contamination levels for ^{99}Tc range from 4.9 ± 0.4 Bq m^{-2} (D1, '94 & '95, L/Of/Oh) to 72.1 ± 2.1 Bq m^{-2} (K2, '94 & '95, Ah/B). In particular, the results for the organic samples are one or two orders of magnitude higher compared to global fallout ^{99}Tc concentrations, which have been reported to range from 0.01 to 0.1 Bq kg^{-1} DW[15,16]. From this result it is evident that most of the ^{99}Tc measured in Chernobyl samples originates from the Chernobyl accident. This conclusion is also supported by the fact that the total ^{99}Tc deposition at K2 (organic + mineral: 130 ± 4 Bq m^{-2}), which is located much closer to the CNPS than D1 and D3, is 6 to 8 times larger compared to the total ^{99}Tc deposition at D1 ((16.5 ± 0.6) Bq m^{-2}) and D3 ((22.5 ± 1.2) Bq m^{-2}) (Table 2). Similar differences in the contamination of K2 compared to D1 and D3 have been observed for many other radionuclides released by the CNPS (see Table 2 for ^{137}Cs, and reference[11] for other radionuclides).

Table 2 Lower limits for the deposition of ^{99}Tc and ^{137}Cs at the investigated sites. Uncertainties include statistical one-sigma measurement errors and one-sigma standard errors for the area-related densities. Additional uncertainties due to the inhomogenous deposition are estimated to be less than 10% (L/Of/Oh) and less than 20% (Ah/B).

Site	^{99}Tc [Bq m^{-2}]	^{137}Cs [kBq m^{-2}]	$^{99}Tc/^{137}Cs$
D1	16.5 ± 0.6	156 ± 8	(1.06 ± 0.06) x 10^{-4}
D3	22.5 ± 1.2	154 ± 10	(1.46 ± 0.12) x 10^{-4}
K2	130 ± 4	2046 ± 74	(6.4 ± 0.3) x 10^{-5}

$^{99}Tc/^{137}Cs$ Activity Ratios and Their Mobilities in the Soils

The investigated samples were taken 8 and 9 years after the accident. During this time, some ^{99}Tc and ^{137}Cs might have reached deeper mineral layers than the layers investigated in this study. At present, no information on ecological half-lives for ^{137}Cs is available for the different soil layers at the investigated sites. However, ecological half-lives at a forest in Bavaria, Germany ranged from 2.8 ± 0.5 years in the L horizon to 7.7 ± 4.9 years in the Ah horizon[17], so it is expected that less than half of the initially deposited cesium had migrated to mineral layers by 1995. Since we have included, in this study, even the first 6 to 9 cm of mineral soil, loss of ^{137}Cs is expected to be of minor importance. Since mobility for ^{99}Tc might be higher compared to ^{137}Cs (see below), loss of ^{99}Tc to deeper layers might be larger than for ^{137}Cs. It should be bare in mind, therefore, that the results for the total ^{99}Tc deposition released by the Chernobyl accident might represent only lower limits.

In order to compare the mobility of ^{99}Tc and ^{137}Cs, $^{99}Tc/^{137}Cs$ ratios were separately calculated for the organic and mineral layers, and decay-corrected back to the accident date of 26 April 1986 (Table 1). With one exception (sample K2, '95, L/Of/Oh), all organic samples showed significantly lower $^{99}Tc/^{137}Cs$ ratios than those of the mineral samples in the corresponding sites. This can be interpreted in terms of a higher mobility of ^{99}Tc compared to ^{137}Cs, allowing ^{99}Tc to penetrate to deeper layers within the given time, and increasing the $^{99}Tc/^{137}Cs$ ratios in deeper layers while possibly decreasing these ratios in the organic layers. This is in line with results from experiments on undisturbed forest soil columns, where it was shown that after simulating artificial rain showers, ^{95m}Tc applied as pertechnetate was more mobile compared to ^{137}Cs[18, 19].

Since the Chernobyl accident, only one publication has appeared reporting on the simultaneous measurement of ^{137}Cs and ^{99}Tc originating from the Chernobyl accident in the same sample: Aarkrog *et al.*[9] determined the ratio of $^{99}Tc/^{137}Cs$ in a heavily contaminated motor filter of a fishing boat in the western Baltic Sea, which had passed through the Chernobyl cloud at the end of April 1986. These authors found a ratio of 1.01×10^{-5}. For comparison, we calculated $^{99}Tc/^{137}Cs$ ratios from the total depositions deduced for each site, again decay-corrected back to the accident date of 26 April 1986 (Table 2). Our results range from $(0.6 \pm 0.03) \times 10^{-4}$ (K2) to $(1.46 \pm 0.12) \times 10^{-4}$ (D3). These values are higher than the result reported by Aarkrog *et al.*[9], but close to the theoretical ratio of 1.4×10^{-4} estimated from the corresponding fission yields and half-lives.

It should be noted that Aarkrog's data and our data are difficult to compare, since ^{99}Tc and ^{137}Cs are expected to behave differently in the environment with respect to volatility, deposition velocities, and migration rates, due to their differences in the actual physicochemical forms in which both nuclides appear. For example, $^{99}Tc/^{137}Cs$ ratios are expected to be influenced by the different mobilities of ^{99}Tc and ^{137}Cs in our soil samples (see above), but not in Aarkrog's filter sample. Atmospheric transport is also expected to influence ratios calculated for different radionuclides. For example, it was reported that $^{103}Ru/^{137}Cs$ ratios decreased by a factor of 20 over a distance of approximately 1000 km[10]. Since the characteristics of Tc are expected to be similar to those of Ru[9, 20], it is possible that in comparison to

^{137}Cs, ^{99}Tc would be apt to deposit close to the Chernobyl region, and subsequently, the corresponding $^{99}Tc/^{137}Cs$ ratios could be higher close to the CNPS than those obtained from other areas far from it.

^{99}Tc Released from the Chernobyl Accident

Recently a procedure was suggested to estimate the release of ^{137}Cs from the Chernobyl accident[10]. We followed this procedure and plotted our data for ^{137}Cs in addition to the data given in Aarkrog's report (1988)[10] versus distance from the CNPS. A least squares fit of these data gives a regression function of $D_{Cs} = 5.14 \times 10^4 \times R^{-1.477}$, where D_{Cs} is the ^{137}Cs deposition on the ground (GBq km^{-2}) and R, the distance from the CNPS (km) (see Fig. 1). Assuming the same horizontal distribution of the ^{137}Cs

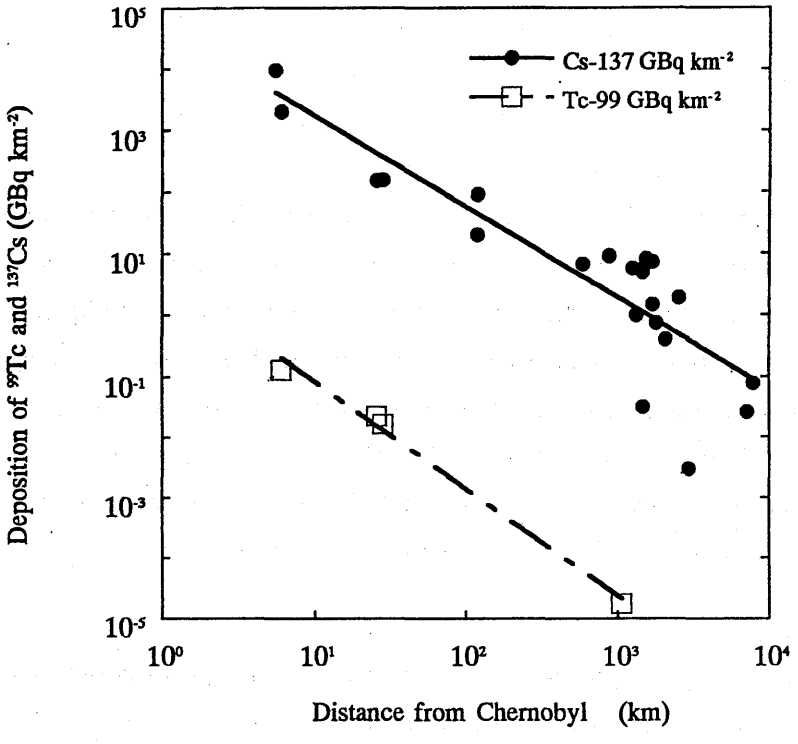

Fig. 1 ^{137}Cs and ^{99}Tc deposition as function of distance from Chernobyl. ^{137}Cs deposition data are from this study and from (10). ^{99}Tc deposition data are from this study and from (9) which was estimated for a distance of 1000 km (see text).

deposition in all directions from the CNPS, we calculate the ^{137}Cs release as

$$\int_1^{10000} 2\pi R \times 5.14 \times 10^{-2} \times R^{-1.477}\, dR \approx 76 \text{ PBq}$$

This is close to the ^{137}Cs release estimated for the Chernobyl accident[20, 21].

We applied a similar procedure in order to estimate the release of ^{99}Tc due to the Chernobyl accident, using our ^{99}Tc depositions (Table 2) for distances of 6 km (K2), 26 km (D3), and 28.5 km (D1). For a distance of 1000 km, we assumed that the $^{99}Tc/^{137}Cs$ ratio of 1.01×10^{-5} given in the report of Aarkrog *et al.*[9], and the ^{137}Cs deposition of about 1 GBq km^{-2} given in Fig. 1, produce a representative ^{99}Tc deposition of about 1×10^{-5} GBq km^{-2}. The resulting regression function is $D_{Tc} = 4.88 \times R^{-1.771}$, where D_{Tc} is the ^{99}Tc deposition on the ground (GBq km^{-2}) and R, the distance from the CNPS (km) (see Fig. 1). Again, the release may be calculated by integration over R as

$$\int_1^{10000} 2\pi R \times 4.88 \times R^{-1.771}\, dR \approx 970 \text{ GBq}$$

The total core inventory of ^{137}Cs is estimated to range from 210 to 290 PBq[20, 21]. A ^{137}Cs release of 76 PBq, as estimated in this paper, corresponds therefore to a fraction of 26% to 36% of the total ^{137}Cs core inventory. From the inventory of ^{137}Cs and from the theoretical ratio of ^{99}Tc to ^{137}Cs of 1.4×10^{-4}, the total inventory of ^{99}Tc can be calculated to range from 30 to 40 TBq. Consequently, the percentage of ^{99}Tc released into the atmosphere by the accident could be estimated to range from 2% to 3%. This result is close to the estimate given by Aarkrog *et al.* who suggested the release percentage of ^{99}Tc would be an order of magnitude less than that of ^{137}Cs. However, our result is higher by a factor of 3 to 4 compared to the estimate of the release percentage of ^{103}Ru and ^{106}Ru given in the report of Gudiksen *et al.*[20], which is believed to be similar to the release percentage of ^{99}Tc[9]. At this point we emphasize that all estimates of the ^{99}Tc release of the Chernobyl accident still have a large uncertainty, since data on ^{99}Tc concentrations in environmental samples are quite limited. Further investigations are required for a precise estimate of the amount of ^{99}Tc released by the Chernobyl accident.

ACKNOWLEDGMENT

This work was carried out in the National Institute of Radiological Sciences (NIRS), Japan. W. R. gratefully acknowledges the Science and Technology Agency of Japan for financial support during a 3-month stay in Japan.

REFERENCES

1. L. Devell, H. Tovedal, U. Bergström, A. Appelgren, J. Chyssler and L. Andersson, Initial observations of fallout from the reactor accident at Chernobyl, *Nature* **321**, 192-193 (1986).
2. N. E. Whitehead, S. Ballestra, E. Holm and A. Walton, Air radionuclide patterns observed at Monaco from the Chernobyl accident, *J. Environ. Radioact* **7**, 249-264 (1988).
3. J. L. Ferrero, M. L. Jordá, J. Milió, L. Monforte, A. Moreno, E. Navarro, F. Senent, A. Soriano,

A. Baeza, M. del Río and C. Miró, Atmospheric radioactivity in Valencia, Spain, due to the Chernobyl reactor accident, *Health Phys*. **53**, 519-524 (1987).

4. H. O. Denschlag, A. Diel, K. H. Gläsel, R. Heimann, N. Kaffrell, U. Knitz, H. Menke, N. Trautmann and G. Herrmann, Fallout in the Mainz area from the Chernobyl reactor accident, *Radiochim. Acta* **41**, 163-172 (1987).
5. H. Hötzl, G. Rosner and R. Winkler, Long-term behaviour of Chernobyl fallout in air and precipitation, *Radiochim. Acta* **41**, 181-190 (1987).
6. I. Winkelmann, H. J. Endrulat, S. Fouasnon, P. Gesewsky, R. Haubelt, P. Klopfer, H. Köhler, R. Kohl, D. Kucheida, C. Leising, M. K. Müller, P. Neumann, H. Schmidt, K. Vogl, S. Weimer, H. Wildermuth, S. Winkler and E. Wirth, E., Wolff, S. *Institute for Radiation Hygiene, German Federal Office of Radiation Protection, ISH Report 116* (1987).
7. P. J. Coughtrey, D. Jackson and M. C. Thorne, *Radionuclide Distribution and Transport in Terrestrial and Aquatic Ecosystems, A Critical Review of Data, Vol. 3*, pp.210-217, A. A. Balkema, Netherlands (1983).
8. J. E. Till, F. O. Hoffman and D. E. Dunning Jr., A new look at ^{99}Tc releases to the atmosphere, *Health Phys.* **36** 21-30 (1979).
9. A. Aarkrog, L. Carlsson, Q. J. Chen, H. Dahlgaard, E. Holm, L. Huynh-Ngoc, L. H. Jensen, S. P. Nielsen and H. Nies, Origin of technetium-99 and its use as a marine tracer, *Nature* **335**, 338-340 (1988).
10. A. Aarkrog, The radiological impact of the Chernobyl debris compared with that from nuclear weapons fallout, *J. Environ. Radioact*.**6** 151-162 (1988).
11. D. Lux, L. Kammerer, W. Rühm and E. Wirth, Cycling of Pu, Sr, Cs, and other long-living radionuclides in forest ecosystems of the 30-km zone around Chernobyl, *Sci. Total Environ.* **173/174**, 375-384 (1995).
12. T. Sekine, M. Konishi, H. Kudo, K. Tagami and S. Uchida, Separation of carrier free ^{95m}Tc from niobium targets irradiated with alpha particles, *J. Radioanal. Nucl. Chem.* (in press).
13. K. Tagami and S. Uchida, Analysis of technetium-99 in soil and deposition samples by inductively coupled plasma mass spectrometry, *Appl. Radiat. Isot.* **47** 1057-1060 (1996).
14. K. Tagami and S. Uchida, Use of a combustion apparatus for low-level ^{99}Tc separations from soil samples, *Radioact. and Radiochem.* (in press).
15. T. R. Garland, D. A. Cataldo, K. M. McFadden, R. G. Schreckhise and R. E. Wildung, Comparative behaviour of ^{99}Tc, ^{129}I, ^{127}I and ^{137}Cs in the environment adjacent to a fuels reprocessing facility, *Health Phys.* **44**, 658-662 (1983).
16. K. Tagami and S. Uchida, Concentration of global fallout ^{99}Tc in rice paddy soils collected in Japan, *Environ. Pollut.* **95**, 151-154 (1997).
17. W. Rühm, L. Kammerer, L. Hiersche and E. Wirth, Migration of ^{137}Cs and ^{134}Cs in Different Forest Soil Layers, *J. Environ. Radioact.* **33**, 63-75 (1996) and Erratum. *J. Environ. Radioact.* **34**, 103-106 (1997).
18. W. Schimmack, K. Bunzl and D. Klotz, Infiltration of radionuclides with high mobility (^{82}Br and

^{95m}Tc) into a forest soil. Effect of the irrigation intensity, *Sci. Total Environ.* **138**, 169-181 (1993).

19. W. Schimmack, K. Bunzl, F. Dietl and D. Klotz, Infiltration of radionuclides with low mobility (^{137}Cs and ^{60}Co) into a forest soil. Effect of the irrigation intensity, *J. Environ. Radioact.* **24**, 53-63 (1994).
20. P. H. Gudiksen, T. F. Harvey and R. Lange, Chernobyl source term, atmospheric dispersion, and dose estimation, *Health Phys.* **57**, 697-706 (1989).
21. United Nations Scientific Committee on the Effects of Atomic Radiation. *1988 Report to the General Assembly, Annex D*; pp. 312-314, New York: United Nations (1988).

Journal of Radioanalytical and Nuclear Chemistry, Vol. 243, No. 2 (2000) 403–408

Transfer of technetium from paddy soil to rice seedling

K. Yanagisawa, H. Takeda, K. Miyamoto, S. Fuma

Environmental and Toxicological Sciences Research Group, National Institute of Radiological Sciences, 4-9-1 Anagawa, Inage-ku, Chiba-shi, 263-8555 Japan

(Received September 16, 1999)

Tracer experiments on the chemical transformation of technetium in paddy soil and the transfer to rice seedlings have been carried out using ^{95m}Tc as a tracer. Two common Japanese soils, Andosol and Gray lowland soil were used in the soil incubation experiments. The chemical form of soluble Tc in soil water was a mixture of Tc-organic matter complex, Tc-iron complex and pertechnetate. An uptake experiment with rice seedlings using nutrient solution showed that the Tc-organic matter complex was less available than pertechnetate or the Tc-iron complex. These chemical forms of Tc were also observed in the root bleeding sap of rice seedlings when introduced to the nutrient solution containing soluble Tc. These results suggested that the transfer of technetium from soil to rice would depend on the chemical form of Tc and they would transport from the root to the leaf without chemical transformation.

Introduction

Technetium-99 is one of the important radionuclides for radiation protection because of its long half-life ($2.1 \cdot 10^5$ y) and relatively high fission yield. In the chemical form of TcO_4^-, this radionuclide is well dissolved in soil water and easily available to plants.[1] The transfer factor of technetium recommended by the IAEA is 5 for food crops.[2] This value is higher than other radionuclides such as ^{137}Cs (0.03) or ^{90}Sr (0.3). For nuclear safety assessment, it is necessary to obtain information on the behavior of this nuclide in the soil-plant system. In Japan, rice is one of the most important agricultural products and its consumption is very high. Studies on this plant are important for dose assessment through the intake of foodstuffs. Since the transfer factor is expected to vary with different crops, we have performed laboratory experiments on the transfer of technetium from soil to various Japanese crops using ^{95m}Tc as a tracer.[3–5] In this, we found the transfer factors for brown rice (hulled rice grain) grown in a flooded condition were markedly lower than those for other cereals grown in a non-flooded condition. It was suggested that TcO_4^- added to the soil rapidly transformed to an insoluble form due to the reducing conditions caused by the flooding. The chemical form of Tc fixed with soil is thought to be TcO_2 and/or the Tc-humic acid complex as suggested by VAN LOON et al.[6] and SEKINE et al.[7] VAN LOON et al. found from their incubation experiment that minor quantities of Tc were present in an aqueous extract with distilled water at pH 6. They suggested that the Tc was associated with organic matter dissolved in the water. We found that the chemical form of the soluble Tc in flooded soils was not pertechnetate since it was associated with soluble organic matter.[8] The availability of this Tc-organic matter complex to a rice seedling was lower than pertechnetate. However, a more detailed study was necessary to know whether the Tc-organic matter complex is the only chemical form that was generated in the flooded soil. In addition, the chemical transformations of Tc in the plant root are still unknown. Therefore, we have carried out following three experiments. In the first experiment, we determined the precise chemical form of soluble Tc in the flooded soil. In the second one, we examined the influence of the chemical form of Tc on the plant availability, and in the third, determined the chemical form of Tc in the root bleeding sap of a rice seedling.

Experimental

Soil incubation and determination of chemical form of soluble Tc

Andosol and Gray lowland soil were used in the experiments. Andosol was collected in Tokai Village, Ibaraki, and Gray lowland soil was collected in Mito City, Ibaraki. The chemical properties of these soils are listed in Table 1. Both soils were air dried and sieved to pass a 1 mm mesh. Soil (5 g), deionized water (10 ml) containing 3.7 MBq of $^{95m}TcO_4^-$, and glucose (10 mg) to enhance microbial activity, were mixed thoroughly and placed in a 50 vial. The soil mixtures were incubated at room temperature (about 20 °C) for 40 days and the soluble Tc was extracted as follows. After mixing thoroughly, the samples were centrifuged at 5000 rpm for 20 minutes. The supernatant was filtered with a 0.4 μm pore diameter filter.

The chemical form of Tc was examined by gel filtration chromatography (Sephadex G-15, column diameter = 1 cm; column length = 30 cm; eluents = 0.01M $CaCl_2$; flow rate = 12/h; injection volume = 2; fraction size = 1). To detect soluble organic matter in the solution, the optical density of the effluent was measured at 254 nm (Tokyo Rikakikai UV-9000).

0236–5731/2000/USD 17.00

Akadémiai Kiadó, Budapest
Kluwer Academic Publishers, Dordrecht

Table 1. Chemical properties of soil used in the experiments

	Gray lowland soil	Andosol
CEC,* meq/100 g of dry soil	10.2	16.6
Total carbon, %	2.4	4.3
pH	5.7	5.3

* Cation exchange capacity.

Samples of the fractionated effluents were placed in polyethylene vials and ^{95m}Tc concentration was measured with a scintillation counter (Aloka ARC-300). Decay corrections were made to the beginning of the experiment.

Determination of availability to rice seedling

Since the concentration of soluble ^{95m}Tc in Andosol was low, the soluble fraction of Gray lowland soil was used in this experiment. Fractions obtained from Gel filtration chromatography, were diluted with nutrient solution (Kasugai solution: N=40 mg/l; P_2O_5=20 mg/l; K_2O=30 mg/l; CaO=4 mg/l; MgO=6 mg/l)[9] to a volume of 200. As a control, 200 of nutrient solution containing 2 kBq of $^{95m}TcO_4^-$ was prepared. These solutions were placed in glass beakers and shaded with black polyethylene film. Rice seedlings (*Oryza sativa L.* C.V. Kosihikari) were pre-cultivated on a floating mesh (nylon mesh: 2 mm) using nutrient solution in a growth chamber for 20 days, before they were exposed to the nutrient solutions mentioned above. Five plants were used for determination of the availability of Tc for each solution. After a 24 hours exposure, the concentrations of ^{95m}Tc in the leaves and roots of each rice plant were measured. During the exposure experiments, the temperature in the chamber was controlled at 30 °C during the daylight period (14 h) and 25 °C during the night. The light intensity at the plant level in the chamber was about 20000 lux. At the harvest, each plant was separated into leaves and roots. Samples of the plant parts (0.5–0.8 g) or the nutrient solutions (2) were placed in polyethylene vials and measured with an automatic well type sodium iodide scintillation counter. Values of the concentration ratio between plant parts and the nutrient solution were calculated as "the activity per unit weight of plant (on a fresh weight basis)" divided by "the activity per unit weight of the nutrient solution".

Determination of the chemical form of Tc in the root bleeding sap

Soluble Tc obtained from two kinds of soil incubation (about 5 ml) was diluted with nutrient solution to a volume of 30 ml. These solutions were placed in polyethylene vials and shaded with black polyethylene film. Immediately after the rice seedling was transplanted to the vial, the stem of the seedling was cut near the root and bleeding sap was collected from rice seedling. For the collection, absorbent cotton was placed on the cutting surface of the rice seedling and covered by polyethylene film to prevent evaporation. After 12-hour collection, bleeding sap was extracted from the absorbent cotton with water and analyzed by gel filtration chromatography as mentioned above.

Results and discussions

Determination of chemical form of soluble Tc

Table 2 shows the distribution of ^{95m}Tc between the soil solid phase (insoluble form) and the soil solution (soluble form). More than 98% of the ^{95m}Tc in both soils was distributed in the soil-solid phase.

As we observed in the cultivation experiment with rice,[5] the transformation of TcO_4^- to the insoluble form occurred due to the reducing condition generated by soil micro-organisms. Between the two soils, the concentration of the soluble ^{95m}Tc in Gray lowland soil was markedly higher than that of Andosol. This tendency was consistent with the results obtained in our previous experiments.[5] The chromatograms of soluble ^{95m}Tc in the two soils are shown in Fig. 1 (Gray lowland soil) and Fig. 2 (Andosol). In the two soils, three peaks were observed in the elution pattern of ^{95m}Tc. The first peak corresponded to the peak of the optical density, which represents the elution of soluble organic matter. This result indicates that ^{95m}Tc eluted in the first peak of both soils were associated with soluble organic matter. The peak of ^{95m}Tc-organic matter complex and the optical density of Gray lowland soil (Fig. 1) were higher than those of Andosol (Fig. 2). This difference would depend on the amount of soluble organic matter released from each soil to water.

In the second and third peak, there was no distinct difference between the two soils. Concerning the second peak, we assumed that the chemical form of ^{95m}Tc eluted in this position might be formed by the reaction of Fe^{2+} ion and $^{95m}TcO_4^-$. To confirm this assumption, we mixed 10 ml of 2% $FeSO_4$ solution and 1 kBq of $^{95m}TcO_4^-$ in a 50 ml vial and analyzed the solution by gel filtration chromatography. The results (Fig. 3) showed that a small amount of the ^{95m}Tc was eluted in the same position of the second peak. This suggested that the ^{95m}Tc eluting in the second peak would be associated with iron ion or iron hydroxide.

Table 2. Distributions of ^{95m}Tc in the soil solid phase and soil solution

Phase	Percent of total, %	
	Gray lowland soil	Andosol
Soil solid phase (insoluble)	98.3	99.9
Water phase (soluble)	1.7	0.1

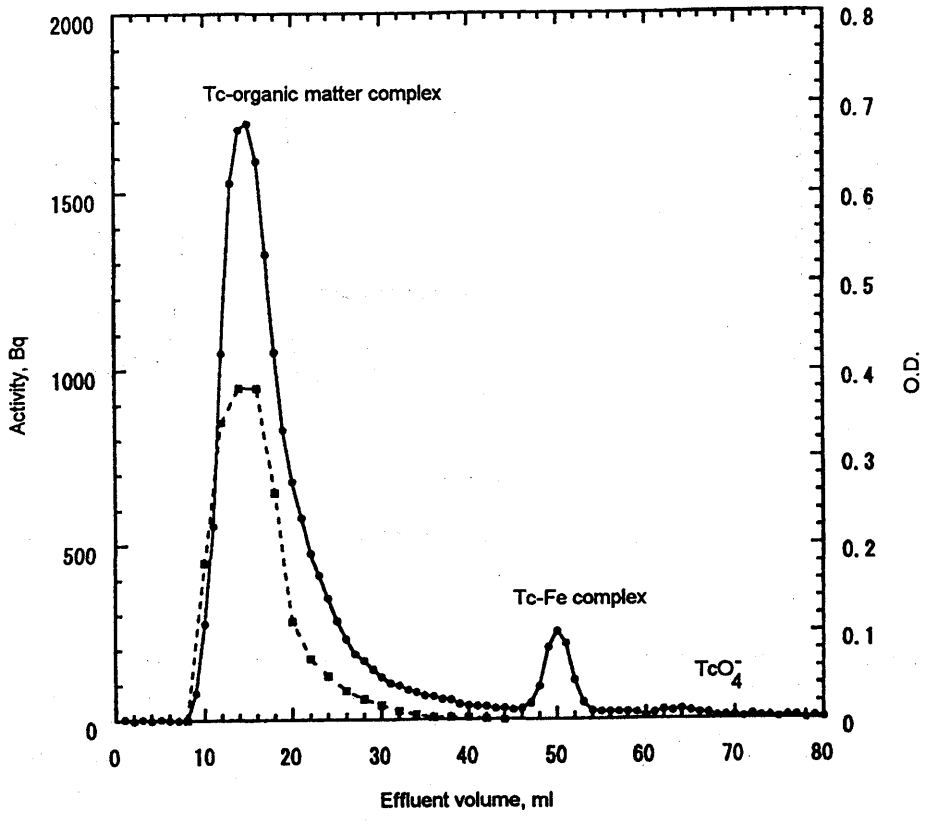

Fig. 1. Chromatogram of soluble ^{95m}Tc isolated from Gray lowland soil; ● ^{95m}Tc; ■ optical density

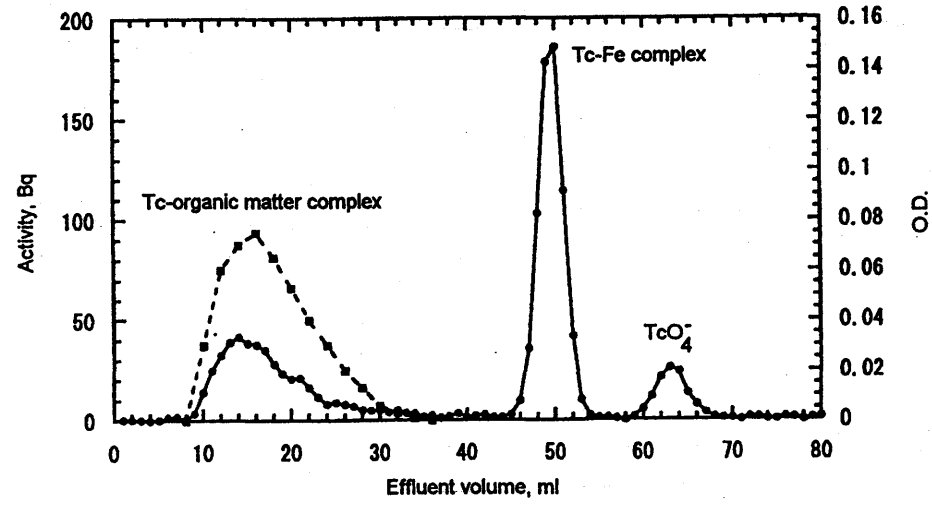

Fig. 2. Chromatogram of soluble ^{95m}Tc isolated from Andosol; ● ^{95m}Tc; ■ optical density

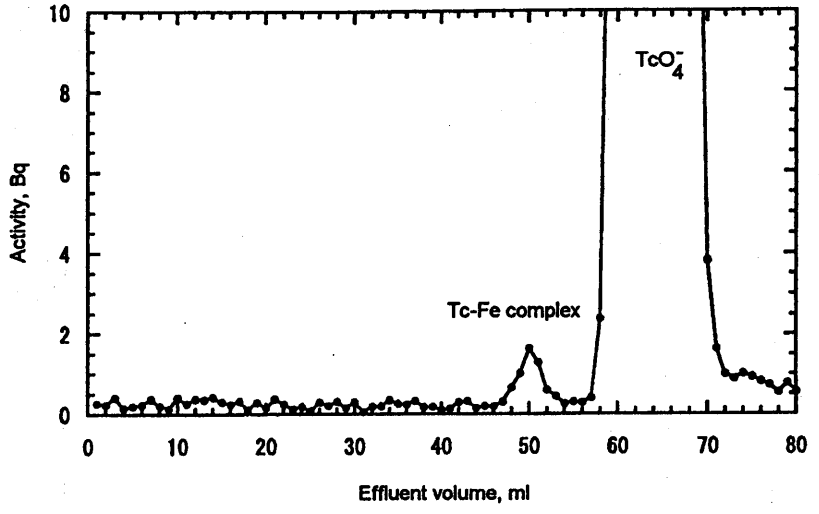

Fig. 3. Chromatogram of ^{95m}Tc mixed with $FeSO_4$ solution as $^{95m}TcO_4^-$

Table 3. Distribution of ^{95m}Tc (in Bq) in various chemical forms isolated from the soil solution

Chemical form	Gray lowland soil	Andosol
Tc-organic matter complex	861	53
Tc-iron complex	58	76
Pertechnetate	12	13

Note: 3.7 MBq of $^{95m}TcO_4^-$ added in the incubation of two soils.

Since this chemical form of Tc is soluble in water and can filter through the column, it would differ from Tc-iron hydroxide aggregates.[10] Details of this form of Tc remain to be investigated. In this paper, we describe this chemical form as Tc-iron complex for convenience. The third peak was pertechnetate, which was confirmed by the analysis of $^{95m}TcO_4^-$. The amount of soluble ^{95m}Tc in each chemical form is shown in Table 3. The amounts of pertechnetate and Tc-iron complex were similar for the two soils. The production of soluble Tc-organic matter complex in the soils might relate to the soil nature, e.g., quantity and quality of soil organic matter.

Availability of soluble Tc to rice seedling

Plant availability of different chemical forms of Tc is shown in Table 4. The concentrations of ^{95m}Tc in the plant samples were not less than 100 $Bq \cdot g^{-1}$. The concentration ratios observed in the leaves of the rice plant were as follows: 2.7 for Tc-organic matter complex, 23 for Tc-iron complex and 43 for pertechnetate. The concentration ratio observed in Tc-organic matter complex was markedly lower than that for other two chemical forms of Tc, suggesting that Tc-organic matter complex is less available than Tc-iron complex or pertechnetate. For the root, the concentration ratio was opposite to that of the leaves: 15 for Tc-organic matter complex, 9.4 for Tc-iron complex and 5.9 for pertechnetate. The higher concentration ratio of the Tc-organic matter complex observed at the root of the rice seedling can be explained by its lower efficiency of transportation from root to leaf than those of other form of Tc.

Chemical form of Tc in the root bleeding sap

Chromatograms of the root bleeding sap collected from rice seedling transplanted in the nutrient solution containing the soluble fraction of ^{95m}Tc isolated from Gray lowland soil and Andosol are shown in Figs 4 and 5. Compared with the soluble Tc (Figs 1 and 2), the chemical forms of Tc does not seem to be changed.

Table 4. Concentration ratios for rice plant seedling and nutrient solution after a 24 hour exposure

Chemical form	Leaves*	Root*
Tc-organic matter complex	2.7 ± 0.2	14 ± 0.6
Tc-iron complex	23 ± 1.3	9.4 ± 0.5
Pertechnetate	43 ± 2.9	5.9 ± 0.4

* ± Standard deviation for 5 samples.

Table 5. Concentration ratios of each chemical form of Tc between root bleeding sap and nutrient solution containing soluble technetium from two soils

Chemical form	Andosol	Gray lowland soil
Tc-organic matter complex	0.6	0.6
Tc-iron complex	0.6	0.6
Pertechnetate	8.0	5.2

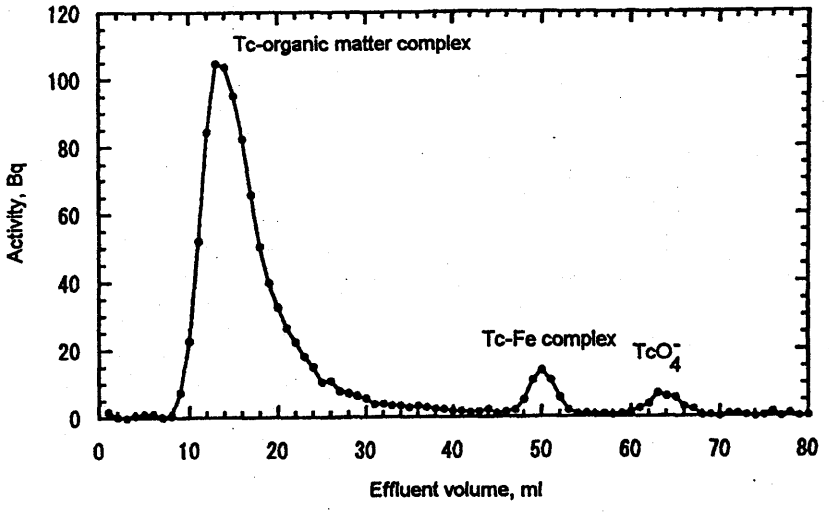

Fig. 4. Chromatogram of bleeding sap collected from rice seedling transplanted in the nutrient solution containing soluble fraction of ^{95m}Tc isolated from Gray lowland soil

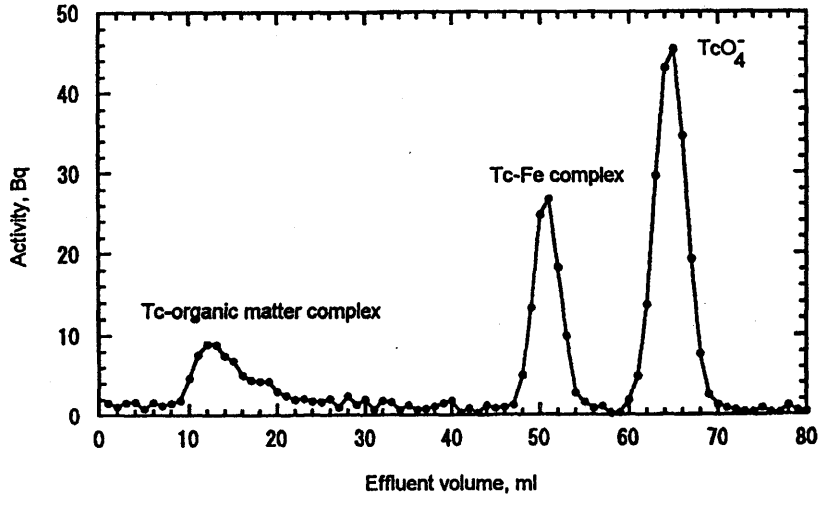

Fig. 5. Chromatogram of bleeding sap collected from rice seedling transplanted in the nutrient solution containing soluble fraction of ^{95m}Tc isolated from Andosol

The concentration ratios between the root bleeding sap and nutrient solutions in each chemical form are shown in Table 5. The concentration ratio of the pertechnetate was higher than that of Tc-organic matter complex and Tc-iron complex. This suggested that the uptake and transport of TcO_4^- was more efficient than the other two chemical forms and that the chemical transformation of Tc into other chemical forms would not occur in the root. Technetium absorbed at the root is supposed to transport to the leaves without chemical transformation.

Conclusions

Most of the ^{95m}Tc added as pertechnetate to flooded soil was transformed into an insoluble form due to the reducing condition generated by soil micro-organisms and subsequently it was fixed in the soil. Although the concentration was very low, a soluble form of ^{95m}Tc was present in the soil solution. The concentrations of the soluble ^{95m}Tc in Gray lowland soil were higher than in Andosol. From the gel filtration chromatographic

determination, three chemical forms of the ^{95m}Tc were found in the soluble fraction: Tc-organic matter complex, Tc-iron complex and pertechnetate. An uptake experiment with rice seedlings using nutrient solution showed that the Tc-organic matter complex was less available than pertechnetate or the Tc-iron complex. Chromatograms of the root bleeding sap collected from rice seedlings showed that the chemical form of ^{95m}Tc was not different from the nutrient solution containing soluble ^{95m}Tc from the two soils. These results suggested that the transfer of technetium from soil to rice depends on the chemical form in the soil solution and there was no chemical transformation in the transfer process.

References

1. J. M. MOUSNY, P. ROUCOUX, C. MYTTENAERE, Environ. Exp. Bot., 19 (1979) 263.
2. IAEA, Generic Models and Parameters from Assessing the Environmental Transfer of Radionuclides from Routine Releases, IAEA Safety Ser. No. 57, IAEA, Vienna, 1994, p. 20.
3. K. YANAGISAWA, Y. MURAMATSU, H. KAMADA, Radioisotopes, 41 (1992) 397.
4. K. YANAGISAWA, Y. MURAMATSU, J. Radiat. Res. 36 (1995) 171.
5. K. YANAGISAWA, Y. MURAMATSU, J. Radioanal. Nucl. Chem., 197 (1995) 203.
6. L. VAN LOON, M. STALMANS, A. MAES, A. CREMERS, M. COGNEAU, Technetium in the Environment, Elsevier Applied Science Publishers, London, 1986.
7. T. SEKINE, A. WATANABE, K. YOSHIHARA, J. I. KIM, Radiochim. Acta, 63 (1993) 87.
8. K. YANAGISAWA, Y. MURAMATSU, T. BAN-NAI, J. Radioanal. Nucl. Chem., 226 (1997) 221.
9. S. KASUGAI, Journal of Science of Soil and Manure, Japan, 13 (1939) 669 (in Japanese).
10. M. A. DAVIS, Radiology, 95 (1970) 347.
11. IAEA, Generic Models and Parameters from Assessing the Environmental Transfer of Radionuclides from Routine Releases, IAEA Safety Ser. No. 57, IAEA, Vienna, 1994, p. 20.
12. K. YANAGISAWA, Y. MURAMATSU, H. KAMADA, Radioisotopes, 41 (1992) 397.
13. K. YANAGISAWA, Y. MURAMATSU, J. Radiat. Res., 36 (1995) 171.
14. K. YANAGISAWA, Y. MURAMATSU, J. Radioanal. Nucl. Chem., 197 (1995) 203.

ELSEVIER

J. Environ. Radioactivity, Vol. 41, No. 2, pp. 183–205, 1998

Printed in Great Britain
PII: S0265-931X(97)00098-2 0265-931X/98 $19.00 + 0.00

Concentrations of Alkali and Alkaline Earth Elements in Mushrooms and Plants Collected in a Japanese Pine Forest, and Their Relationship with ^{137}Cs

Satoshi Yoshida & Yasuyuki Muramatsu

National Institute of Radiological Sciences, 4-9-1 Anagawa, Inage-Ku, Chiba-Shi, Chiba 263-8555, Japan

(Received 11 August 1997; accepted 13 November 1997)

ABSTRACT

^{137}Cs and stable Na, K, Rb, Cs, Mg, Ca, Sr, Ba and Al were determined in 29 mushrooms and 8 plants collected from a Japanese pine forest. Concentrations of ^{137}Cs, Cs and Rb in mushrooms were one order of magnitude higher than those in plants growing in the same forest. On the other hand, concentrations of Ca and Sr in mushrooms were obviously lower than those in plants. A good correlation ($r = 0{\cdot}99$, $p < 0{\cdot}01$) between ^{137}Cs and stable Cs concentrations was observed for mushrooms. The $^{137}Cs/Cs$ ratios were almost constant ($^{137}Cs/Cs = 134 \pm 36\ Bq\,mg^{-1}$ in 1990) and were significantly higher than that in the surface soil ($27\ Bq\,mg^{-1}$). The ratios for plants were almost the same as those for mushrooms. In plant samples, good correlations were observed among the concentrations of K, Rb, Cs and Mg. Correlation between those of Ca and Sr was also good. In contrast, Cs was not correlated with K in mushrooms, indicating that the mechanism of Cs uptake was different from that for K. Rb showed a correlation with Cs ($r = 0{\cdot}82$).

INTRODUCTION

Radiocesium discharged to the environment through nuclear weapons testing and nuclear accidents is accumulated in forest ecosystems, mainly due to the wide surface areas of tree canopies and the ability of forest soils to hold radiocesium. Even 10 years after the Chernobyl accident, radiocesium contamination of forest products is high in contrast to agricultural products. Since removal of radiocesium from a contaminated forest is difficult,

studies on the distribution and transfer of radiocesium in forest ecosystems are important in order to predict the future contamination of forest product. Many studies were carried out before and after the Chernobyl accident (e.g. Waller and Olsen, 1967; Yamagata *et al.*, 1969; Heinrich *et al.*, 1989; Schimmack *et al.*, 1993; Wirth *et al.*, 1994). Accumulation and migration of radiocesium in the soil profiles have been discussed and many studies indicate that radiocesium deposited in the forests is accumulating at the surface of the forest soils (e.g. Thiry and Myttenaere, 1993; Yoshida and Muramatsu, 1994*a*; Bunzl *et al.*, 1995).

Concentrations of radiocesium in biological samples were also measured. A great deal of effort has gone into the measurement of radiocesium in mushrooms, because mushrooms accumulate radiocesium. High concentrations of radiocesium in mushrooms were reported in European forests (e.g. Haselwandter *et al.*, 1988; Baldini *et al.*, 1989; Römmelt *et al.*, 1990) and also in Japanese forests (Muramatsu *et al.*, 1991; Yoshida and Muramatsu, 1994*a*, *b*; Yoshida *et al.*, 1994; Sugiyama *et al.*, 1994). Many factors controlling the radiocesium concentration in mushrooms, e.g. type of forest (Heinrich, 1992), soil pH (Eckl *et al.*, 1986; Sugiyama *et al.*, 1994) and species of mushrooms (Fraiture *et al.*, 1990; Dighton *et al.*, 1991), were discussed. The relationship between the habitat of the mycelium and the radiocesium concentration in the fruit body has also been studied (Giovani *et al.*, 1990; Guillitte *et al.*, 1990; Yoshida and Muramatsu, 1994*a*; Yoshida *et al.*, 1994; Rühm *et al.*, 1997). Recent studies (Olsen *et al.*, 1990; Guillitte *et al.*, 1994; Brückman and Wolters, 1994) indicated the importance of mycelium on the accumulation of radiocesium in surface soils. Many of them demonstrated that more than 30% of ^{137}Cs existing in the surface soil is accumulated in the mycelia of fungi.

These experimental measurements in forest ecosystems have provided information for the development of models which explain radiocesium transport through several compartments in a forest ecosystem. Some different types of models were developed as summarized by Schell *et al.* (1994, 1996). However, the prediction of radiocesium behaviour in forest ecosystems is still difficult.

Analytical data of stable elements must be useful to understand the long-term behaviour of radionuclides. Chemical behaviour of radiocesium is expected to be similar to that of stable Cs and the other alkali elements. Myttenaere *et al.* (1993) summarized the relationship between radiocesium and K in forests, and suggested the possible use of K behaviour for the prediction of radiocesium behaviour.

There are many studies on the behaviour of major nutrient elements such as K, Mg and Ca in forests (e.g. Eaton *et al.*, 1973; Likens *et al.*, 1977) because these elements are directly related to the forest growth. Effect of

acid deposition on the behaviour of these elements was also studied in the last two decades (e.g. Mayer and Ulrich, 1977; Yoshida and Ichikuni, 1989; Liechty *et al.*, 1993). However, information on the relationship between radionuclides and the major nutrient elements in forest ecosystems is still limited. In addition, analytical data about the nutrient elements in wild mushrooms are very much limited, although some studies such as Tyler (1980) are available. The data for trace alkali and alkaline earth elements such as Rb, Cs, Sr and Ba in forest ecosystems are limited because of the lack of simple analytical methods. Recently, inductively coupled plasma-mass spectrometry (ICP-MS) has been used for accurate and precise determination of trace elements in environmental samples for more than 50 elements including Rb, Cs, Sr and Ba (Casetta *et al.*, 1990; Yamasaki and Tamura, 1990; Alaimo and Censi, 1992; Schönberg, 1993; Yoshida *et al.*, 1996).

In the previous papers (Yoshida and Muramatsu, 1994*a*, *b*; Yoshida *et al.*, 1994), the authors studied the behaviour of radiocesium in a Japanese pine forest on sandy soil near the coast in Tokai-mura, Ibaraki Prefecture. Radiocesium in plants, mushrooms and soils were determined and accumulation of it in mushrooms was discussed. However, data for stable elements, which can be discussed with the radiocesium concentrations are limited, except for some plant and soil samples (Yoshida and Muramatsu, 1997).

In this paper, the stable alkali (Na, K, Rb and Cs), alkaline earth (Ca, Sr and Ba) elements and Mg in mushrooms collected in the pine forest were determined by ICP-MS or inductively coupled plasma-atomic emission spectrometry (ICP-AES), and the data of stable elements for mushrooms, plants and soils were summarized together with those of ^{137}Cs. Al was also measured to check the contamination due to soil particles adhering on the surface of the samples. Concentration ratio between mushroom or plant and surface soil was estimated for each stable element and ^{137}Cs. Relationships among the concentrations of ^{137}Cs and the above-mentioned stable elements were discussed.

MATERIALS AND METHODS

Sampling of mushrooms and plants

Samples were collected from a pine forest where the behaviour of radiocesium has been studied by the authors (Yoshida and Muramatsu, 1994*a*, *b*; Yoshida *et al.*, 1994). The forest is situated in lat. 36° 26′ N. and long. 140° 36′ E. on sandy soil near the coast in Tokai-mura, Ibaraki Prefecture. Mushroom samples were collected in 1989–1991 and plant

samples (leaves for trees and leaves and stems for shrubs and grasses) were collected in November 1990. The samples were cleaned by using a brush or cellulose wiper, gently removing attached soil and humus. They were not rinsed with water to avoid possible loss of a part of the elements by leaching. After cleaning, samples were freeze-dried and pulverized with a cooking blender. Soils from different depths were also sampled in the forest. The organic layer of the soil was thin in this forest. Therefore, after removing the litter layer, the soil was separately sampled at four depths (0–2, 2–5, 5–10 cm and deeper). The organic layers except litter layer were included in the first 0–2 cm. Analyses of the soils were described in Yoshida *et al.* (1994) and Yoshida and Muramatsu (1997). The soils were sampled at one place in the forest. Therefore, the analytical data for soils might be less representative than those for mushrooms and plants.

Determination of ^{137}Cs

Each dried sample (usually 20–40 g) was placed in a plastic bottle (diameter: 50 mm) and concentration of ^{137}Cs was determined by counting with a Ge-detector for 40 000–80 000 s. The decay correction was made as to October 1990. The approximate detection limit for ^{137}Cs by the counting system for a 30 g dry sample was 3 Bq kg^{-1}. The results of the radiocesium determination were already reported in the previous papers (Muramatsu *et al.*, 1991; Yoshida *et al.*, 1994; Yoshida and Muramatsu, 1994*a*, *b*). The concentrations of ^{137}Cs were under the detection limit in some mushroom samples. One of the most important objectives of the present study is to get information about the relationship between radiocesium and stable elements in mushrooms. Therefore, the 29 mushrooms in which ^{137}Cs was detected were selected and analyzed for stable elements. Samples used in the present study are listed in Table 1. They were mycorrhizal or saprophytic fungi growing on the soil. Saprophytic fungi growing on dead trees were not included. The concentrations of ^{137}Cs in this type of mushrooms were below the detection limits because of relatively low concentrations of ^{137}Cs in their substrata (dead trees).

Determination of stable elements

A mushroom sample (0·4 g) was digested in Teflon™ PFA pressure decomposition vessel with HNO_3, HF and $HClO_4$. After leaving the vessels on a hot plate (80°C) overnight for pre-decomposition, the samples were heated in a microwave digester (CEM, MDS-2000) for 1–2 h. After digestion, the samples were evaporated to dryness. Then, the residues were dissolved in 1–2% HNO_3.

TABLE 1
List of Samples Collected from a Pine Forest in Tokai-mura, Ibaraki

Sample code	*Species*	*Sample type*[a]	*Sampling date*
Mushrooms			
MR-006	*Russula emetica*	M	Oct. 1989
MR-007	*Suillus granulatus*	M	Oct. 1989
MR-011	*Suillus bovinus*	M	Oct. 1989
MR-023	*Lactarius hatsudake*	M	Oct. 1989
MR-024	*Lactarius hatsudake*	M	Oct. 1989
MR-075	*Russula mariae*	M	1 July 1990
MR-089	*Astraeus hygrometricus*	M/S	13 July 1990
MR-093	*Russula mariae*	M	18 July 1990
MR-097	*Russula mariae*	M	18 July 1990
MR-128	*Agaricus sp.*	S	22 Sep. 1990
MR-132	*Amanita pantherina*	M	6 Oct. 1990
MR-133	*Russula nigricans*	M	6 Oct. 1990
MR-145	*Russula nigricans*	M	9 Oct. 1990
MR-146	*Suillus luteus*	M	9 Oct. 1990
MR-147	*Suillus granulatus*	M	9 Oct. 1990
MR-149	*Armillariella tabescens*	S	9 Oct. 1990
MR-151	*Amanita pantherina*	M	9 Oct. 1990
MR-152	*Amanita pantherina*	M	9 Oct. 1990
MR-171	*Suillus granulatus*	M	Oct. 1990
MR-175	*Suillus granulatus*	M	Oct. 1990
MR-180	*Lactarius chrysorrheus*	M	18 Oct. 1990
MR-184	*Inocybe* sp.	M	18 Oct. 1990
MR-185	*Gymnopilus aeruginosus*	S	18 Oct. 1990
MR-210	*Lactarius hatsudake*	M	31 Oct. 1990
MR-211	*Tricholoma flavovirens*	M	6 Nov. 1990
MR-274	*Suillus granulatus*	M	17 Oct. 1991
MR-278	*Lactarius hatsudake*	M	17 Oct. 1991
MR-280	*Bankera fuligineo-alba*	M	17 Oct. 1991
MR-281	*Phellodon niger*	M	17 Oct. 1991
Plants			
TL-2a[b]	*Pinus thunbergii*	TL	6 Nov. 1990
TL-2b[c]	*Pinus thunbergii*	TL	6 Nov. 1990
TL-4	*Morus bombycis*	TL	6 Nov. 1990
GR-5	*Indigofera pseudo-tinctoria*	GR	6 Nov. 1990
GR-6	*Vitex rotundifolia*	GR	6 Nov. 1990
GR-8	*Oenothera lamarckiana*	GR	6 Nov. 1990
GR-9	*Miscanthus sinensis*	GR	6 Nov. 1990
GR-10	*Ophiopogon japonicus*	GR	6 Nov. 1990

[a] Sample type: (M) mycorrhizal fungi, (S) saprophytic fungi, (M/S) unknown fungi, (TL) tree leaves, (GR) leaves and stems of shrubs and grasses.
[b] Current needles.
[c] 1 and 2 year old needles.

Trace elements (Rb, Cs, Sr and Ba) were measured by ICP-MS (Yokogawa Analytical Systems, PMS-2000). Rh was used for internal standard to compensate for changes in analytical signals during the operation. Major elements, Na, K, Mg, Ca and Al were determined by ICP-AES (Seiko Instruments, SPS7700). Standard solutions were prepared from SPEX Multi-Element Plasma Standards (SPEX Industries Inc.) and used to get calibration curves. Tomato Leaves (1573a) and Orchard Leaves (1571) supplied by the National Institute of Standards and Technology were used to validate the analytical procedure. Details for the analyses have been described by Yoshida and Muramatsu (1997).

RESULTS AND DISCUSSION

Validation of analytical procedure

Good agreements between the certified and measured values were observed for standard reference materials (see Table 2). In the case of Tomato Leaves, errors of measured values were less than 10% of the certified values for Na, K, Ca, Rb and Cs, and 10–20% for Mg, Al, Sr and Ba. Precisions calculated using 6 independent runs of Tomato Leaves were better than 5% relative

TABLE 2
Analytical Results of Tomato Leaves (NIST; 1573a) Obtained by ICP-MS and ICP-AES in Comparison with Certified Values

Elements	*Observed values*[a] *(mg kg^{-1})*	*RSD (%)*	*Certified values (mg kg^{-1})*	*Obs./Cer.*
ICP-AES				
Na	130	3·0	136	0·96
Mg	10700	3·8	12000[b]	0·89
Al	515	4·5	598	0·86
K	25900	4·7	27000	0·96
Ca	49200	6·0	50500	0·97
ICP-MS				
Rb	14·8	7·1	14·89	0·99
Sr	67·9	5·1	85[b]	0·80
Cs	0·053	14	0·053	1·00
Ba	51·7	5·8	63[b]	0·82

[a] Mean values of six independent runs.
[b] Not certified but provided as an additional information value.

standard deviation (RSD) for Na, Mg, Al and K, 5–10% RSD for Ca, Rb, Sr and Ba, and 14% RSD for Cs.

Concentrations of ^{137}Cs and stable elements in mushrooms and plants

Analytical results of alkali and alkaline earth elements in 29 mushrooms collected from a pine forest are shown in Table 3 together with the data for plants and soils collected in the same forest (Yoshida and Muramatsu, 1997). The data for ^{137}Cs (Muramatsu *et al.*, 1991; Yoshida *et al.*, 1994; Yoshida and Muramatsu, 1994*a*, *b*) are also listed in the table. The mean and median concentrations are summarized in Table 4. The median values seemed to be more representative than the mean values for ^{137}Cs and most stable elements in mushrooms and plants, because of the high variations of their concentrations.

The concentrations of ^{137}Cs in mushrooms varied very widely, ranging from 5·4 to 3110 Bq kg^{-1} (dry wt). The median value for all the mushroom species was 135 Bq kg^{-1} (dry wt). In comparison with the median concentration in 124 species of mushrooms collected from all over Japan of 53 Bq kg^{-1} (dry wt), reported by Yoshida and Muramatsu (1994b), the present result is more than two times higher, because mushrooms with relatively high concentration of ^{137}Cs were used in the present study as mentioned before. In comparison with the values reported in Europe after the Chernobyl accident (e.g. Haselwandter *et al.*, 1988; Baldini *et al.*, 1989; Römmelt *et al.*, 1990), the present results are generally 1–2 orders of magnitude lower.

The highest median concentration in mushrooms was found for K followed by Mg, Na, Ca, Rb, Ba, Sr and Cs. For plants (leaves and stems), the highest median value was found for Ca followed by K, Mg, Na, Sr, Ba, Rb and Cs. In comparison with the element composition of plants, the mushroom composition can be characterized by high Rb and Cs concentrations and low Ca and Sr concentrations. Tyler (1980) analyzed 200 mushrooms belonging to 130 species, which were rinsed with water, for several elements including Na, K, Rb, Mg, Ca and Al. Takahashi (1974) summarized the concentrations of many elements in plants (angiosperms). These values are listed in Table 4 for comparison. The present results agree with these previous studies, except for Na and Al in mushrooms. Higher Al concentrations in mushrooms observed in the present study might be attributable to the effect of soils adhering on the surface of mushrooms as mentioned below. Seeger and Schweinshaut (1981) determined stable Cs in 433 mushroom species and obtained the mean value, 7 mg kg^{-1} (dry wt). The present result of stable Cs in mushrooms is comparable with this previous study.

TABLE 3

Concentration of Alkali and Alkaline Earth Elements and ^{137}Cs in Mushrooms, Plants and Soils Collected in a Pine Forest in Tokai, Ibaraki

Sample code	*Dry/wet ratio*	*^{137}Cs (Bq kg^{-1}, dry wt)*	*Na*	*K*	*Rb*	*Cs*	*Mg*	*Ca*	*Sr*	*Ba*	*Al*
			(mg kg^{-1}, dry wt)								
Mushrooms											
MR-006	0·149	42·4	1630	35 500	75·4	0·304	863	201	1·74	2·03	228
MR-007	0·139	449	319	30 300	115	2·32	1100	199	2·05	5·12	415
MR-011	0·108	179	1000	33 800	88·2	1·02	1200	174	1·89	3·31	352
MR-023	0·096	182	208	26 800	110	2·55	1340	450	2·22	2·86	332
MR-024	0·085	230	191	23 000	105	2·19	1050	124	0·93	1·48	169
MR-075	0·224	28·7	1200	28 600	56·5	0·212	777	356	2·88	3·13	347
MR-089	0·202	8·2	1290	25 000	31·0	0·163	1410	1910	17·3	19·3	2640
MR-093	0·121	36·0	1430	34 200	47·7	0·351	963	203	2·27	3·36	377
MR-097	0·120	34·0	1520	32 100	49·8	0·285	874	202	2·68	6·75	454
MR-128	0·211	5·4	1090	27 100	59·8	0·044	1310	432	4·61	6·66	842
MR-132	0·063	55·6	614	40 900	93·1	0·364	976	469	4·80	7·96	1040
MR-133	0·078	127	1780	33 800	85·4	1·01	1100	870	11·7	28·1	3040
MR-145	0·052	65·2	1820	38 400	87·6	0·552	1070	1010	13·2	26·0	3190
MR-146	0·051	317	1030	30 800	137	2·75	976	558	7·68	22·4	1790
MR-147	0·062	675	809	27 200	133	3·79	948	368	4·79	9·63	1030
MR-149	0·081	44·5	1410	18 800	29·5	0·347	1080	512	3·69	4·32	568
MR-151	0·080	45·9	165	27 400	76·5	0·328	683	81	0·93	1·77	185
MR-152	0·083	27·4	197	26 800	73·9	0·239	721	254	2·45	3·90	556
MR-171	0·055	1150	557	25 200	159	6·52	934	99	0·77	1·24	102
MR-175	0·087	246	75	25 400	98·4	2·56	876	63	0·50	0·39	118
MR-180	0·085	356	265	28 100	95·2	1·99	943	278	1·77	1·58	156
MR-184	0·066	287	1570	51 700	68·5	1·85	1520	969	8·32	12·1	1220
MR-185	0·109	75·3	1970	19 300	31·2	0·559	1370	389	2·27	2·82	198
MR-210	0·085	58·1	141	21 400	81·7	0·802	1040	138	0·82	1·26	161

MR-211	0·060	3110	1710	49 500	214	20·0	1380	631	5·77	8·89	1020
MR-274	0·070	598	910	23 900	125	3·78	1140	761	11·0	23·9	2540
MR-278	0·086	602	838	19 900	98·5	3·09	1050	526	5·79	9·66	1350
MR-280	0·113	135	1150	15 500	101	1·01	1580	1990	15·2	18·4	2180
MR-281	0·137	143	882	12 700	78·6	0·920	1330	1280	12·0	14·2	1690
Plants											
TL-2a	0·380	< 2·5	93	6900	8·32	0·024	1300	2570	13·7	2·73	293
TL-2b	0·425	< 3·3	331	4250	3·04	0·017	1100	6440	27·4	6·40	506
TL-4	0·284	< 2·4	6040	15 300	10·4	0·048	3450	29 800	108	15·3	305
GR-5	0·287	< 2·0	713	8890	14·9	0·100	5660	58 300	151	13·5	
GR-6	0·213	< 4·3	1860	8830	8·02	0·037	1300	25 900	99·3	8·20	188
GR-8	0·137	8·0	900	24 500	31·9	0·112	4710	28 700	113	13·6	201
GR-9	0·832	< 5·9	892	3960	4·06	0·022	1200	5820	38·8	8·69	62
GR-10	0·366	7·5	670	17 900	16·0	0·052	2290	6700	42·3	15·0	254
Soils											
Litter		7·8	416	614	1·75	0·047	410	2050	10·8	8·50	893
0–2 cm		34·5	15 300	18 400	42·7	1·28	5180	11 400	78·0	241	44 400
2–5 cm		34·8	16 500	21 800	65·0	1·28	7400	12 300	146	381	52 400

TABLE 4
Mean and Median Concentration of Alkali and Alkaline Earth Elements and ^{137}Cs in Mushrooms, Plants and Soils

	^{137}Cs (*Bq kg^{-1}, dry wt*)	*Na*	*K*	*Rb*	*Cs*	*Mg*	*Ca*	*Sr*	*Ba*	*Al*
		(mg kg^{-1}, dry wt)								
Mushrooms ($n = 29$)										
Mean	321	957	28 700	89·8	2.14	1090	535	5·24	8·71	976
Median	135	1000	27 200	87·6	1·01	1050	389	2·88	5·12	556
Min	5·4	75	12 700	29·5	0·044	683	63	0·50	0·39	102
Max	3110	1970	51 700	214	20·0	1580	1990	17·3	28·1	3190
Tyler (1980)		(100)[a]	32 000	(140)[a]		(1200)[a]	105			30
Plants ($n = 8$)										
Mean	4·5[b]	1440	11 300	12·1	0·052	2630	20 500	74·1	10·4	259
Median	3·8[b]	802	8860	9·35	0·043	1800	16 300	70·8	11·1	254
Min	< 2·0	93	3960	3·04	0·017	1100	2570	13·7	2·73	62
Max	8·0	6040	24 500	31·9	0·112	5660	58 300	151	15·3	506
Takahashi (1974)		1200	14 000	20	0·2	3200	18 000	26	14	550
Soils (0–5 cm)										
Mean	34·7	15 900	20 100	53·9	1·28	6290	11 900	112	310	48 400

[a] Values in parentheses are not given in the paper but estimated from the figures.
[b] In the calculation of the mean and median values of ^{137}Cs, values described as 'detection limit' were also included.

In the case of wild mushrooms, surfaces were often contaminated by nearby soils, and removing all particles was quite difficult. Therefore, the analytical results of some specific elements might be affected by the adhering soils. Al, which is one of the major elements in soils, is not accumulated in biological samples except certain Al accumulating plants such as *Thea sinensis* and *Hydrangea macrophylla.* Worldwide average concentrations of Al in soils and plants are 71 000 mg kg^{-1} (dry wt) and 550 mg kg^{-1} (dry wt), respectively (Takahashi, 1974). Al is often used as the indicator of the contribution of soils to the analytical data of environmental samples. Figure 1a and b summarize the binary plots of Al and alkali and alkaline earth elements including Mg for mushrooms and plants. The ratio of each element to Al in surface (0–5 cm) soils were calculated from the data in Table 4 and shown in the figures as the solid lines. For Ca, Sr and Ba, plots for mushrooms were distributed near the solid lines although the ratios in mushrooms were slightly higher than those in surface soil, indicating that the concentration of these elements in mushrooms was strongly affected by soils adhering on the surface of the samples. Concentration of Na in mushrooms with high Al concentration (>1000 mg kg^{-1}) might also be affected by the soil, because the plots were closer to the line in these samples. For the other elements, the plots for mushrooms were clearly far from the lines, indicating that the effect of adhering soil was negligible. In the case of plants, the plots were far from the lines for all measured elements, showing that the effect of adhering soil is negligible for these elements.

Plant surfaces can act as a filter for aerosols because of their wide surface area (e.g. Aylor, 1975; Lindberg and Lovett, 1985; Yoshida and Ichikuni, 1989). Therefore, the concentration of the elements in plant materials can be influenced by particulate materials deposited on the surface. The effect of soil particles is negligible for plants as already mentioned above. The effect of sea spray is also negligible, because there is no correlation between Na and the other elements as shown later in Table 6a and b. There is no other local source for the alkali and alkaline earth elements around the forest. Therefore, the contribution of the aerial particulate materials is negligible in the present study.

In order to compare the concentrations in mushrooms or plants with those in soil, the concentration ratio defined as 'median concentration in mushrooms or plants on a dry weight basis' divided by 'concentration in the surface 0–5 cm soil on a dry weight basis' was calculated for each element and ^{137}Cs as shown in Table 5. The concentration ratios of higher than 1 were observed for ^{137}Cs, K and Rb in mushrooms and for Ca in plants. The ratios between 0·1 and 1 were observed for Cs and Mg in mushrooms and ^{137}Cs, K, Rb, Mg and Sr in plants. The ratios for the others were lower than 0·1.

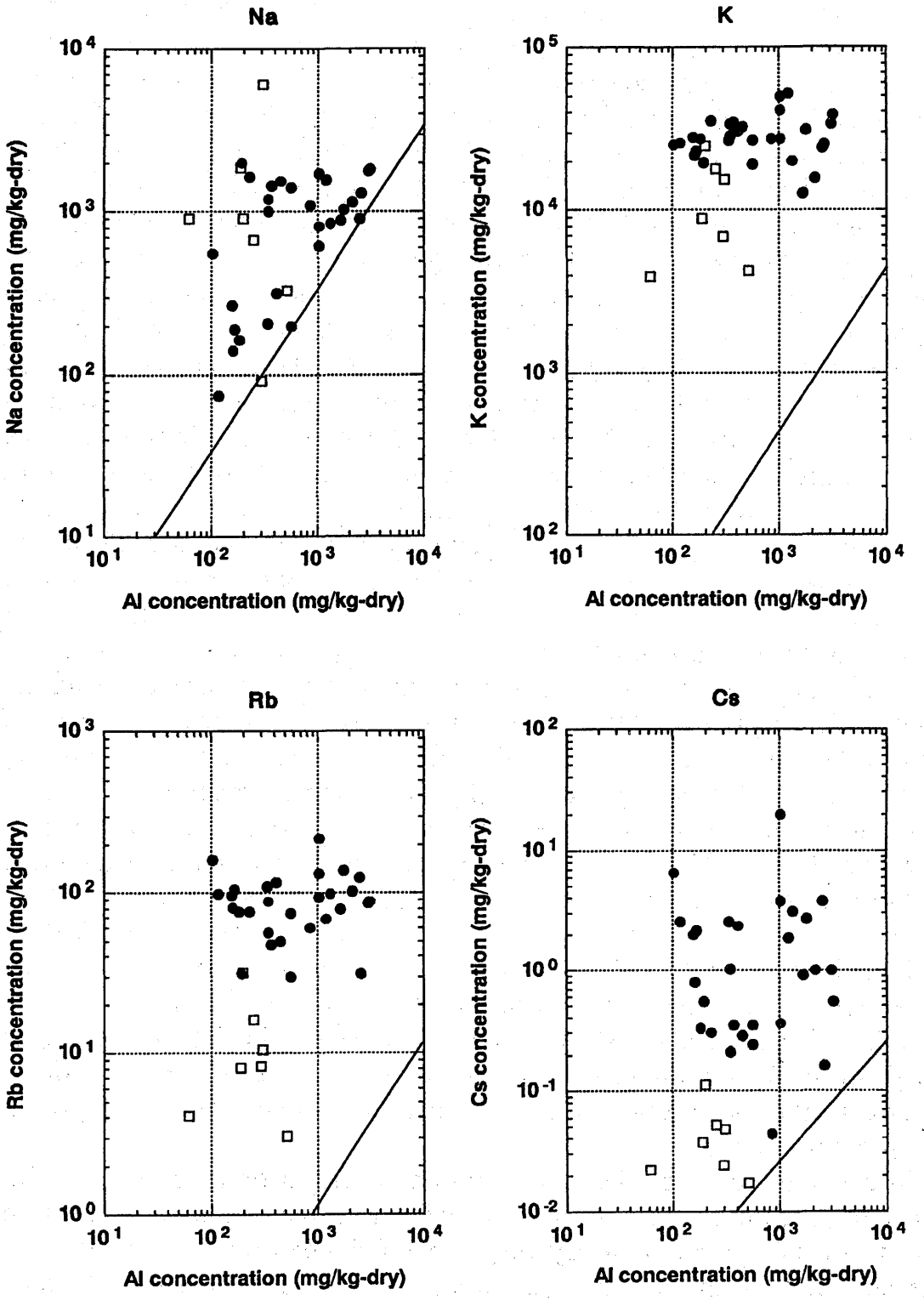

Fig. 1(a). Binary plots of Al and alkali elements for mushrooms (●) and plants (□) collected in a pine forest. Solid line indicates the ratio of each element to Al in surface 0–5 cm soil.

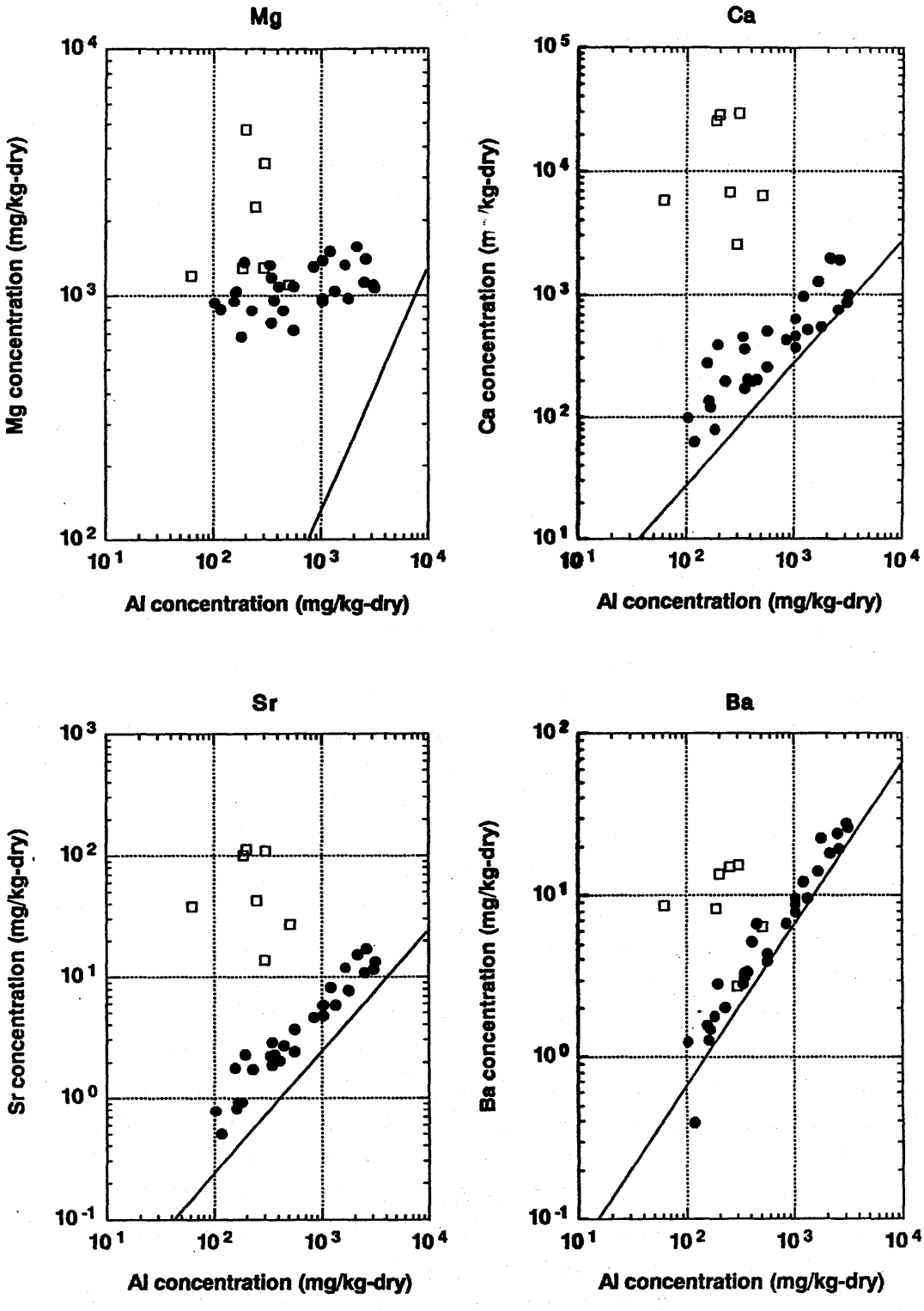

Fig. 1(b). Binary plots of Al and alkaline earth elements for mushrooms (●) and plants (□) collected in a pine forest. Solid line indicates the ratio of each element to Al in surface 0–5 cm soil.

TABLE 5
Concentration Ratio of Alkali and Alkaline Earth Elements and ^{137}Cs for Mushrooms and Plants

Sample	*^{137}Cs*	*Na*	*K*	*Rb*	*Cs*	*Mg*	*Ca*	*Sr*	*Ba*	*Al*
Mushrooms	3·9	0·06	1·4	1·6	0·80	0·2	0·03	0·03	0·02	0·010
Plants	0·2	0·05	0·4	0·2	0·03	0·3	1·40	0·60	0·04	0·005

The concentration ratios of ^{137}Cs, Cs and Rb for mushrooms were one order of magnitude higher than those for plants growing in the same forest. High concentrations of ^{137}Cs discharged through nuclear weapons testing and nuclear accidents were reported for mushrooms in many countries as described in the introduction. The high concentration ratio for stable Cs obtained in this study indicates that mushrooms are important Cs accumulators and ^{137}Cs is taken up from soils together with stable Cs. Accumulations of Cs and Rb in mushrooms were also observed by Ban-nai *et al.* (1994, 1997) from cultivation experiments in flasks using radiotracers. High transfer of Rb from substrata to mushrooms was also reported by Tyler (1982). The concentration ratios of ^{137}Cs were different from those of stable Cs for both plants and mushrooms. The surface 0–5 cm soil is a mixture of organic materials and minerals (sand). Stable Cs is originally contained in the mineral components and this stable Cs is difficult for plant and mushrooms to take up. Therefore, the concentration ratio for stable Cs estimated by using 0–5 cm soil layer was lower than that for ^{137}Cs. Oughton *et al.* (1992) applied a sequential extraction procedure to study the speciation of Chernobyl-derived radionuclides (^{137}Cs and ^{90}Sr), stable Cs and Sr in contaminated 0–4 cm soils and found that higher fraction of ^{137}Cs was extractable into the exchangeable fraction compared with stable Cs.

The low concentration ratios for Ca, Sr and Ba observed in mushrooms suggest no appreciable accumulation of these elements in mushrooms. As demonstrated in Fig. 1b, most part of these elements were derived from soils adhering on the surface of the samples. This result was consistent with the low concentrations of ^{90}Sr in mushrooms after the Chernobyl accident reported by Mascanzoni (1990). The activity ratio of ^{90}Sr to ^{137}Cs in mushrooms given by Mascanzoni ranged in 0·001–0·021%, while the ratio in fallout from the accident was about 1%. Lower concentration ratios for Sr in mushrooms than those in plant were also observed by radiotracer experiments in a laboratory (Ban-nai *et al.*, 1994). Tyler (1982) reported the low transfer of Ca from substrata to mushrooms.

Concentrations of major nutrient elements in plants can fluctuate due to many factors such as differences of sampling season and age of plants. As

shown in Table 3, concentrations of K, Rb and Cs in young pine needles (TL-2a) were higher than those in older needles (TL-2b), while concentrations of Ca, Sr and Ba were higher in older needles. The higher concentration of K and the lower concentration of Ca in younger leaves and needles than older ones were also reported in Yoshida and Ichikuni (1988). K migrates easily in the plant body and tends to be translocated from old tissue to new tissue (Bukovac and Witter, 1957; Johnson *et al.*, 1982). Ca exists in an insoluble form such as calcium oxalate and does not migrate easily in the plant body (Biddulph *et al.*, 1959). The higher concentration of ^{90}Sr in mugwort (*Artemisia vulgaris*) in autumn than in spring was observed by Fujinami *et al.* (1996). In the present study, plants were sampled only in autumn. Further studies may be required to discuss the concentrations of elements in plants sampled in other seasons. In the case of mushrooms used in the present study, they grow quickly and are decomposed within 1 or 2 weeks. Therefore, the effect of age is probably much smaller.

Relationship among ^{137}Cs and alkali and alkaline earth elements

Correlation coefficients among alkaline and alkaline earth elements and ^{137}Cs were calculated for mushrooms and plants (Table 6a and b).

As shown in Fig. 2, a good correlation ($r = 0{\cdot}99$, significance level: $p < 0{\cdot}01$) between ^{137}Cs and stable Cs was observed for mushroom samples, although the species of mushrooms differed. The $^{137}Cs/Cs$ ratios were almost constant. The mean value for autumn in 1990 was 134 ± 36 Bq mg^{-1}. The ratios for 2 plant samples, in which ^{137}Cs was detected, were almost the same as those for mushrooms. The similar ratio, 166 Bq mg^{-1}, was observed also in the litter layer of the forest floor. These findings suggest that

TABLE 6a

Correlation Coefficients among Alkali and Alkaline Earth Elements and ^{137}Cs in Mushrooms

	^{137}Cs	*Na*	*K*	*Rb*	*Cs*	*Mg*	*Ca*	*Sr*	*Ba*
Na	0·10								
K	0·37	0·34							
Rb	0·81	−0·23	0·26						
Cs	0·99	0·09	0·37	0·82					
Mg	0·19	0·37	0·01	0·03	0·21				
Ca	−0·04	0·39	−0·13	−0·10	−0·04	0·69			
Sr	−0·03	0·45	−0·04	−0·04	−0·03	0·57	0·94		
Ba	0·01	0·46	0·10	0·11	0·01	0·36	0·71	0·89	
Al	−0·01	0·44	0·06	0·06	−0·01	0·39	0·78	0·94	0·98

TABLE 6b
Correlation Coefficients among Alkali and Alkaline Earth Elements in Plants

	Na	*K*	*Rb*	*Cs*	*Mg*	*Ca*	*Sr*	*Ba*
K	0·23							
Rb	− 0·03	0·94						
Cs	0·10	0·94	0·98					
Mg	0·40	0·92	0·88	0·92				
Ca	0·68	0·59	0·50	0·64	0·70			
Sr	0·64	0·64	0·56	0·69	0·72	0·99		
Ba	0·55	0·78	0·57	0·64	0·74	0·57	0·64	
Al	0·00	− 0·14	− 0·22	− 0·24	− 0·11	− 0·16	− 0·26	− 0·19

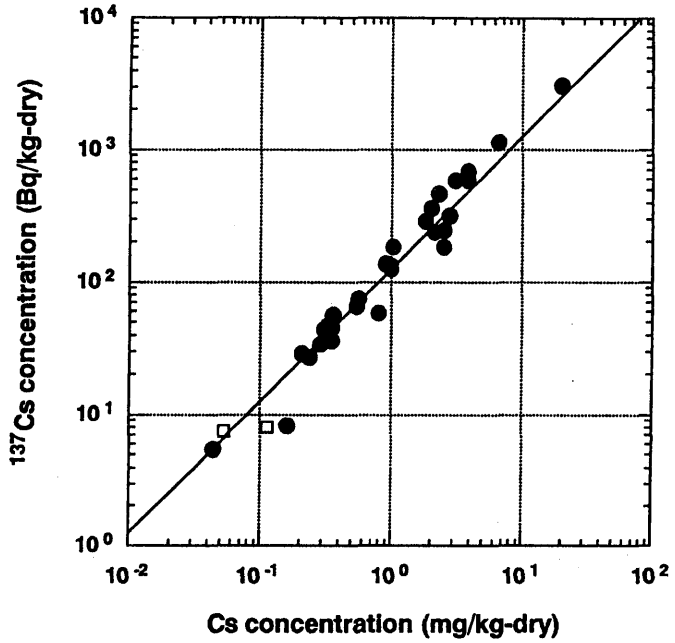

Fig. 2. Relationship between Cs and ^{137}Cs in mushrooms (●) and plants (□) collected in a pine forest. Solid line indicates the mean value of the ^{137}Cs/Cs ratios for mushrooms (^{137}Cs/Cs = 134 ± 36 Bq mg^{-1} in 1990).

the ^{137}Cs/Cs ratios are almost constant in the biological samples in this pine forest. Mushrooms and plants can take up the available part of total ^{137}Cs and total stable Cs in soil. The ^{137}Cs/Cs ratio in surface 0–5 cm soils in the forest was calculated to be 27 Bq mg^{-1} by using the data in Table 4. This value is clearly smaller than that for mushrooms. This is due to the fact that stable Cs is originally contained in the mineral components of the sandy soil and this stable Cs is difficult for plants and mushrooms to take up as mentioned before in the discussion of concentration ratio. Yoshida and Muramatsu (1994*b*) calculated the proportions of ^{137}Cs originating

from the Chernobyl accident in Japanese mushrooms by using $^{134}Cs/^{137}Cs$ ratio, and demonstrated that ^{137}Cs in Japanese mushrooms originates mainly from the fallout of nuclear weapons testing, particularly in the 1960s. These findings suggest that ^{137}Cs, mainly deposited to the forest ecosystem in the 1960s, has become equilibrated with stable Cs biologically, and available Cs for mushrooms and plants is recycling in the pine forest with the constant $^{137}Cs/Cs$ ratio. The $^{137}Cs/Cs$ ratio might be a useful criterion for judging the equilibrium of deposited ^{137}Cs to stable Cs in a forest ecosystem.

Correlations among alkali elements are shown in Fig. 3. In plant samples, good correlations were observed among K, Rb and Cs. Correlations between these elements and Mg in plant samples were also good (Table 6b).

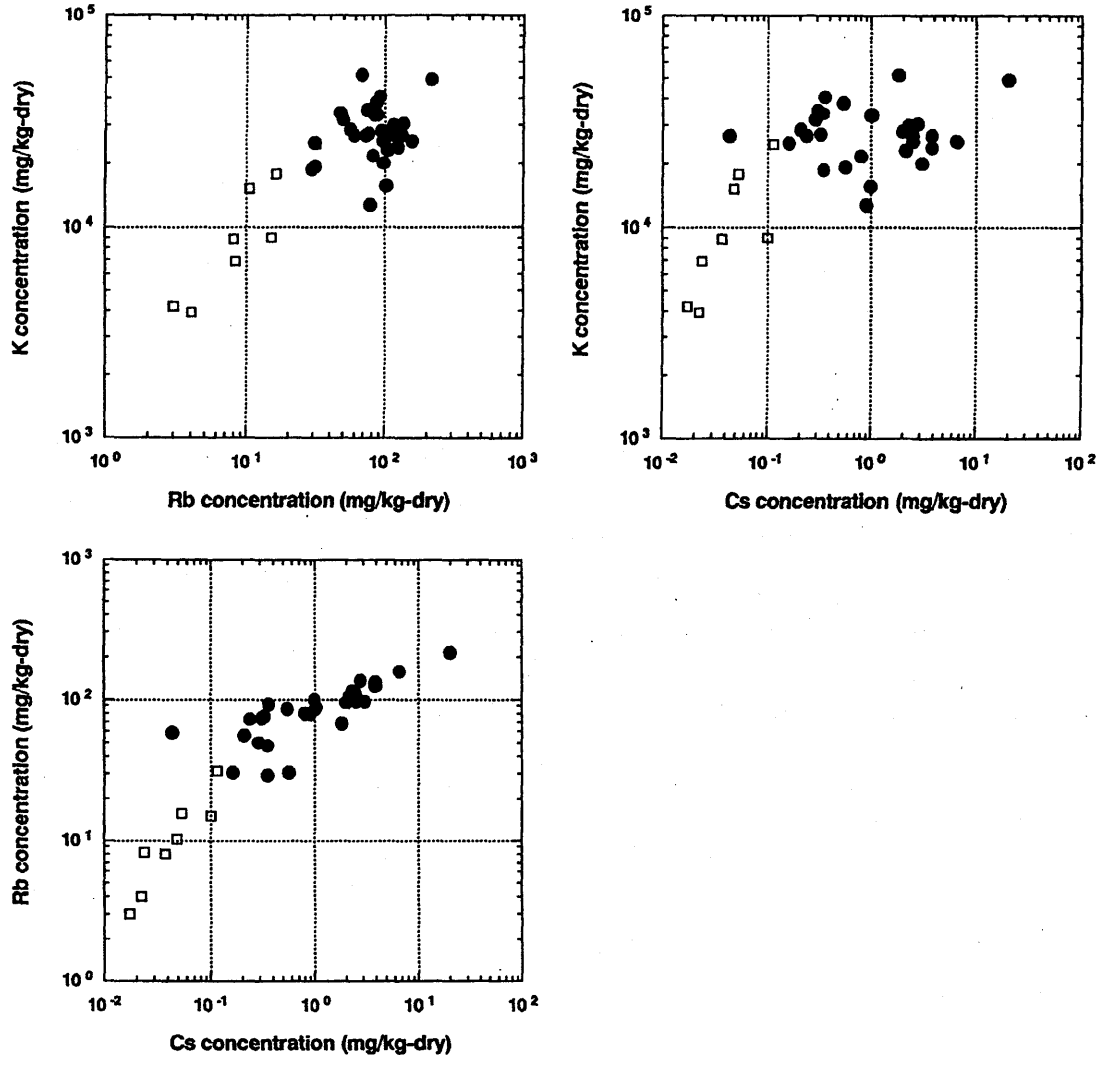

Fig. 3. Relationship among K, Rb and Cs in mushrooms (●) and plants (□) collected in a pine forest.

Ronneau *et al.* (1991) observed the good correlation between ^{137}Cs and K in throughfall waters collected under spruce trees in a forest in Belgium. Myttenaere *et al.* (1993) measured the seasonal change of stable Cs and K in spruce needles, and demonstrated good correlation between them. These findings suggest that K could be used as an indicator of the behaviour of ^{137}Cs in the soil-plant systems in forests. Correlations between Ca and Sr in plants were also good as shown in Table 6b, suggesting the possibility of using the behaviour of Ca to predict the behaviour of ^{90}Sr. No correlations were observed between Na and the other elements studied.

In mushroom samples, good correlations were observed among Ca, Sr, Ba and Al. These elements were not accumulated in mushrooms and most parts in mushrooms were derived from soils adhering on the surface of the samples as already discussed in Fig. 1b. Cs was not correlated with K in mushrooms in contrast with plant samples. The K concentration seemed to be controlled within a narrow range regardless of the mushroom species, while the concentrations of Cs in mushrooms varied very widely. These findings suggested that the mechanism of Cs uptake was completely different from that of K. Rb showed intermediate behaviour between K and Cs. There was a correlation between Rb and Cs ($r = 0{\cdot}82$). However, the Rb/Cs ratio was not constant as shown in Fig. 3. The ratio decreased with increasing Cs concentration in mushrooms, indicating that Rb might be partly taken up by mushrooms by the same mechanism as Cs is.

CONCLUSIONS

The stable alkali (Na, K, Rb and Cs), alkaline earth (Ca, Sr and Ba) elements and Mg in mushrooms collected in a Japanese pine forest on sandy soil were determined, and the data of the stable elements for mushrooms, plants and soils were summarized together with the data of ^{137}Cs. The following conclusions have been drawn.

(1) The element composition of mushrooms could be characterized by the high ^{137}Cs, Cs and Rb concentrations and low Ca and Sr concentrations in comparison with the composition of plants. Concentrations of ^{137}Cs, Cs and Rb for mushrooms were one order of magnitude higher than those for plants growing in the same forest. Ca, Sr and Ba were not accumulated in mushrooms, and their concentrations were affected by soils adhering on the surface of the samples.

(2) A good correlation ($r = 0{\cdot}99$, $p < 0{\cdot}01$) between ^{137}Cs and stable Cs concentrations was observed for mushrooms. The $^{137}Cs/Cs$ ratios were almost constant ($^{137}Cs/Cs = 134 \pm 36$ Bq mg^{-1} in 1990) and were

significantly higher than that in the surface soil (27 Bq mg^{-1}). In the case of the 2 plant samples in which ^{137}Cs was detected, the ratios are almost the same as those for mushrooms. These findings suggested that ^{137}Cs deposited to this pine forest due to nuclear weapons testings has been equilibrated with stable Cs biologically, and available Cs for mushrooms and plants is recycling in the pine forest with the constant $^{137}Cs/Cs$ ratio.

(3) In the plant samples, good correlations were observed among the concentrations of K, Rb, Cs and Mg. Correlation between those of Ca and Sr was also good. These findings suggested that the possibility of using the behaviour of alkali and alkaline earth elements to predict the ^{137}Cs and ^{90}Sr behaviour in soil-plant systems in forests. In contrast, Cs was not correlated with K in mushrooms, indicating that the mechanism of Cs uptake was different from that for K.

Analyses for stable elements have provided much information on the behaviour of elements which are related to radionuclides in a pine forest on sandy soil with a thin organic layer. Such studies must be useful in predicting the migration of radionuclides in forests contaminated by accidental releases such as the Chernobyl accident. Further studies on other forests with other types of soil, vegetation, source of contamination and in other seasons are earnestly desired.

ACKNOWLEDGEMENTS

Mr T. Ohuchi and Ms K. Ebine are acknowledged for their help in sample preparation and measurements.

REFERENCES

Alaimo, R. and Censi, P. (1992) Quantitative determination of major, minor, and trace elements in USGS rock standards by inductively coupled plasma-mass spectrometry. *Atomic Spectroscopy* **13,** 113–117.

Aylor, D. E. (1975) Deposition of particles in a plant canopy. *Journal of Applied Meteorology* **14,** 52–57.

Baldini, E., Bettoli, M. G. and Tubertini, O. (1989) Further investigation on the Chernobyl pollution in forest biogeocenoses. *Radiochimica Acta* **46,** 143–144.

Ban-nai, T., Muramatsu, Y., Yoshida, S., Uchida, S., Shibata, S., Ambe, S., Ambe, F. and Suzuki, A. (1997) Multitracer studies on the accumulation of radionuclides in mushrooms. *Journal of Radiation Research* **38,** 213–218.

Ban-nai, T., Yoshida, S. and Muramatsu, Y. (1994) Cultivation experiments on uptake of radionuclides by mushrooms. *Radioisotopes* **43,** 77–82 (in Japanese).

Biddulph, O., Cory, R. and Biddulph, S. E. (1959) Translocation of calcium in the bean plant. *Plant Physiology* **34,** 512–519.

Brückmann, A. and Wolters, V. (1994) Microbial immobilization and recycling of ^{137}Cs in the organic layers of forest ecosystems: relationship to environmental conditions, humification and invertebrate. *The Science of the Total Environment* **157,** 249–256.

Bukovac, M. J. and Witter, S. H. (1957) Absorption and mobility of foliar applied nutrients. *Plant Physiology* **32,** 428–435.

Bunzl, K., Kracke, W. and Schimmack, W. (1995) Migration of fallout $^{239+240}Pu$, ^{241}Am and ^{137}Cs in the various horizons of a forest soil under pine. *Journal of Environmental Radioactivity* **28,** 17–34.

Casetta, B., Giaretta, A. and Mezzacasa, G. (1990) Determination of rare earth and other trace elements in rock samples by ICP-mass spectrometry: comparison with other techniques. *Atomic Spectroscopy* **11,** 222–227.

Dighton, J., Clint, G. M. and Poskitt, J. (1991) Uptake and accumulation of ^{137}Cs by upland grassland soil fungi: a potential pool of Cs immobilization. *Mycological Research* **95,** 1052–1056.

Eaton, J. S., Likens, G. E. and Bormann, F. H. (1973) Throughfall and stemflow chemistry in a northern hardwood forest. *Journal of Ecology* **61,** 495–508.

Eckl, P., Hofmann, W. and Tüerk, R. (1986) Uptake of natural and man-made radionuclides by lichens and mushrooms. *Radiation and Environmental Biophysics* **25,** 43–54.

Fraiture, A., Guillitte, O. and Lambinon, J. (1990) Interest of fungi as bioindicators of the radiocontamination in forest ecosystems. In *Proc. CEC Workshop, Transfer of Radionuclides in Natural and Semi-Natural Environments,* eds G. Desmet, P. Nassimbeni and M. Belli. Elsevier Applied Science, London, pp. 477–484.

Fujinami, N., Watanabe, T., Tsuzuki, H. and Ibuki, K. (1996) Behavior of strontium-90 in mugwort. *Hoken-butsuri* **31,** 357–360 (in Japanese).

Giovani, C, Nimis, P. L. and Padovani, R. (1990) Investigation of the performance of macromycetes as bioindicators of radioactive contamination. In *Proc. CEC Workshop, Transfer of Radionuclides in Natural and Semi-Natural Environments,* eds G. Desmet, P. Nassimbeni and M. Belli. Elsevier, London, pp. 485–491.

Guillitte, O., Fraiture, A. and Lambinon, J. (1990) Soil-fungi radiocesium transfers in forest ecosystems. In *Proc. CEC Workshop, Transfer of Radionuclides in Natural and Semi-Natural Environments,* eds G. Desmet, P. Nassimbeni and M. Belli. Elsevier, London, pp. 468–476.

Guillitte, O., Melin, J. and Wallberg, L. (1994) Biological pathways of radionuclides originating from the Chernobyl fallout in a boreal forest ecosystem. *The Science of the Total Environment* **157,** 207–215.

Haselwandter, K., Berreck, M. and Brunner, P. (1988) Fungi as bioindicators of radiocesium contamination: pre- and post- Chernobyl activities. *Transactions of the British Mycological Society* **90,** 171–174.

Heinrich, G. (1992) Uptake and transfer factors of ^{137}Cs by mushrooms. *Radiation and Environmental Biophysics* **31,** 39–49.

Heinrich, G., Muller, H. J., Oswald, K. and Gries, A. (1989) Natural and artificial radionuclides in selected Styrian soils and plants before and after the reactor accident in Chernobyl. *Biochemic und Physiologic der Pflanzer* **185,** 55–67.

Johnson, D. W., West, D. W., Todd, D. E. and Mann L. K. (1982) Effect of sawlog vs. whole-tree harvesting on the nitrogen, phosphorus, potassium and calcium budgets of an upland mixed oak forest. *Soil Science Soceity of American Journal* **46,** 1304–1309.

Liechty, H. O., Mroz, G. D. and Reed, D. D. (1993) Cation and anion fluxes in northern hardwood throughfall along an acidic deposition gradient. *Canadian Journal of Forest Research* **23,** 457–467.

Likens, G. E., Bormann, F. H., Pierce, R. S., Eaton, J. S. and Johnson, N. M. (1977) *Biogeochemistry of a Forested Ecosystem.* Springer, New York.

Lindberg, S. E. and Lovett, G. M. (1985) Field measurements of particle dry deposition rates to foliage and inert surfaces in a forest canopy. *Environmental Science and Technology* **19,** 238–244.

Mascanzoni, D. (1990) Uptake of ^{90}Sr and ^{137}Cs by mushrooms following the Chernobyl accident. In *Proc. CEC Workshop, Transfer of Radionuclides in Natural and Semi-Natural Environments*, eds G. Desmet, P. Nassimbeni and M. Belli. Elsevier, London, pp. 459–467.

Mayer, R. and Ulrich, B. (1977) Acidity of precipitation as influenced by the filtering of atmospheric sulphur and nitrogen compounds — its role in the element balance and effect on soil. *Water, Air and Soil Pollution* **7,** 409–416.

Muramatsu, Y., Yoshida, S. and Sumiya M. (1991) Concentrations of radiocesium and potassium in basidiomycetes collected in Japan. *The Science of the Total Environment* **105,** 29–39.

Myttenaere, C., Schell, W. R., Thiry, Y., Sombre, L., Ronneau, C. and van der Stegen de Schrieck, J. (1993) Modelling of Cs-137 cycling in forests: recent developments and research needed. *The Science of the Total Environment* **136,** 77–91.

Olsen, R. A., Joner, E. and Bakken, L. R. (1990) Soil fungi and the fate of radiocesium in the soil ecosystem — a discussion of possible mechanisms involved in the radiocesium accumulation in fungi, and the role of fungi as a Cs-sink in the soil. In *Proc. CEC Workshop, Transfer of Radionuclides in Natural and Semi-Natural Environments*, eds G. Desmet, P. Nassimbeni and M. Belli. Elsevier, London, pp. 657–663.

Oughton, D. H., Salbu, B., Riise, G., Lien, H., Østby, G. and Nøren, A. (1992) Radionuclide mobility and bioavailability in Norwegian and Soviet soils. *Analyst* **117,** 481–486.

Römmelt, R., Hiersche, L., Schaller, G. and Wirth, E. (1990) Influence of soil fungi (basidiomycetes) on the migration of Cs 134 + 137 and Sr 90 in coniferous forest soils. In *Proc. CEC Workshop, Transfer of Radionuclides in Natural and Semi-Natural Environments*, eds G. Desmet, P. Nassimbeni and M. Belli. Elsevier, London, pp. 152–160.

Ronneau, C., Sombre, L., Myttenaere, C., Andre, P., Vanhouche, M. and Cara, J. (1991) Radiocaesium and potassium behaviour in forest trees. *Journal of Environmental Radioactivity* **14,** 259–268.

Rühm, W., Kammerer, L., Hiersche, L. and Wirth, E. (1997) The $^{137}Cs/^{134}Cs$ ratio in fungi as an indicator of the major mycelium location in forest soil. *Journal of Environmental Radioactivity* **35,** 129–148.

平成１３年１１月刊行

放射線医学総合研究所
研究交流・情報室
千葉市稲毛区穴川４丁目９番１号（〒２６３－８５５５）
電話　千葉（０４３）２０６－３０２７（ダイヤルイン）
http://www.nirs.go.jp　　E-mail：kouryu@nirs.go.jp